THE FRACTIONATION OF DEXTRAN POLYMER BY ULTRAFILTRATION TO YIELD CLINICAL PRODUCTS

A thesis submitted by Keith Robert Poland (BSc) for the degree of Doctor of Philosophy to the Faculty of Engineering, Aston University, Birmingham.

June 1986

THE UNIVERSITY OF ASTON IN BIRMINGHAM

THE FRACTIONATION OF DEXTRAN POLYMER BY ULTRAFILTRATION TO YIELD CLINICAL PRODUCTS

Keith Robert Poland (BSc) PhD June 1986

SUMMARY

A review of ultrafiltration (UF) theory and equipment has been made.

Dextran is fractionated industrially by ethanol precipitation, which is a high energy intensive process.

The aims of this work were to investigate the fractionation of dextran using UF and to compare the efficiency and costs of UF fractionation with ethanol fractionation. This work is the continuation of research conducted at Aston, which was concerned with the fractionation of dextran using gel permeation chromatography (GPC) and hollow fibre UF membranes supplied by Amicon Ltd.

Initial laboratory work centred on determining the most efficient make and configuration of membrane. UF membranes of the Millipore cassette configuration, and the DDS flat-sheet configuration, were examined for the fractionation of low molecular weight (MW) dextran. When compared to Amicon membranes, these membranes were found to be inferior. DDS membranes of 25 000 and 50 000 MW cut-offs were shown to be capable of fractionating high MW dextran with the same efficiency as GPC.

The Amicon membranes had an efficiency comparable to that of ethanol fractionation. To increase this efficiency a theoretical UF membrane cascade was adopted to utilize favourable characteristics encountered in batch mode membrane experiments. The four stage cascade used recycled permeates in a counter-current direction to retentate flow, and was operated 24 hours per day controlled by a computer. Using 5 000 MW cut-off membranes the cascade improved the batch efficiency by at least 10% for a fractionation at 6 000 MW.

Economic comparisons of ethanol fractionation, combined GPC and UF fractionation, and UF fractionation of dextran were undertaken. On an economic basis GPC was the best method for high MW dextran fractionation. When compared with a plant producing 100 tonnes pa of clinical dextran, by ethanol fractionation, a combined GPC and UF cascade fractionation could produce savings on operating costs and an increased dextran yield of 5%.

Key words:

Dextran, Polymer, Fractionation, Ultrafiltration, Membranes

ACKNOWLEDGEMENTS

The author is indebted to the following:

Professor GV Jeffreys and the Department of Chemical Engineering for making available the facilities for research.

Professor PE Barker who supervised the work, for his help and guidance throughout this project.

Mr RM Alsop of Fisons plc, Pharmaceutical Division for his technical advice and support.

For the provision of a scholarship by the Science and Engineering Research Council and the Directors of Fisons plc, for their financial support.

Mr N Roberts and the technical staff, especially Mr M Santoro for his unique workmanship in the construction of experimental equipment, and Mr D Bleby without whose electronics expertise and patience the cascade equipment would not have been possible

Tracy for her patience during the typing of this thesis.

Finally, my parents for their support throughout my PhD.

Dedication

To my parents

AND

Fiona

LIST OF CONTENTS

LIST OF FIGURES

1.0 INTRODUCTION

1.0 INTRODUCTION

Dextran is a polymer of glucose in which at least 60% of the glucosidic bonds are of the α-1, 6 type. It is used in the field of medicine as:

(i) a blood plasma volume restorer, and

(ii) for the production of iron dextran, which is then used in the treatment of anaemia (1-3).

The present manufacturing process involves the fermentation of sucrose to yield a product known as "native dextran". The molecular weight of the native dextran ranges from several hundred thousand to several hundred million daltons. This very high molecular weight range makes the native dextran unusable as a blood expander (clinical dextran), since it would interfere with the normal coagulation processes of the blood. Therefore, the native dextran is subjected to partial acid hydrolysis which produces a product with a molecular weight range of 180 daltons to 3,000 000 daltons. This product is known as dextran hydrolysate.

Befcre the dextran can be used as a clinical product, the remaining high molecular weight, and some of the low molecular weight dextran must be removed (Figure 1.1). The amount of material to be removed depends on the required specification of the clinical product. An example is dextran 40 which requires 85% of its molecular weight range to be between 12,000 daltons and 98,000 daltons (4).

The removal of the unwanted material is accomplished by means of a two stage ethanol precipitation. The first addition of ethanol to an aqueous solution of dextran results in the precipitation of the largest dextran molecules. In thc second stage the ethanol concentration is increased and the smaller molecules are precipitated (5,6). This procedure results in a process which has high energy costs due to the need for ethanol recovery by distillation, and is a potential fire hazard. Therefore, a process involving no ethanol fractionation would probably be preferable from an economic viewpoint, although maintaining sterility will be more difficult in aqueous solution than in ethanol.

Figure 1.1. Clinical Dextran Separation from the Hydrolysate

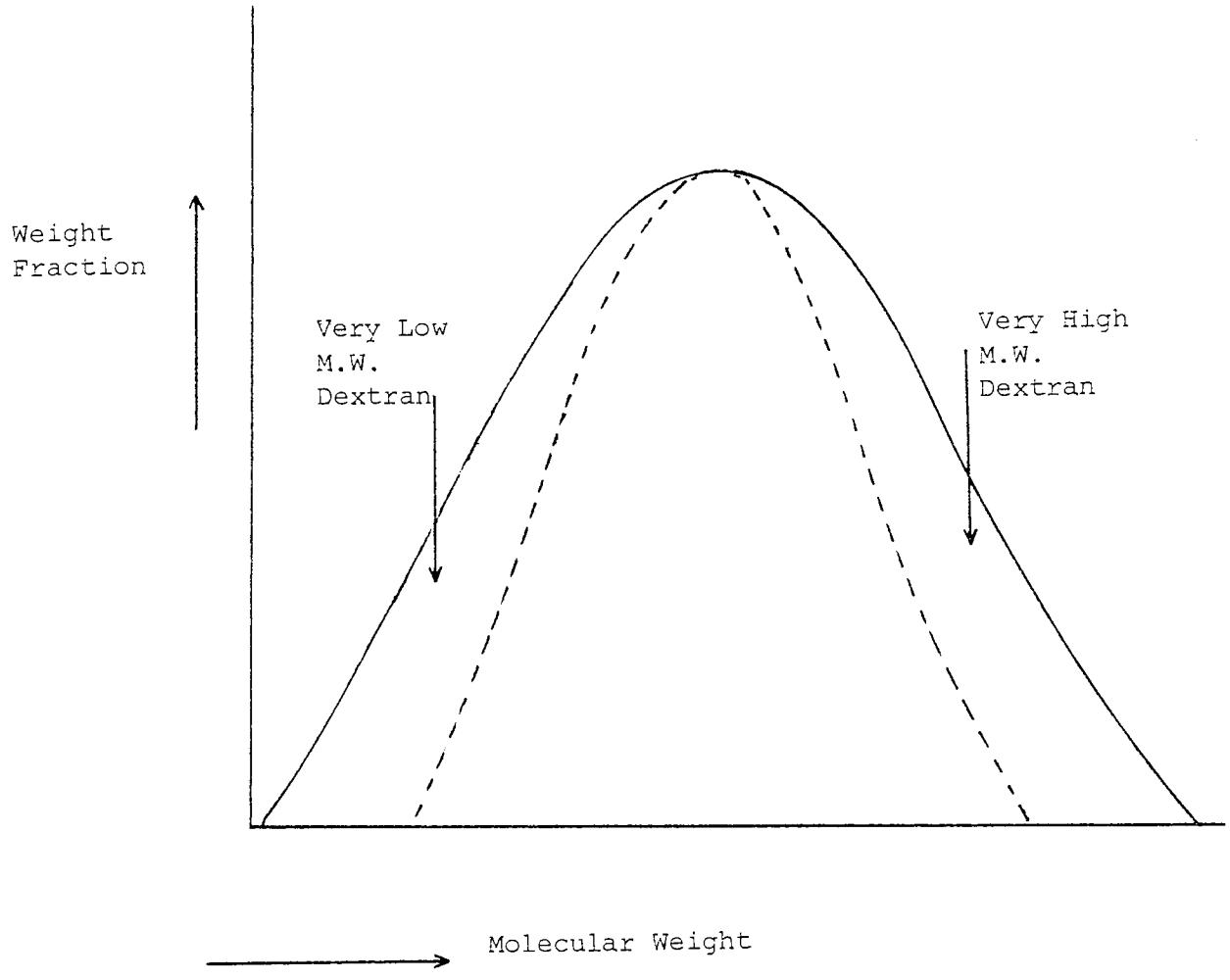

Specification of Clinical Dextran 40

British Pharmacopeia
M.W. 12,000<85% of dextran<98,000 M.W.

Fisons Ltd
M.W. 12,000<90% of dextran<98,000 M.W.

Two possible alternative processes are gel permeation chromatography (GPC) and ultrafiltration (UF).

GPC is a form of liquid chromatography based on the unique properties of the gels for separating polymers, primarily on the basis of molecular size.

Ultrafiltration also separates molecules according to their molecular size but utilises porous membranes as a separation means instead of gels.

The use of GPC for dextran fractionation has been investigated extensively by Barker and co-workers over the last 15 years (7-11, 15,16). This work resulted in the development at Aston (12-14) of an ethanol free fractionation process (Figure 1.2). This process utilises GPC for the fractionation of high molecular weight dextran, ultrafiltration for the fractionation of the low molecular weights and an ion exchange bed for the removal of any silica eluted from the porous silica GPC columns. Vlachogiannis found that an efficiency comparable with or greater than ethanol fractionation could be obtained.

The ultrafiltration section of the proposed new process was based on experiments conducted by Vlachogiannis (12) on only one manufacturer's membrane (AMICON). Therefore, the aims of this project were as follows:

(a) to investigate different makes and configurations of membranes, in order to determine the most efficient one in the fractionation of low molecular weight dextran. It had been agreed that Fisons Pharmaceuticals (Holmes Chapel) staff would investigate the performance of membranes in fractionating high molecular weight dextran

(b) To investigate whether the ultrafiltration single stage batch efficiency could be improved by means of a cascade system utilising several membrane stages.

Figure 1.2: A New Process for the Manufacture of Clinical Dextran (12)

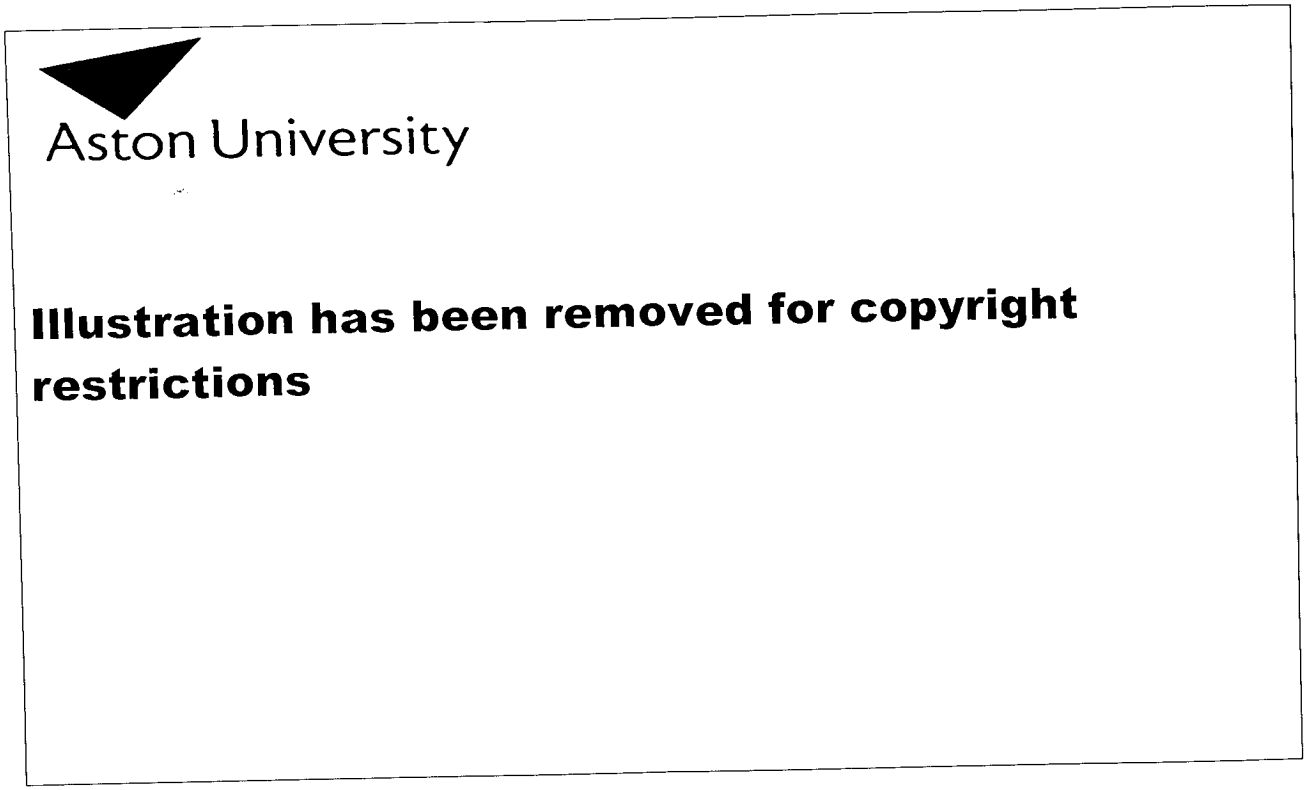

(c) To determine, by an economic comparison, the most efficient method of fractionation, ie. ethanol, GPC, UF or a combination of UF and GPC.

2.0 LITERATURE SURVEY

2.0 LITERATURE SURVEY

2.1 INTRODUCTION

Until 1960 ultrafiltration was essentially a laboratory curiosity, but it has recently been gaining prominence as a practical industrial process for the concentration and purification of macromolecular and colloidal species in solution. Increased interest in the process has been closely tied to the development of finely produced, high flux membranes capable of distinguishing among molecular species in a 1nm to 10μm size range. These new commercially available ultrafiltration membranes are a direct spin-off from the rapid development of reverse osmosis technology. The cellulose acetate membranes available are often produced using the same formulation as for a reverse osmosis membrane, but without the final heat shrinkage. Also much of the technology for making polysulphone ultrafiltration membranes was derived from the manufacture of base films for composite reverse osmosis membranes. As well as these main two materials almost every polymeric material can be used for the construction of membranes.

As well as improvements in the actual membranes there has been a great advance in the design of equipment to utilize the characteristics of the membranes. This equipment comes in many different forms, ie. spiral wound, hollow fibre, flat sheet or tubular modules. Between them these various designs are able to cater for a very wide range of different processing conditions.

Theoretically, and now in practice, ultrafiltration (UF) offers an attractive alternative to a number of unit operations in the food processing, chemical processing, pharmaceutical and medical industries, eg. for concentration, purification and sterilisation. One of the major applications of interest on the industrial scale is the replacement of heat drying and even vacuum evaporation by UF. The UF process is athermal and permits removal of up to 90% of the water at ambient temperature avoiding thermal and oxidative degradation of the products. Also, the absence of phase change results in lower energy costs.

Retained particle size is one characteristic distinguishing UF from other filtration processes. Viewed on a spectrum of membrane separation processes, UF is only one of a series of membrane methods that can be used for macromolecular separations (see Figure 2.1). Reverse osmosis (RO) is used to separate smaller molecules, and microporous filters are capable of virus and bacteria retention. Conventional industrial filters retain normal particulate material.

2.2 PRINCIPLES OF ULTRA-FILTRATION

2.2.1 MODES OF OPERATION

2.2.1.1 CONCENTRATION MODE

A UF system can be used to concentrate a macromolecular solution by removing solvent and some low molecular weight material. As the concentration of macromolecules in the feed/retentate solution increases, its volume decreases (Figure 2.2.).

2.2.1.2 DIAFILTRATION (CONSTANT CONCENTRATION) MODE

Purification from low molecular weight contaminants is partially effected during concentration, since the removed solvent contains some of these contaminants. Purification of solutes at constant concentration can also be achieved. Figure 2.3 features a batch diafiltration operation for the removal of low molecular weight contaminants. In diafiltration the species to be purified is neither diluted or concentrated with respect to the solvent. As permeate, containing lower molecular weight materials, is removed (washed) through the membrane, dialysate (pure solvent) flows into the retentate reservoir at the same rate. The matching of dialysate flow rate and permeate rate is normally achieved by use of a pressure balance between the dialysate reservoir and the retentate reservoir.

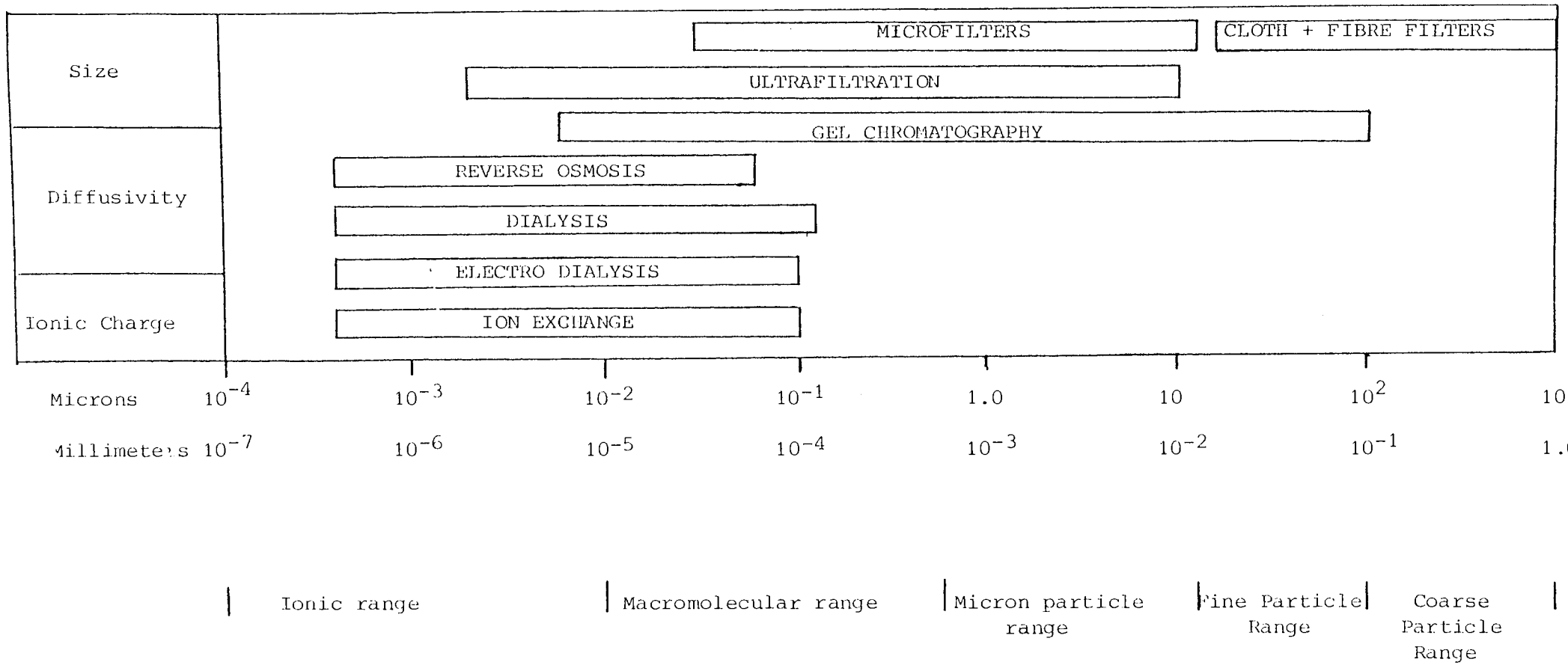

Figure 2.1: Comparison of Membrane Processes

Figure 2.2: UF Unit in Concentration Mode Operation

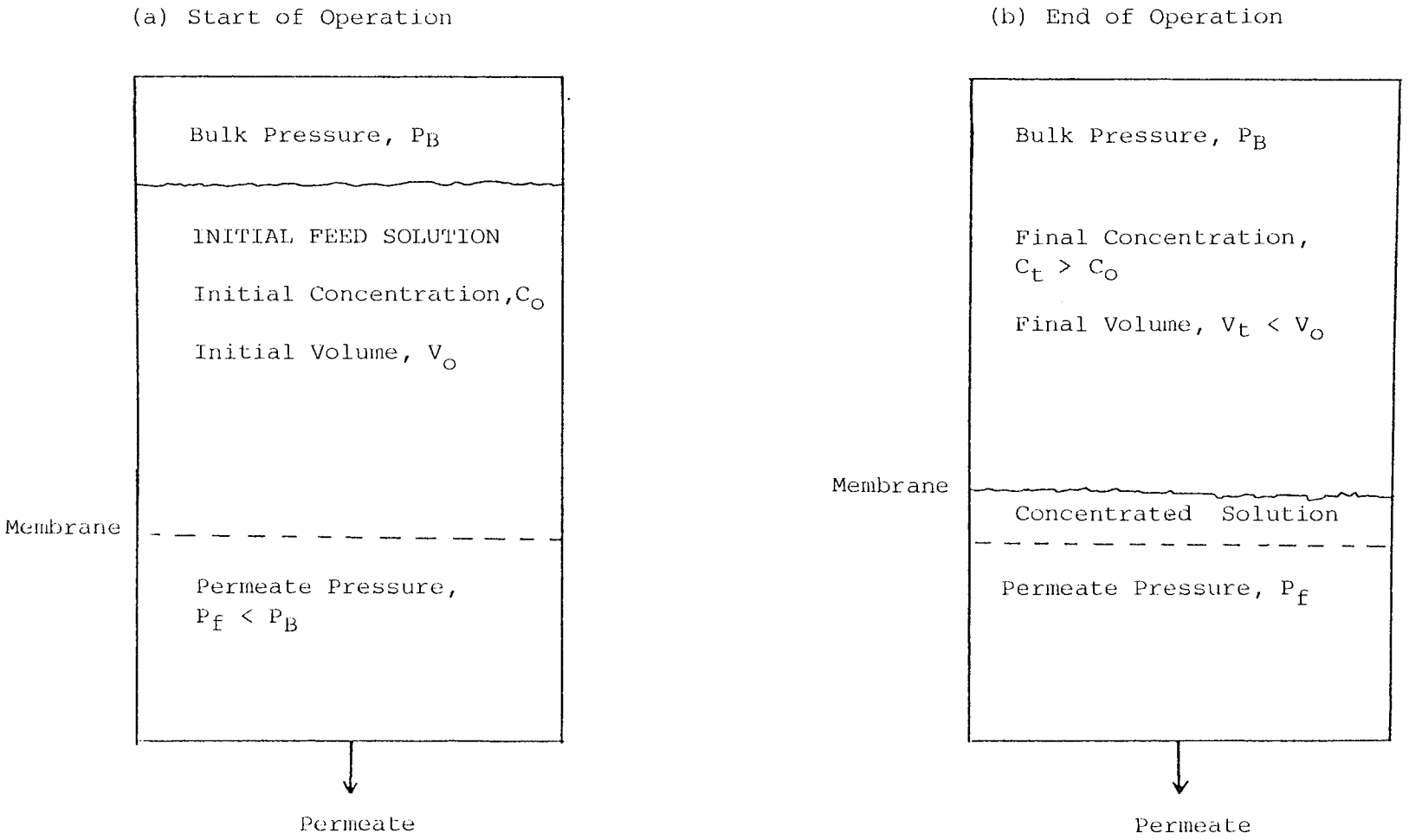

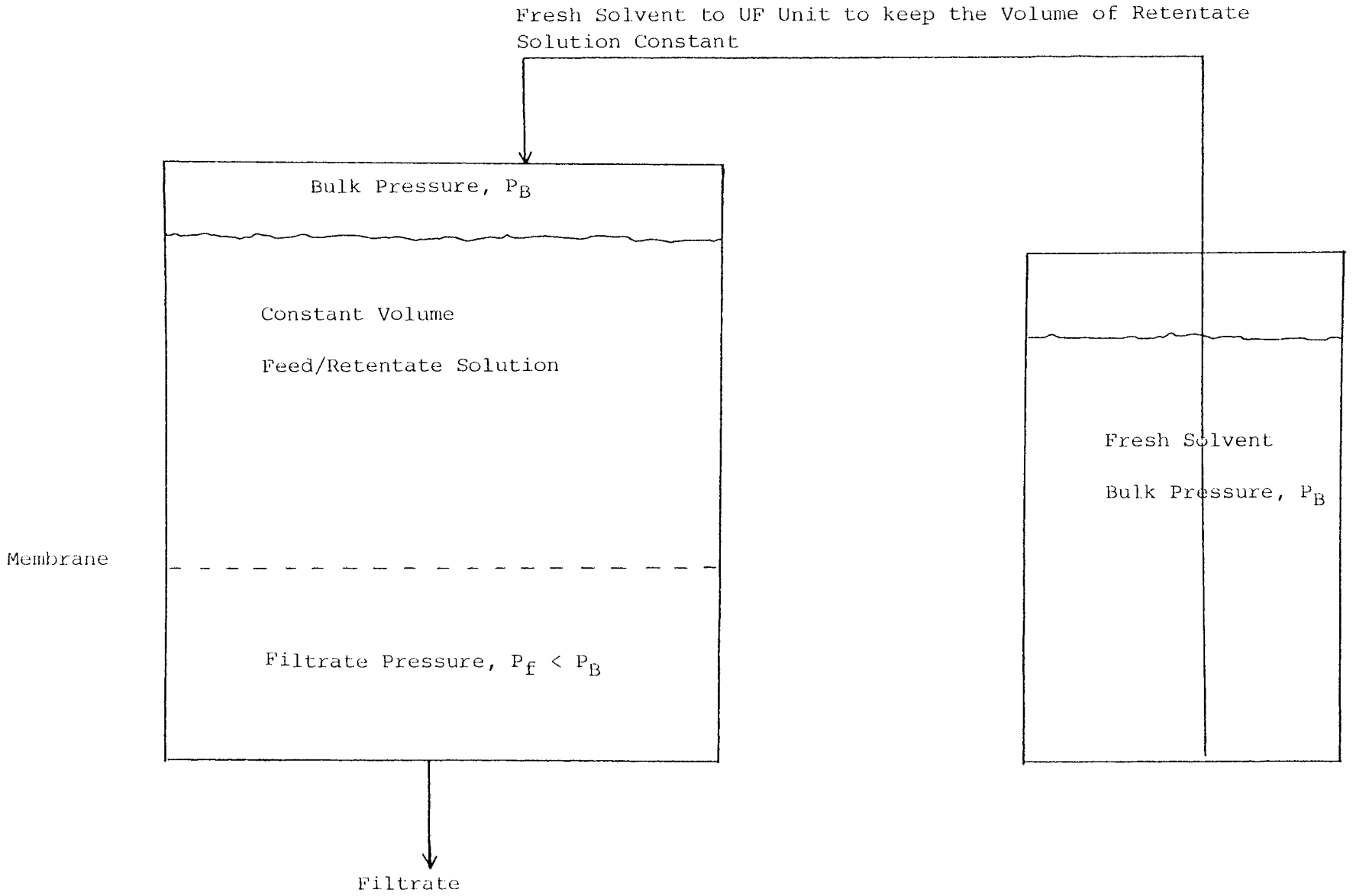

Figure 2.3: UF Unit in Diafiltration Mode Operation

2.2.1.3 DIALYSIS MODE

A UF system working in the dialysis mode has the feed solution flowing across the membrane in the high pressure section and fresh solvent flowing across the other side of the membrane (Figure 2.4). Rapid removal of microsolutes from process fluids can be accomplished in this mode because microsolutes are removed from the process solution in two ways: (1) microsolute diffuses into the dialysate liquid through the membrane wall; (2) liquid with microsolute is convectively transported through the membrane walls as permeate.

2.2.2 IDEAL SYSTEMS

2.2.2.1 RETENTIVITY

The two major characteristics of any membrane are its pore size distribution which defines the selectivity of the membrane, and its solvent flux which depicts the performance of the membrane.

The majority of models for the selectivity assume that colloidal and suspended matter will be filtered from the feed solution by the sieving action of pores in the membrane structure. However, in reality the membrane contains a distribution of pore sizes and a certain fraction (R) of these pores will be too small to allow passage of the solute through the membrane. Assuming that all the larger pores allow the solute to pass unhindered, the solute flux (J_2) is given by:

$$J_2 = C_B (1- R) J_1 \qquad \text{..... 2.1}$$

where J_1 is the solvent flux through the membrane and C_B is the bulk concentration of solute in the retentate.

Since mass balance dictates that:

$$J_2 = J_1 C_P \qquad \text{..... 2.2}$$

where C_P is the concentration of solute in the permeate, then:

Figure 2.4: UF Unit in Dialysis/Concentration Mode Operation

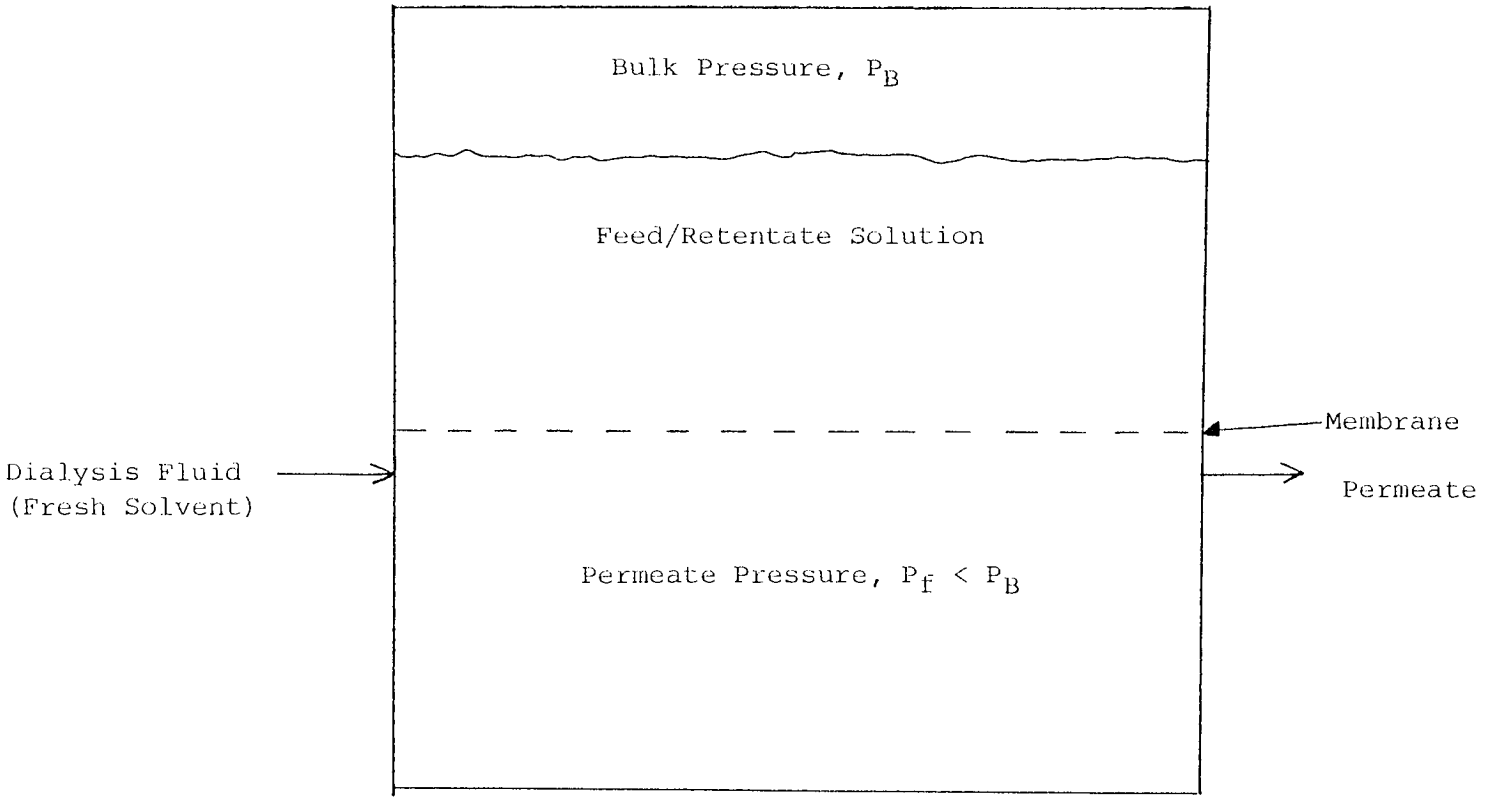

$$R = 1 - \frac{C_P}{C_B} \qquad \text{..... 2.3}$$

The selectivity (R) of a membrane is currently obtained from experiments conducted with a series of compounds of progressively increasing molecular weights. During evaluation of a membrane a UF unit is charged with a test solution of a well characterized solute and pressurised. After a small volume of permeate is collected the remaining retentate and the collected permeate are both analysed. The selectivity of the membrane, for the particular solute tested, is then found from equation 2.3.

Even though this is the most commonly used equation for calculating the rejection coefficient (selectivity) it is only applicable if the concentration of the solute in the retentate stays constant. This would only be true if the concentration of the permeate (C_P) was equal to the concentration of the retentate (C_B), ie. the membrane allowed the solute to pass through unrestricted, and R equals zero. In any case where some of the solute is retained (R > O) the concentration of the retenate would change, thus changing C_P. This in turn would then affect C_B. To overcome this problem very large quantities of test solution are used as feed and only very small quantities of permeate are collected. Therefore any change in C_B would be negligible and it can be considered constant.

Another method of calculating the rejection coefficient is to take into account the change in volume of the retentate. Since solute permeation is an exponential function of the decreasing volume of solution in the unit (17), expressions for the rejection coefficient derived from either retentate or permeate are:

$$R_{ret} = \frac{\ln (C_t/C_o)}{\ln (V_o/V_t)} \qquad \text{..... 2.4}$$

$$R_{per} = \left\{ \frac{V_o}{V_P} - \frac{C_P}{C_o} \left(\frac{V_o}{V_P} - 1 \right) \right\} \Big/ \ln \left(\frac{V_o}{V_P} \right) \qquad \ldots\ 2.5$$

where C_o and V_o are the initial concentration and volume of the feed respectively, C_t and V_t are the final concentration and volume of the retentate, and C_P and V_P are the final concentration and volume of the permeate.

The above equations are only valid if the concentration mode of operation is used. If the diafiltration mode is used the following equations can be derived from a simple mass balance:

$$C_{r(t)} = C_{r(o)} \exp \left[- \frac{V_{(t)}}{V_o} (1 - R) \right] \qquad \ldots\ldots\ 2.6$$

$$\ln C_{P(t)} = \text{const} - (1 - R) \frac{V_{(t)}}{V_o} \qquad \ldots\ldots\ 2.7$$

where $V_{(t)}$ is the volume of permeate collected from the beginning of the experiment until time (t); V_o is the volume of the UF cell (which is constant); $C_{r(t)}$, $C_{P(t)}$ are the concentrations of the retentate and permeates at time (t) respectively, $C_{r(o)}$ is the initial concentration of the retentate, and R is the rejection coefficient.

Hence a plot of $\ln C_{P(t)}$ versus $V_{(t)}/V_o$ gives a slope of - [1 - R].

In both the concentration and diafiltration mode of testing, dilute solutions must be employed to minimise the effects of solute polarisation or the formation of a gel layer (to be discussed later). By repeating this test for a range of solutes with different molecular weights, the molecular weight cut-off for the membrane, ie. the molecular weight above which 90+% of the solute is retained, can be determined.

A further operational definition of solute permeation often refers to membranes as possessing either 'sharp' or 'diffuse' cut-off levels. Figure 2.5 illustrates this aspect of performance and is plotted with the usual rejections versus molecular weight convention. When R equals one the solute is totally rejected and when R equals zero the solute passes unhindered through the membrane. Theoretically, an ideal membrane with a narrow distribution of pore diameters would display the more vertical inflection (sharp). In general however, membranes tend to display a more 'diffuse' cut-off under actual operating conditions than when used with very dilute solutions. This is due to the phenomenon of 'concentration polarisation', which is an accumulation of macromolecules at the membrane/solution interface. It restricts solvent flow and may impair or enhance solute permeation.

The simple rejection models used above indicate that the rejection coefficient is essentially constant and pressure independent. However, they take no account of solute shape, charge or adsorption on the membrane or any form of membrane fouling by the solute. The effect of these phenomena will be discussed later.

2.2.2.2 MEMBRANE PERMEATION

Consider a system operating at steady-state under isothermal conditions, with a semi-permeable membrane separating two fluid compartments, as illustrated in Figure 2.6. An aqueous solution of a single solute, at a concentration C_A, flows continuously by the upstream surface of the membrane and is at a pressure P_A. The membrane is totally permeable to the solvent but only partially permeable to the solute, so that a concentration of solute in the permeate, C_P, is obtained which is less than C_A. A permeate flux, J_1, is continuously removed from the downsteam compartment of the membrane at a pressure P_P which is lower than P_A. The flow of solution

Figure 2.5. Solute Retentivity by 'Sharp' and 'Diffuse' Cut-off UF Membranes

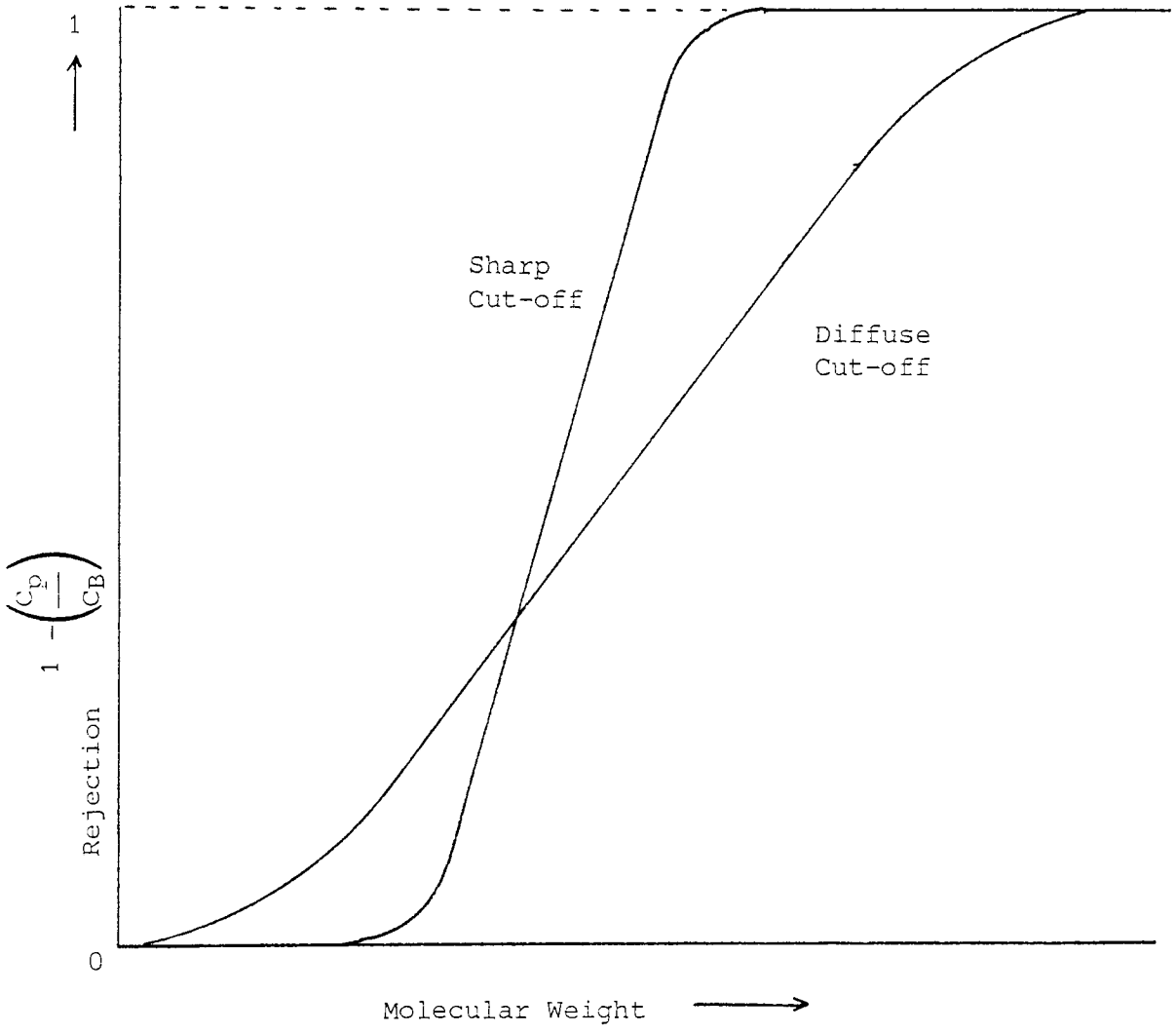

Figure 2.6 Schematic Diagram of Membrane UF Process

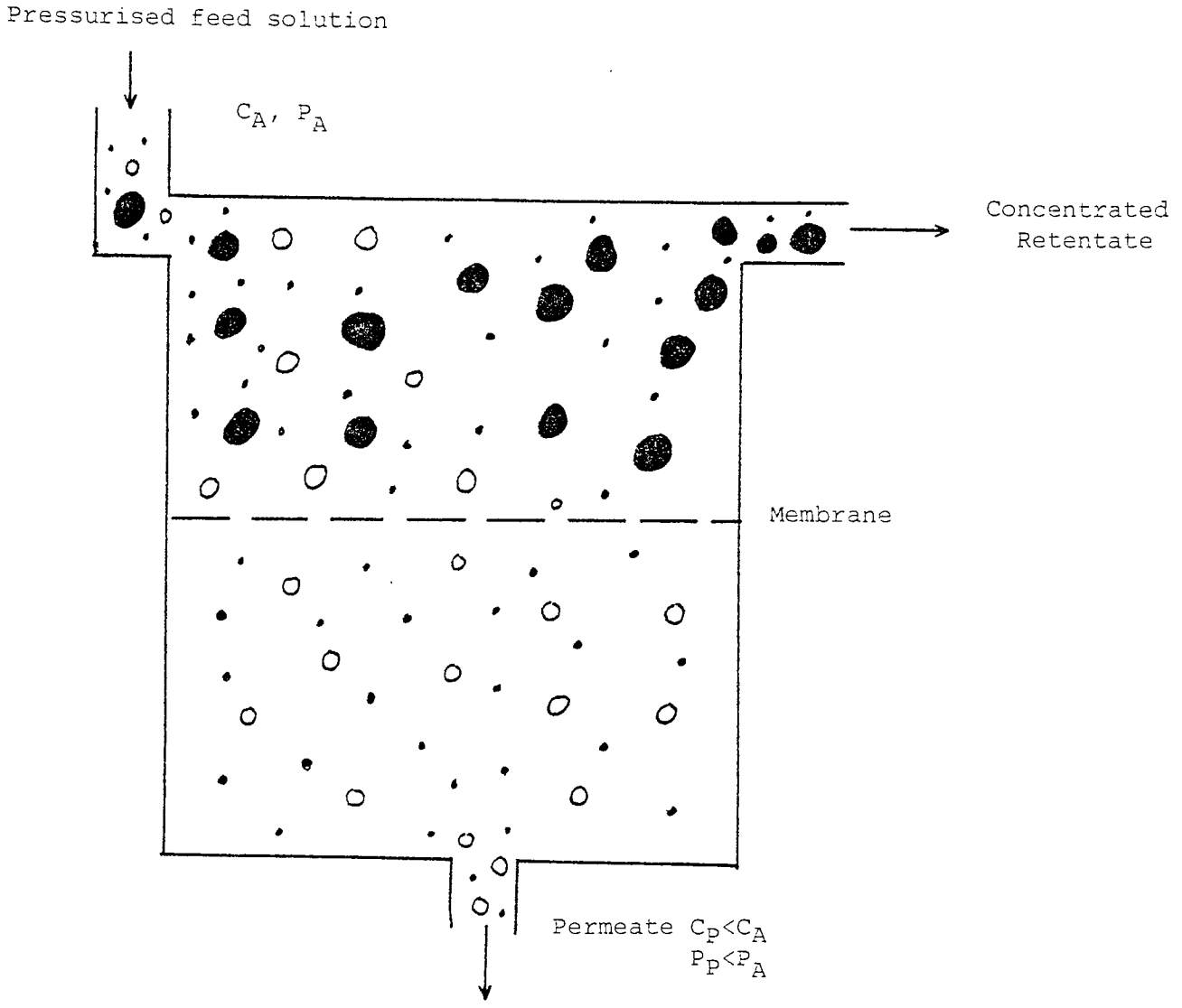

across the upstream face of the membrane is high relative to the permeate flux J_1, so that the concentration change in the upstream compartment is negligible. Under these conditions the flux, J_1, can be described by the basic relationship proposed by Kadem and Katchalsky (18).

$$J_1 = L_P \{ (P_A - P_P) - (\pi_A - \pi_P)\} = L_P (\Delta P - \Delta \pi) \quad \ldots\ldots\ 2.8$$

where π_A and π_P are the osmotic pressures corresponding to the solution concentrations C_A and C_P respectively, and L_P is the membrane permeability constant which is stable over a range of pressures and concentrations.

In most ultrafiltration processes a solution of large molecules is purified by the removal of low molecular-weight solutes. The membrane used usually retains only the large molecules, which have a negligible osmotic pressure, and allows the unrestricted passage of the small molecular solute. The concentration of small molecules on both sides of the membrane will then be equal, and the transmembrane osmotic pressure difference will be negligible compared to the applied pressure. Therefore, equation 2.8 approximates to:

$$J_1 = L_P \Delta P \quad \ldots\ldots\ 2.9$$

This simple model is based on theory initially derived for reverse osmosis (RO) membranes where the main flux transport is by diffusion.

In RO the surface of the membrane can be considered to be a dense polymer, whereas UF membranes have a surface containing pores of approximately 10-27 Å diameter (19). These pores can be assumed to be uniform, cylindrical and to pass straight through the membrane (20). The water flux can, therefore, be determined by the Hagen-Poiseuille equation for viscous flow through a cylindrical pipe:

$$J_1 = \frac{\varepsilon r^2 \Delta P}{8 \mu \Delta x} \quad \ldots\ldots\ 2.10$$

where J_1, is the volumetric water flux through the membrane, ε is the fraction of the membrane containing pores, r is the pore radius, ΔP is the pressure drop acros the membrane, μ is the fluid viscosity and Δx the membrane thickness. This assumption that the pores have a uniform diameter straight through the membrane only holds true for track-etched membranes. In reality the diameter of the membrane's pores tends to increase through the membrane (see later). Hence, in practice it would be necessary to apply a correction term to take into account the non-uniformity of the pores.

Another model to predict the water flux in UF membranes was proposed by Rautenback (21). This is based on the Carman-Kozeny equation and was developed for flow through a porous bed containing irregular pores, from equation 2.10:

$$J_1 = \frac{\varepsilon^2}{2K_C(1-\varepsilon)^2 F(V)^2} \times \frac{\varepsilon \Delta P}{\mu \Delta x} \qquad \ldots\ldots\ 2.11$$

where F(V) is the surface area per unit volume and K_C is the Carman factor.

Equation 2.11 should give a better estimate of the water flux (J_1) but it still contains a correction term (K).

The solute flux of the membrane is given by equation 2.1:

$$J_2 = J_1 (1 - R) C_B \qquad \ldots\ldots\ 2.1$$

These simple models indicate that, under ideal conditions, the solvent flux of the membrane is directly proportional to the applied pressure, and the solute flux is dependent upon the solvent flux.

2.2.3 NON-IDEAL SYSTEMS (CONCENTRATION POLARISATION)

2.2.3.1 INTRODUCTION

Although ultrafiltration is generally applied to the retention of macrosolutes that exert little osmotic effect, a phenomenon occurs which must be understood and

managed before any viable application can be made. This phenomenon is concentrated polarisation.

When a molecular mixture is brought to a membrane surface by a driving force, some molecules permeate the membrane while others are retained. This leads to an accumulation of the retained components, and to a depletion of the permeating components in the boundary layer adjacent to the membrane surface. This occurrence is known as concentration polarisation and is a consequence of all mass separation processes. However, its adverse effect is especially severe in membrane processes.

The solubility of these accumulated particles in the boundary layer at the membrane surface is frequently exceeded. This then causes the particles to precipitate and a solid gel layer is formed on the membrane surface. This gel layer often exhibits membrane properties itself and can reduce the flux through the membrane. Since the gel is acting as a secondary membrane the observed rejection characteristics of the UF membrane in the non-ideal situation will be different to that obtained in the ideal situation.

To try to understand the effect of the non-ideal situation many workers (43-49) have attempted to model either the concentration polarisation or the gel layer regimes. Many of these workers have based their work on two basic models. These models will now be described.

2.2.3.2 Film Model

Concentration polarisation effects can be described mathematically by the so-called film model which was originally developed for reverse osmosis by Sourirajan (22) and then applied to ultrafiltration (23, 24, 25). This model assumes that even in turbulent flow a laminar boundary layer is obtained next to the membrane surface. This boundary layer can be considered to be of thickness Y_b (see Figure 2.7).

Figure 2.7. Concentration Profile in the Boundary Layer for Well Developed Turbulent Flow

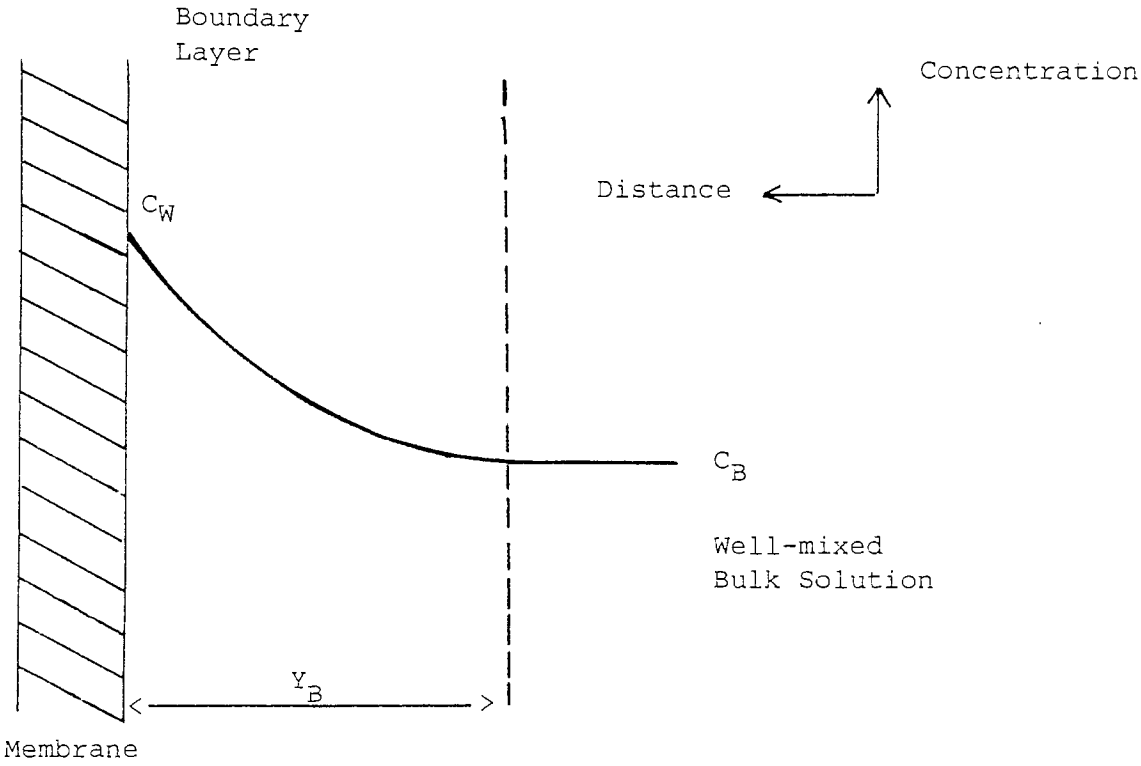

C_W: solute concentration at membrane wall.

During the filtration process a steady-state is reached where the convective transport of retained solute to the membrane wall, is counterbalanced by a diffusive flow of the rejected and accumulated material from the membrane surface back into the bulk solution. This back diffusion of the solute away from the membrane will be according to Fick's Law:

$$B = D \frac{dC}{dy} \qquad \text{..... 2.12}$$

where B is the back diffusion, D is the diffusivity of the species and (dC/dy) is the rate of change of the solute concentration.

The transport of retained solute is equal to the total convective transport of solute to the membrane wall minus the loss of solute in the permeate:

$$J_1 C - J_1 C_p \qquad \text{..... 2.13}$$

where J_1 is the solvent flux and C_P is the concentration of solute in the permeate. At steady-state:

$$J_1 (C - C_P) = -D \frac{dC}{dy} \qquad \text{..... 2.14}$$

Rearranging 2.14 and integrating over the boundary layer:

$$\frac{J_1 Y_b}{D} = \ln\left(\frac{C_w - C_P}{C_b - C_P}\right) \qquad \text{..... 2.15}$$

where the membrane rejects all or most of the solute, $C_P = 0$ and equation 2.15 becomes:

$$\emptyset = \frac{C_w}{C_b} = \exp\left(\frac{J_1 Y_b}{D}\right) = \exp\left(\frac{J_1}{K}\right) \qquad \text{..... 2.16}$$

where K is the overall mass transfer coefficient:

$$K = \frac{D}{Y_b} \qquad \ldots\ldots\ 2.17$$

The ratio C_w/C_b (Ø) is generally referred to as the concentration polarisation modulus.

If the solute is not totally rejected C_p can be related to the membrane rejection coefficient by equation 2.3. Combining 2.15 and 2.3 gives:

$$\frac{C_w}{C_b} = \frac{\exp\ (J_1/K)}{R + (1 - R) \exp\ (J_1/K)} \qquad \ldots\ldots\ 2.18$$

This equation only holds true under the condition that the diffusion coefficient is independent of the solute concentration, and that the boundary layer is constant over the entire membrane and is unaffected by the solvent flux (J_1). These assumptions can only be made approximately in dilute solutions,in the downstream region of turbulent flow (26).

According to equations 2.16 and 2.18 the concentration polarisation is mainly determined by the filtration rate, the diffusion coefficient of the solute, and the thickness of the boundary layer. The diffusion coefficient is usually determined by the solute and the solvent, and the filtration rate is normally as high as possible, therefore, the concentration polarisation can only be effectively controlled by the thickness of the boundary layer, which should be as thin as possible. This is normally achieved in practice by the creation of high turbulance near the membrane surface. This high turbulance is generated by vigorous stirring in batch type operations or by high feed flow velocities in a continuous flow-through system.

Since ultrafiltration membranes have high solvent fluxes and retain large macromolecules, of low diffusivities, this tends to cause a high concentration polarisation modulus at the membrane surface. This higher surface concentration places a limit on the flux attainable from a membrane system. A typical plot of

membrane flux versus transmembrane pressure is given in Figure 2.8. As the transmembrane pressure increases the flux initially increases. However, at a certain pressure the flux reaches a certain value and then becomes independent of the applied hydrostatic pressure.

The main explanation of these phenomena was first suggested by Michaels (24) and then developed by Blatt (25). This theory suggests that preceeding the pressure independent region any increases in the transmembrane pressure causes an increase in flux, but also causes an increase in the resistance of the concentration polarisation layer to solvent flux. Hence solutions of macromolecules do not follow the pure water flux line and the rate of increase of their flux decreases.

At the start of the pressure independent region the theory suggests that the concentration polarisation modulus is so high the solute precipitates out as a gel layer on the membrane surface. As this occurs equations 2.16 and 2.17 no longer hold true. Once the gel layer is formed, however, the concentration gradient between the membrane surface and the bulk solution reaches its maximum. At this point the back diffusion again equals the convective solute flow towards the membrane. The concentration profile for this system is given in Figure 2.9. The concentration of this gel layer is designated C_g and is constant.

When the hydrostatic pressure is increased this will cause more solute to be transported by convection to the membrane surface. However, since the concentration of the gel cannot be increased these additional solutes will then precipitate and thicken the gel layer. This in turn increases the hydraulic resistance of the gel membrane to such an extent that, in spite of the increase in hydrostatic pressure, the same filtration rate will be obtained.

As with the concentration polarisation case described above the gel layer phenomenon can be modelled by film theory. In this case equation 2.16 becomes:

Figure 2.8. Filtration Rate of Haemoglobin Solutions of Various Concentrations as a Function of the Applied Hydrostatic Pressure (26)

Figure 2.9. Gel Formation in Concentration Polarisation

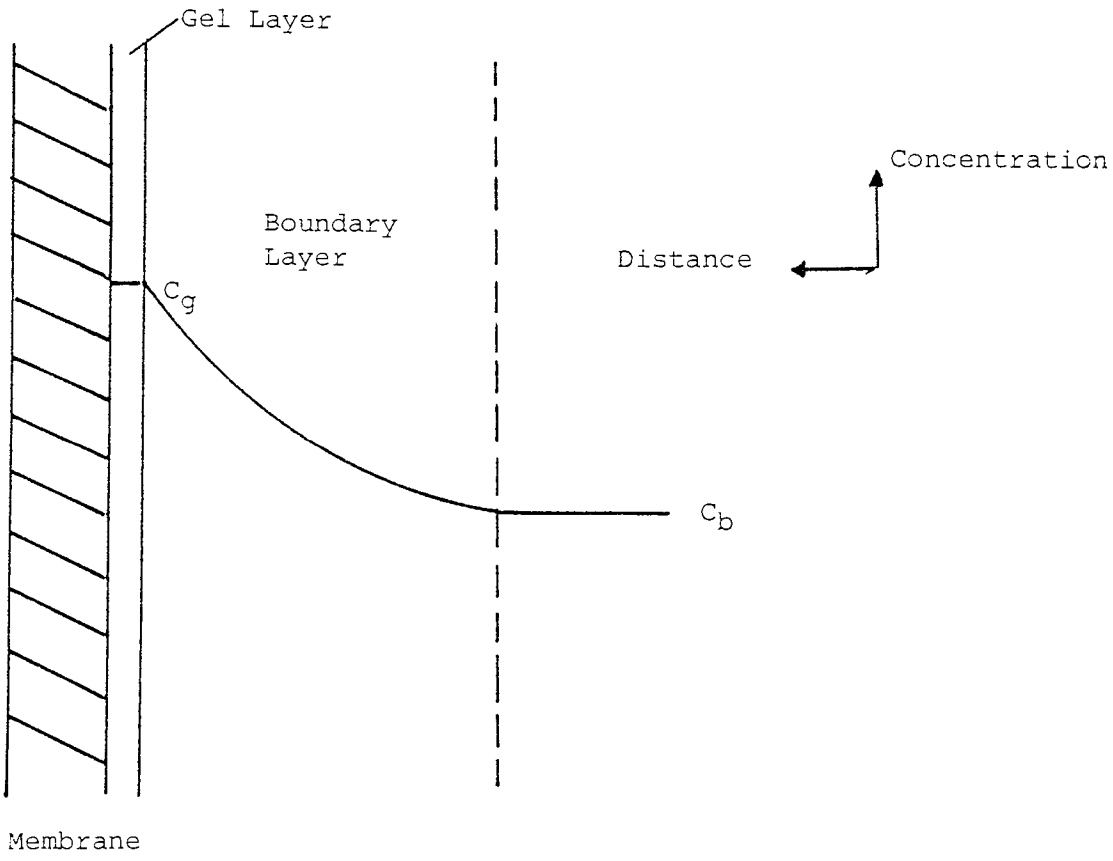

C_g: solute concentration at gel/solution interface (concentration of gel layer).

$$J_1 = K \ln \frac{C_g}{C_b} \quad \text{..... 2.19}$$

Equation 2.19 shows that, when the gel layer is formed, the filtration rate is only affected by the boundary layer thickness, which again is a function of the flow distribution. The value of C_g is usually found by a plot of J_1 versus ln C_b for data in the gel polarised region. When the resultant graph is extropolated to $J_1 = O$ the value of C_g can be found (see Figure 2.10).

The value of the mass transfer coefficient K can be found from mass transfer heat transfer analogies. Porter (27) found that for laminar flow the Graetz (28) or Lévêque (29) solutions for convective heat transfer, modified for mass transfer, gave good agreement between experimental and model results.

For turbulent flow Porter found that the Dittus and Boelter correlation gave the best comparison between experimental and the model.

2.2.3.3 OSMOTIC PRESSURE MODEL

One of the major assumptions of the above concentration/gel polarisation model is that the osmotic pressures of macromolecular solutions are always negligible. Goldsmith (30) pointed out that this assumption is not really correct, and it has long been known to specialists of macromolecular physical chemistry that concentrated solutions of macromolecules have quite appreciable osmotic pressures (31, 32). In the high concentrations found in the ultrafiltration polarisation layer the osmotic presure can be of the same order of magnitude as the applied pressure generally used in ultrafiltration.

The proponents of the osmotic pressure model believe that it is an increase in the osmotic pressure of the macromolecules, which causes the rate of increase of the membrane flux to decrease, as the transmembrane pressure is increased (Figure 2.8).

Figure 2.10 Plot of Permeate Flux Versus Bulk Concentration at Varying Recirculation Rates (27)

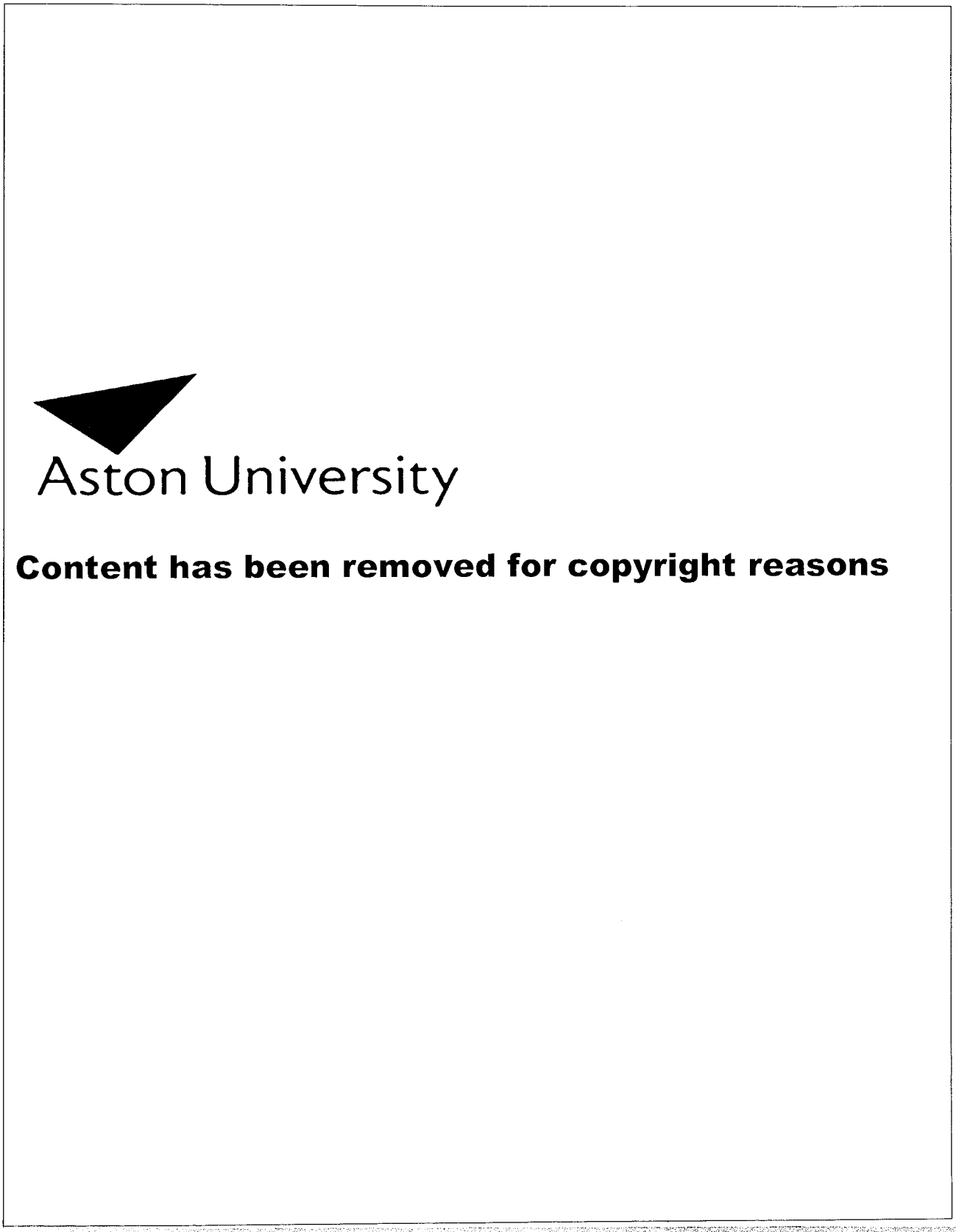

The pressure independent flux region occurs when an increase in transmembrane pressure causes a corresponding equal increase in osmotic pressure. Thus the effective increase in pressure is zero.

In the absence of any membrane fouling, the only effect which operates to reduce the membrane permeation rate is the osmotic pressure of the solution in contact with the membrane. Therefore, the basic equation describing the permeate flux is:

$$J_1 = L_P (\Delta P - \Delta \pi) \quad \text{..... 2.8}$$

where $\Delta \pi$ is the osmotic pressure difference between the macromolecules at the membrane wall and the solute in the permeate. The variation of osmotic pressure with concentration is given by the relationship (33):

$$\pi (c) = (RT/\bar{M}_n) (C + \Gamma_2 C^2 + \Gamma_3 C^3) \quad \text{..... 2.20}$$

where the first term in this expression corresponds to the van't Hoff Law, Γ_2 and Γ_3 are virial coefficients.

This basic model has been used with some alteration by workers such as Wales (34) and Clifton (35) to show that in the pressure dependent region the flux is dependent upon the osmotic pressure. However, Wijmans (36) has shown that for the pressure dependent region, both this model and the forementioned film model both appear to predict the obtained experimental results, and that these two approaches are essentially equivalent.

2.2.3.4 EFFECT OF NON-IDEALITY ON REJECTION

When concentration polarisation occurs the increased solute concentration at the membrane wall results in the rejection coefficient being lower than expected when based on the bulk solute concentration. By using the Colton (37) polarisation correction Nguyen (38) and Capanelli (39) were able to relate the observed rejection to the true rejection.

$$\text{Observed rejection} = R_o = 1 - \frac{C_P}{C_b} \qquad \text{..... 2.3}$$

$$\text{True rejection} = R = 1 - \frac{C_P}{C_w} \qquad \text{..... 2.21}$$

where C_w is the membrane wall concentration.

When steady-state is achieved the convective solute transport to the membrane equals the back diffusion of the solute plus the convective transport of solute into the permeate (see Section 2.2.3.2). This gives a relationship between C_b and C_w and, therefore, a correlation between true and observed rejection:

$$R = R_o \exp\left(\frac{J_v}{K_m}\right) \Big/ ((1 - R_o) + R_o \exp\,(J_v/K_m)) \qquad \text{..... 2.22}$$

where J_v is the total volume of flux and K_m is the mass transfer coefficient of the solute.

Another model to describe the effect of polarisation on rejection uses a sieving coefficient (Ø), which was defined by Goldsmith (30) as:

$$Ø = \frac{C_P}{C_w} \qquad \text{..... 2.23}$$

where Ø is a function of pore and molecular dimensions only, ie. the size (radius) of the macromolecules in solution and the size (radius) of the membrane pores, which are assumed to be cylindrical.

Again, at steady state, equations 2.3, 2.15 and 2.23 can be combined to give:

$$\frac{1 - R}{R} = \frac{Ø}{1 - Ø} \exp\,(J/K) \qquad \text{..... 2.24}$$

This model was proposed for dilute solutions and a fixed sieving factor, where a fixed proportion of the solute presented to the membrane wall will pass through. Therefore, with increased polarisation the rejection will decrease. This is because C_P must increase as C_w increases to keep Ø constant. This also shows that for dilute solutions, as the pressure increases, the rejection decreases (Figure 2.11). This is due to the increased pressure increasing the concentration polarization as above.

When concentrated solutions are considered the above equations do not apply and the forementioned flux/pressure-rejection phenomenon does not occur. With high concentrations the concentration polarisation tends to form a secondary membrane. This is especially true if a gel layer is formed. This secondary membrane is often more retentive than the primary membrane and, therefore, the rejection coefficients tend to increase as the concentration polarisation and pressure increases.

Recently Nakao (40, 41) proposed a model to take into account the effect of the formation of a gel layer. This model assumes the gel layer acts as a membrane in series with the ultrafiltration membrane. Therefore, the gel is considered to have a specific pore size, solute permeability (P_g), and a rejection coefficient (σ_g).

For this analysis, transport equations for water and solute flow through two different membranes in series are necessary, and have been developed by Jagur-Grodzinski and Keden (42). The real rejection of these series is given by:

$$R = \frac{(1 - F_g)(1 - \sigma_M) + F_g(1 - \sigma_g)(1 - F_M \sigma_M) - (1 - \sigma_g)(1 - \sigma_M)}{(1 - F_g)(1 - \sigma_M) + F_g (1 - \sigma_g)(1 - F_M \sigma_M)} \quad \text{..... 2.25}$$

In the case of a membrane with a gel layer, suffix g corresponds to the gel layer and M corresponds to the membrane.

Aston University

Content has been removed for copyright reasons

Figure 2.11. Plot of Rejection Against Hydrostatic Operating Pressures for Varying Molecular Weight Dextrans (74).

$$F_g = \exp\left\{ - \frac{J_v (1 - \sigma_g)}{P_g} \right\} \qquad \ldots\ldots\ 2.26$$

$$F_M = \exp\left\{ - \frac{J_v (1 - \sigma_M)}{P_M} \right\} \qquad \ldots\ldots\ 2.27$$

When Nakao used a steric-hinderance pore model to determine the parameters σ and P he found good agreement between theory and experimental. However, before this agreement was obtained Nakao had to incorporate a correction factor to take into account the compressibility of the gel layer. The chief drawbacks of this model are its complexity and the considerable amounts of experimental data required to evaluate some of the parameters used in the model.

As well as the effect of concentration polarisation and gel layer formation on the rejection of a solute, adsorption of the solute on to the membrane also has a significant effect. However, this occurrence is very specific to the membrane and solute under consideration and no generally applicable theories exist.

2.3 MEMBRANE CONSTRUCTION AND ITS EFFECT ON THE MEMBRANE'S PERFORMANCE

2.3.1 INTRODUCTION

Ultrafiltration membranes can be made from any polymeric material. The actual material used, and the manner in which a membrane is formed, can give a range of final performance characteristics. A membrane's performance depends substantially on the following factors: membrane properties, solution properties, polarisation and fouling phenomena.

The membrane properties depend on the chemical nature of the base polymer of the membrane, and also on its morphological structure , ie. the thickness and

porosity (size, number and distribution of the pores) of the skin layer and on the structure of the porous sublayer. The morphological structure of a membrane is greatly related to its preparation conditions.

Transport through the pores of a membrane can be affected by interfacial forces at the membrane-solution interface, as well as interactions between the solute and the membrane (72, 73). The interactions concern attractive forces such as van der Waal's forces or the formation of chemical bonds (50). These membrane-solution interactions are dependent upon the polymer material used in the membrane construction.

The membrane performance quoted by most manufacturers is derived from the pure water flux and usually the rejection coefficient obtained after tests with pure, spherical proteins of specific molecular weights. However, this quoted performance data gives no indication of the effect of the pore distribution or solute adsorption. Therefore, significant efforts have recently been made to determine these membrane characteristics (51).

2.3.2 MEMBRANE MANUFACTURE

Membranes with a variety of physical structures can be used for ultrafiltration, but the most common type is the asymmetric membrane. This membrane is highly porous but has larger pores at one surface than the other, with the finely porous surface exposed to the liquid to be filtered. As these fine pores pass through the membrane their diameter increases. The finely porous surface is usually an ultra-thin layer supported by the main porous bulk of the membrane (Figure 2.12). Asymmetric membranes are produced by a process called phase-inversion.

The two other main types of membranes are composite membranes and track-etched membranes. Composite membranes are similar to asymmetric membranes but the fine pore layer and the support layer are made from two different materials, and in two different stages.

Figure 2.12: Schematic Diagram of Asymetric Membrane

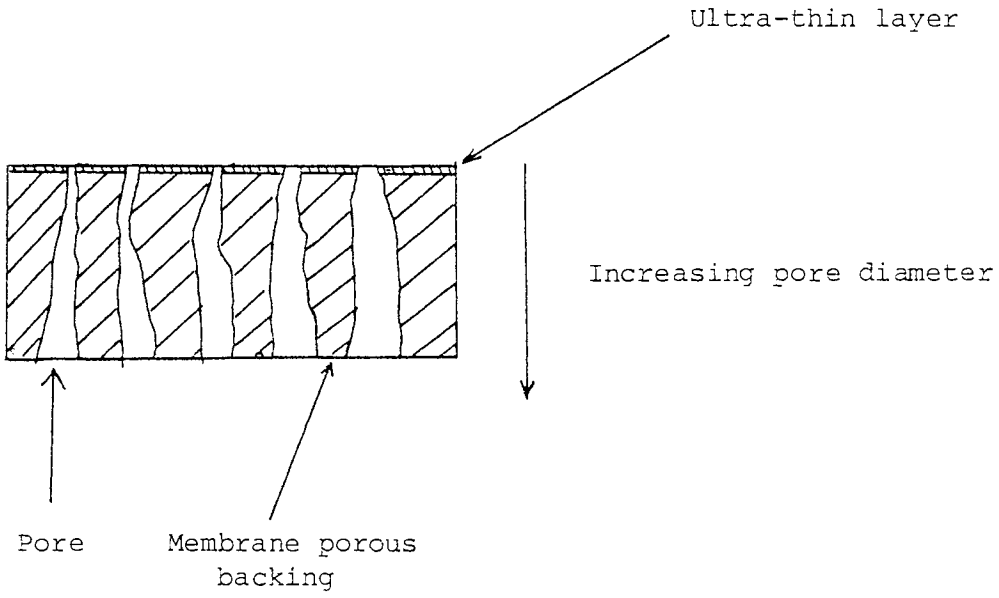

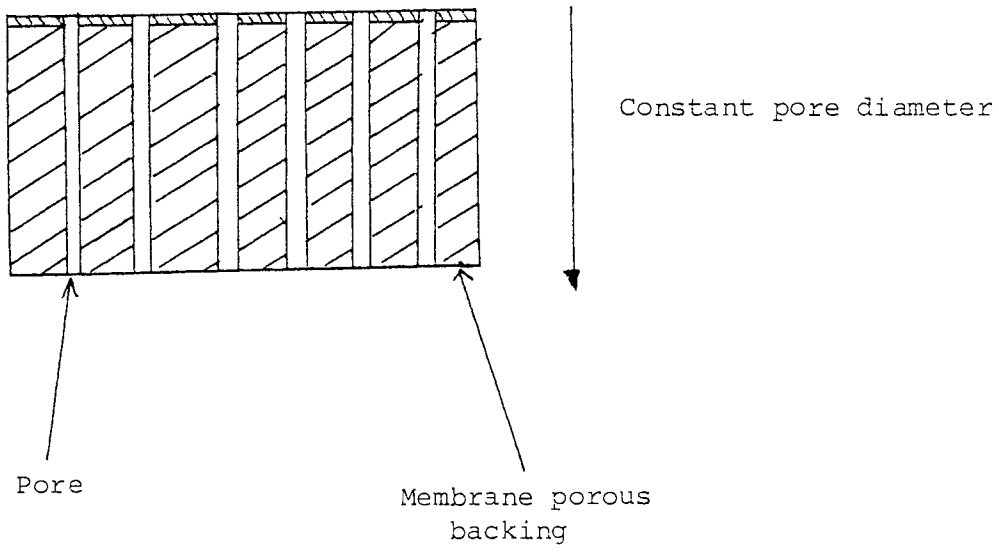

Figure 2.12(a): Schematic Diagram of Track-etched Membrane

Track etched membranes have little or no asymmetry in their structure and their pores can be considered to be uniform, straight through, and cylindrical. These membranes are made from thin polymeric films, which are typically about 10% of the thickness of phase inversion membranes. Nuclepore membranes are made by irradiating the membrane film in a field of α particles and then chemically etching the film to produce the pores.

2.3.3 MEMBRANE SURFACE CHARACTERISTICS

2.3.3.1 PORE SIZE AND PORE SIZE DISTRIBUTION

It is a widely accepted concept (39, 50-57), that the distribution in membrane pore sizes and the adsorption of solute polymer molecules on the membrane surface (see later), govern the transport of solute and solvent in ultrafiltration membranes. In an ideal membrane all the pore sizes would be equal. In reality, however, in any membrane surface there will be a proportion of pores which are: (a) too small to allow passage of the solute but will allow passage of solvent; (b) small enough to allow passage of small solute molecules and solvent; and (c) large pores which will allow passage of any solute and solvent. If the proportion of small pores is high the membrane will have very good rejection characteristics but a small solvent flux. This is because the small pores can become blocked by solute. The intermediate size pore would give a membrane with a good rejection characteristic and good solvent flux. In this case not many pores would become blocked. The large pore size would give a membrane with a bad rejection characteristic but very good solvent flux. Hence, any narrowing in the distribution of pore sizes in a membrane could make its performance better and more practicable.

The determination of pore size distributions in membranes can be traced back to the experiments of Bechhold (52) in 1908 for obtaining the average pore size and pore size distribution of acetic collodion membranes. The use of the rejection coefficients of macromolecules to measure pore diameter was first considered by Ferry

(53). The relationships between the sieving coefficient (rejection coefficient) and the hydrodynamic diameter of solutes were then investigated by Du Bois (54). Green (58) further developed the above theories and reported that the sieving coefficients of two membranes used in his experiment exhibited straight line correlations to the Stokes Law radius of solute molecules on normal probability co-ordinates. This led to the hypothesis that the pore sizes in the membranes were normally distributed. Michaels (59), however, showed that a log-normal distribution function correlated the data equally well. Using this method Schwarz (55) found that for increasing pressure, the standard deviation of the pore distribution also increased. This suggests the pores in the membrane were deformed.

Bodzek (56) used this sieving coefficient method to determine the effect of the manufacture of membranes on their pore size characteristics. He found that increasing the polymer concentration in the casting solution increased the membrane skin thickness and decreased the mean pore radius of the membrane. This resulted in a decrease in the pure water permeability and an increased macrosolute rejection. These results, however, were only qualitative and the prediction of the ultrafiltration membrane performance, under a given set of operating conditions was not feasible.

Work carried out by Chan (50, 60) on the development of a surface force-pore flow model has resulted in a method of predicting the performance of a given membrane. This model enables one to calculate solute separation from the data on the size of the solute molecule (such as that represented by Stokes Law radius), the average pore size and the pore size distribution. This model also takes into account the interaction force working between the membrane polymer surface and the solute.

Experiments conducted by Fane (57) showed that the surface area of the pores, which is available for solvent flow, is less than 1% of the total surface area of the membrane. Similar findings were also reported by Green (58), and, therefore, these observations challenge the assumption that the membrane surface is homogeneously permeable.

Several workers (39, 61, 62, 67, 68) have proposed that the capillary flow of solvent through the pores of a membrane can be modelled using the Hagen-Poiseuille equation:

$$J_1 = N \pi d_P^4 \Delta P/(128 \mu L) \quad \text{..... 2.28}$$

$$= S d_P^2 \Delta P/(32 \mu L) \quad \text{..... 2.29}$$

where d_P is the capillary diameter, L the capillary length, N the number of capillaries per unit area and S is the (fractional) surface porosity.

This model has been shown by these workers to calculate water fluxes in reasonable agreement with those quoted in the literature. However, the above equations use the mean pore diameter, and Fane (57) modified equation 2.28 to allow for the known distribution of pore sizes:

$$J_1 = \sum_{d_P\ min}^{d_P\ max} N f_i \pi d_{Pi}^4 \Delta P/(128 \mu L) \quad \text{..... 2.30}$$

where f_i is the fraction of pores of characteristic diameter, d_{Pi}. He then proposed that the fraction, q_i, of the total water flow passing through pores of diameter d_{Pi}, may be estimated by:

$$q_i = f_i d_{Pi}^4 / \sum_{d_P\ min}^{d_P\ max} f_i d_{Pi}^4 \quad \text{..... 2.31}$$

Fane then used equation 2.31 to calculate the flow passing through specific pore diameters. Figure 2.13 gives the flow distribution, calculated by Fane, for two membranes. This clearly shows the significant contribution of the large pores and in these cases50% of the solvent flow passes through only 20-25% of the pores of the membranes.

Figure 2.13 Effect of Large Membrane Pores on Membrane Flux (57)

Aston University

Content has been removed for copyright reasons

Since the solvent flux passes through only a small portion of the membrane pores, this will cause a localised concentration polarisation. The main theory for this phenomenon, described in Section 2.2.3, assumes a homogeneously permeable membrane, which is clearly not the case. Therefore, Fane proposed a correction factor for the main model for this phenomenon:

$$J = x_e\ k\ \ln\left(\frac{C_g}{C_b}\right) \qquad \text{..... 2.19a}$$

where x_e is the correction factor and is described as the effective free area of the membrane. Using this theory Fane showed that a thin polarised layer is sensitive to the surface properties of the membrane. This thin layer occurs at high stirring speeds or high recirculation rates, and both operating parameters are exploited in well designed membrane equipment.

2.3.3.2 ADSORPTION EFFECTS

In the majority of the work already mentioned the solute rejection is assumed to be governed almost totally by a sieving mechanism. This assumption ignores the interaction force between a solute macromolecule and the membrane material (69-71). However, work done by Michaels (24) on the comparison of sieving curves for ionically charged dextran , with those for neutral dextran showed that this assu mption is not always valid. He showed that negatively charged macromolecules were sieved more effectively, while positively charged ones less effectively, than neutral macromolecules. This result is consistent with the existence of negative charges on the membrane surface.

This interaction between the membrane and the solute is very specific to the two materials being considered, but it is well documented (63, 64) that water soluble macromolecules adsorb readily on polymeric ultrafiltration membranes. In spite of this recorded phenomenon relatively little work has been done on the effect of this adsorbed material on the membranes' rejection performance.

Initially workers, such as Rowland and Eirich (65), measured the thickness of macromolecular layers adsorbed in pores. They found a linear correlation between the adsorbed thickness, $[\Delta r_3]$, and the intrinsic viscosity, $[\eta]$, of the solute. This indicated a dominating effect of polymer conformation in solution on the adsorbed layer. The relative thickness of the adsorbed layer in the pore can be obtained from water flux measurements. For cylindrical pores and laminar flow, Poiseuille equation gives:

$$\frac{\Delta r_3}{r_3} = 1 - \left(\frac{J_{w,2}}{J_{w,1}} \right)^{0.25} \qquad \text{..... 2.32}$$

where r_3 is the membrane capillary radius, $J_{w,1}$ is the water flux prior to solute adsorption, and $J_{w,2}$ is a water flux after adsorption.

Using this thickness of adsorbed solute, Δr_3, workers such as Zeman (66) have predicted the change in rejection of the membrane. The basic equation describing the normal steric rejection of a non-adsorbing sphere was first derived by Ferry (53).

$$R = 1 - \frac{C_P}{\overline{C_r}} = [\lambda (\lambda - 2)]^2, \ \lambda \leq 1 \qquad \text{..... 2.33}$$

where $\lambda = r_2/r_3$ and r_2 is the solute radius.

Zeman stated this equation is still applicable if a λ value reflecting the changes in the pore dimensions due to adsorption is used. For the simplest case of adsorbing rigid spheres:

$$\lambda = \frac{r_2}{r_3 - 2 r_2} \qquad \text{..... 2.34}$$

For random coils

$$\lambda = \frac{r_2}{r_3 - K[\eta]_2} \qquad \ldots\ldots\ldots 2.35$$

where $[\eta]_2$ is the intrinsic viscosity of the solute and K is a proportionality constant. In this latter case Zeman assumed that a random coil behaves like a sphere with a diameter proportional to $[\eta]_2$.

Using the above correction factors Zeman was able to obtain reasonable agreement between predicted rejection coefficients and experimentally obtained coefficients. These results showed the adsorbed layer had a significant effect on the membranes' performance. He concluded that the "cut-off" values of membranes depend on the physiochemical properties of both membrane and solute. It is, therefore, possible for a solute to adsorb on to one membrane and not another. Also, hydrophobic solutes should give higher rejection coefficients than hydrophilic solutes of the same size, with the same membrane. This is because increased hydrophobicity of the solute leads to an increased entropy gain due to hydrophobic dehydration on adsorption. This results in stronger attractive forces between the membrane and solute.

2.4 ULTRAFILTRATION OF DEXTRAN

2.4.1 EXPERIMENTAL WORK

Since dextran is cheap, easily soluble in water and available in a range of molecular weights it has been used extensively in research work involved with the ultrafiltration of polymers, and in the characterization of membranes (80). In the late 1960s Baker (74, 75) used dextran to test the new 'sharper' cut-off membranes available at that time. He showed that the new membranes could be used to fractionate polymers and also that the rejection characteristics of the membranes were strongly

dependent upon the operating pressure (Figure 2.11). He also showed that in ultrafiltration experiments dextran molecules have the same retention as proteins one-tenth their molecular weight. Baker postulated that this phenomenon was due to the high shear forces present in ultrafiltration. These forces could deform large diameter dextran molecules and allow them to pass through small diameter pores (see later).

In his experiments Baker calculated the molecular weights of his samples from the intrinsic viscosity. Hence, if he had a product of low viscosity he assumed it only contained low molecular weight material. However, the sample could contain high molecular weight material as well as low, and the intrinsic viscosity would only measure the average molecular weight. Therefore, this technique could not be used to characterise the actual rejection performance of a membrane at specific molecular weights of dextran. This problem was solved to a certain degree in the work of Edberg (76) where he calculated the weight average ($\bar{M}_W$) and number average ($\bar{M}_N$) molecular weights of his samples by the sedimentation equilibrium method of van Holde and Baldwin. From the ratio of these two average molecular weights he was able to find the range of the molecular weight distributions in his samples. Using a number of membranes in series Edberg was able to fractionate a dextran feed into several products of different weight average molecular weights and narrow range distributions.

This problem of measuring actual molecular weights of dextran instead of averages was solved with the advent of gel permeation chromatography (GPC) as an analytical tool (see later). Using GPC Cooper (77) was able to characterise membranes using dextrans of several molecular weight distributions (T fractions). He found that if the rejection coefficient versus molecular weights are plotted on log probability paper linear relationships were observed. This plot then allowed the rejection (R) molecular weight (MW) relationship to be defined by two parameters; (a) the mean value of log MW at P = 0.5, and (b) the standard deviation, which is one-half the value of the difference in log MW at R = 0.84 and 0.16.

From his results Cooper found that most membranes had a rejection coefficient of approximately 70% for a dextran molecule with a molecular weight equal to the quoted cut-off of the membrane, ie. a 10 000 cut-off membrane rejects 70% of 10 000 molecular weight dextran. Cooper also found that the Rejection-Molecular Weight (R-MW) relationship was not independent of the molecular weight distribution of the polymer probe, ie. the polymer used to characterise the membrane's rejection performance. Using a 10 000 cut-off membrane he found the R-MW relationship with two different distributions. The first distribution had a weight average molecular weight ($\overline{M}_W$) of 10 000 and gave a rejection coefficient of 85% for 10 000 molecular weight dextran molecules. The second probe had a $\overline{M}_W$ of 40 000 and gave a R of 70% for a 10 000 MW dextran molecule. When the two probes were mixed they behaved like the first (see Figure 2.14). The R-MW data obtained by Cooper indicated that the membranes had very 'diffuse' cut-offs with dextran. Similar results were obtained by Nguyen (78) with polyethylene glycol (PEG) and as with Baker these diffuse cut-offs were assumed to be due to the 'deformability' of the dextran and PEG molecules.

The effect of operating conditions on the ultrafiltration of dextran solutions was investigated by Bottino (79). He found that the flux of a membrane with dextran not only depends upon the normal operating parameters, such as pressure, recirculation rate and concentration, but also on the weight average molecular weight of the dextran in the sample (Figure 2.15). Dextrans of low $\overline{M}_W$ gave higher fluxes than dextrans with a high $\overline{M}_W$, at the same concentration. He also found that lowering the $\overline{M}_W$ value also reduced the dependency of the flux on the recirculation rate. To determine the effect of low $\overline{M}_W$ material on the rejection characteristics of a high $\overline{M}_W$ material Bottino mixed a sample of PEG of 35 000 $\overline{M}_W$ with a sample of 3 000 $\overline{M}_W$. He found that even in small quantities the low MW material increased the rejection coefficients of the mixture above that of the pure 35 000 $\overline{M}_W$ material. This result is

Figure 2.14 Effect of Molecular Weight and its Distribution on the Determination of Rejection - Molecular Weight Relationships (77)

Figure 2.15 Influence of Recirculation Rate on Membrane Flux for Varying Weight Average Molecular Weights of Dextran (79)

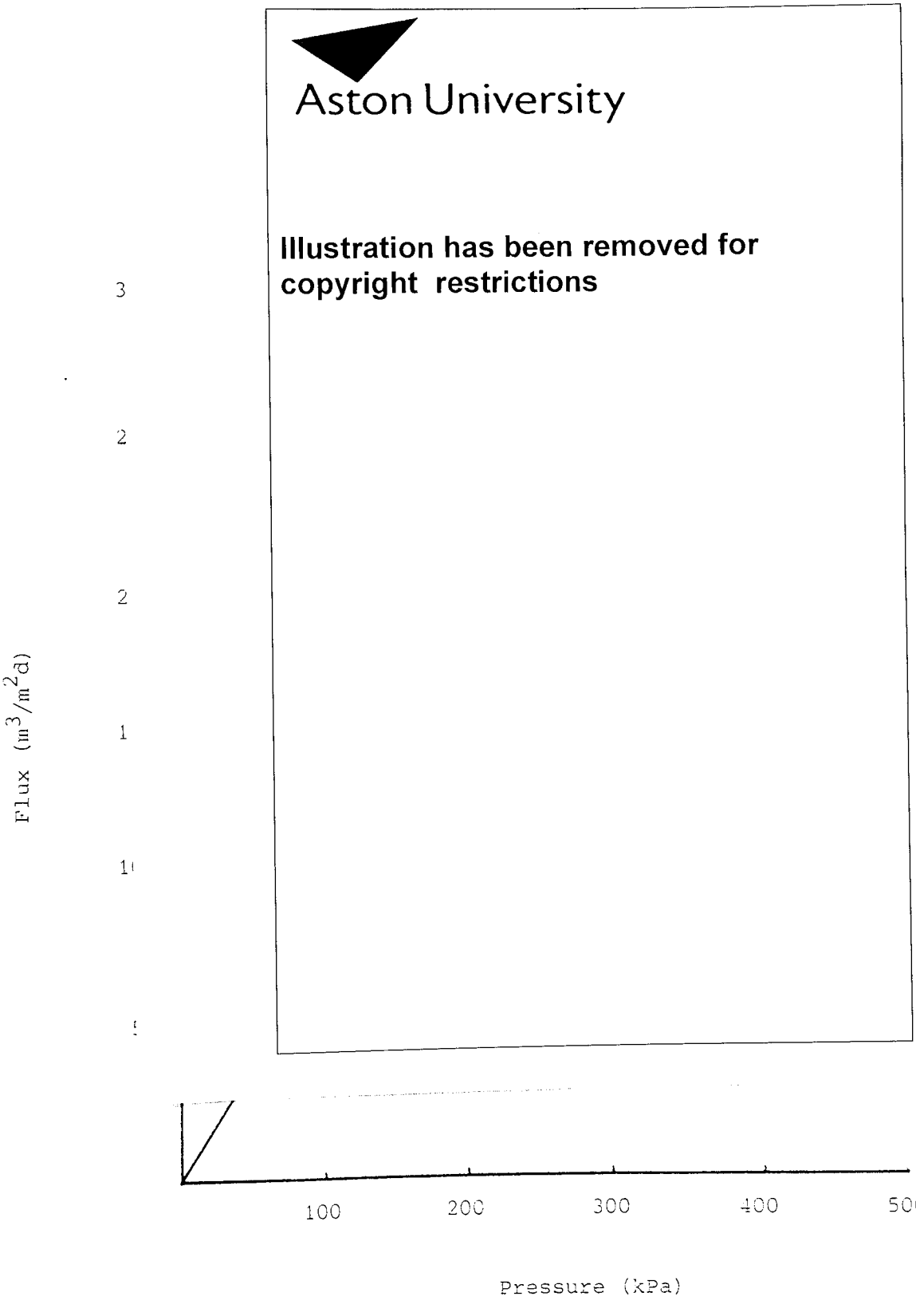

similar to that obtained by Cooper.

All the work mentioned above is concerned with either using dextran to characterise membranes or showing that membranes can be used to separate dextran in to products of differing $\overline{M}_W$. However, work done by Barker and Vlachogiannis (12, 14) has proved that ultrafiltration can be used to fractionate dextran on a commercial basis. This work was concerned with removing dextran of 12 000 molecular weight and less, from an industrial hydrolysate with a wide molecular weight range. This material had to be removed with little or no loss of material above 12 000 molecular weight. This was accomplished by using a membrane of 5 000 molecular weight cut-off with an efficiency comparable to that presently obtained with ethanol fractionation. A 5 000 MW cut-off membrane was used due to the 'diffuse' cut-off performance experienced by membranes with dextran, ie. molecules of 70 000+ MW will readily pass through the 5 000 MW cut-off membrane. Barker and Vlachogiannis also showed that dextran solutions could be easily concentrated from low concentrations (1%) up to high concentrations (20%) by use of either a 5 000 or 2 000 MW cut-off membrane. During this concentration it was shown that additional fractionation of the dextran hydrolysate took place. Even though some fractionation took place during the concentration mode of operation this was insufficient to provide a product within the required specification. Barker and Vlachogiannis also showed that diafiltration was the ideal operating mode for fractionating dextran hydrolysate below 12 000 molecular weight.

2.4.2 MATHEMATICAL MODELLING OF DEXTRAN PERFORMANCE WITH MEMBRANES

2.4.2.1 FLEXIBLE MOLECULE MODEL

In most of the work cited above, the workers hypothesised that the 'diffuse' cut-off performance of dextran was a result of the high shear forces involved in ultrafiltration. These high forces are present in an attempt to control concentration polarisation, but can also cause dextran molecules to deform so that large diameter molecules can pass through membrane pores of smaller diameter.

This deformation occurs when the retentate flow is fast enough to set up a high longitudinal gradient at the pore entrance, and the macromolecule is then stretched in the flow direction to such a point that it arrives at the pore entrance with a transversal section smaller than the pore entrance. At this point the macromolecule is carried through the pore by the solvent flux.

Investigations undertaken by several workers (81-84) has shown that a soluble macromolecule exposed to a shear flow can be distorted but the Brownian fluctuations in the chain configuration tends to produce a relaxation of the distortion. De Gennes (81) showed that there is a critical value of the shear rate (S_c) and the distortion will decay if the system shear rate is less than this critical value. If the shear rate is higher than S_c, the stretching force is greater than the restoring (Brownian) force and the polymer chain becomes strongly stretched. In the latter case the chain follows perfectly the deformation imposed by the solvent flow and the molecule is deformed in the same way as a fluid element. This type of deformation is called affine (84).

The critical value, S_c is of the same order as the relaxation frequency of the soluble polymer. In a dilute solution the relaxation frequency of a macromolecule is the Zimm relaxation frequency of the polymer chain (84). Therefore, S_c is given by:

$$S_c \simeq r_z^{-1} \simeq \frac{k_B \quad T}{\eta_0 \; R_F^3} \qquad \ldots\ldots\ldots 2.36$$

where r_z is the Zimm relaxation time, η_0 is the viscosity of the solvent, R_F is the Flory radius of gyration of a dissolved molecule, T is the Kelvin temperature and k_B is the Boltzmann constant.

In semi-dilute solutions polymer coils tend to overlap and in this region the relaxation frequency is the characteristic time for the reorganization of this transient network and defined as the reptation time (r_R). Therefore:

$$S_c \simeq r_R^{-1} \quad \text{..... 2.37}$$

The reptation time is linked to the Zimm relaxation time, r_z, and the concentration by the relationship:

$$r_R \simeq r_z (C/C^*)^{3/2} \quad \text{..... 2.38}$$

$$C^* \simeq N/R_F^3 \quad \text{..... 2.39}$$

where N is the number of monomer units in a macromolecule.

To drive a deformed macromolecule, with a solvent flow, in to a pore, Daoudi (83) has established that the elongational shear should attain the critical threshold S_c at a minimal distance from the pore opening. This distance is of the order of the characteristic dimension of the dissolved macromolecule. This condition is necessary to obtain the transversal dimension of the deformed chains equal to that of the pores. For a dilute solution the characteristic dimension is the radius of gyration (R_F). For a semi-dilute solution the characteristic dimension is the correlation length $\zeta \simeq R_F (C^*/C)^{3/4}$,(78).

The shear rate near the membrane wall is dependent upon the solvent flux, and, therefore, there will be a critical flux (J*) at which the critical shear rate, S_c, is obtained. Using the above theory Nguyen (85) found J* to be given by the following equation for a dilute solute:

$$J^* \gtrsim k_B T \varepsilon / \eta_o R_o^2 \quad \text{..... 2.40}$$

For semi-dilute solutions:

$$J^* \gtrsim \frac{k_B T \varepsilon}{\eta_o R_o^2} \left(\frac{C^*}{C}\right)^{15/4} \quad \text{..... 2.41}$$

where ε is the surface porosity of the membrane skin and R_o is the radius of the pore opening.

From these equations it can be seen that the value of the critical flux depends on the membrane skin parameters as well as the macromolecule parameters. For the dilute regime the critical flux is independent of the concentration but in the semi-dilute regime it decreases rapidly with the concentration (as $C^{-15/4}$). This behaviour is explained by the difference in the physical state of the macromolecules in the two regimes. In dilute solution the relaxation of the independent molecules is rapid and of the same frequency. In the semi-dilute regime the polymer coils become more entangled with increased concentration and the thermic motion of their segments is retarded. The steady shear required for their deformation is consequently lowered.

Since the critical flux is dependent upon concentration only in the semi-dilute region, this therefore suggests that there will be a critical concentration at the transition point from the dilute to the semi-dilute regime. This was confirmed by Nguyen (85) when he conducted ultrafiltration experiments with macromolecules at varying concentrations. For low concentrations the rejection coefficient of the macromolecules remained constant. At this point the critical flux was higher than the actual flux and no deformation of macromolecules occurred. As the concentration was increased the rejection remained constant until the critical concentration was reached, at this point the rejection dropped sharply. After the critical concentration point the critical flux dropped according to $C^{-15/4}$ and was consequently lower than the actual flux. At this point the macromolecules deformed, passed through the membrane and lowered the rejection coefficient.

2.4.2.2 HARD SPHERE MODEL

The idea that a membrane rejects or passes a molecule by means of a sieving action was based on the original assumption by Ferry (53) that the molecule could be considered a hard sphere. With this assumption the rejection of the molecule by a membrane pore can be given by.

$$R = (\lambda (\lambda - 2))^2 \qquad \text{..... 2.42}$$

However, in the enclosed space of a pore the terminal velocity of a sphere, with respect to a moving liquid, is not the same as in free space. This gives rise to 'hydrodynamic lag' so that the velocity of the sphere with respect to a wall is not the same as that of the liquid. The viscous drag force on a solute sphere that reflects the proximity of a wall can be written as (86):

$$F = - 6\pi \mu a (K_1 U - K_2 V) \qquad \text{..... 2.43}$$

where a is the radius of the sphere, U is the velocity of the solute, V is the velocity of the solvent, μ is the viscosity of the solution and K_1 and K_2 are the drag coefficients. At steady state:

$$U/V = K_2/K_1$$

and the hinderance to convection is (87):

$$W = 1 - R = \frac{K_2}{K_1} (1 - (\lambda (\lambda - 2))^2) \qquad \text{..... 2.45}$$

The values of K_1 and K_2 have been calculated by Paine (88) who showed that this was a good approximation for the calculation of the hydrodynamic lag.

Equation 2.45 was used by Zeman (87) to predict the rejection coefficients of dextran samples found by experimentation. Zeman found close agreement between the equation and experiments for low values of λ but at high λ values there was a discrepancy. In his theoretical calculations Zeman used Stokes radius as the radius of the dextran 'sphere'. When Long (89) and also Bodzek (56) undertook similar work with dextran they both used Einstein's expression for the intrinsic viscosity of rigid spheres to calculate the radius of the dextran sphere:

$$\eta = 2.5 \left(\frac{4 \pi r_e}{3} \right) N_A / \bar{M}_v \qquad \text{..... 2.46}$$

where η is the intrinsic viscosity of the dextran sample, N_A is Avogadro's number, $\bar{M}_v$ is the viscosity average molecular weight and r_e is the Einstein radius of the sphere. Since neither workers had a value for $\bar{M}_v$ they used an average of the weight and number average molecular weights for each sample.

With a radius calculated via this method Long obtained a good correlation between equation 2.42 and his experimental results at both low and high λ values.

In the experiments conducted by both Zeman and Long the operating conditions were chosen so that concentration polarization was not a problem. However, this also resulted in very low shear rates at the membrane surface and, therefore, in a normal ultrafiltration process, where high shear rates are present, this model would probably not hold. This hypothesis is confirmed by the work of Deen (90) and Munch (91) who found little agreement between their flexible marcomolecule experimental results and the hard sphere theory.

2.5 ENHANCEMENT OF BATCH ULTRAFILTRATION EFFICIENCY

2.5.1 INTRODUCTION

Ultrafiltration processes are generally concerned with the purification of one solute by the removal of a second. In many cases the first solute is not totally retained and the impurity solute is retained to a small degree. Therefore, it is not always possible to obtain the necessary purity or efficiency in one process step so this leads one to the idea of using a cascade system.

A cascade process is a system, where by means of permeate and retentate recycling, a purity and efficiency greater than a one step batch process can be obtained. There are two basic designs of cascade configuration with one based on a concentration mode of operation and the second on a diafiltration mode of operation. These will now be described.

2.5.2 CONCENTRATION CASCADE CONFIGURATION

The simplest design of a concentration cascade is shown in Figure 2.16. This was the method used by Baker (74) to fractionate a dextran hydrolysate sample (see Section 2.4.1) into different $\bar{M}_W$ products. In the initial two stages the high molecular weight products are removed using a membrane which is totally permeable to the middle and low MW dextrans. Since the high MW material is slightly permeable with this membrane some of this product is lost from the first stage, but is then recovered from the first stage permeate in the second stage. The permeate product from the second stage contains only middle and low MW material. In the remaining stages the initial membrane is changed for a tighter membrane, which allows no passage of middle MW material and almost 100% passage of the low MW material. Therefore, in stage three just low MW material is removed and the retentate then passes to stages four, five and six for the removal of the final low molecular weight material. By choosing the correct number of stages any required purity of medium MW material can be obtained.

An alternative concentration cascade design is given in Figure 2.17. This design is based on the gaseous diffusion cascade for the separation of uranium isotopes, which was developed during the second world war. The process is split into two sections, an enriching section and a stripping section with the feed inlet between the two. The required product is removed from the 'top' of the cascade, stage N, and the unwanted waste product from the bottom, stage one. This type of cascade is designed for the separation of two or more components, which have almost the same rejection characteristics with membranes. In this design the same membrane is used in all the stages, unlike the previous design where different membranes could be used in each stage.

The initial separation of the wanted and unwanted solutes takes place at the feed stage. In this stage the majority of the unwanted material is removed in the

Figure 2.16 Concentration Cascade for the Fractionation of Dextran (74)

permeate but a large portion of the wanted solute is also removed since the retentions are so similar. This permeate is then passed down the stripping section of the cascade where the wanted material is recovered in the retentates and recycled back up to the feed stage. By choosing the correct number of stages in the stripping section it is theoretically possible to recover all the wanted material.

The retentate from the feed stage is sent to the enriching section where the remaining 'unwanted' solute is removed, with the additional loss of 'wanted' material. Therefore, the permeates in this section are recycled back down the cascade to recover this lost 'wanted' material. As with the stripping section the number of stages can be chosen to give the required purity. The main limit on the total number of stages is a purely economic factor, ie. the capital costs of the equipment.

Another use for this type of cascade is for the removal of a single solute from its solvent phase where it is only partially rejected by a membrane under consideration. The cascade system removes the need to use a 'tighter' more retentive membrane which would require higher operating pressures hence higher operating costs. In this case the extra capital costs of the cascade method would have to be compared with the 'tighter' membrane's higher operating costs.

The performance of a concentration cascade depends upon the number of stages used, the position of the feed point within the cascade, the difference in the rejection coefficients of the solutes and the ratio of permeate product to retentate product. The effect of varying any one of these parameters was demonstrated by Tutunjian and Reti (92). These workers modelled a five stage cascade unit for the purification of a solute. This modelling was accomplished by analysis of a set of mass balances over the whole system and over each individual stage. A summary of their results is given graphically in Figures 2.18-2.21. In these Figures the passage (P) is the fraction of material passing through the membrane (1 - R), the flow ratio (W_i/W_o) is the ratio of the flow rate at the inlet to the retentate outlet of a stage, N is the number

Figure 2.18 Permeate Product as a Function of Passage (92)

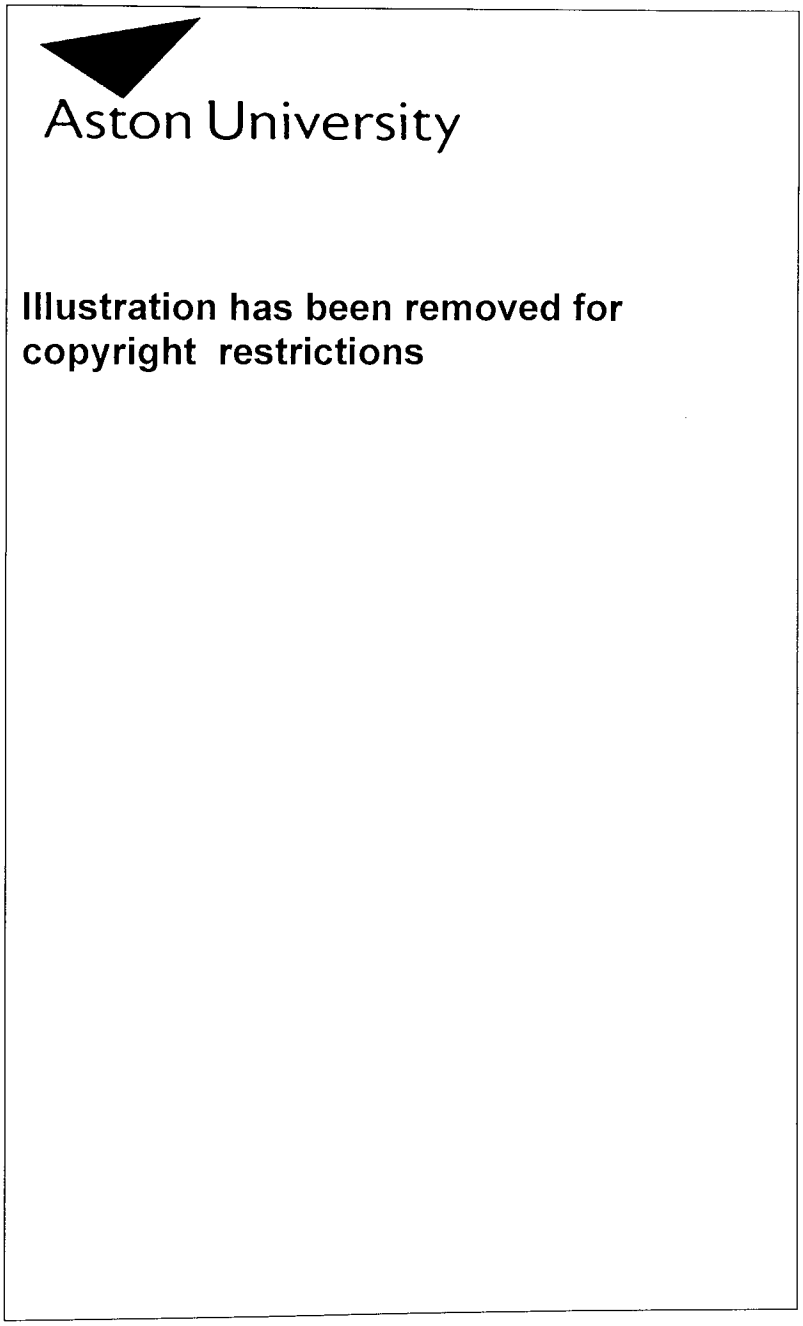

Figure 2.20 Permeate product for various number of stages (92)

of stages and F is the stage number where the feed enters. In these calculations Tutunjian assumed the flow ratio was equal for all stages to simplify the calculations.

Using these plots the relative separation of a multi-component feed can be examined. For example, consider a feed that has two components of equal concentration, A and B, with a passage of 0.7 and 0.3 (Rejections of 0.3 and 0.7) respectively, and enters at stage three. For a flow ratio of 6, the fraction of each solute in the permeate can be read directly from Figure 2.18.

PERMEATE: A = 0.94 (78% purity)

B = 0.26

RETENTATE: A = 0.06

B = 0.74 (93% purity)

EQUIVALENT BATCH RESULTS:

PERMEATE: A = 0.71 (63% purity)

B = 0.42

RETENTATE: A = 0.29

B = 0.58 (67% purity)

Tutunjian repeated this method for different flow ratio values and showed that when the ratio is reduced the purity of the permeate stream increases, but the recovery of the main component (A) decreases. This is shown in Figure 2.19, as the ratio is decreased, the fraction of any component in the permeate is decreased. The effect on the retentate for changing flow ratios is the opposite of the permeate.

The separation dependence on the number of stages is shown in Figure 2.20. It can be seen that as the number of stages is increased, the separation is increased. Figure 2.21 shows that moving the feed stage away from the permeate product stage decreases the fraction of any component in the permeate product and increases the fraction in the retentate.

Since the system considered by Tutunjian was for only five stages and the flow ratio was constant for each stage, the mass balance equations were relatively simple to solve. However, some cascade systems contain many more stages with varying amounts of permeate removal at each stage. In these cases numerical iteration methods such as the multidimensional Newton-Raphson method have to be used and the solving of these equations has been investigated by many workers (93-96).

2.5.3 DIAFILTRATION CASCADE CONFIGURATION

When a solute is purified under diafiltration conditions many volumes of dialysate (wash solvent) are usually required for the complete removal of the contaminant. These large volumes would be both a storage, pumping and effluent problem on any industrial sized process and therefore, a continuous counter-current diafiltration cascade was suggested by Porter and Michaels (97) as a method of reducing these volumes. A schematic diagram of their cascade is given in Figure 2.22.

In this three stage process the pure dialysate is added to stage three, and the permeate produced from this stage is then recycled back to stage two. This permeate from stage three is then used as dialysate for stage two and the permeate from stage two as dialsate for stage one. By this method only one volume of dialysate is used for the same purification as approximately three volumes on a batch mode. As with the previous cascade configuration the capital investment cost of this method is higher than batch diafiltration, but the added investment may be warranted if the wash solvent is an expensive buffer.

A process where the wash solvent is expensive to recover is in the purification of water soluble polymeric dyes, since in this case the solvent is either pyridine or alcohols. In an attempt to reduce the use of these alcohols Cooper (98) proposed a process based on the concept of partial recycling of permeates. A schematic diagram of this process is given in Figure 2.23. As with the Porter cascade the pure dialysate solvent enters at the last retentate stage and the permeates are

Figure 2.22: Continuous Counter-current Diafiltration Cascade (97)

Figure 2.23: Schematic Diagram of Diafiltration Cascade for Decreased Solvent Use (98)

recycled back to the initial feed stage, ie. the permeates pass counter-current to the retentates. However, in this process the final permeate is sent to a solvent recovery stage.

As with the concentration cascade configuration this method is best modelled by means of material balances. From these balances Cooper was able to obtain a relationship which showed the effect of the number of stages (K) and the rejection coefficient (σ) of the impurity on the purity of the final product (ψ). In his calculations Cooper assumed that the required product was totally rejected. From this relationship Cooper found the final product purity for varying values of N and σ, see Figures 2.24 and 2.25. In these calculations the effect of the rejection (σ) and the number of diavolumes used (N) were grouped as a constant $Z = (1 - \sigma)N$. Cooper found that for increasing values of K and Z, the value of ψ increases non-linearly at low Z values and linearly at higher Z values.

To illustrate the economic benefits of a cascade system Cooper calculated the cost per Kg of a product from cascading, and a product from a batch system. The main processing costs, such as solvent price, fractional loss of solvent in the recovery stage and individual membrane life were the same for both methods. For a product of given purity the cascade cost 0.75 currency units/Kg and the batch 1.13 currency units/Kg. He then repeated the calculations for varying solvent costs and concluded that the economic advantage of cascade over batch was most pronounced at high solvent costs.

2.6 METHODS FOR THE FRACTIONATION OF DEXTRAN

As well as using ultrafiltration for the fractionation of dextran there are two other main techniques. These are ethanol precipitation and gel permeation chromatography (GPC). Ethanol precipitation is the method currently used on industrial scale processes, and is based on the solubility difference of different

Figure 2.24 Effect of High Values of Z, for Various Numbers of Stages (k), on Product Purity from a Diafiltration Cascade (98)

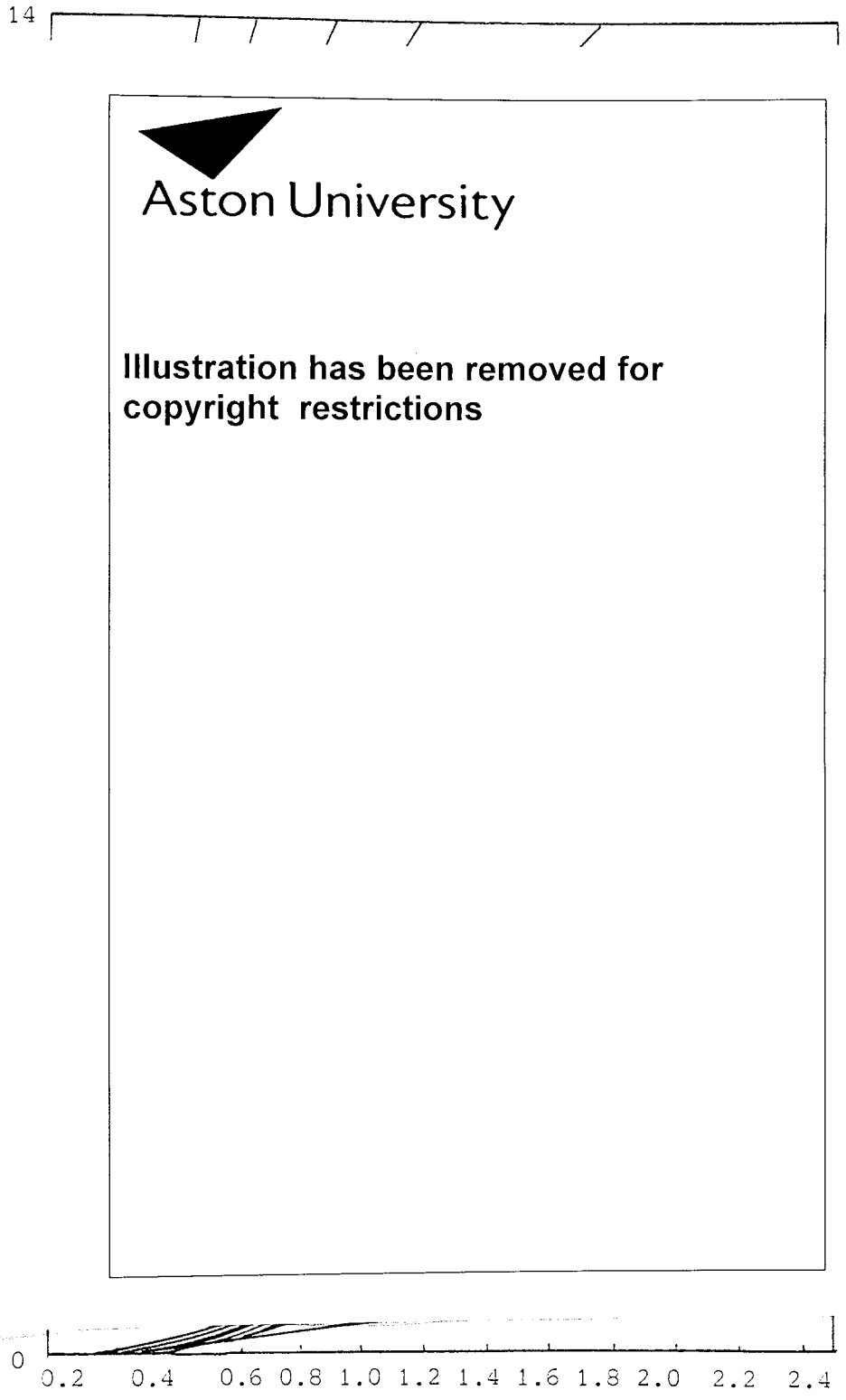

Figure 2.25 Effect of Low Values of Z, for Various Numbers of Stages (k), on Product Purity from a Diafiltration Cascade (98)

molecular weights of dextran. If a given amount of ethanol is added to an aqueous solution of dextran hydrolysate, agitated for a period of time, and then allowed to stand, phase separation will occur. The ethanol phase will contain a precipitate of high molecular weight dextran and the water phase the remaining dextran hydrolysate. By altering the amounts of ethanol added different fractions can be precipitated out and the original dextran hydrolysate can be fractionated to the required specification.

On an industrial plant the low molecular weight material is usually removed first by precipitating out the high and middle molecular weight material. The high molecular weight material is then removed to leave the required middle range material. This process of fractionation is very costly in energy terms since the ethanol used has to be recovered by distillation from the final product and the waste products. To try to reduce the amount of ethanol used, hence distillation costs, workers such as Bhambra (100) have modelled the relationship between the amounts of ethanol and the fractions of dextran obtained.

Since the ethanol recovery costs are so high an ethanol free means of fractionation was desired, and Barker (7, 15) and Vlachogiannis (16) succeded in this aim using GPC. This method of chromatography uses a porous gel as the separating medium. When a solution of dextran is pumped through a column of this gel the dextran molecules can diffuse into and out of the pores to a degree dependent upon their molecular weight, ie. small dextran molecules enter the pores fully, medium dextran molecules enter the surface of the pore and very large molecules are excluded from the pore. Therefore, the large molecules leave the column first, followed by the middle range dextran and lastly the small molecules. Hence, the dextran sample is fractionated in to molecular weight bands. The advantage of this process is that only aqueous solutions are needed. The disadvantage of this method was that initially this system was only available in a batch mode of operation. However, Barker and Ellison

(7) solved this problem with the design and construction of a continuous counter-current chromatographic unit. Using this unit Vlachogiannis showed that GPC could fractionate dextran, at the high specification, as efficiently as the present ethanol method. In the fractionation of dextran at the low molecular weight specification level GPC was shown to have an efficiency comparable to that of ethanol fractionation.

2.7 ULTRAFILTRATION EQUIPMENT

2.7.1 INTRODUCTION

For the efficient application of ultrafiltration the design of the membrane module and the layout of the system in which the module is installed are as important as the selection of the membrane. This is mainly due to the control of concentration polarisation and gel formation, which is to a large extent determined by the module design. One of the most important parameters in designing UF modules, therefore, is the flow control of the feed solution at the membrane surface.

Several module designs, which have significant differences in feed distribution, operating pressure, capital and operating costs, are available. The main large scale units are shown in Figure 2.26.

2.7.2 TUBULAR MEMBRANE MODULE

The tubular membrane module gives significant advantages in terms of control of concentration polarisation and membrane fouling. The construction of such a system is shown schematically in Figure 2.27. This construction can be easily cleaned by means of foam swabs without dismantling the equipment. The membrane is placed on the inside of a porous stainless steel tube and the pressurised feed solution flows down the tube bore. The product permeates into the outer shell. These tubes may be installed in series or parallel array and the modules vary in tube diameter from

Figure 2.26

Module Type	Membrane Surface for Module Volume	Investment Cost	Operating Cost	Flow Control	Ea Cl in

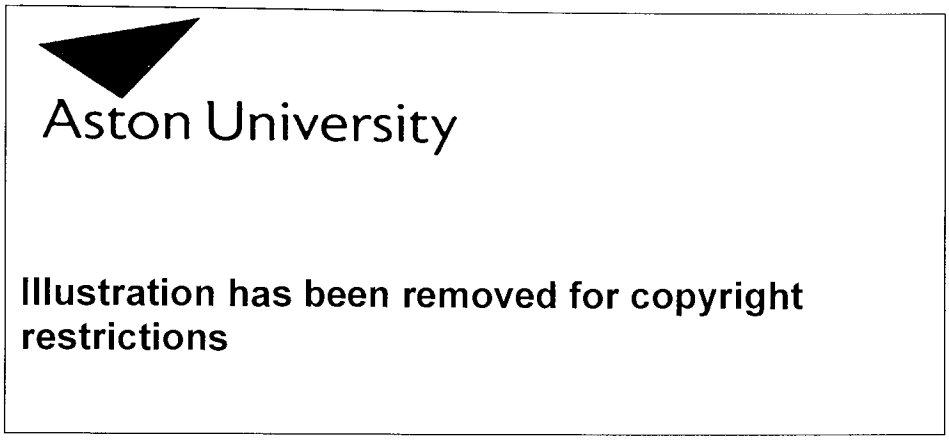

Ultra Filtration Membrane Modules used on large scale (26)

Figure 2.27: Tubular Membrane Module

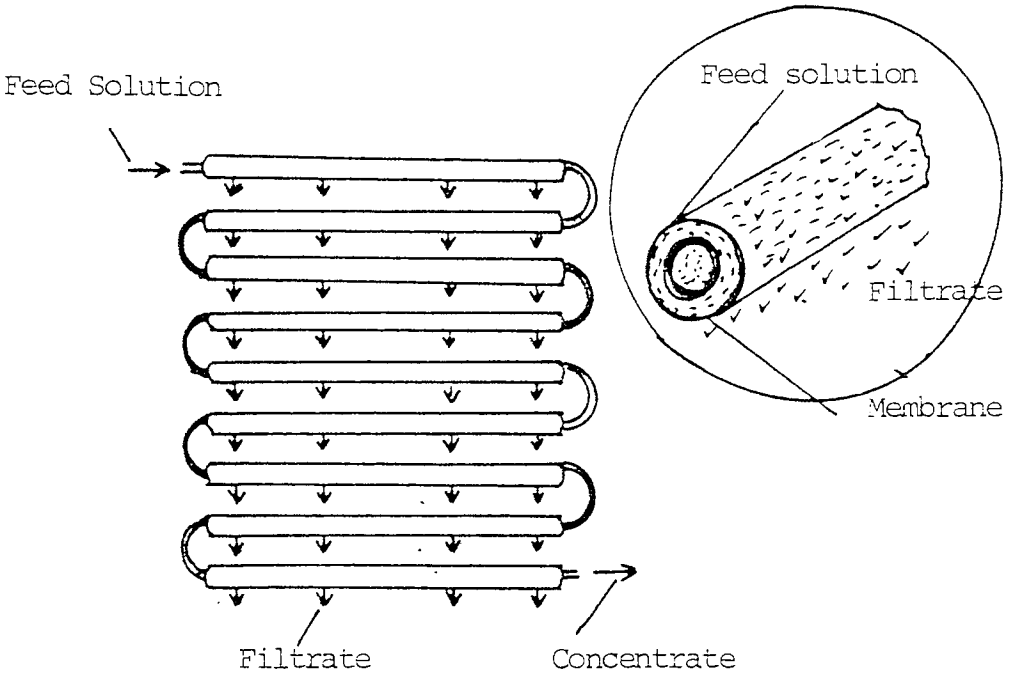

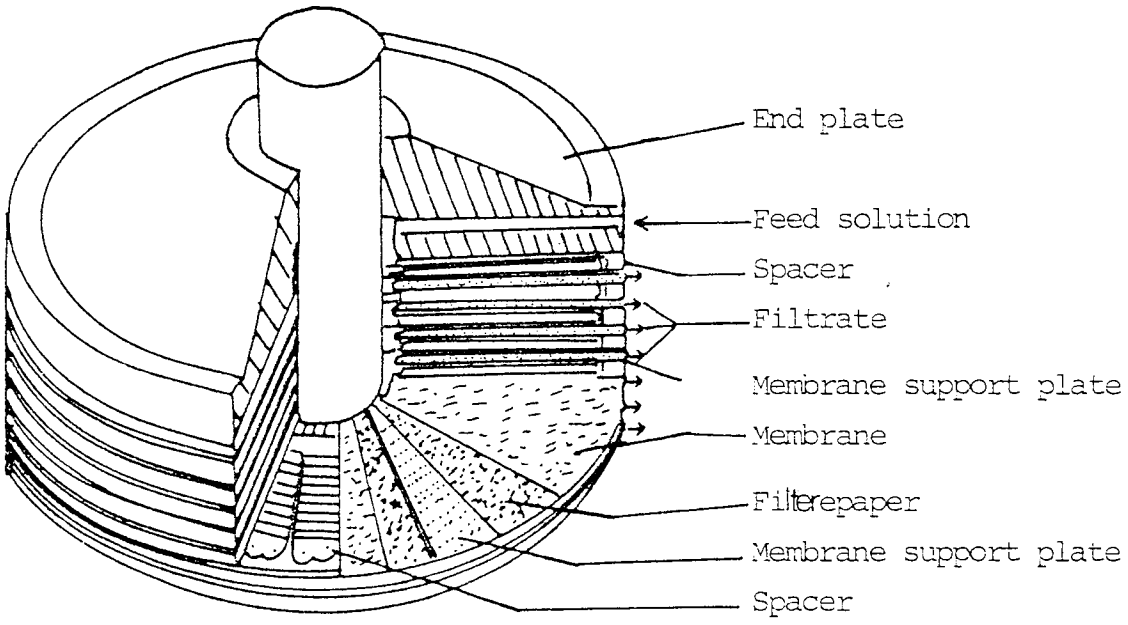

Figure 2.28: Plate-and-Frame Membrane-module

1 to 2.5cm. These units are produced by Abcor and Nitto Electric Industrial. The advantages of tubular systems are that the feed velocity can be adjusted over a wide range for control of concentration polarisation and also the system can be mechanically cleaned when excessive membrane fouling occurs. The disadvantages are the relatively high investment and operating costs and a low ratio of membrane surface area to system volume.

2.7.3 PLATE-AND-FRAME MEMBRANE MODULE

Plate-and-frame membrane systems were among the first ones introduced in large scale UF and reverse osmosis units. These designs have their origins in the conventional filter press concept. The membranes, porous membrane support materials, and spacers forming the feed flow channel, are clamped together and stacked between two end plates. The feed solution is channelled across the surface of the membrane by the feed spacers. A schematic diagram is shown in Figure 2.28. This basic design of module is made by De Danske Sukkerfabrikker, but there are several variations on this design. In some modules the membrane can be removed from the porous support plate, whereas in others it is directly cast onto the plate. The control of concentration polarisation is more difficult with these units than with tubular systems, and plugging of the feed flow channel can be a problem especially with solutions containing large quantities of suspended solid matter. The investment cost of plate-and-frame units depends on the specific module design. Overall, however, they are lower than in tubular systems, and generally the operating costs are lower than tubular systems.

2.7.4 SPIRAL-WOUND MEMBRANE MODULE

The spiral wound membrane module is used mainly in reverse osmosis and is shown schematically in Figure 2.29. In principle it is a plate-and-frame system which has been rolled up. The feed flow channel, the membrane and the membrane support are rolled up and inserted in an outer tubular pressure shell. The permeate is

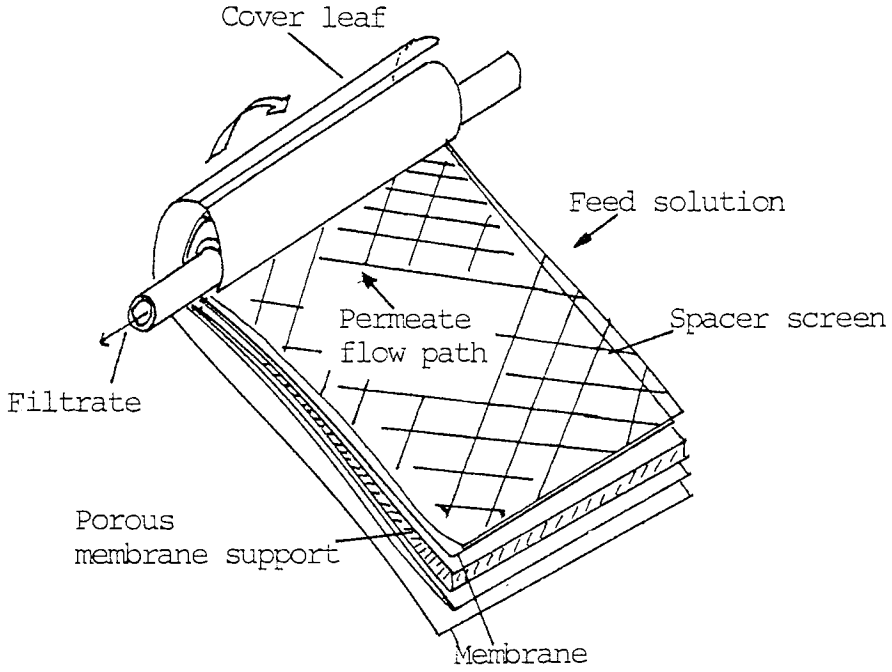

Figure 2.29: Spiral Wound Membrane Module

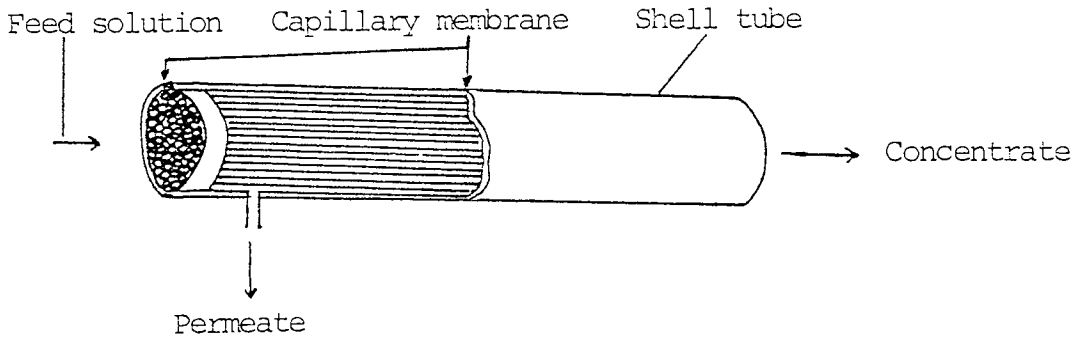

Figure 2.30: Capillary Membrane Module

collected in a tube in the centre of the roll. In this module the membrane surface area per unit volume is very high and capital and operating costs are low. However, it is very difficult to control concentration polarisation effects and severe membrane fouling may occur with solutions containing only moderate concentrations of suspended solids.

2.7.5 CAPILLARY MEMBRANE MODULE

A schematic of this module system is shown in Figure 2.30. It consists of a large number of membrane capillaries with a diameter in the range 0.5 to 1.5mm. The feed solution is passed down the centre of the capillary and the permeate passes through its wall. Since the membranes are produced by fibre spinning technology and the capillaries are unsupported, capital costs are low.

This system provides a good feed flow control and a large membrane surface area per unit volume. However, the operating pressure is limited and the system is sensitive to operating errors. Plugging of the capillaries can be a problem when the inner diameter of the capillaries are too low, and in all cases an effective prefiltration of the feed solution is required.

2.7.6 COMPARISON BETWEEN UF MODULES

In general the tubular module is the most expensive design in terms of capital and operating costs. However, in some applications tubular systems are used more widely than other modules, eg. the recovery of electro coating paints. In this situation the good control of concentration polarisation, the proven reliability and the ability not to use prefiltration compensates for the high capital and operating costs.

Plate-and-frame systems have been used successfully in the dairy industry in spite of their relatively high capital cost since they offer major advantages in the fields of membrane replacement, cleaning procedures and high operating reliability.

Capillary membranes have been used successfully for applications ranging from waste water treatment to surface water sterile filtration. Even though a

preflitration is required their relatively low capital and operating costs make the module more attractive. Due to the diversified nature of UF applications no one module design dominates the field and each system has its own application area.

3.0 ANALYTICAL EQUIPMENT

3 ANALYTICAL EQUPMENT

3.1 INTRODUCTION

To assess the performance of a given membrane, data is required on how that membrane rejects dextran of chosen molecular weight bands. Two analytical techniques were used in this work.

To obtain the total weight of dextran in a sample the concentration of the sample was measured using either high performance liquid chromatography (HPLC) or a polarimeter (see Section 3.2).

The molecular weight distribution of the sample was then found using analytical gel permeation chromatography (GPC) (Section 3.3). Using this distribution the sample could then be subdivided in to weight fractions at any molecular weight band.

From the weight fractions and the total weight of the sample, the weight of the molecular weight bands could be calculated. This procedure was repeated for both the feed and product of any experiment and rejection values calculated for selected molecular weight bands.

3.2 CALCULATION OF SAMPLE CONCENTRATION

3.2.1 HPLC METHOD

A schematic diagram of the equipment layout is given in Figure 3.1. The equipment basically consisted of an eluent reservoir, water bath, thermoregulator, pump, sample injection valve, HPLC column, hot water circulator, glass column, detector and an integrator.

An eluent of deionised water was used. This water was kept at a constant temperature of 80^{o}C to ensure it was degassed.

The eluent was pumped with a positive displacement pump (series II, Metering Pumps Ltd, London, UK). Samples were injected using a six-port sample

Figure 3.1 Schematic Diagram of HPLC Analytical System

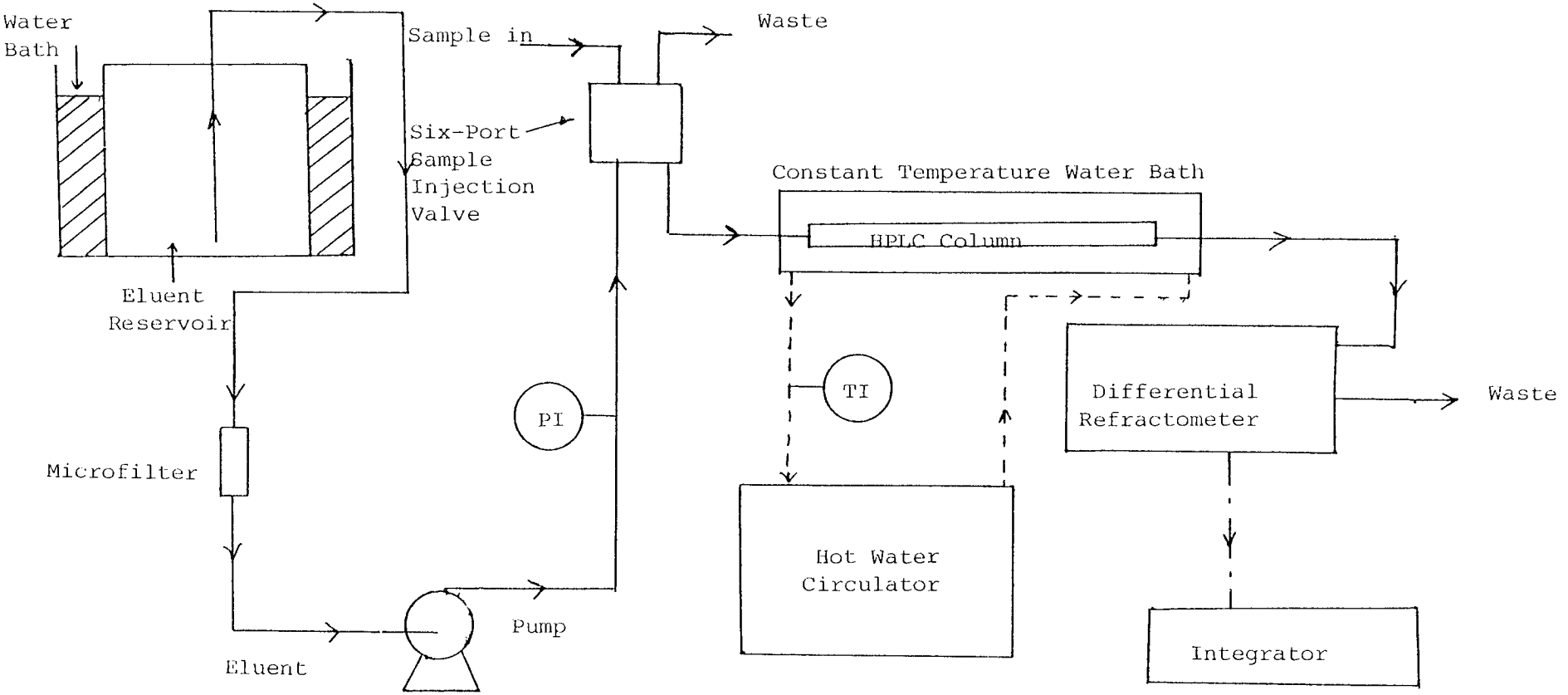

injection valve (type 3.100) supplied by Spectroscopic Accessory Co, London, and fitted with a constant volume (20 μl) sample loop. All the samples were filtered before injection into the column using a disposable syringe filter of 0.45 μm mesh supplied by Millipore, London.

The HPLC column used was a WATERS SUGAR-PAK carbohydrate column, supplied by Millipore, London. The column was enclosed in a glass column 26.0cm long x 5.0cm ID filled with water and kept at a constant 85°C by a hot water circulator (C-400, Techne, Cambridge, UK).

The eluent from the column then passed into a differential refractometer (Model R401, Waters Associates Ltd). The refractometer produced a voltage peak whose area was directly proportional to the concentration of dextran in the sample. The area was measured using an integrator (Model 3390A, Hewlett Packard). By comparing the area of the sample to that of a standard of known concentration, the concentration of the sample was found.

3.2.2 POLARIMETER METHOD

Towards the end of this work a polarimeter became available for use, courtesy of FISONS PHARMACEUTICALS LTD (Holmes Chapel). The polarimeter showed the degree of optical rotation of any solution placed in its sample compartment. This degree of rotation was shown to be directly proportional to the concentration of the sample, (Figure 3.2).

3.2.3 COMPARISON OF CONCENTRATION MEASUREMENT TECHNIQUES

The initial experiments conducted could be completed in one day. In these cases the concentrations measured using HPLC were found to be adequate. However, due to the nature of the latter experiments this time period increased from one day to several days. In these experiments it was necessary to add an anti-bacteria agent (sodium azide) to the feed solution. This agent then passed through the membrane

Figure 3.2: Calibration of Polarimeter

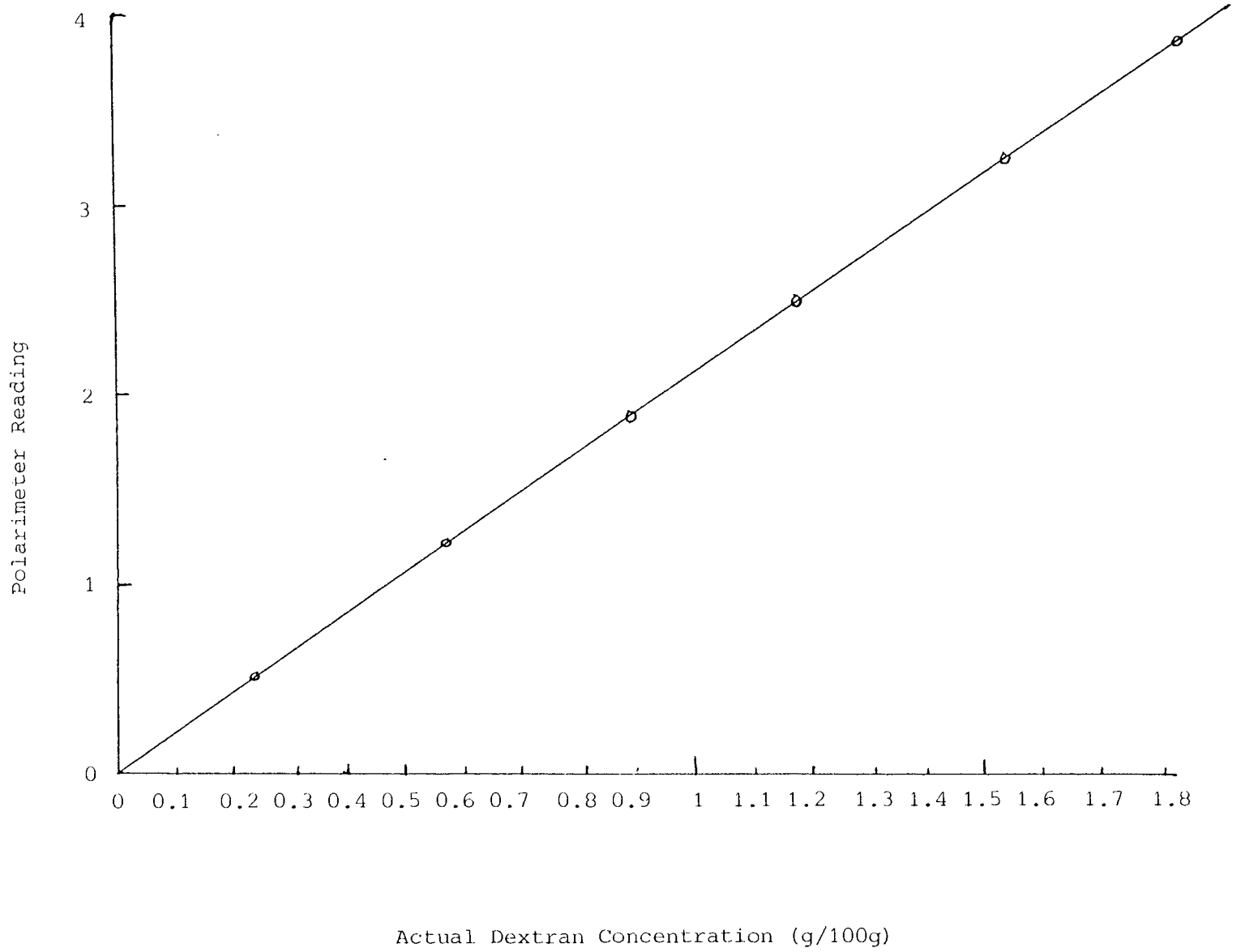

during the experiments and distorted the concentrations measured by HPLC. This was due to the sodium azide concentration being superimposed upon the dextran concentration when measured by a differential refractometer.

When a dextran plus sodium azide sample is measured using a polarimeter only the dextran concentration is measured. Therefore, the polarimeter was found to be more accurate for samples containing sodium azide. This is shown in Figure 3.3 where the concentrations for one typical experiment are shown. The polarimeter concentrations show an expected trend whereas the HPLC results are more random.

The polarimeter was found to be superior also on analysis time. The polarimeter took approximately 1 minute per sample and the HPLC took 10 minutes.

3.3 ANALYTICAL GPC

3.3.1 EQUIPMENT DISCRIPTION

The equipment layout used is given in Figure 3.4. The equipment consisted of an eluent reservoir, water bath, thermoregulator, microfilter, pump, a sample injection valve, fractionating columns, hot water circulator, glass column, detector, chart recorder and a PET computer.

The eluent used was a 0.02% w/v solution of sodium azide in distilled water. The sodium azide solution was used to prevent bacterial growth in the columns. The samples to be injected were made up to a concentration of 2% w/v dextran and 0.02% w/v sodium azide. The sodium azide was present to prevent any negative (absence of sodium azide) peaks on the chromatogram.

The eluent was pumped with a positive displacement pump (Series II, Metering Pumps Ltd, London, UK). This pump has recently been changed to a more accurate dual piston, low pulsation pump (model 1330, Bio-Rad Laboratories, Watford, UK). Samples were injected using a six port sample injection valve (model 30.100, Spectroscopic Accessory Co, London) fitted with a constant volume (100 µl) sample loop. Before injection into the columns all the samples were filtered using a

Figure 3.3 Comparison of Concentrations Measured by Polarimeter and HPLC

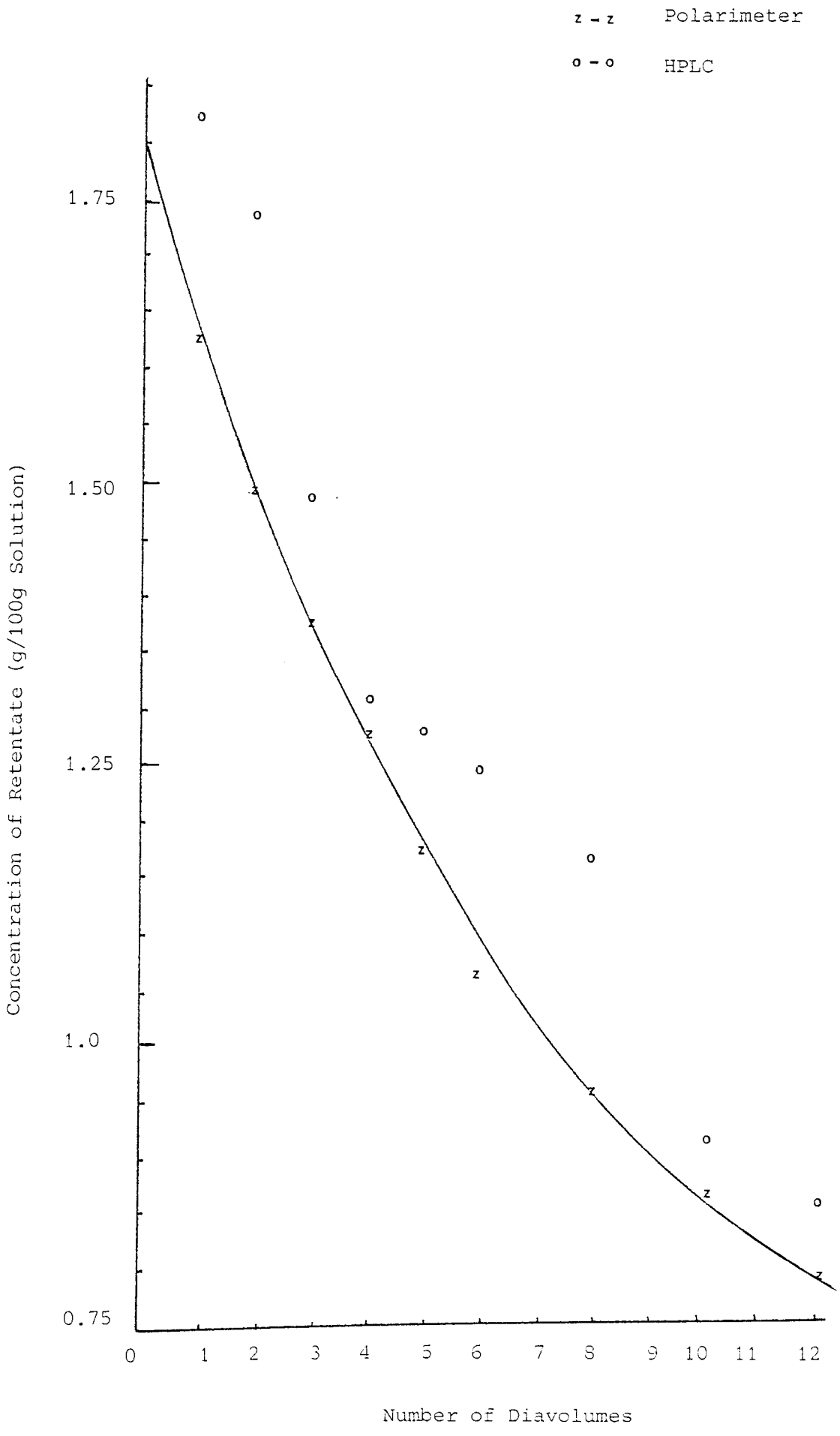

Figure 3.4 Schematic Diagram of the Analytical GPC System

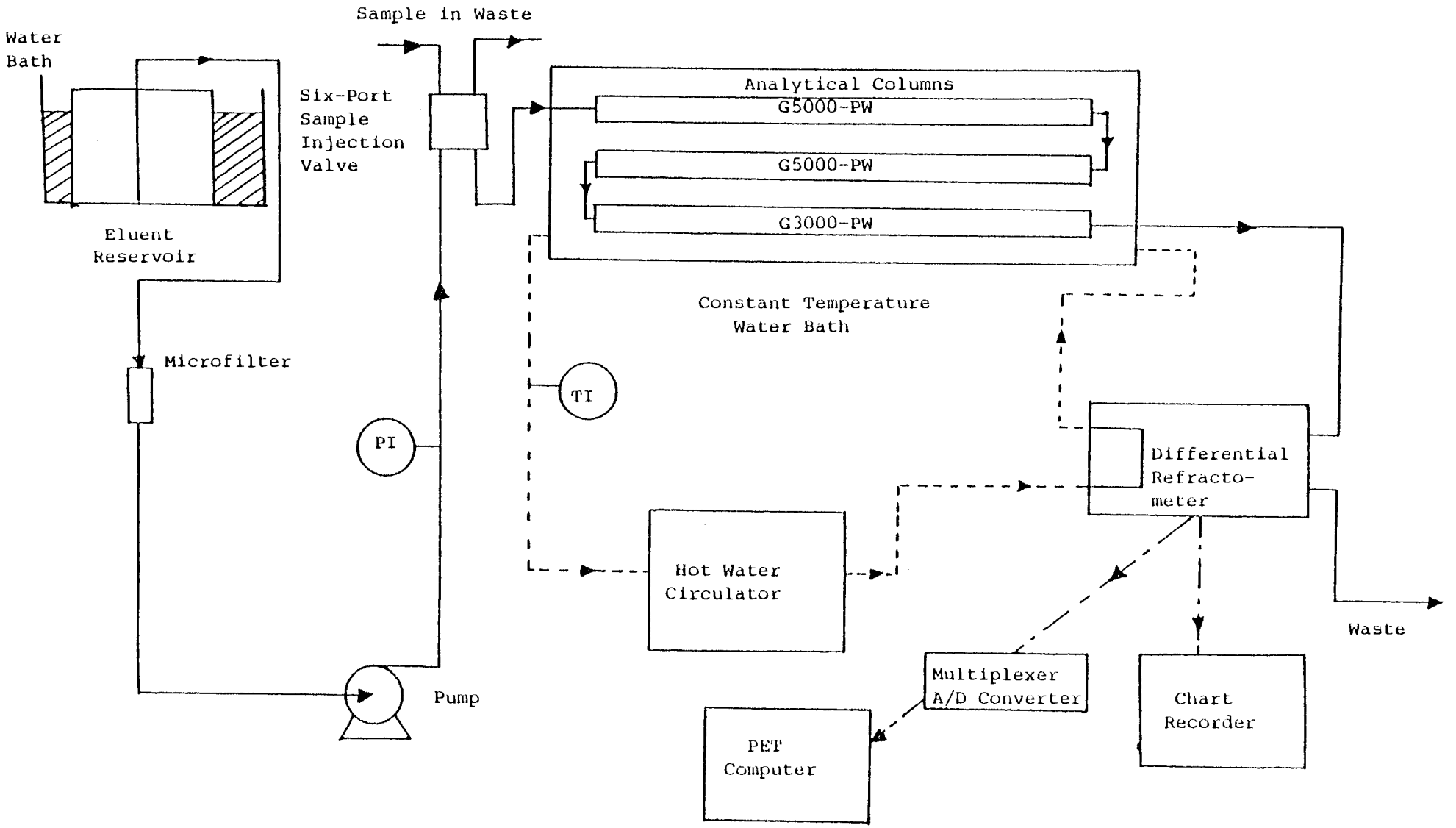

0.45 μm disposable syringe filter supplied by Millipore, London.

The GPC columns used will be described in detail in Section 3.3.2. The columns were enclosed in a glass column (70cm long x 7.5cm ID) filled with water and kept at a constant 35°C by a hot water circulator (C-4OO, Techne, Cambridge, UK).

The product from the GPC columns then passed into a differential refractometer (Model R401, Waters Associates Ltd, London) and the refractometer compared this product against a standard reference of 0.02% w/v sodium azide. The resulting change in the product concentration was registered on a flat-bed potentiometric chart recorder (Venture Servoscribe, RE 541.2 Smiths ltd). The anologue output from the refractometer was also registered by a multiplexer (Model PCI 1001, CIL Electronics Ltd, Sussex) which then converted it to a digital signal. This digital signal was then recorded by a PET computer (MODEL CBM 4032, 32K bytes, Commodore, UK). The programming involved and the subsequent calculation of the sample's molecular weight distribution will be described in detail in Section 3.3.5.

3.3.2 GPC FRACTIONATING COLUMNS

The GPC fractionating columns used throughout this research project were the TSK-PW type marketed by Toyo Soda Manufacturing Co Ltd, Tokyo, Japan (101, 102).

To fractionate the whole range of dextran molecular weights three GPC columns were used in series. The first two were G 5000 PW columns and the third was a G 3000 PW column. The G 5000 PW columns have a particle size of 17 ± 2 μm and fractionates dextran in the molecular weight range of 10 000 - 2×10^6. The G 3000 PW has a particle size of 13 ± 2 μm and fractionates dextran up to a molecular weight of 10 000. The columns are 60cm in length by 0.75cm ID.

The flowrate through the columns was 1.0cm^3/min and the analysis time for dextran-glucose solutions was approximately one hour.

The GPC columns used in the first part of this research work were originally installed by Vlachogiannis (12, 103, 104) and after three and a half years of intensive use showed signs of deterioration. Therefore, a new set of three columns were purchased from Toyo Soda.

Before the new columns were installed the number of theoretical plates (N), and the asymmetry factor (A_S), of the old and new columns were calculated. These two parameters are widely used in chromatography to describe the efficiency of a column.

There are several methods available for measuring N, but if the peak obtained from a column is symmetrical and close to Gaussian shape, N can be expressed in variables that are easily measured experimentally. The most commonly used approximation is:

$$N = 5.54\left(\frac{V_R}{W_{0.5}}\right)^2 \qquad \text{..... 3.1}$$

where $W_{0.5}$ is the peak width at one-half the peak height. V_R is the total liquid volume of the column and is calculated from the time for the peak to be eluted and the flow rate (see Figure 3.5).

The assymmetry factor (A_S) is calculated at one-tenth the peak height (see Figure 3.5) and is given by the following equation:

$$As = \frac{b}{a} \qquad \text{..... 3.2}$$

The results obtained using a 1% w/v ethylene glycol solution are given in Figure 3.6, together with the manufacturer's recommended values.

The old columns were found to be below specification, but the new columns were better than specification and were subsequently installed at Aston.

Figure 3.5 Illustration of Parameters for Determining HETP and Asymmetry Factor

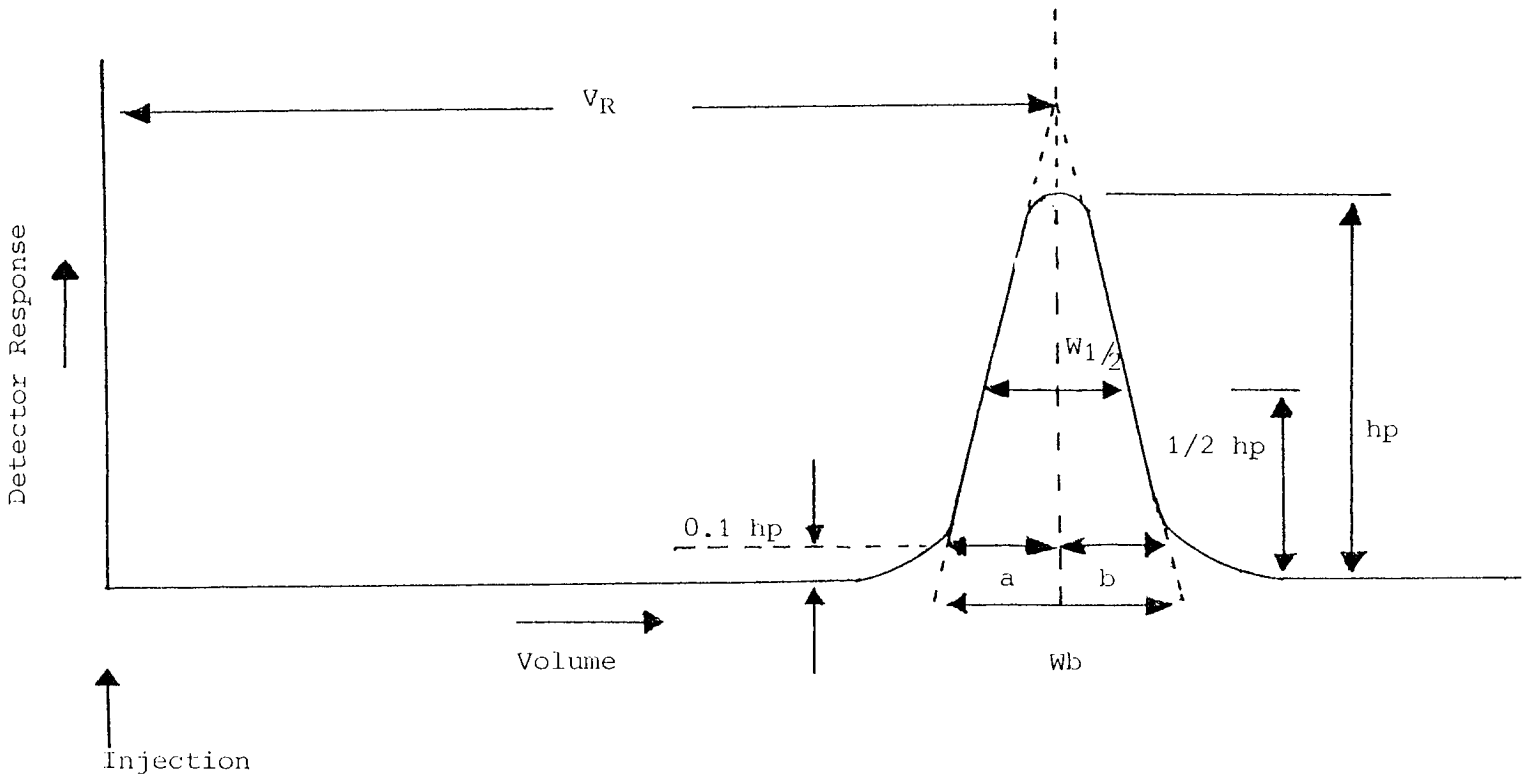

Figure 3.6

RESULTS OF THEORETICAL PLATES AND ASYMMETRY FACTORS FOR TSK-PW COLUMNS

Column Type	Toyo Soda Quality Specifications		Aston Analysis	
	N/Metre	As	N/Metre	As
G5000-PW OLD I	10000	0.7~1.6	3732	2.52
G5000-PW OLD II	10000	0.7~1.6	9098	1.28
G3000-PW OLD	16000	0.7~1.6	14508	1.70
G5000-PW NEW I	10000	0.7~1.6	16083	0.94
G5000-PW NEW II	10000	0.7~1.6	16667	1.01
G3000-PW NEW	16000	0.7~1.6	19777	1.08

3.3.3 CALIBRATION OF THE GPC COLUMNS

The raw data from a GPC analysis consists of an elution profile of detector response against elution volume. A typical chromatogram obtained is shown in Figure 3.7. The ordinate represents the variable being measured by the detector, but as this is directly proportional to the concentration of the polymer present, concentration will be used for convenience. The abscissa is the elution volume, or elution time. The area under the curve represents the weight of sample injected in to the column. The shaded area represents the weight between V_{R1} and V_{R2}.

To be able to convert this data into the molecular weight distribution of the sample the columns must be calibrated. This calibration relates the elution volume of the chromatogram to the molecular weight.

There were various calibration methods available (105-114), but after extensive work by Vlachogiannis (12) and Bhambra (100) it was found that the best method for dextran was the one proposed by Nilsson and Nilsson (115). This approach is based on a polynominal of the type:

$$M = b_5 + \exp \{b_4 + b_1 (K_d) + b_2 (K_d)^2 + b_3 (K_d)^3\} \quad \ldots\ldots\ 3.3$$

where M is the molecular weight to be calculated. b_1-b_5 are constants.

K_d is a distribution coefficient, which is related to the elution volume (V_R) of the sample according to the equations:

$$V_R = V_o + K_d V_i \text{ or } K_d = \frac{V_R - V_o}{V_i} \quad \ldots\ldots\ 3.4$$

Figure 3.7 A Typical GPC Polymer Chromatogram

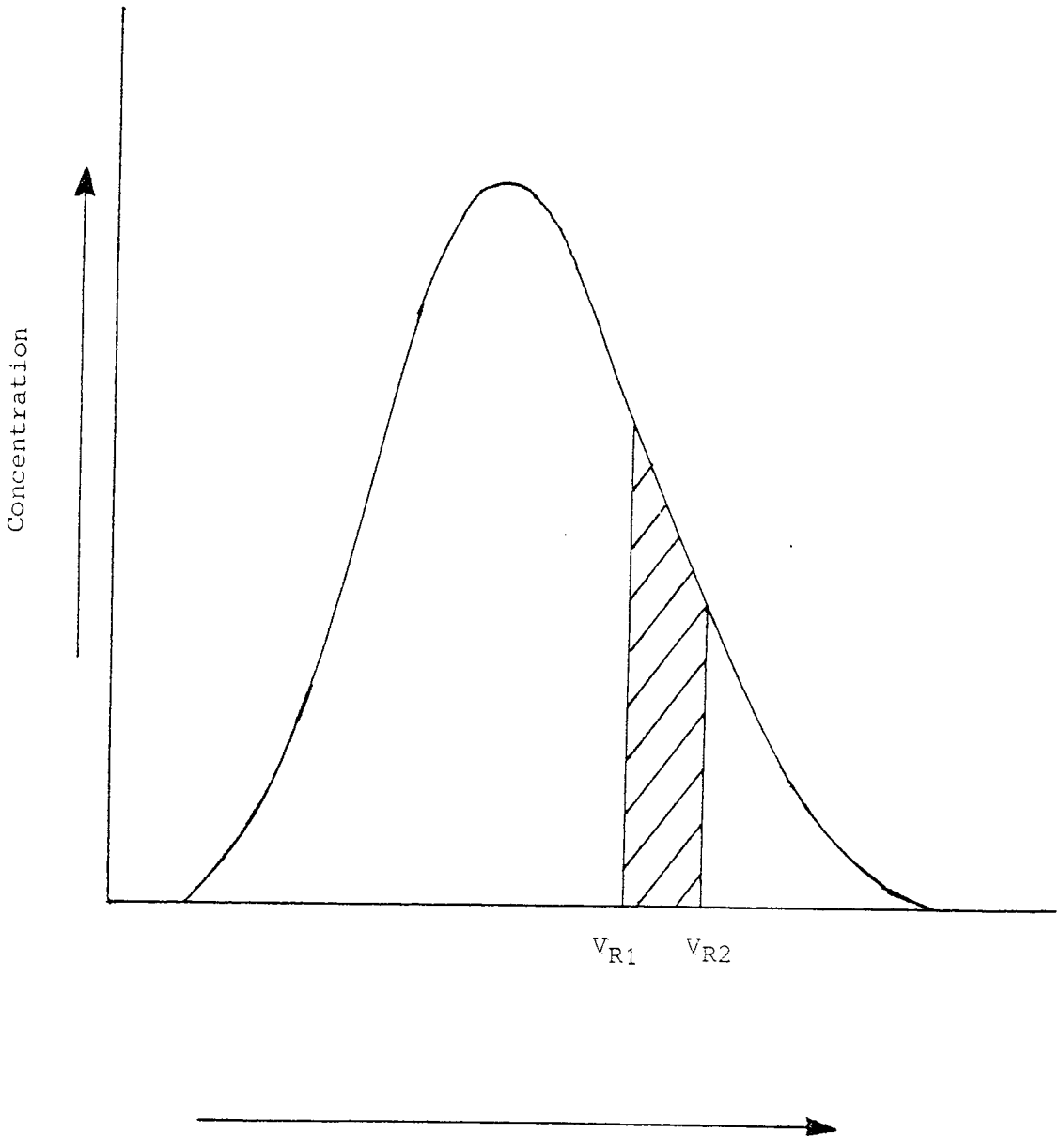

and

$$V_i = V_t - V_o \qquad \text{..... 3.5}$$

where

V_i is the internal (pore) volume of the columns.

V_o is the void volume of the columns.

V_t is the total liquid volume of the columns.

Therefore, once the values of V_o, V_t and b_1-b_5 are found the molecular weight (M) can be directly related to the elution volume (V_R).

The values of V_o, V_t were found by injecting a solution of high molecular weight dextran and glucose . The elution time for the dextran is equal to V_o and the elution time of the glucose is equal to V_t.

The values of the calibration constants b_1-b_5 were obtained by the following procedure.

(a) A series of chromatograms were obtained for several Pharmacia dextran T-fractions (3, 4, 117, 118) whose weight average molecular weights, $\bar{M}_W$ (see Section 3.3.6), had been measured previously by light-scattering. The eluent flowrate for each chromatogram was measured.

(b) The heights, elution volumes (converted to K_d values), $\bar{M}_W$ (measured by light-scattering) of the T-fraction chromatograms and guessed values of the calibration constants b_1-b_5 were entered into a computer calibration program. This program had been written by Vlachogiannis and used the Hartley modification of the Gaussian-Newton (116) method to calculate the new values of the calibration constants b_1-b_5. These new values then gave the optimum agreement between the actual values

of $\overline{M}_W$ (measured by light-scattering) for each T-fraction and the calculated values obtained from the GPC elution profiles.

(c) The resulting calibration was then checked by analysing a dextran T-40 sample (batch BT1J, $\overline{M}_W$ 41 500 by LS) and comparing the values of the $\overline{M}_W$s between light-scattering and GPC. This dextran T-40 sample was analysed frequently as a check on the calibration.

Once the columns were calibrated the limits of the calibration had to be determined. These limits are the maximum and minimum molecular weights for which the calibration still holds.

These limits are found by plotting a calibration curve. A typical curve is shown in Figure 3.8 and shows the relationship between molecular weight and elution volume (V_R) on a semi-logarithmic scale. This is a typical S-shaped calibration curve and five regions can be identified on this curve. Above a certain molecular weight (M_X) no fractionation occurs (sections a-b) as all these molecules are too large to penetrate any pores of the packing. Therefore, all these molecules elute at the void volume (V_o) and K_d equals zero.

Below molecular weight M_Y the molecules are not fractionated (sections e-f) as they all completely penetrate the pores ($K_d = 1$), and therefore they are the last to elute at a retention volume of V_t. Molecules between these two points are fractionated and these two points are the limits of the calibration.

In the section c-d the calibration can be represented by a straight line and one normally chooses a column that fractionates the whole of a sample in this region. Between these two points the fractionating power of the columns are greatest.

Figure 3.8 A Typical Calibration Curve for a GPC Column

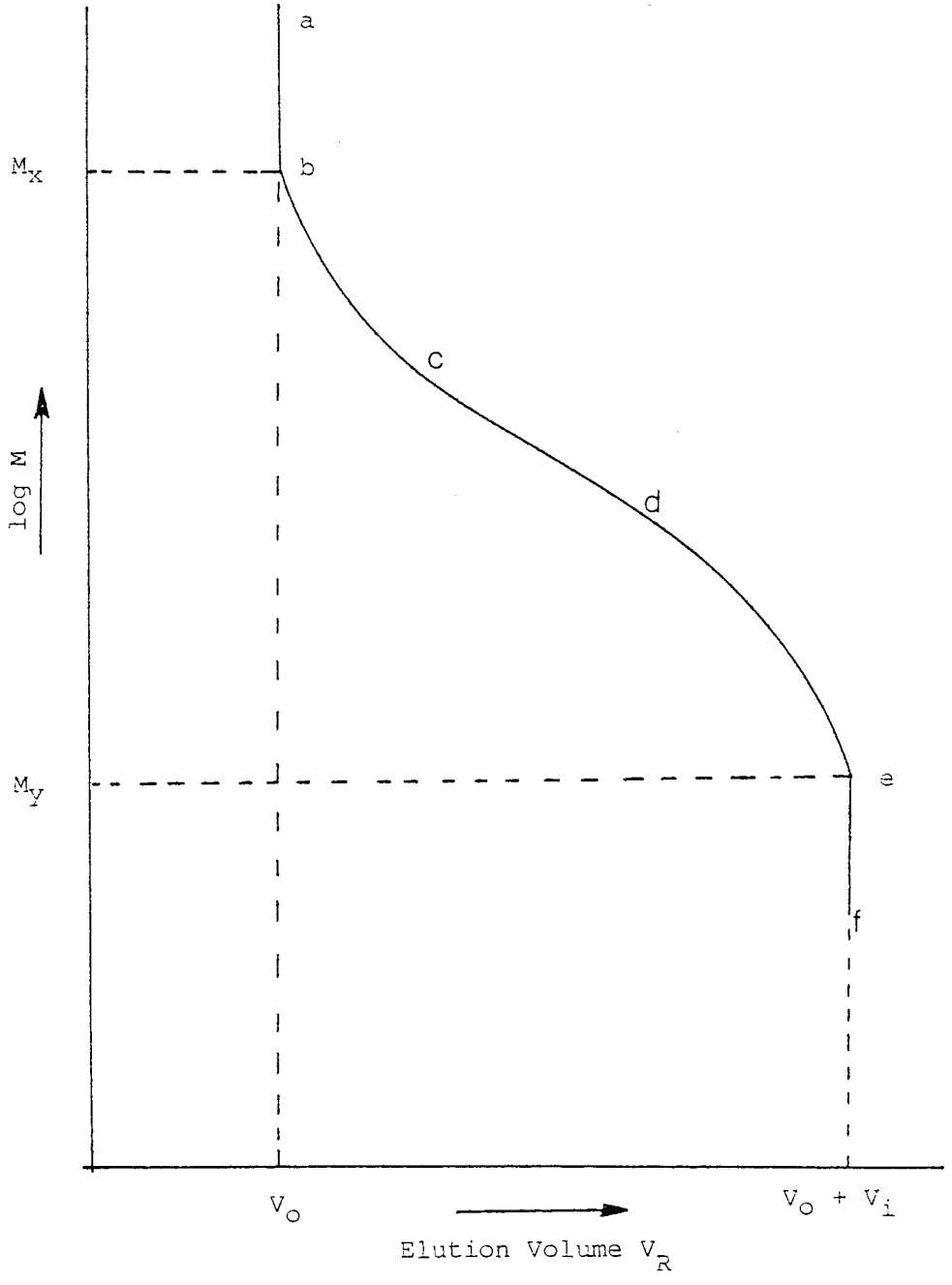

In sections b-c and d-e fractionation is still occurring, but the relationship between log M and V_R is non-linear. However, it is necessary to calibrate over the whole region that is likely to be covered by a sample because extrapolation of calibration curves will give erroneous results.

The calibration results obtained by Bhambra (2) on the old set of columns are given in Figures 3.9 and 3.10 and the results obtained with the new columns in Figures 3.11 and 3.12. In both cases, when new, the columns had an upper molecular weight limit of 10×10^6 and a lower limit of 180 (glucose).

3.3.4 ANALYTICAL TECHNIQUES

The preparation of a sample to be injected on the analytical columns fell into one of two categories. These were:

(a) The preparation of 2% w/v solutions of known molecular weights, for the calibration of the columns. These solutions were prepared by dissolving a known amount of dextran powder (of known average molecular weights) in a precise volume of 0.02% w/v sodium azide aqueous solution. Glucose and very high molecular weight dextran markers were then added to these solutions. These markers indicated the total inclusion (V_t) and total exclusion (void, V_o) volumes respectively.

(b) The feed and product solutions from the experiments usually did not need any preparation. Solutions which were too dilute were concentrated to 2% w/v using a Buchi Rotary evaporator. Solutions which were too concentrated were diluted to 2% w/v.

If the experimental samples contained no sodium azide, sufficient azide was added to obtain a sample with a 0.02% w/v sodium azide concentration.

Where sodium azide was present no extra azide was added. This was due to the fact that the azide concentration could not be measured. Therefore, the correct amount of sodium azide could not be calculated.

Figure 3.9

The Results of Aston's GPC Calibration (Old Columns)

Batch Numbers	Weight Average Molecular Weights		GPC x 100 / L.S.
	L.S.	GPC	
3202	490000	493715	100.76
1343	231000	229485	99.34
921	154000	153382	99.60
5403	72000	71594	99.44
2540	44400	44588	100.42
2514	41800	42595	101.90
7968	22300	22280	99.91
3205	9300	9171	98.61
Stachyose	667	671	100.60
Glucose	180	180	100.00

Calibration Constants

b_1	b_2	b_3	b_4	b_5
-16.634	21.702	-16.606	16.067	87.798

Figure 3.10 GPC Calibration Curve on Aston's Old TSK-PW Columns

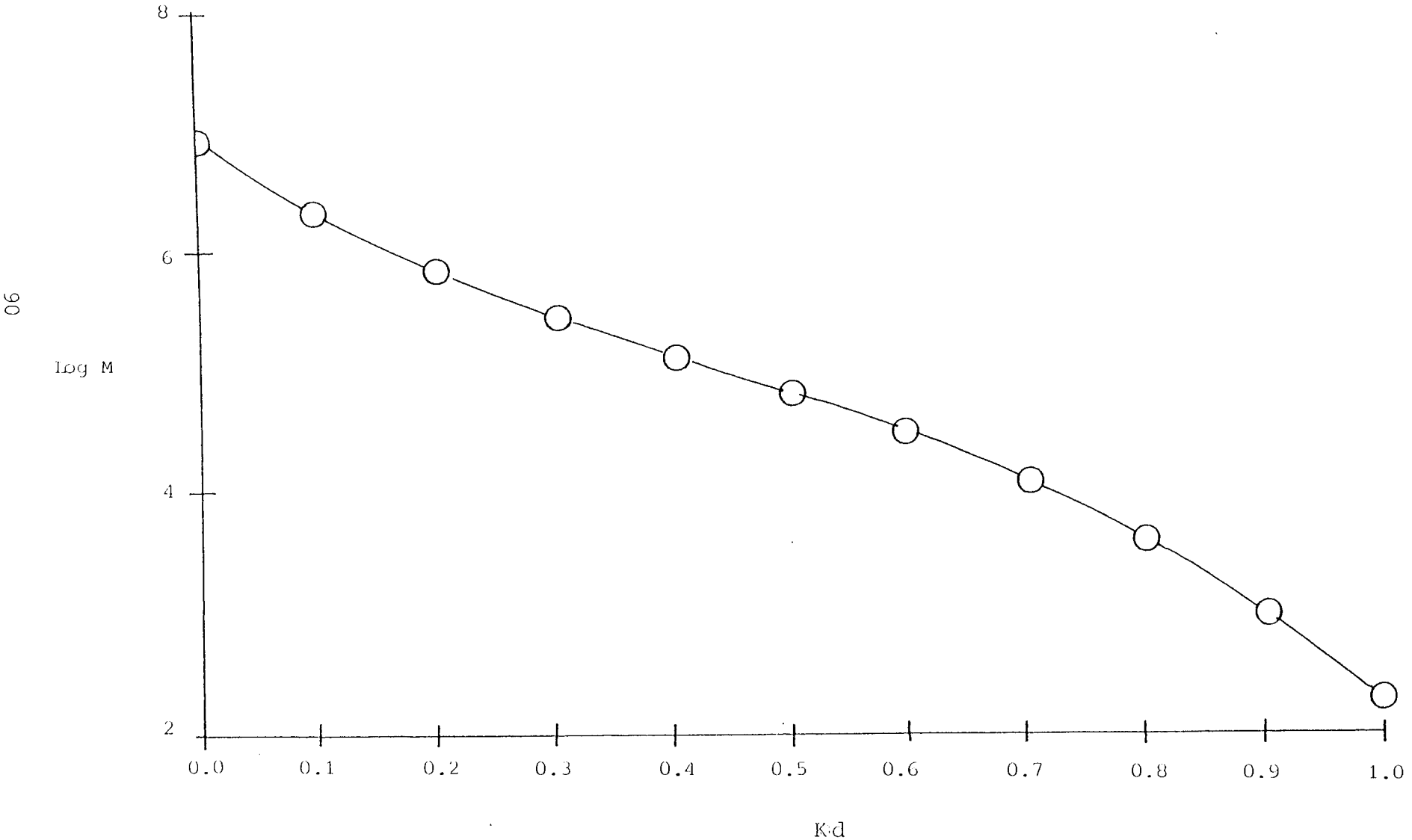

Figure 3.11

The Results of Aston's GPC Calibration (New Columns)

Batch Numbers	Weight Average Molecular Weights		GPC x 100 / L.S.
	L.S.	GPC	
PT 3636	239825	244153	101.80
PH 1078	149600	144398	96.52
PG 7427	104450	103450	99.04
PF 1601	73625	74003	100.51
PB 5227	42150	42457	100.73
PE 5382	21975	23451	106.72
PA 0094	11500	10892	94.71
JD 2985	8825	8377	94.92
DK 8868	5250	5140	97.90
PD 2335	4100	4331	105.63
Glucose	180	180	100.00

Calibration Constants

b_1	b_2	b_3	b_4	b_5
-13.663	12.758	-9.547	15.987	-73.385

Figure 3.12 GPC Calibration Curve on Aston's New TSK-PW Columns

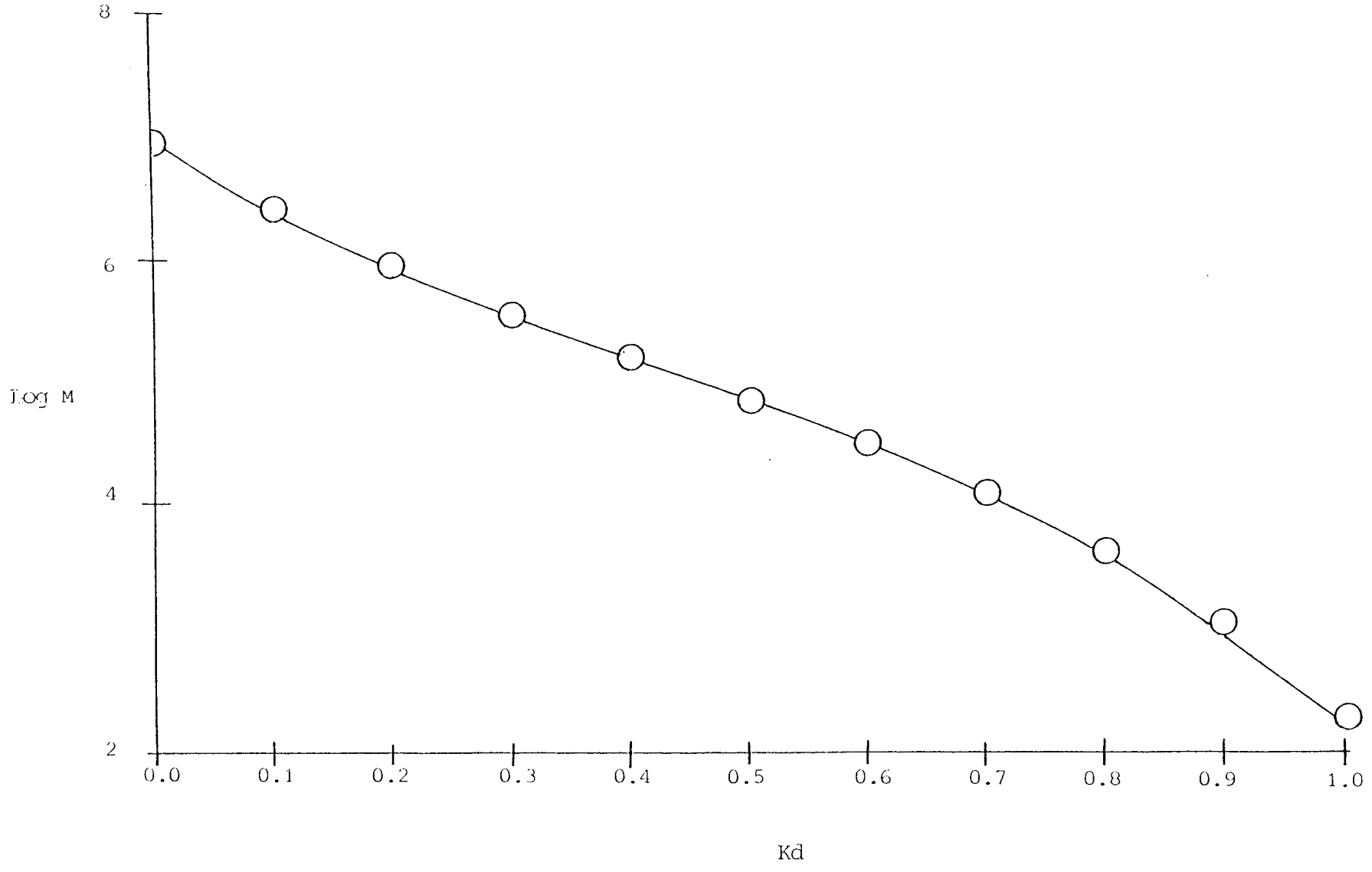

In all cases glucose was added as a V_t marker.

The samples were then filtered and injected into the columns via the six-port injection valve.

The differential refractometer had a full scale deflection of 100 mV. The chart recorder and the multiplexer were both adjusted to this value. The zeroing of the differential refractometer and the chart recorder are explained by Waters Associates (122) and Smiths manual (123) respectively.

The eluent flowrates through the columns were measured by weighing the eluate collected in a known period of time.

The interstitial volume was taken to be at the peak maximum of the V_o (high molecular weight dextran) marker chromatogram.

The total liquid volume of the columns (V_t) was marked by the peak maximum of the glucose chromatogram.

3.3.5 DATA ACQUISITION USING A PET COMPUTER

To be able to calculate the molecular weight distribution of a sample, from its chromatogram, the heights at set time periods are required from the chromatogram.

When the GPC analytical system was first installed at Aston these heights were obtained by measuring the chromatogram with a ruler. This method was time consuming and laborious. Also, if the heights were not measured at an exact perpendicular to the base-line large variations in the final molecular weight distribution would be obtained. Therefore, when this research was begun this manual method was replaced by an on-line data acquisition system.

This system consisted of a multi-plexer, Commodore PET computer (Model CBM 4032) and a Commodore printer (Model CBM 4022 P).

A listing of the programme used for this data acquisition is given in Appendix 1. This program recorded the heights of the chromatogram in the following step.

(a) At the moment a sample was injected into the columns the data acquisition programme was started and the initial reading of the differential refractometer was recorded via the multi-plexer (see Section 3.3.1). Also at this point the internal clock of the computer was set to zero.

(b) After a two second delay another reading was then taken from the refractometer. This procedure was repeated until five readings had been taken. These five readings were then averaged to give one reading for the first 10 seconds of the chromatogram.

(c) Once the average for the first 10 seconds was obtained, the programme then started measuring the heights, every two seconds, for the next 10 second average. This procedure was repeated over the whole time period of the sample. To help the operator of the analysis these two second readings and the run time since the injection of the sample were continually displayed on the computer's VDU. This display helped with the zeroing of the refractometer during the initial part of an analysis.

(d) The end of the chromotogram could be determined either when the sample peak returned to the base-line or by a timer within the data acquisition programme.

Once the sample had finished the recorded heights were printed out, within one minute, and were ready for use in the calculation of the average molecular weights and the molecular weight distribution.

3.3.6 CALCULATION OF THE MOLECULAR WEIGHT DISTRIBUTION AND THE AVERAGE MOLECULAR WEIGHTS

To convert the chromatogram of a sample into a molecular weight distribution the following information was required:

(a) The heights measured at regular time intervals along the chromatogram.

(b) The elution time of the very high molecular weight dextran peak (for calculation of the void volume, V_o).

(c) The elution time of the glucose peak (for calculation of the total liquid volume, V_t).

(d) The start and finish on the chromatogram.

(e) The calibration constants b_1-b_5.

Once this data was available the distribution was calculated using the following equations:

(a) $$M_i = b_5 + \exp [b_4 + b_1 (K_{di}) + b_2 (K_{di})^2 + b_3 (K_{di})^3] \quad \ldots\ldots 3.3$$

(b) $$K_{di} = \frac{V_i - V_o}{V_t - V_o} \quad \ldots\ldots 3.4$$

(c) $$\text{Weight fraction, } (h_i) = \frac{\text{chromatogram height, } h_i}{\text{Total chromatogram heights } \Sigma h_i} \quad \ldots\ldots 3.6$$

An example of a molecular weight distribution is given in Appendix 2 together with a listing of the computer program used.

Due to the polydisperse nature of dextran it is not generally possible to characterise it by a single molecular weight and the mass of the polymer can only be completely described by a molecular weight distribtion. However, instead of a single molecular weight, various averages can be used. Of these averages the most common are:

$$\text{Weight Average, } \bar{M}_W = \frac{\Sigma h_i M_i}{\Sigma h_i} \quad \ldots\ldots 3.7$$

$$\text{Number Average, } \bar{M}_N = \frac{\Sigma hi}{\Sigma h_i/M_i} \quad \ldots\ldots 3.8$$

For polydisperse polymers $\bar{M}_W$ is always greater than $\bar{M}_N$, except that the values are equal for a monodisperse polymer.

The term polydispersity is often used to describe the breadth of the molecular weight distribution and is defined as:

$$\text{Polydispersity, } D = \frac{\overline{M}_W}{\overline{M}_N} \qquad \ldots\ldots\ 3.9$$

This polydispersity ratio is 1.0 for a monodisperse sample, while most commercial synthetic polymers have ratios in the range 2-20.

4.0 DETERMINATION OF THE MOST EFFICIENT MAKE OF MEMBRANE

4 DETERMINATION OF THE MOST EFFICIENT MAKE OF MEMBRANE

4.1 INTRODUCTION

As stated previously, this research was a continuation of the ultrafiltration work conducted by Vlachogiannis (12, 13, 14). The results obtained by Vlachogiannis were based almost solely on membranes manufactured by Amicon Ltd (124). Therefore, the initial part of this work was concerned with investigating whether there were more efficient makes of membrane on the market for fractionating dextran polymer solutions.

Initially a search of the literature was conducted to find suppliers of ultrafiltration membranes. A list of these suppliers is given in Figure 4.1.

Unfortunately, most of the membrane makes discovered each required unique equipment for their operation. The purchase, or construction costs of this equipment was prohibitive and therefore several membrane manufacturers were approached for the loan of the necessary equipment. An example of these high costs is the De Danske Sukkerfabrikker (DDS) membranes which requires a £4000 membrane holder unit and a £9000 pump.

However, of the firms approached only two were willing to loan the necessary equipment. These were Millipore (UK) Ltd (125) and DDS (5).

4.2 EXPERIMENTS CONDUCTED USING MEMBRANES MANUFACTURED BY MILLIPORE LTD

4.2.1 INTRODUCTION

The Millipore membranes have a molecular weight cut-off range of 1000 to 1000 000 and are produced in either membrane disc or cassette form. A schematic of the cassette system is given in Figure 4.2 and the actual unit in Figure 4.3. This cassette system can accommodate a total membrane area of 0.5 to 2.5 m^2 (5 to 25 ft^2). The membranes come preassembled and pretested in layers of filters and screens, ready to install, with a total membrane area of 0.5 m^2 (5 ft^2).

MWCO	NUCLEPORE	AMICON	DDS	MILLIPORE	PATERSON-CANDY	SARTORIUS	DORR-OLIVER	MICRO-FILTRATION SYSTEMS
1000	D, FS, SW	D, HF	-	D	-	-	D	D
2000	-	HF	-	-	-	-	-	-
3000	-	HF	-	-	-	-	-	-
5000	D, FS, SW	D, HF	-	-	-	-	D	-
6000	-	-	FS	-	T (7000)	-	-	-
10000	D, FS, HF,SW	D, HF	-	C,D	T (12000)	D	D	D
20000	D, FS, SW	-	FS	-	T	D	-	D
25000	-	-	FS	D	T	-	-	-
30000	-	D	FS	-	-	D	D	-
50000	D,FS,HF,SW	D,HF	-	-	-	D	D	D
65000	-	-	FS	-	-	D (70000)	-	-
100000	D,FS,HF,SW	D,HF	-	C,D	-	D	D	-
300000	-	D	-	-	-	D	D	D (200000)
5000000	D,FS,SW	-	-	-	-	-	-	-

MWCO: Molecular Weight Cut-off

C = Cassette; D = Disk; FS = Flat Sheet: HF = Hollow Fibre; SW = Spiral Wound; T = Tubular

Figure 4.1: Trade Survey of Ultra-Filtration Membrane Manufacturers

Figure 4.2: Schematic Diagram of Millipore Cassette Membrane System

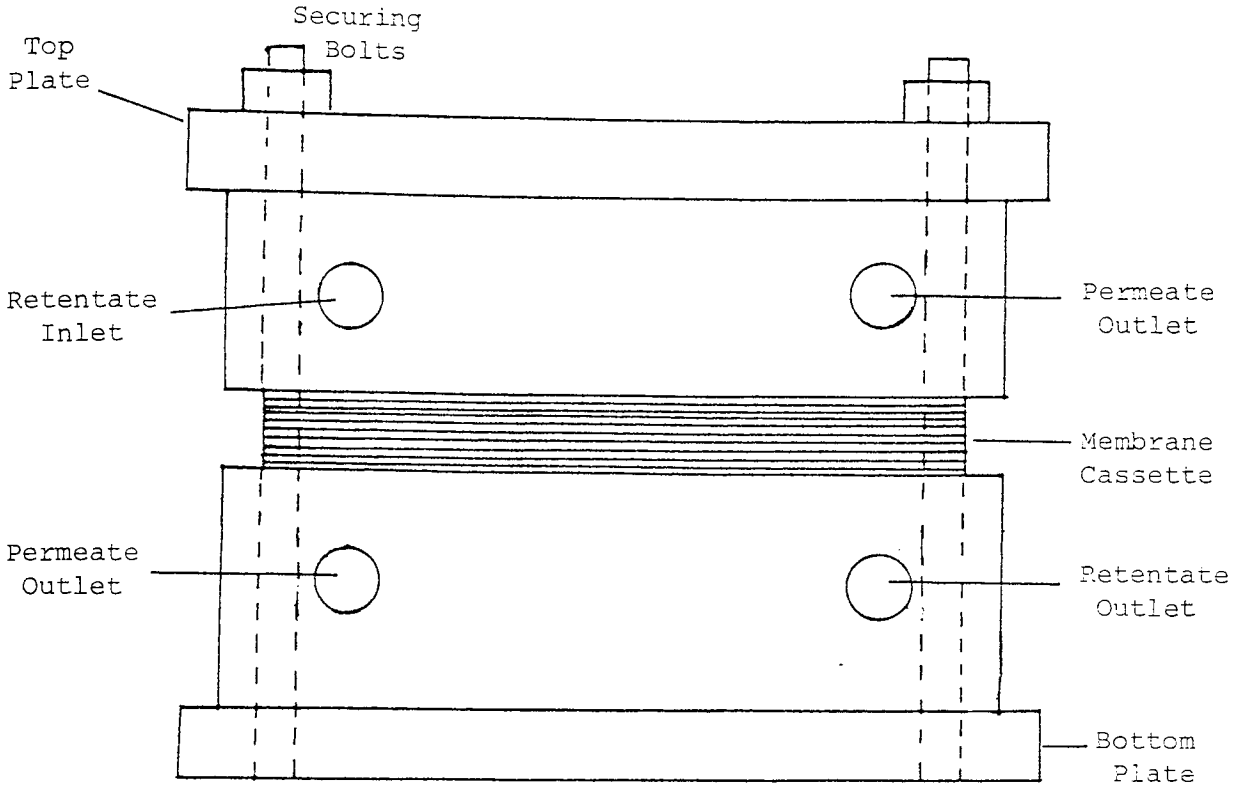

Composition of Cassette Membrane

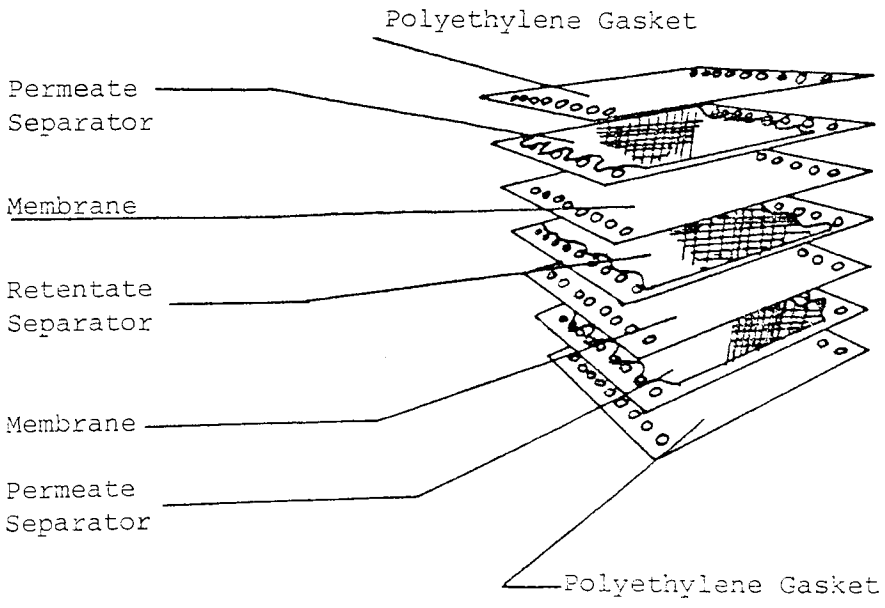

Figure 4.3: Photograph of a Millipore Cassette Membrane Holder Unit

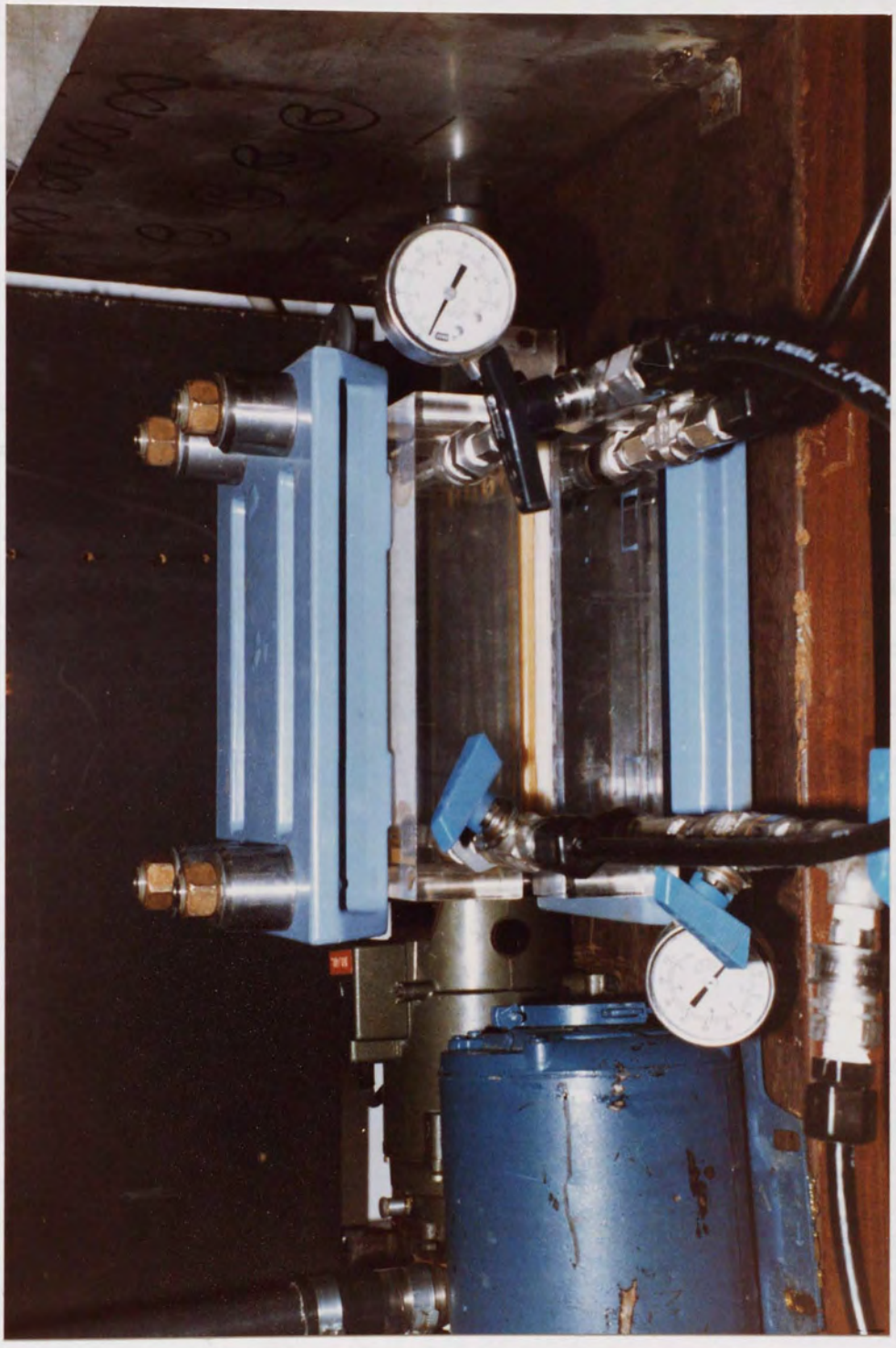

The Millipore membranes are constructed from polysulphone, with the exception of the 1000 and 1000 000 cut-off membranes which are constructed from Cellulosic polymer.

These Millipore membranes were to be compared to the Amicon 5 000 molecular weight (MW) cut-off membrane used and recommended by Vlachogiannis (14). Ideally a Millipore 5 000 MW cut-off membrane was required. Unfortunately such a MW cut-off membrane was not produced and therefore the Millipore 10 000 MW cut-off membrane was tested. This membrane was the closest standard Millipore membrane to the Amicon 5 000 and also it was produced in an equivalent larger industrial size unit. This need for the membrane to have an industrial equivalent was important if the results were to be used in calculating the size and costs of an actual industrial process.

Even though the 10 000 MW cut-off membrane was the tightest standard one available, a Millipore 1000 MW cut-off membrane was also tested. This membrane was said by Millipore Ltd to be experimental and had to be obtained from the USA. It was tested because although experimental, it too was to be produced in an industrial sized equivalent if successful.

Both the 10 000 MW cut-off and the 1000 MW cut-off membranes were of the cassette configuration.

4.2.2 MILLIPORE 10 000 MW CUT-OFF MEMBRANE

The equipment layout used is shown in Figure 4.4. The equipment consisted of two stainless-steel tanks, a recirculation pump (centrifugal) and the Millipore cassette holder unit.

The two tanks were used as a feed tank and permeate collection tank, with the processed retentate being recycled back to the feed tank. Since this experiment was to be conducted under the dia-filtration constant volume mode of operation as recommended by Vlachogiannis, a level controller was added to the feed tank. This level controller added de-ionised water (from two storage tanks) to the feed solution at the same rate as permeate was produced.

Figure 4.4 Schematic Diagram of the Equipment Layout used to Test Millipore Membranes

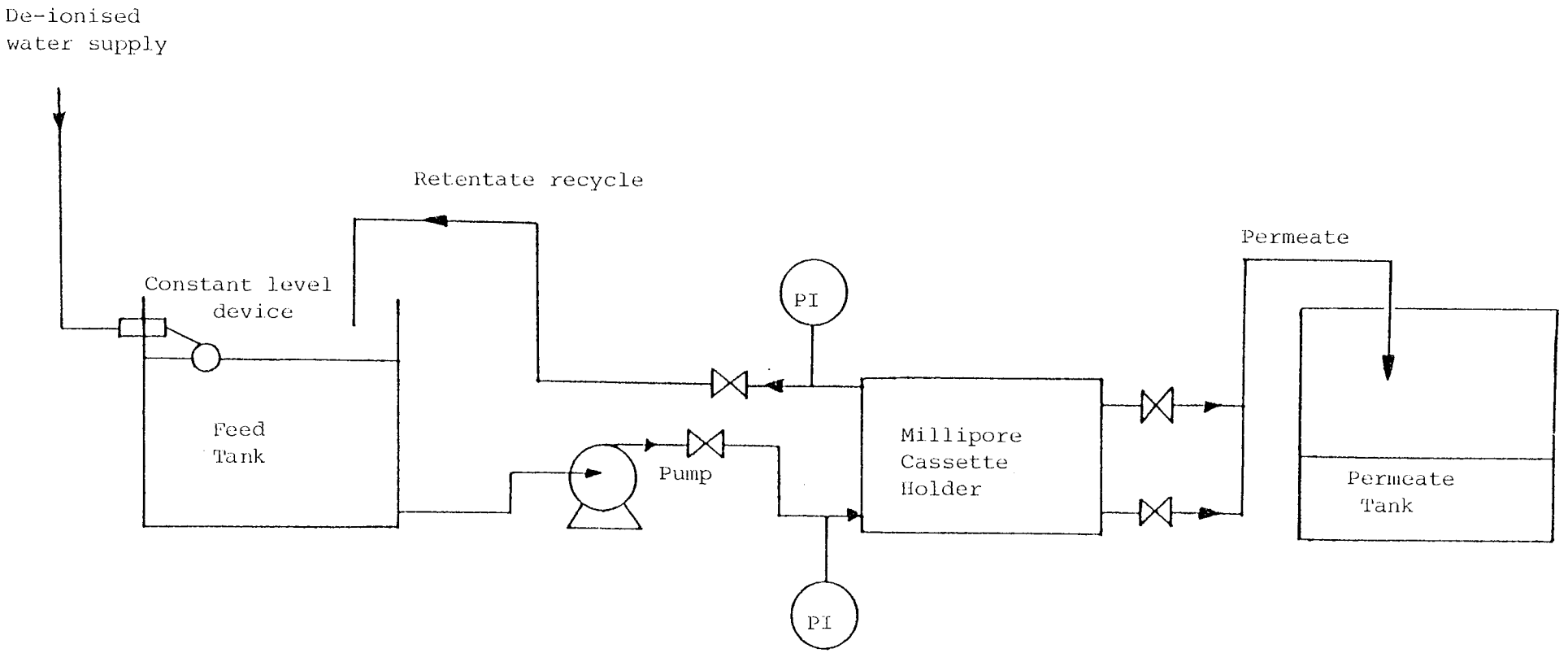

The cassette holder unit supplied by Millipore had a capability to hold five sets of membrane cassette units. However, in this experiment only two sets were used giving a total membrane surface area of 0.9 m^2 (10 ft^2).

The pump was set to give the required minimum recirculation rate of 300cm^3/min m^2.

The pressure in the cassette unit could be varied by either the inlet or exit valves of the unit. In accordance with recommendations from Millipore the inlet valve was left fully open and the exit valve was used to set a 1.5 Kg/cm^2 transmembrane pressure.

The feed used for this experiment was from a Fisons dextran batch of code HZ16K. This batch had supplied the feed used by Vlachogiannis (12) in his Amicon experiments. It had a weight average molecular weight ($\overline{M}_W$) of 89749, with 30% of its molecular weight distribution below 12 000 daltons.

The initial feed concentration (2%), number of washes (a wash is the ratio of volume of permeate collected to the volume of feed), and operating temperature were also the same as used by Vlachogiannis. These factors therefore ensured that any result obtained from this experiment could be compared to those obtained by Vlachogiannis.

The results obtained for this membrane are summarised in Figure 4.5 to Figure 4.9.

A comparison of the Millipore 10 000 MW cut-off membrane against the Amicon 5 000 MW cut-off membrane (12) is given in Figure 4.10.

From these results it can be seen that the Millipore membrane could be used to fractionate the low molecular weight dextran, since it removed 80% of the material below 12 000 daltons from the feed. However, when this performance is compared with that of the Amicon membrane (Figure 4.10), the Millipore membrane not only removed less material below 12 000 daltons but also removed more material above 12000 (35% compared to 30% for Amicon). Therefore, the Amicon 5000 MW cut-off membrane is more efficient than the Millipore 10 000 MW cut-off membrane in fractionating low molecular weight dextran.

Figure 4.5

Molecular Weight Results for Millipore 10 000 Molecular Weight Cut-ff Membrane

Time (Hrs)	Retentate					Permeate		
	$\bar{M}_W$	$\bar{M}_N$	% Less than 12,000 MW	% Between 12,000 & 98,000 MW	% Greater than 98,000 MW	$\bar{M}_W$	$\bar{M}_N$	Efficiency†
0	89749	10648	28	62	10	-	-	-
0.5	102346	13885	24	64	12	16822	6076	92%
1.0	148483	15971	23	63	14	17766	5844	81%
2	137508	19950	16	69	15	20810	8230	77%
3	131444	26303	14	70	16	22808	10553	68%
4	131008	26723	10	73	17	24169	11959	65%

† Efficiency = $\frac{\text{Weight of 'saleable' Dextran in Product}}{\text{Weight of 'saleable' Dextran in Feed}}$

Table 4.6: MASS BALANCE RESULTS FOR MILLIPORE 10 000 MEMBRANE

Time (Hrs)	RETENTATE				PERMEATE				
	Volume (Litres)	Weight of Dextran (gms)	% Less 12 000 MW	Lowest MW	Volume (Litres)	Weight of Dextran (gms)	Lowest MW	Highest MW	% Less 12 000 MW
0	50	900	28	500	-	-	-	-	-
0.5	50	800	24	451	21	100.8	350	122708	57
1	50	715	23	602	42	180.6	601	77060	55
2	50	620	18	1056	84	285.6	1074	105043	50
3	50	540	14	1414	126	357	1389	115019	48
4	50	495	10	1297	168	411	819	121234	48

Figure 4.7 Overall Mass Balance for Millipore 10,000 Molecular Weight Cut-off Membrane

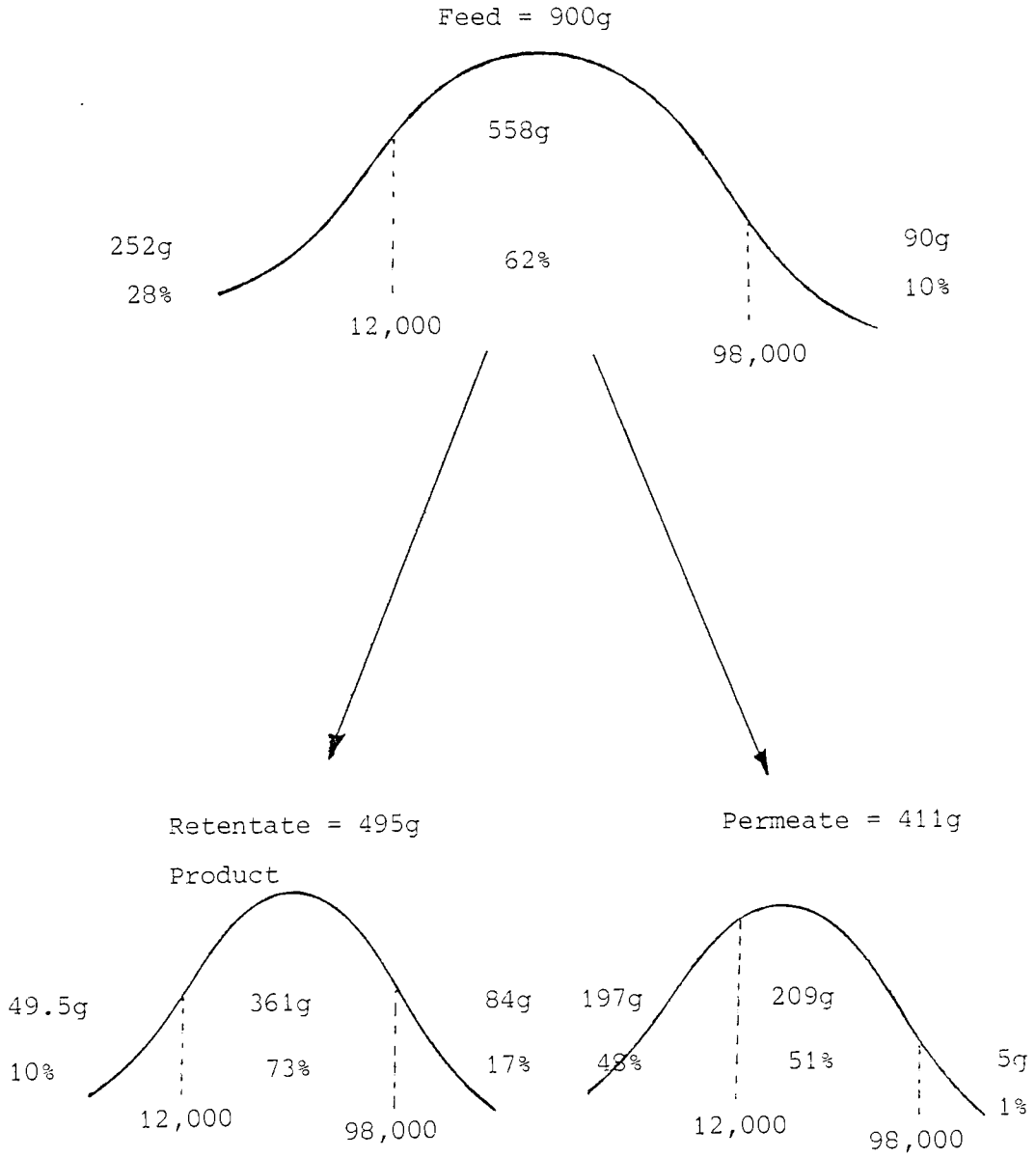

Figure 4.8 Mass of Dextran in Permeate Versus Number of Diavolumes for Millipore 10,000 Molecular Weight Cut-off Membrane

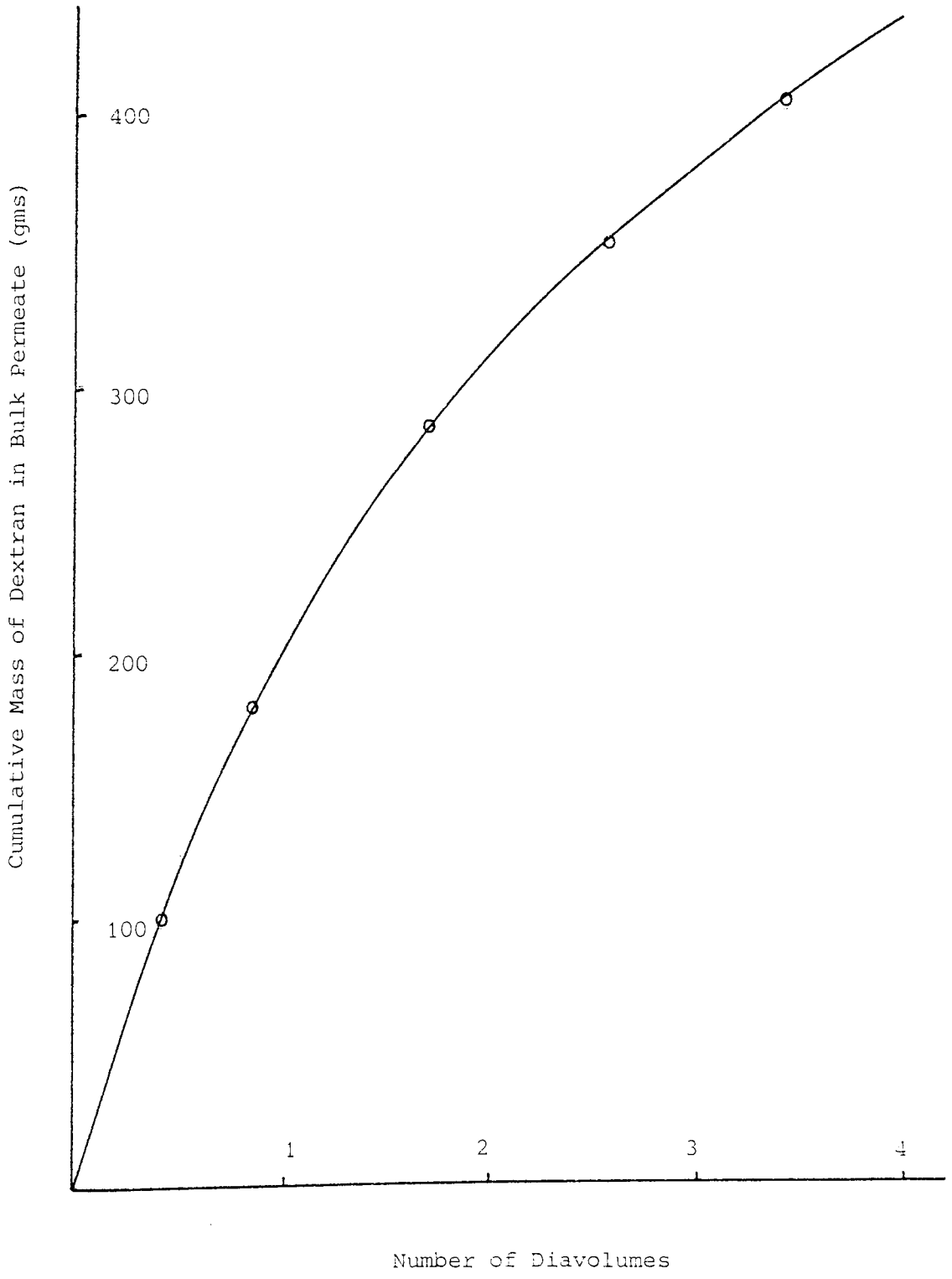

Figure 4.9 Percentage of Dextran in the Retentate, Below 12,000 Molecular Weight, Versus Number of Diavolumes for Millipore 10,000 Molecular Weight Cut-off Membrane

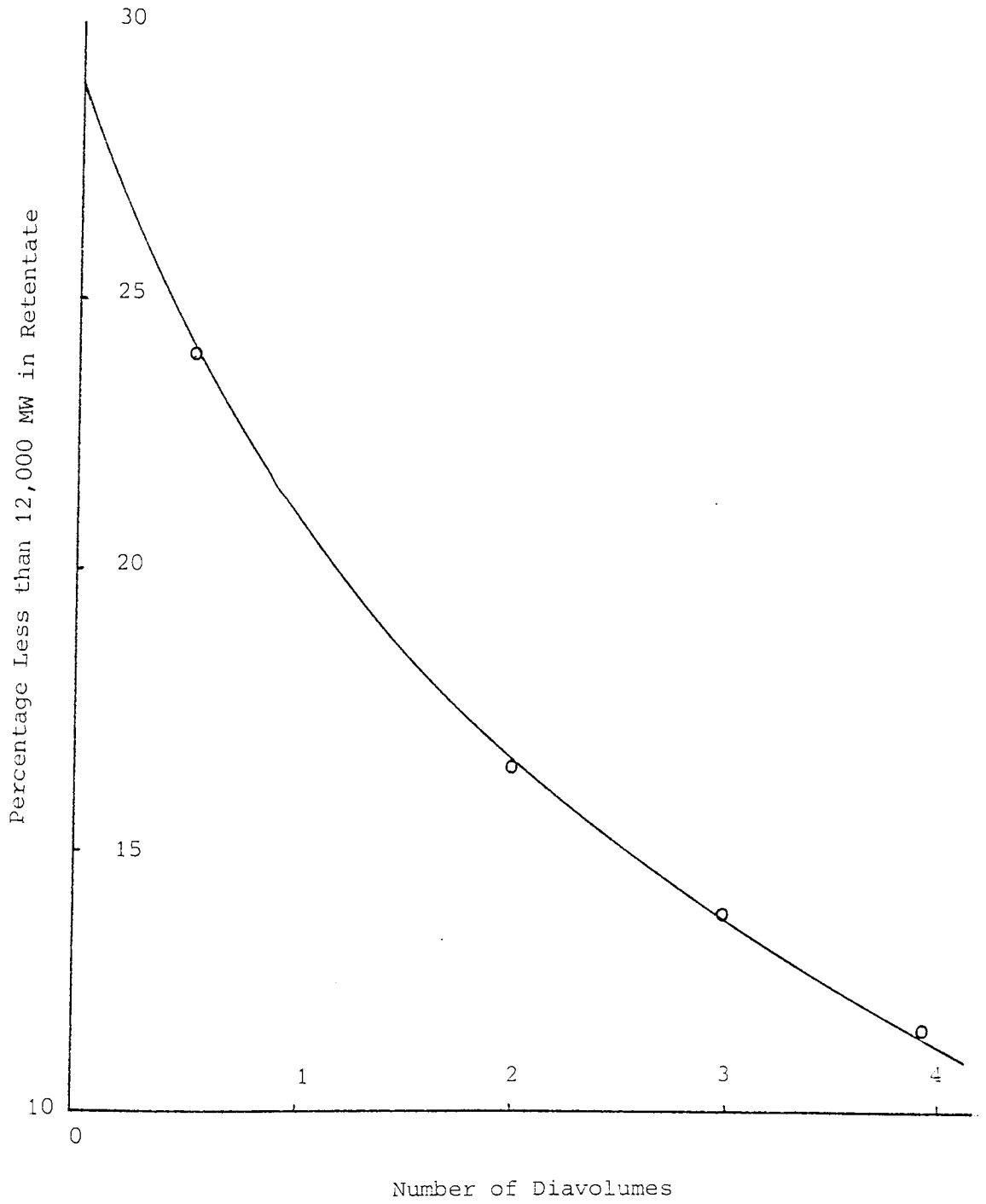

Figure 4.10

COMPARISON OF MILLIPORE 10 000 CUT-OFF MEMBRANE AND AMICON 5000 MEMBRANE (12)

Area used:	Millipore = 0.9 m^2 (10 ft^2) Amicon = 0.9 m^2
Permeate flux:	Millipore = 42 L/m^2 hr Amicon = 28 L/m^2 hr
Trans-membrane pressure used:	Millipore = 1.5 Kg/cm^2 Amicon = 0.8 Kg/cm^2
Maximum MW in permeate:	Millipore = 123 000 Amicon = 90 000
% of material below 12 000 daltons removed from feed:	Millipore = 80% Amicon = 87%
% of material between 12 000 and 98 000 daltons removed from feed:	Millipore = 35% Amicon = 30%

This lower efficiency of the Millipore membrane was due to two main factors. These were (a) the larger pore size present in the 10 000 cut-off membrane compared to the Amicon 5 000 cut-off membrane, and (b) the higher transmembrane pressure used in the Millipore membrane experiments.

Initially it was hoped that these two factors would enable the permeation of the small dextran molecules to be greater than the Amicon membrane, but at the same time still enabling the membrane to reject dextran above the 10 000 cut-off. However, it appears that the greater shear forces produced (by the high transmembrane pressure) in the Millipore membrane caused the larger dextran molecules (ie. 120 000 daltons) to deform and pass through the small pores of the membrane. This therefore agrees with the theory postulated by both Baker (85) and Nguyen (127) (see Section 2.4.2.1).

Throughout this dia-filtration experiment the volumetric permeate flux of the Millipore membrane remained constant (Figure 4.6). This was unexpected since, as the retentate concentration decreased, the flux should have increased according to the equation:

$$J = K \ln\left[\frac{C_w}{C_b}\right] \qquad \ldots\ldots\ 2.16$$

where K is the solute mass transfer coefficient,

J is the volumetric permeate flux,

C_b is the bulk concentration of the retentate,

C_w is the concentration of the retentate at the membrane wall.

As C_b decreased it was expected that J would increase, thus causing C_w to decrease at a lower rate than C_b. C_w decreasing would cause the concentration of solute in the permeate to decrease, but this still would have caused C_b to decrease. This procedure should have been repeated until a pure water flux was obtained (when C_b = O).

Since the permeate flux (J) remained constant this tends to suggest that one particular MW band of dextran controlled the amount of flux produced. This controlling band was assumed to be high MW dextran (200 000 + daltons) since this material was almost totally rejected by the membrane. Therefore, this band had a constant concentration (C_b value), and would give a constant flux (J).

During this experiment a discrepency was noted between the clean water flux before and after the diafiltration run. This discrepency was assumed to be due to the presence of a gel layer on the membrane surface.

The presence of the gel layer could normally be verified by means of the overall mass balance. If a gel layer is formed, the balance would be negative since material is left on the membrane surface. However, in this experiment due to errors incurred in the analytical techniques employed ($\pm$ 2% from HPLC and $\pm$ 2% from GPC) an accurate mass balance could not be obtained.

An indication of the presence of the gel layer was given by the values of the clean water flux, before and after the experiment. Before the experiment the flux was 80 L/m^2 hr. Immediately after the experiment the clean water flux was only 50 L/m^2 hr. After washing the membrane with over 300 Litres of clean water the flux increased to 75 L/m^2 hr. This washing had removed almost all the gel layer present, and therefore the clean water flux returned to normal.

While the volumetric permeate flux remained constant during the experiment the mass rate of dextran passing through the membrane decreased asymptotically (Figure 4.8). Also the actual molecular weights of the molecules passing through the membrane increased during the experiment. This is shown by the increase of $\overline{M}_W$ for the permeate (Figure 4.5). Both of these occurrences were assumed to be due to the depletion of the lower molecular weights as the experiment progressed.

4.2.3 MILLIPORE 1000 MW CUT-OFF MEMBRANE

The Millipore 1000 molecular weight cut-off membrane was tested using the same equipment and operating parameters as the Millipore 10 000 MW cut-off membrane.

The results obtained are summarised in Figures 4.11 to 4.14. A comparison of the Millipore 1000 and 10 000 membranes is given in Figure 4.15.

From these results it can be seen that:

(a) both the Millipore membranes had the same volumetric permeate flux.

(b) the Millipore 1000 MW cut-off membrane allowed through larger molecules than did the Millipore 10 000 membrane.

(c) a higher percentage of the larger molecules (12 000+ daltons) passed through the Millipore 1000 membrane than through the Millipore 10 000 membrane.

(d) less material below 12 000 daltons was removed with the Millipore 1000 membrane than with the Millipore 10 000 membrane.

This last point (d) was expected since the Millipore 1000 membrane was supposed to be a 'tighter' membrane than the 10 000 membrane. However, the first three points were contradictory to what was expected, and tend to indicate that the Millipore 1000 membrane had larger pore sizes than the Millipore 10 000 membrane.

When Millipore were approached with the comparison of these results they agreed that either the membrane or the cartridge itself was faulty.

Unfortunately, no replacement membrane could be obtained and this experiment was abandoned.

4.3 EXPERIMENTS CONDUCTED USING MEMBRANES MANUFACTURED BY DDS LTD

4.3.1 INTRODUCTION

The DDS range of ultra-filtration membranes have nominal molecular weight cut-offs from 6 000 daltons to 100 000 daltons.

These membranes are of the flat-sheet configuration and for the purpose of these experiments a DDS Lab-Module 20 (126) was borrowed to house them. Figures 4.16

Figure 4.11

Molecular Weight Results for Millipore 1000 Molecular Weight Cut-off Membranes

Time	Retentate					Permeate		
	$\bar{M}_W$	$\bar{M}_N$	% Less than 12,000 MW	% Between 12,000 & 98,000 MW	% Greater than 98,000 MW	$\bar{M}_W$	$\bar{M}_N$	Efficiency†
0	81479	8996	30	60	10	-	-	-
2	88764	12560	25.5	63.5	11	26367	5772	83%
4	122508	14504	23	64	13	28654	6725	71%
6	127220	16553	20	66	14	28697	7992	58%
8	128168	18908	17.5	67.5	15	29557	7297	56%

† Efficiency = $\frac{\text{Weight of 'saleable' Dextran in Product}}{\text{Weight of 'saleable' Dextran in Feed}}$

Table 4.12: MASS BALANCE RESULTS FOR MILLIPORE 10 00 MEMBRANE

Time (Hrs)	RETENTATE				PERMEATE				
	Volume (Litres)	Weight of Dextran (gms)	% Less 12 000 MW	Lowest MW	Volume (Litres)	Weight of Dextran (gms)	Lowest MW	Highest MW	% Less 12 000 MW
0	50	965	30.1	380	-	-	-	-	-
2	50	760	25.5	501	42	201.6	381	278000	45.5
4	50	640	22.61	883	83	332	379	310000	41.13
6	50	504	19.9	887	124	465	378	305000	39.44
8	50	480	17.5	1167	168	487	379	310000	38.9

Figure 4.13 Mass of Dextran in Bulk Permeate Versus Number of Diavolumes for Millipore 1000 Molecular Weight Cut-off Membrane

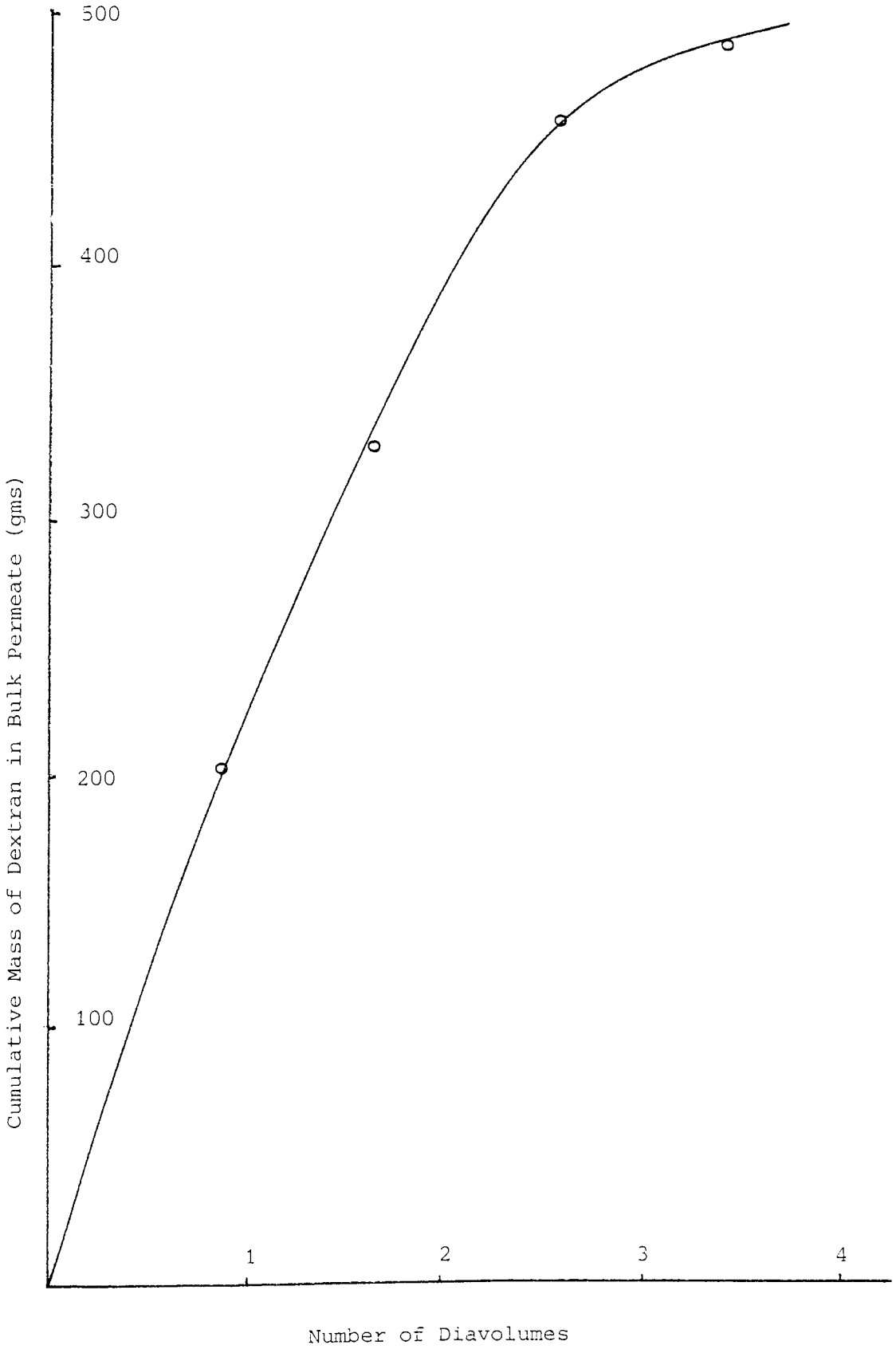

Figure 4.14 Percentage of Dextran in the Retentate, Below 12,000 Molecular Weight, Versus Number of Diavolumes, for Millipore 1000 Molecular Weight Cut-off Membrane

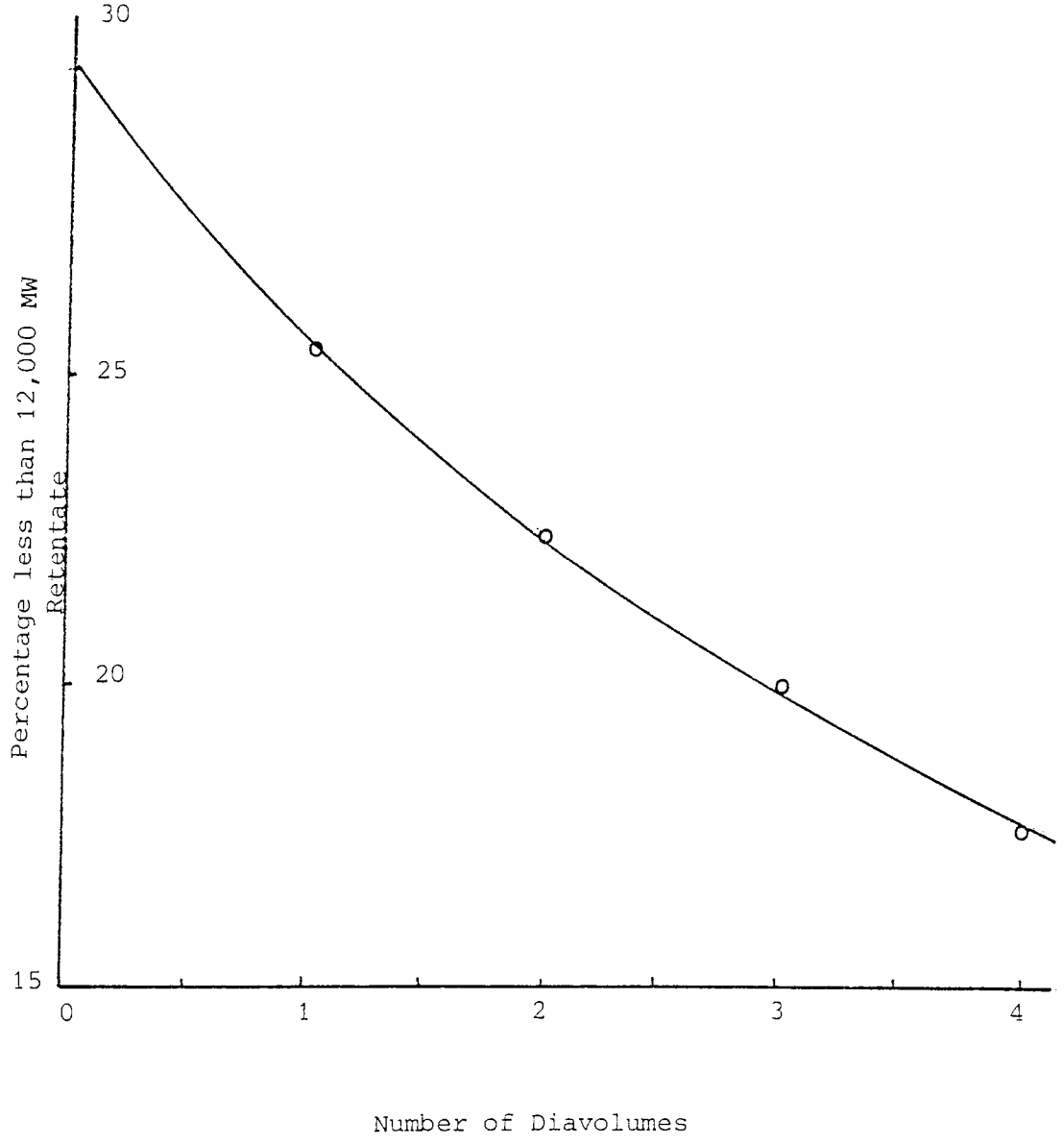

Figure 4.15

COMPARISON OF MILLIPORE 1000 MW CUT-OFF MEMBRANE AND MILLIPORE 10 000 MW CUT-OFF MEMBRANE

Area used:	Millipore 1K = 0.45 m^2 Millipore 10K = 0.9 m^2
Permeate flux:	Millipore 1K = 42 L/m^2 hr Millipore 10K = 42 L/m^2 hr
Maximum molecular weight in permeate:	Millipore 1K = 310 000 Millipore 10K = 123 000
% of material below 12 000 daltons removed from feed:	Millipore 1K = 65% Millipore 10K = 79%
% of material between 12 000 and 98 000 daltons removed from feed:	Millipore 1K = 44% Millipore 10K = 35%

to 4.19 show the construction of this module. The pump used was a high pressure Rannie pump which was also borrowed from DDS.

A schematic of the flow characteristics used in this module is given in Figure 4.20. Two membranes are placed on either side of a support plate and held in place by a plastic ring. This support plate is hollow and its surface is machined with grooves and holes (see Figure 4.21).

The permeate passing through the two membranes is chanelled in the grooves, passes through the holes into the centre of the support plate, then out through an exit port on the outside edge of the plate.

Between each set of two membranes there is a spacer plate (Figures 4.20 and 4.21). This spacer plate is chanelled so that the retentate is spread over the whole of the membrane surface. The processed retentate then passes through holes in the spacer plate to the next set of two membranes.

At the centre of the unit there is a hydraulic ram which is used to clamp the sandwich of membranes together. A pressure of 20 tonnes/cm^2 was used.

The membranes used with this equipment had molecular weight cut-offs of 6000 daltons, 25 000 daltons and 50 000 daltons. All these membranes were constructed from polysulphone.

The 6000 molecular weight cut-off membranes were the closest comparable DDS membranes to the Amicon 5000 membrane.

The DDS 25 000 and 50 000 membranes were used to investigate the fractionation of the high molecular weight dextran.

4.3.2 EXPERIMENTAL OPERATING CONDITIONS AND RESULTS OBTAINED

As with the Millipore experiments, the operating conditions were chosen to be similar to those used by Vlachogiannis (6). The only differences were in the trans-membrane pressure and retentate recirculation rate. These two parameters were set at the manufacturer's recommended values. The actual operating conditions used are given in Figure 4.22.

Figure 4.16: Photograph of a DDS Lab-Module 20, and a Rannie Pump

Figure 4.17: Photograph of a DDS Lab-Module 20 showing Permeate Collection

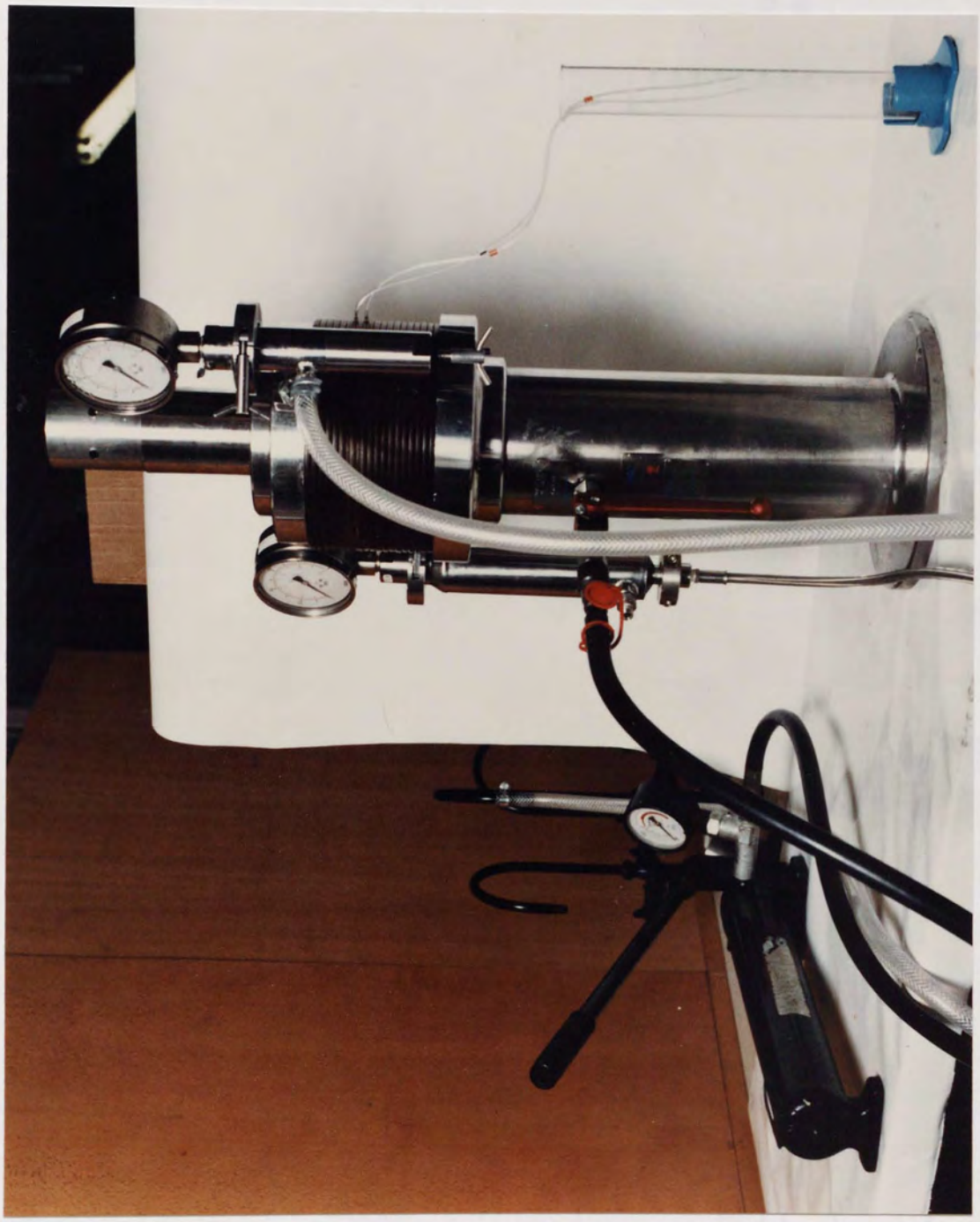

Figure 4.18: Schematic Diagram of DDS Lab-Module 20

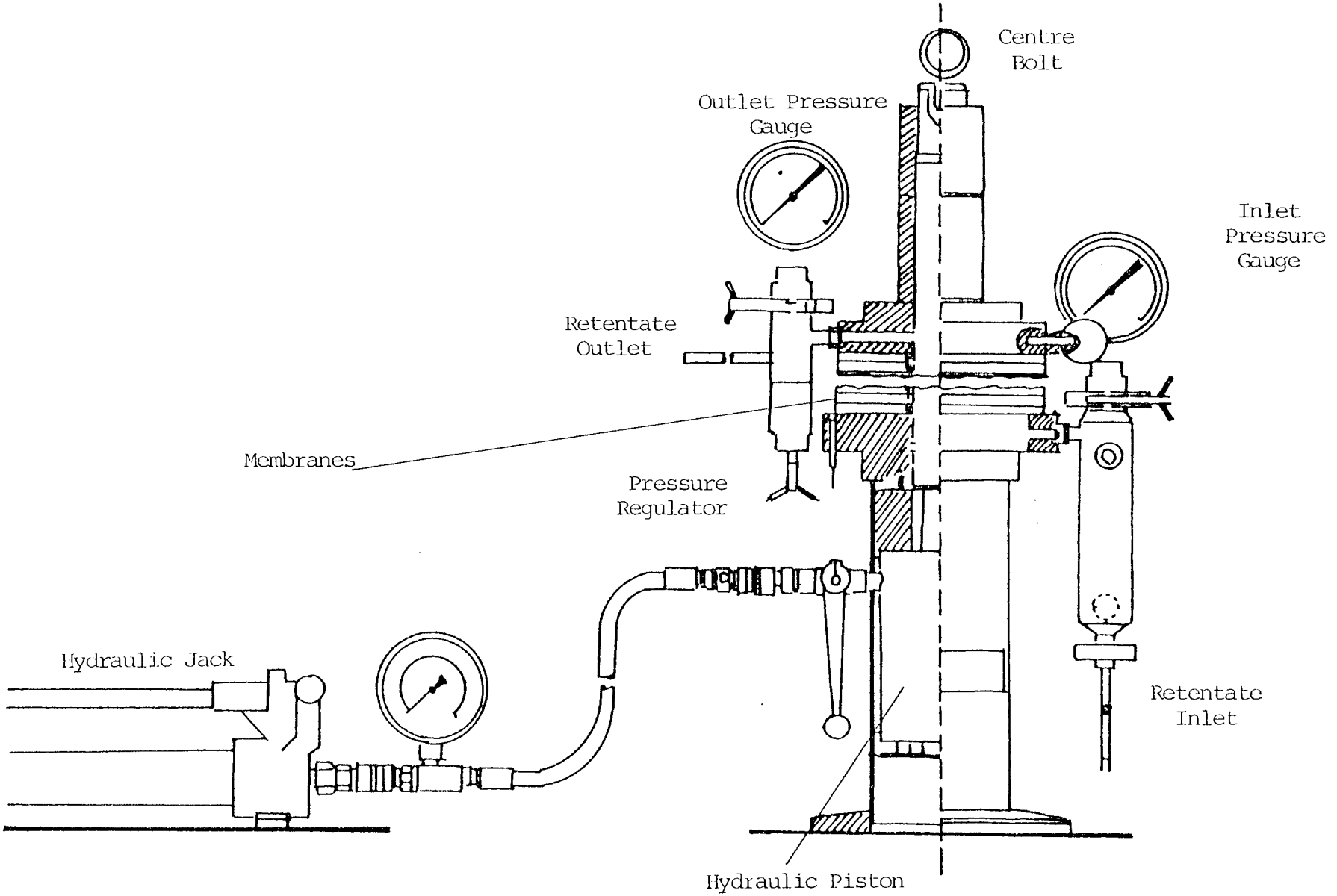

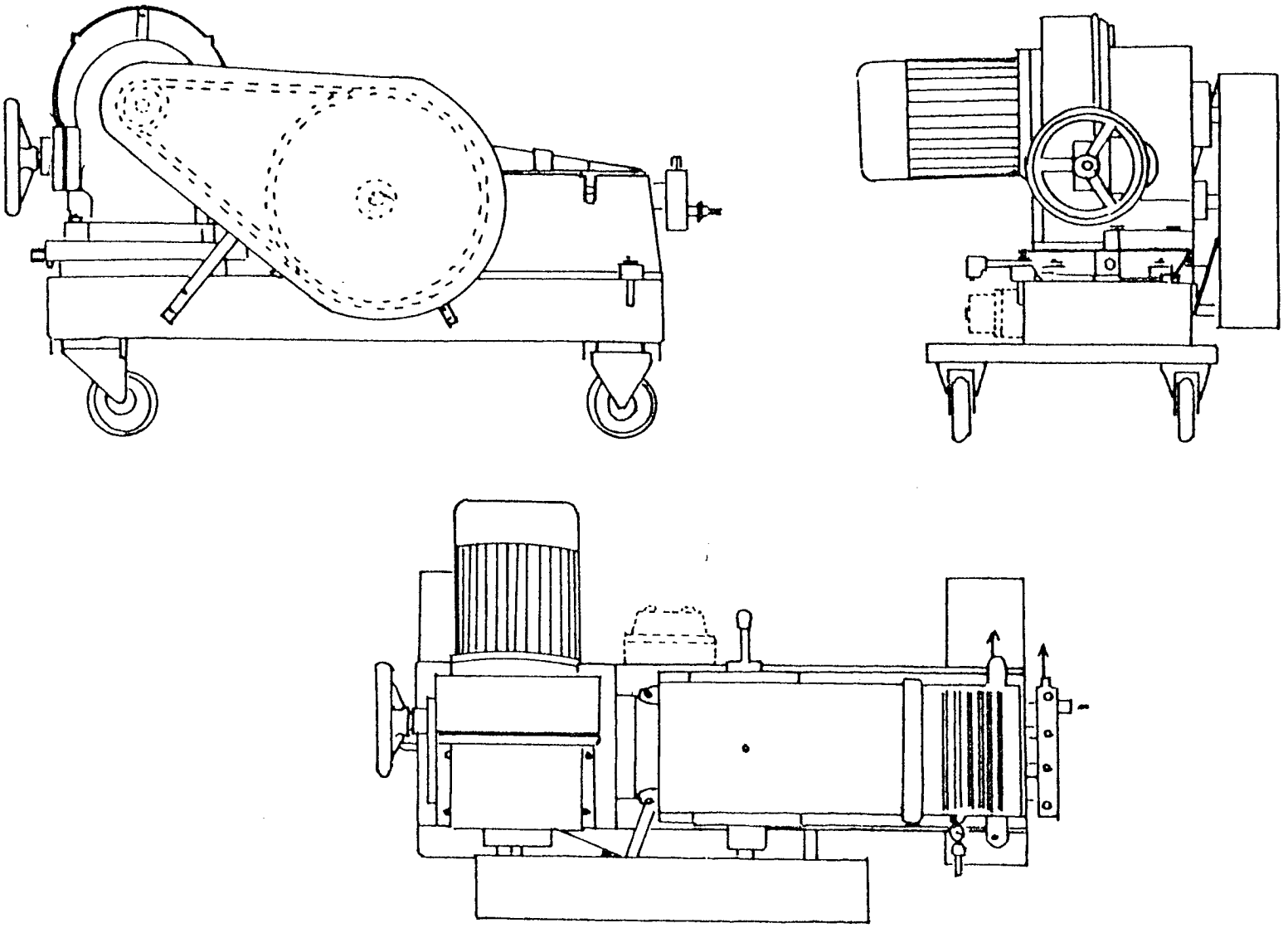

Figure 4.19: High Pressure, Variable Flow Rannie Pump

Figure 4.20 Schematic Diagram of the Flow Characteristics in the DDS UF Module

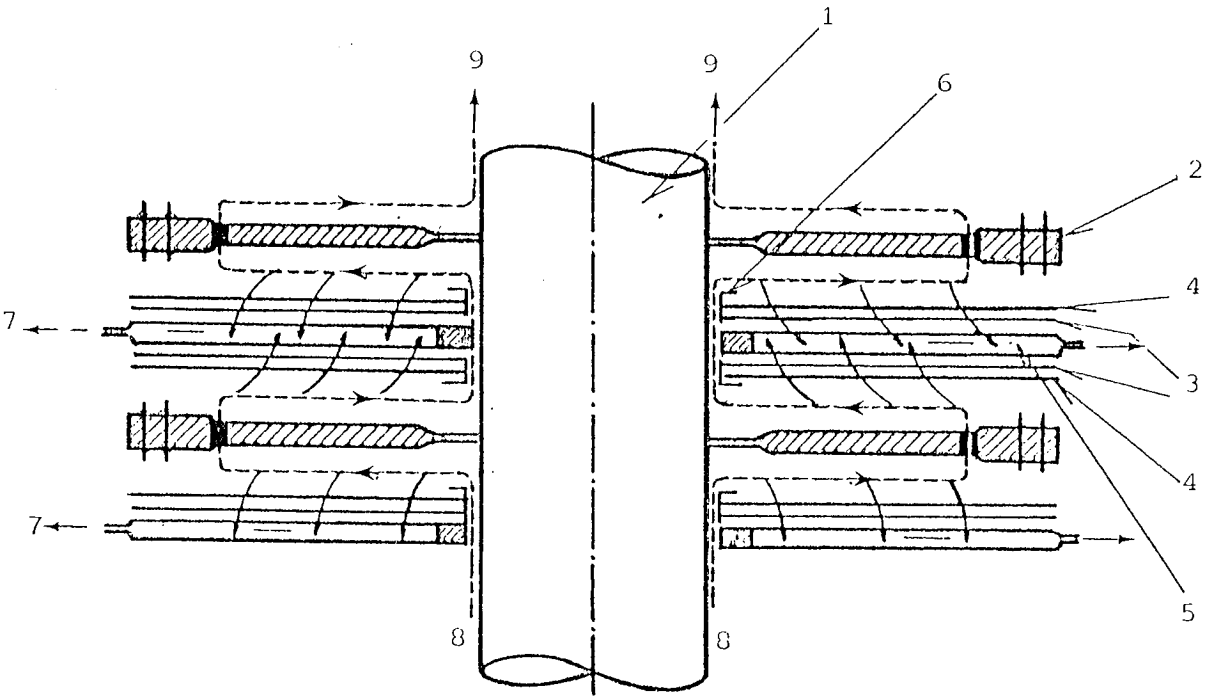

1 Centre Bolt
2 Spacer
3 Drain Paper (DDS Type GR Membrane is cast directly on the drain paper)
4 Membranes
5 Membrane support plate
6 Neck ring
7 Permeate
8 Feed solution
9 Retentate

Figure 4.21: Photograph of a Membrane Support Plate, and a Membrane Spacer Plate

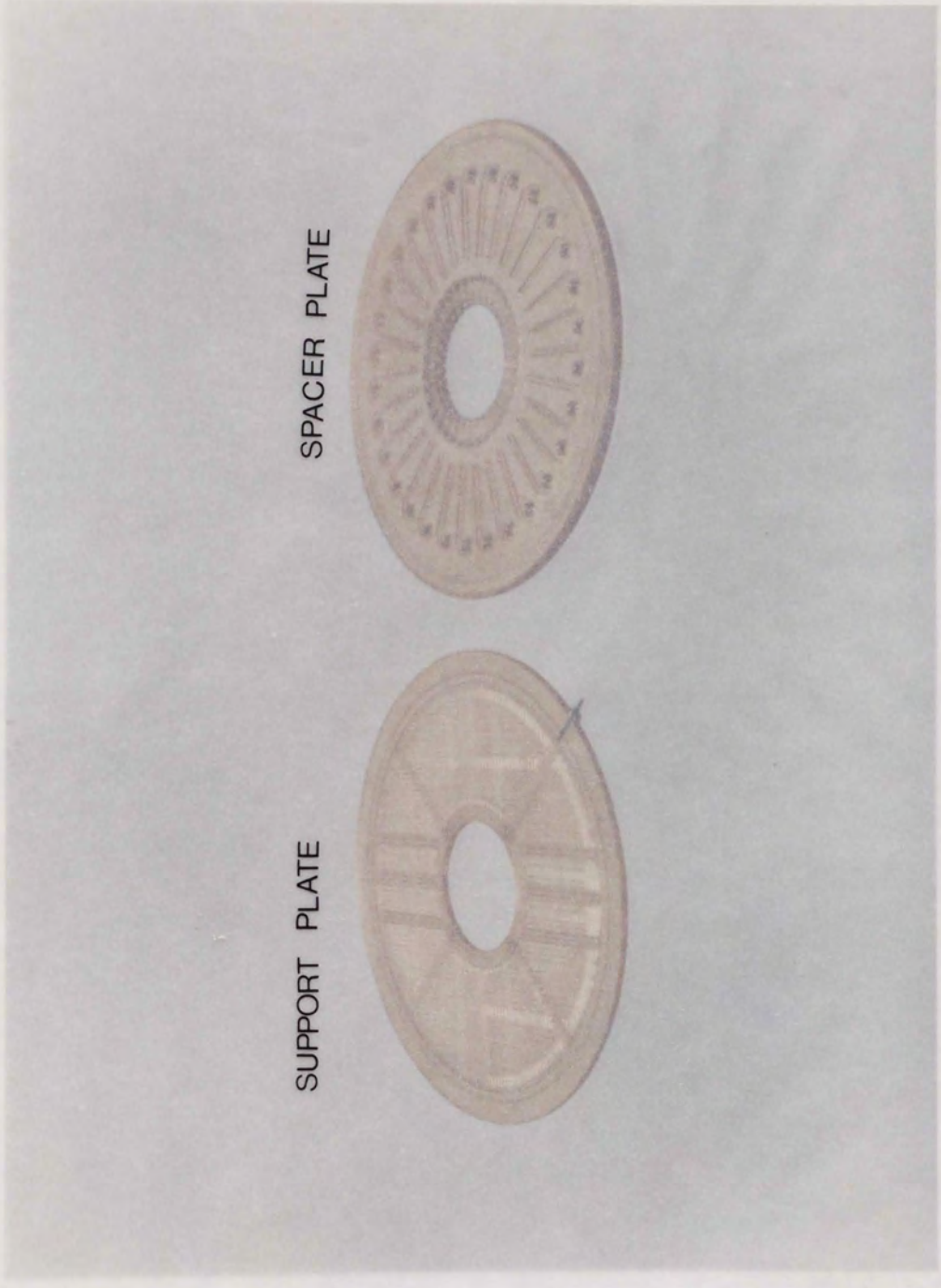

Figure 4.21: Photograph of a Membrane Support Plate, and a Membrane Spacer Plate

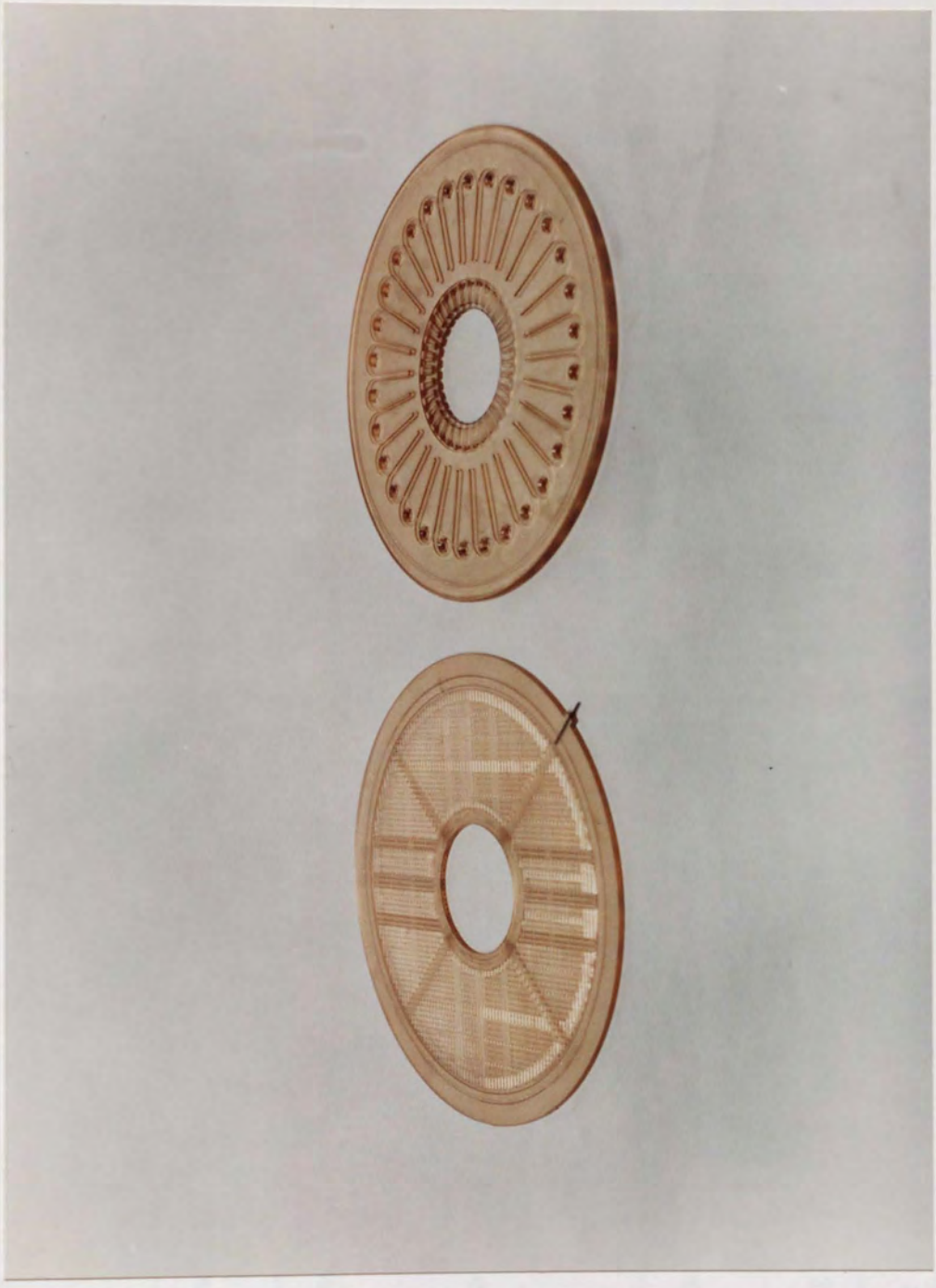

Figure 4.22: Operating Conditions for DDS Runs

	Run 1	Run 2	Run 3	Run 4
Membrane Type	GR 81PP (6000 cut-off)	GR 81PP (6000 cut-off)	GR 51PP (50 000 cut-off)	GR 60PP (25000 cut-off)
Membrane Area	0.144 m^2	0.144 m^2	0.072 m^2	0.072 m^2
Mode of Operation	Dia-filtration	Dia-filtration	Dia-filtration	Dia-filtration
Feed	2% solution (HZ16K)	2% solution (HZ16K)	2% solution (HZ16K)	2% solution (HZ16K)
Mean Operating Pressure	5 bar	5 bar	5 bar	5 bar
Operating temp	20^{o}C	20^{o}C	20^{o}C	20^{o}C
Retentate Flow Rate	6.6 L/min	7.7 L/min	7.7 L/min	7.7 L/min
Permeate Flux (L/min m^2)	1.389 to 0.847	0.438	2.1 to 1.472	1.31 to 1.22

The results obtained for the DDS 6000 molecular weight cut-off membranes are summarised in Figures 4.23-4.26. Figure 4.27 gives a comparison of the DDS and Amicon membranes.

The results for run 1 were obtained with new membranes. After run 1 was completed the membranes were washed with clean, de-ionised water and then stored in 0.02% w/v sodium azide for one week. These membranes were then used for run 2.

As can be seen from Figure 4.22 the permeate flux dropped steadily over run 1. This was assumed to be due to the gradual compression of the membranes inside the DDS Lab-module. When the same membranes were then recompressed for run 2, the permeate flux was again reduced from the final value of run 1. However, during run 2 the permeate flux remained constant, indicating the membranes were compressed to their limit. This was confirmed when the same membranes were again decompressed, then recompressed. The clean water flux obtained was equal to that of run 2.

This declining permeate flux also occurred with the DDS 25 000 and 50 000 molecular weight cut-off membranes, and membranes of larger cut-offs which were subsequently bought by Fisons Plc (127).

The clean water flux at the end of run 2 was found to be less than the initial flux, this indicates that a gel layer had been formed on the membranes' surface. As with the Millipore membranes this was confirmed by continual washing of the surface with clean water. Before run 2 the clean water flux was 3 L min^{-1} m^{-2}. Immediately after run 2 the flux was 0.7 L min^{-1} m^{-2}. After washing the flux increased to 2.9 L min^{-1} m^{-2}. Since this flux did return to normal this indicates that no additional membrane compression had occurred during run 2.

It can only be assumed that a gel layer was formed in run 1 since the operating conditions (ie. feed concentration etc) were the same as run 2. The clean water flux did vary over the experiment but could not be returned to its initial value with washing the membrane. This was due to the membrane being compressed during the experiment.

This membrane compression theory is further supported if the results for run 1 and run 2 are compared (Figure 4.27). From this comparison it can be seen that:

Figure 4.23

Experimental Results for DDS 6000 Molecular Weight Cut-off Membranes (Run 1)

Time (Hrs)	Retentate				Efficiency†
	Concentration (g/100g sol)	% Below 12,000MW	% Between 12,000 & 98,000MW	% Above 98,000 MW	
Feed	1.81	28	62	11	-
0.5	1.61	25	62	13	90%
1.0	1.30	18	68	14	78%
1.5	1.01	14	71	15	65%
2	0.81	12	70	18	51%
3	0.75	10	70	20	47%
4	0.53	4	71	25	34%

† Efficiency = $\frac{\text{Weight of 'saleable' Dextran in Product}}{\text{Weight of 'saleable' Dextran in Feed}}$

Figure 4.24: Overall Mass Balance on DDS 6000 MW Cut-off Membranes (Run 1)

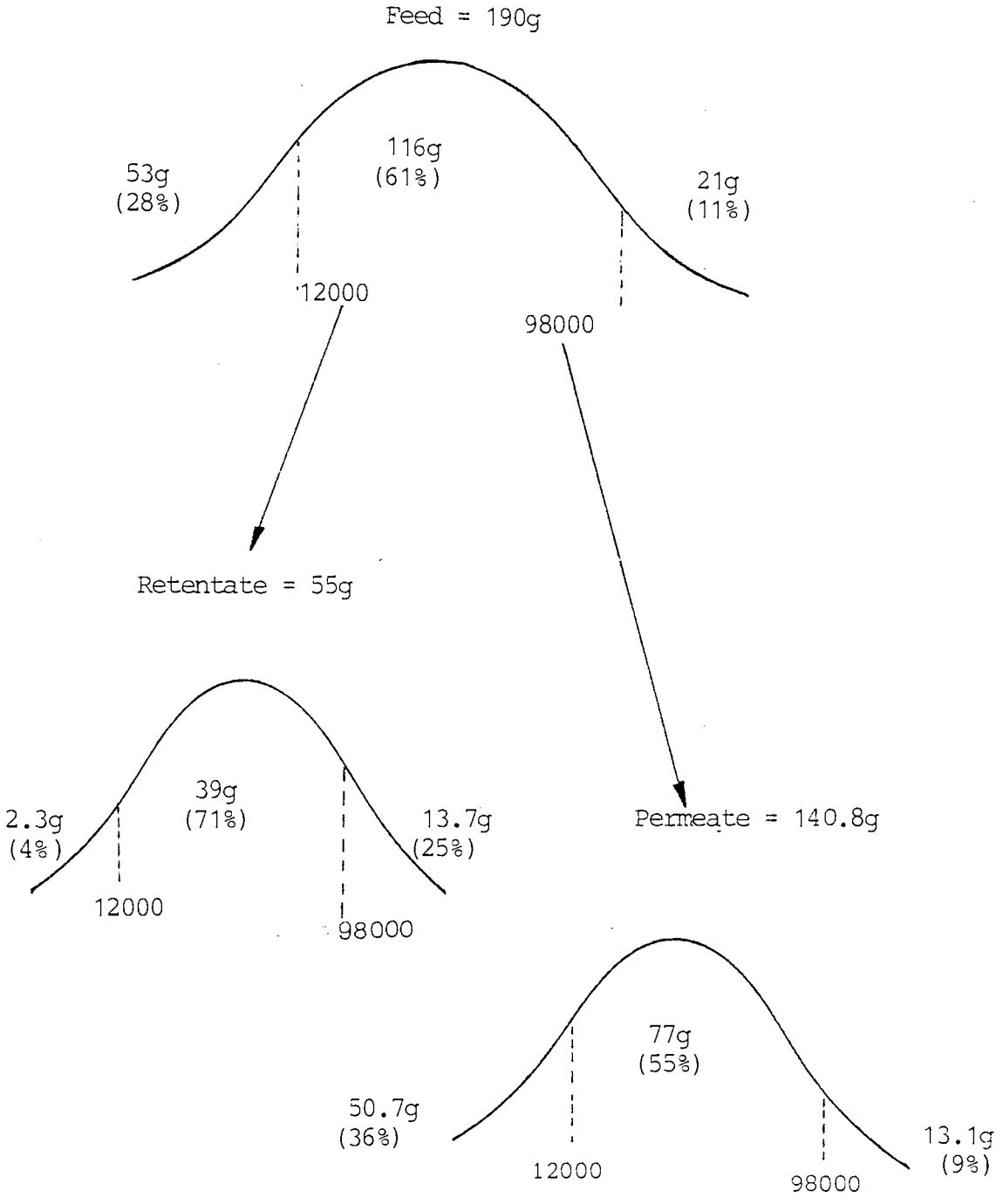

Figure 4.25

Experimental results for DDS 6000 Molecular Weight Cut-off Membranes (Run 2)

Time (Hrs)	Retentate				Efficiency†
	Concentration (g/100g sol)	% Below 12,000MW	% Between 12,000 & 98,000MW	% Above 98,000 MW	
Feed	1.72	28	61	11	-
1	1.62	27.5	61.5	11	95%
2	1.50	25	64	11	92%
3	1.41	24	64.5	11.5	87%
4	1.32	23.5	65	11.5	82%
5	1.25	23	65	12	77%
6	1.16	22.5	65.5	12	72%
8	1.09	21.5	66	12.5	68%
10	0.9	21	66.5	12.5	57%
12	0.86	20	67.5	12.5	54%

† Efficiency = $\frac{\text{Weight of 'saleable' Dextran in Product}}{\text{Weight of 'saleable' dextran in feed}}$

Figure 4.26: Overall Mass Balance for DDS 6000 MW Cut-off Membranes (Run 2)

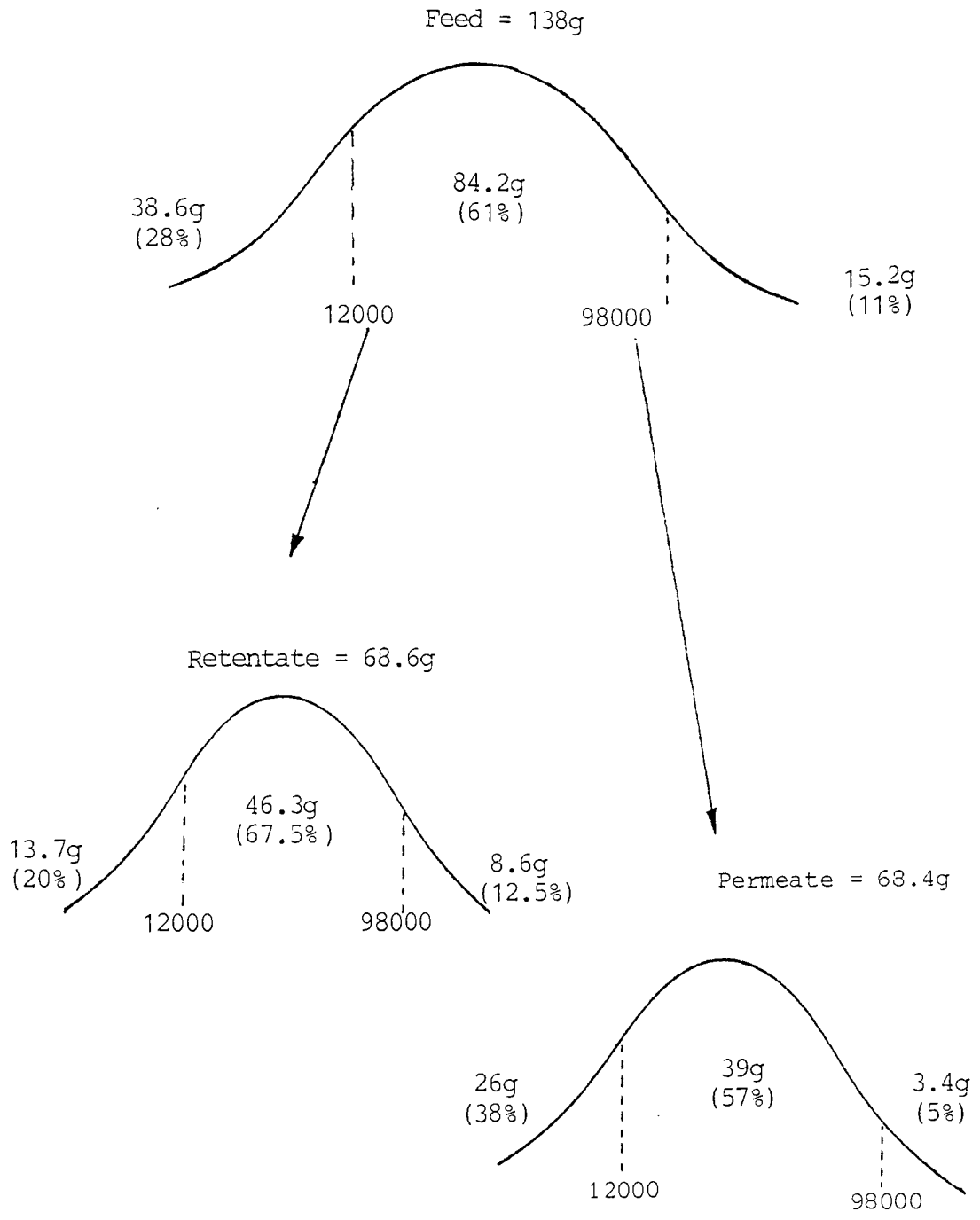

Figure 4.27

COMPARISON OF DDS 6000 MOLECULAR WEIGHT CUT-OFF MEMBRANES AND AMICON 5000 MOLECULAR WEIGHT CUT-OFF MEMBRANES (12)

(a) During run 1 larger molecules passed through the membranes than during run 2.

(b) A larger proportion of the material below 12 000 daltons was removed in run 1 than run 2.

(c) More material between 12 000 and 98 000 daltons was removed as permeate in run 1 than run 2.

These three statements tend to indicate that the membrane pores had become smaller (compressed) between runs 1 and 2.

However, even when run 2 is compared to the performance of the Amicon membrane (Figure 4.27), it can be seen that the Amicon membrane is superior.

The results obtained for the DDS 25 000 and 50 000 molecular weight membranes are summarised in Figures 4.28 - 4.31.

As stated previously, these membranes were used to fractionate the high molecular weight dextran. However, when Vlachogiannis used Amicon membranes for this purpose, he found that GPC was more efficient. Therefore the results for these two membranes are compared with GPC in Figure 4.32.

Unlike the two previous comparisons the product stream in this case is the permeate. This is because the 'unwanted' material, ie. material above 98 000 daltons, is rejected and kept in the retentate. The 'wanted' material, ie. below 98 000 daltons, is passed through the membrane and collected in the permeate. Therefore, an ideal membrane would have a rejection coefficient of 100% for above 98 000 daltons and 0% for below 98 000 daltons.

As can be seen from Figure 4.32 the DDS 25 000 membrane had the best coefficient above 98 000 daltons and the worse below. The 50 000 membrane had the best below 98 000 daltons but the worse above.

These two results are very dependent upon the number of washes conducted during the experiment. To improve the performance of the DDS 25 000 cut-off membrane the number of washes should be increased. This would cause more of the material below 98 000 daltons to pass through the membrane. However, this would also cause more material above 98 000 to pass through, thus lowering the efficiency.

Figure 4.28

Experimental Results for DDS 25,000 Molecular Weight Cut-off Membrane

Time (Hrs)	*Permeate Product				Efficiency†
	Concentration (g/100g sol)	% Below 12,000MW	% Between 12,000 & 98,000MW	% Above 98,000 MW	
Feed	1.85	28	61	11	-
1	0.87	55	44.5	0.5	21%
2	0.70	53	46	1.0	34%
3	0.55	49	48	3.0	42%
4	0.45	46	50.7	3.3	49%
5	0.36	44	52.6	3.4	55%
6	0.30	43	53	4	60%
7	0.25	41	54.5	4.5	61%
8	0.24	40	55.0	5.0	67%
9	0.26	39.6	55.3	5.1	70%

* Permeate is product since high MW fractionation is being undertaken.

† Efficiency = $\frac{\text{Weight of 'saleable' dextran in permeate}}{\text{Weight of 'saleable' dextran in feed}}$

Figure 4.29: Overall Mass Balance for DDS 25 000 Molecular Weight Cut-off Membrane

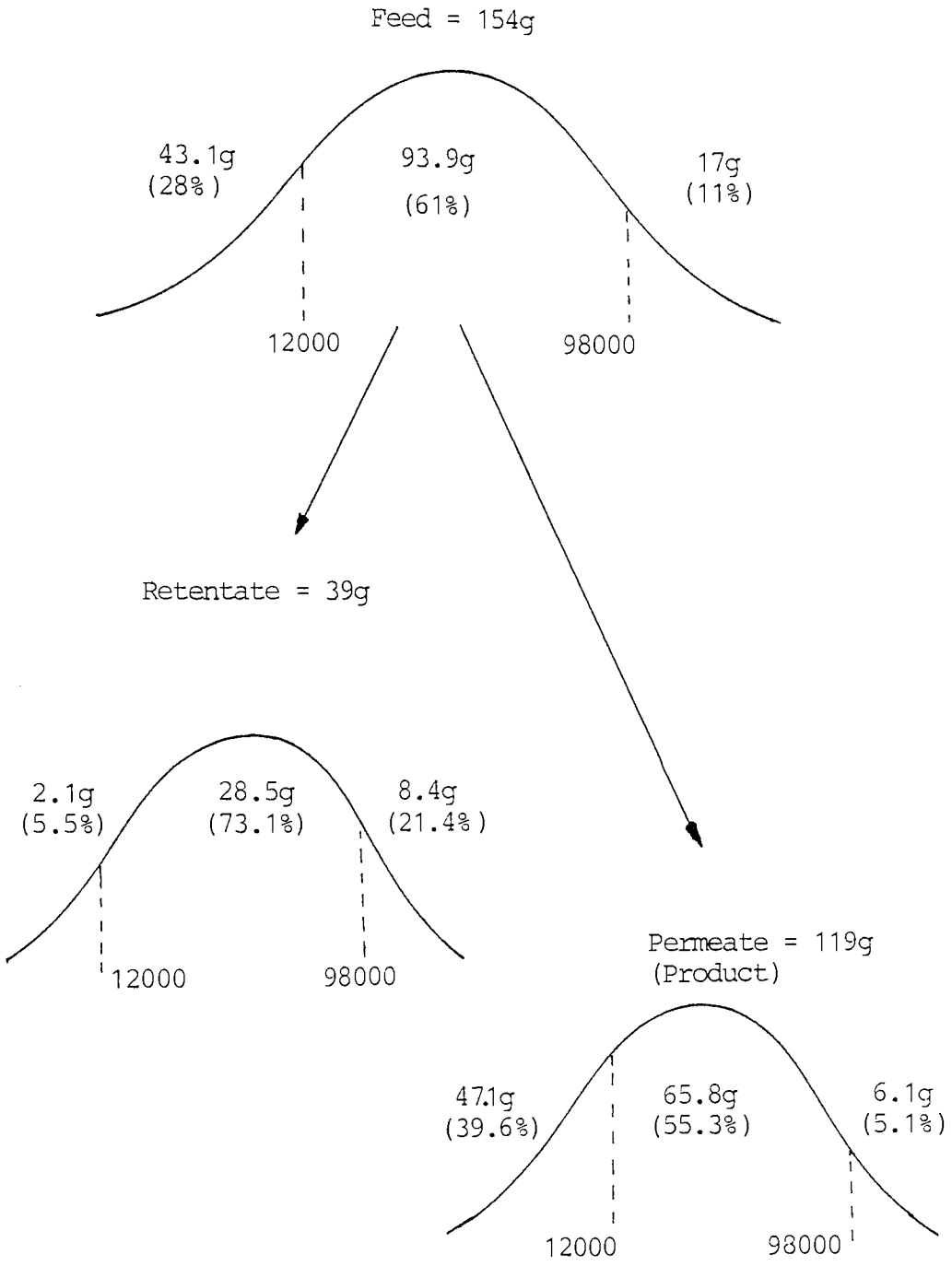

Figure 4.30

Experimental Results for DDS 50 000 Molecular Weight Cut-off Membrane

Time (Hrs)	*Permeate Product				Efficiency†
	Concentration (g/100g sol)	% Below 12,000MW	% Between 12,000 & 98,000MW	% Above 98,000 MW	
Feed	1.88	28	61	11	-
2	0.74	43	56	1	59%
4	0.50	32	64	4	93%
6	0.36	31	63	6	95%
8	0.26	30	63	7	96%

* Permeate is product since high molecular weight fractionation is being undertaken

† Efficiency = $\frac{\text{Weight of 'saleable' Dextran in Permeate}}{\text{Weight of 'saleable' Dextran in Feed}}$

Figure 4.31: Overall Mass Balance on DDS 50 000 Molecular Weight Cut-off Membrane

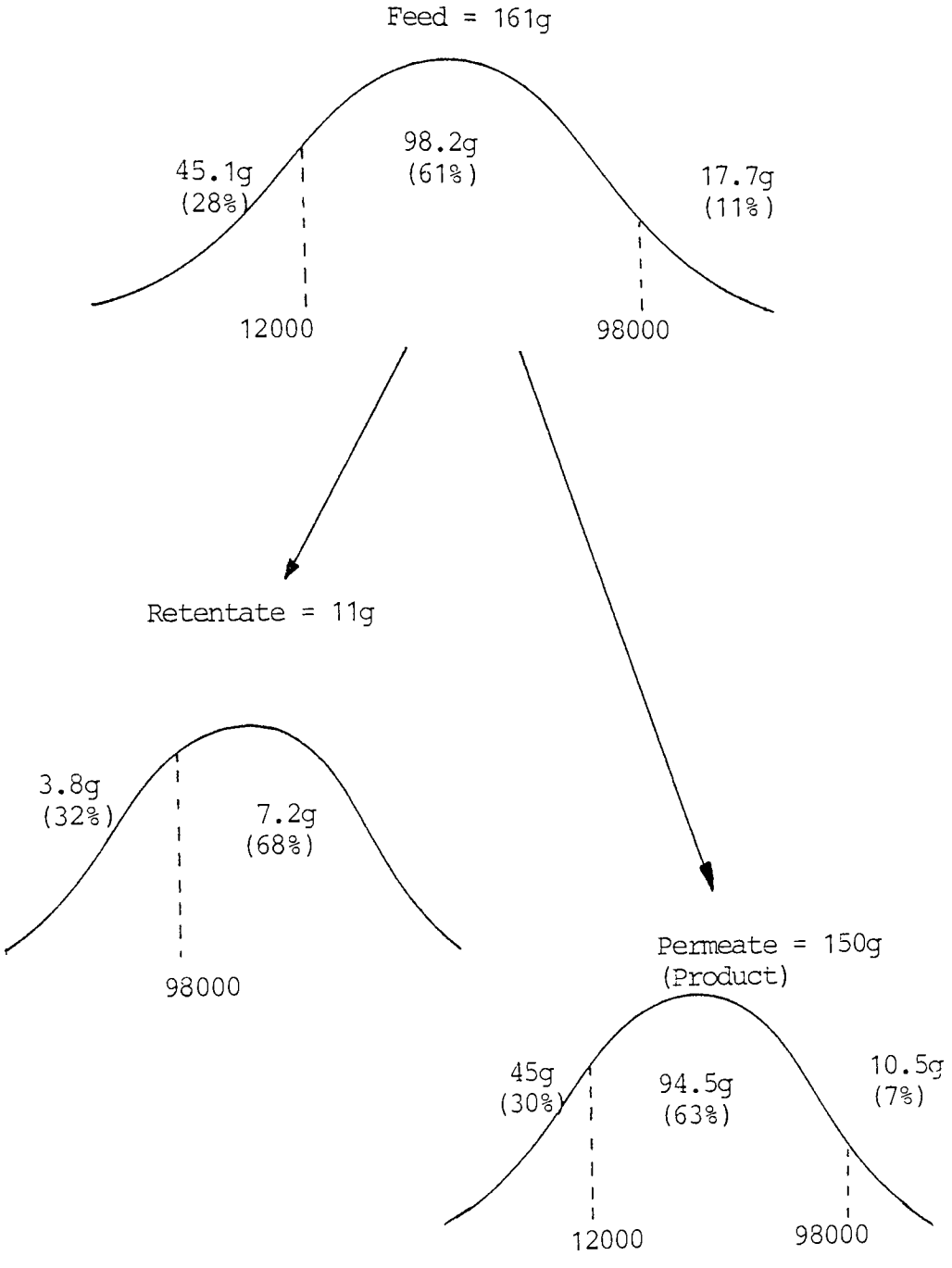

Figure 4.32

COMPARISON OF DDS 25 000 AND 50 000 MOLECULAR WEIGHT CUT-OFF MEMBRANES AND GPC (12)

The number of washes should be decreased for the DDS 50 000 cut-off membrane. This would reduce the amount of material, both above and below 98 000 daltons, passing through the membrane. In both these cases the membrane efficiency would then be comparable to that of the GPC. Unfortunately, the DDS equipment had to be returned to the Company before this could be proved experimentally at Aston.

4.4 EXPERIMENTS CONDUCTED USING MEMBRANES MANUFACTURED BY AMICON LTD

4.4.1 INTRODUCTION

The Amicon 5000 molecular weight cut-off membrane tested by Vlachogiannis had been purchased in 1981. Since then Amicon had informed us that they had improved their manufacturing process. Therefore, it was decided to purchase some new Amicon 5000 membranes. These new membranes were then compared with the membrane used by Vlachogiannis (12, 14).

Both the old and new membranes were made from polysulphone, and were of the hollow fibre configuration. The equipment used for these comparisons was the Amicon DC2A module. A schematic drawing of this equipment is given in Figure 4.33. This equipment can be operated in either concentration, dialysis or dia-filtration mode. For the purpose of these experiments the dia-filtration mode was used.

The transmembrane pressure was pre-set by a pressure cut-off switch which was incorporated into the DC2A system. When the pressure reached 10 psi the pump was automatically cut-out. This cut-off switch ensured that the pressure was the same in all the experiments.

4.4.2 EXPERIMENTAL OPERATING CONDITIONS AND RESULTS OBTAINED

Initially, one new membrane was tested under exactly the same conditions as those chosen by Vlachogiannis. These operating conditions are given in Figure 4.34.

The results obtained for this membrane are summarised in Figures 4.35 - 4.36. Figure 4.37 gives the comparable results obtained by Vlachogiannis (12).

From these results it can be seen that the new membrane removed 61% of the material below 12 000 daltons at an efficiency of 93%. The old membrane removed

Figure 4.33(a): Photograph of the Hollow Fibres in an Amicon Membrane

Figure 4.33: The Amicon DC2A UF System - Diafiltration Mode

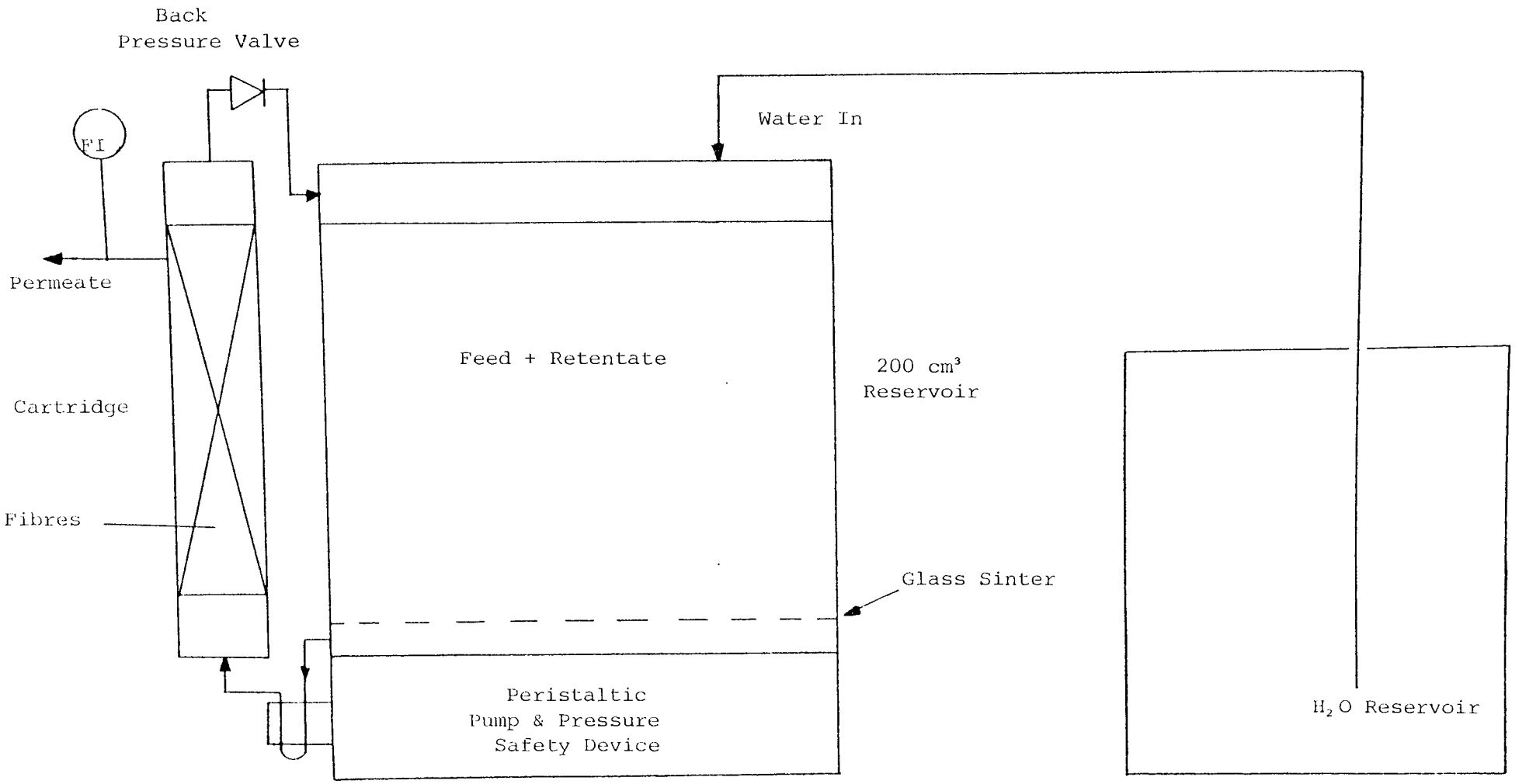

Figure 4.34

Operating Conditions used to Test Amicon 5000 Molecular Weight Cut-off Membrane

Equipment used:	Amicon DC2A
Membrane Area:	600 cm^2
Retentate Recirculation Rate:	300 cm^2/min
Transmembrane Pressure:	1 Kg/cm^2
Operating Temperature:	20°C
Feed:	2% w/w of Fisons Batch HZ 16K
Mode of Operation:	Dia-filtration
Number of Diavolumes Processed:	6

Figure 4.35: Diafiltration Results for a New Amicon 5000 Molecular Weight Cut-off Membrane

Number of Diavolumes used	Retentate Product				Efficiency†
	Concentration (g/100g sol)	% Less than 12 000 MW	% Between 12 000 and 98 000 MW	% Greater than 98 000 MW	
Feed	1.75	31	57	12	-
1	1.65	27.3	60.3	12.4	98.6%
2	1.56	22.7	63.8	13.5	96.6%
3	1.49	19.4	66.3	14.3	95.7%
4	1.43	16.9	68.1	15	94%
5	1.38	14.5	69.8	15.7	93.4%
6	1.34	12.4	71.2	16.4	93%

† Efficiency = $\frac{\text{Weight of 'saleable' Dextran in Product}}{\text{Weight of 'saleable' Dextran in Feed}}$

Figure 4.36: Overall Mass Balance on a New Amicon 5000 Molecular Weight Cut-off Membrane

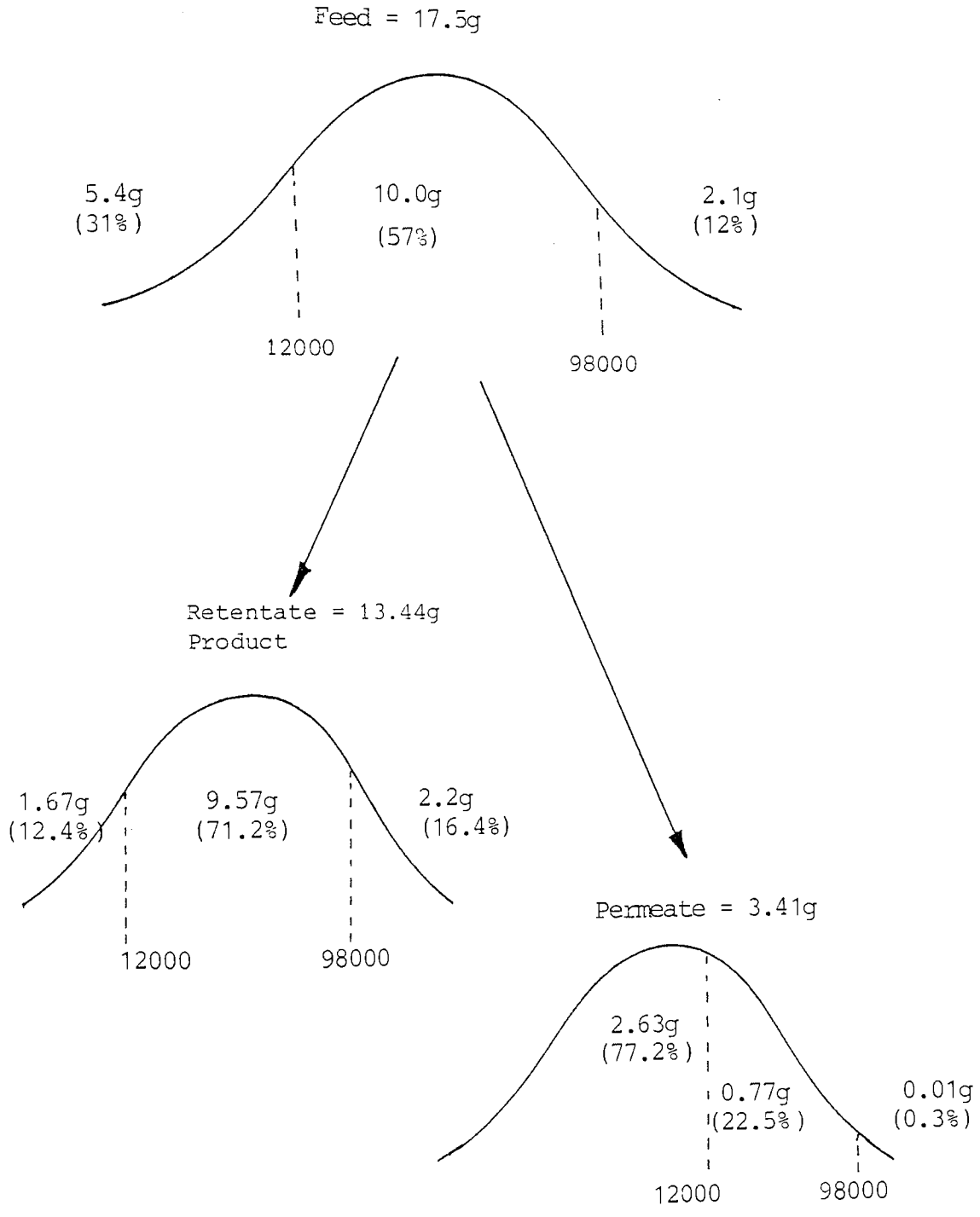

Figure 4.37: Overall Mass Balance on Old Amicon 5000 Molecular Weight Cut-off Membrane (12)

87.5% of the material below 12 000 at an efficiency of 70%. These figures clearly prove that the new membrane is a 'tighter' membrane.

As with the other membrane comparison tests, the feed used in the above experiment was from the Fisons batch HZ16K. This batch contains a high percentage of material below 12 000 daltons and is not representative of the dextran produced on an industrial plant. It was therefore decided to retest the new membrane and other new membranes bought from Amicon, with a new dextran feed.

The new feed was from Fisons batch code RB5R. This new batch contained only 25% of its material below 12 000 daltons compared to 28-30% with HZ16K.

As well as changing the feed, the number of washes used was also changed. For each experiment the number was increased until the concentration of the dynamic permeate remained constant. After this point the retentate changed very little. All the other conditions were kept constant.

The results obtained with these new operating conditions are summarised in Figures 4.38 - 4.47. A comparison of the results is given in Figure 4.48 and Figure 4.49.

From these results it can be seen that in all the experiments the final product was within specification at the low molecular weight end, ie. 7% below 12 000 daltons. However, the individual efficiencies gave a large variation with membrane number 3 being much lower than the rest (Figure 4.48). This very low efficiency is also shown up in Figure 4.49. The rejection coefficient of membrane 3 is at least 15% lower than the other membranes in the 24 - 25 000 molecular weight band width. This shows that membrane number 3 was a faulty membrane.

Even though the efficiencies of membranes 1, 2, 4 and 5 varied by 12%, their actual rejection graphs were very similar. Therefore, these four membranes were considered to be comparable and usable.

Figure 4.48 also gives the efficiency obtained by Vlachogiannis using an 'old' membrane. From these results it would appear that the old membrane was equal to, if

Figure 4.38: Diafiltration Results for Amicon 5 000 Molecular Weight Cut-off Membrane Number One

Retentate Product

Number of Diavolumes Used	Concentration (g/100g solution)	Percentage less than 12 000 mw	Percentage between 12000 & 98000 mw	Percentage above 98000 mw	Efficiency (%) ‡
Feed	1.73	25.8%	62.2%	12%	-
1	1.63	22.3%	64.9%	12.8%	98.6
2	1.55	19.6%	67.4%	13%	97.4
3	1.48	15.6%	69.9%	14.5%	96.1
4	1.40	13.4%	71.4%	15.2%	93.2
5	1.34	11.4%	72.5%	16.1%	90.3
6	1.28	10.9%	72.5%	16.6%	86
8	1.17	8.9%	74.5%	16.6%	81.4
10	1.09	7.0%	74.3%	18.7%	75.3
12	1.03	5.1%	75.5%	19.4%	72.3

‡ Efficiency = $\frac{\text{Weight of 'saleable' dextran in product}}{\text{Weight of 'saleable' dextran in feed}}$

Figure 4.39: Overall Mass Balance on Amicon 5000 Molecular Weight Cut-off Membrane (Number One)

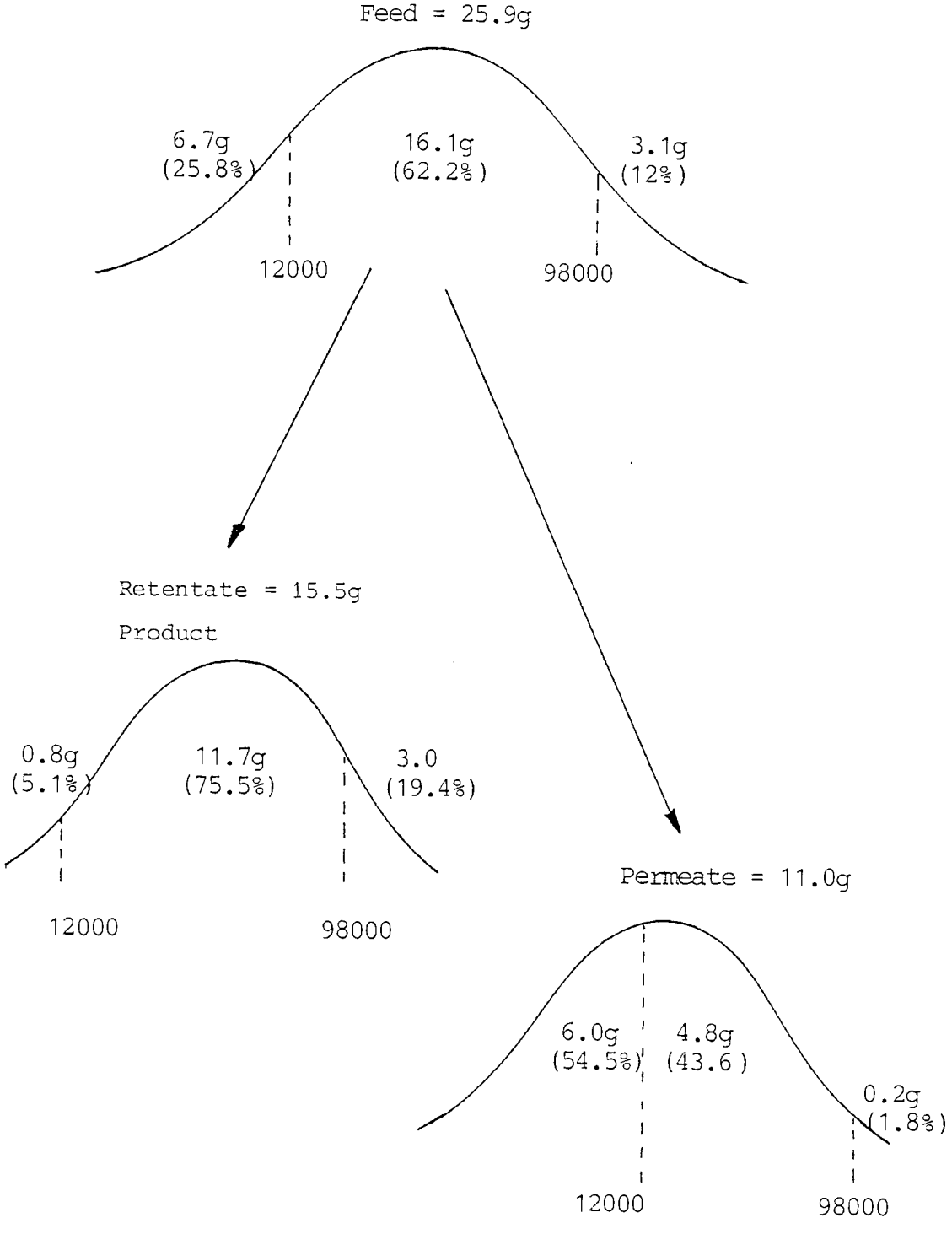

Figure 4.40: Diafiltration Results for Amicon 5 000 Molecular Weight Cut-off Membrane Number Two

		Retentate Product			
Number of Diavolumes Used	Concentration (g/100g solution)	Percentage less than 12 000 mw	Percentage between 12000 & 98000 mw	Percentage above 98000 mw	Efficiency (%) ‡
Feed	1.89	25%	61%	14%	-
1	1.78	24.5%	62.9%	12.6%	97%
2	1.68	21.1%	66.5%	12.4%	97%
3	1.6	20%	66.4%	13.6%	92%
4	1.51	19.5%	66.8%	13.7%	88%
5	1.44	18.8%	67.6%	13.6%	84%
6	1.37	18%	66.7%	15.3%	79%
8	1.24	14%	70%	16%	75%
10	1.14	12.2%	70.8%	17%	70%
12	1.05	9.7%	74.2%	16.1%	68%

‡ Efficiency = $\frac{\text{Weight of 'saleable' dextran in product}}{\text{Weight of 'saleable' dextran in feed}}$

Figure 4.41: Overall Mass Balance on Amicon 5000 Molecular Weight Cut-off Membrane (Number Two)

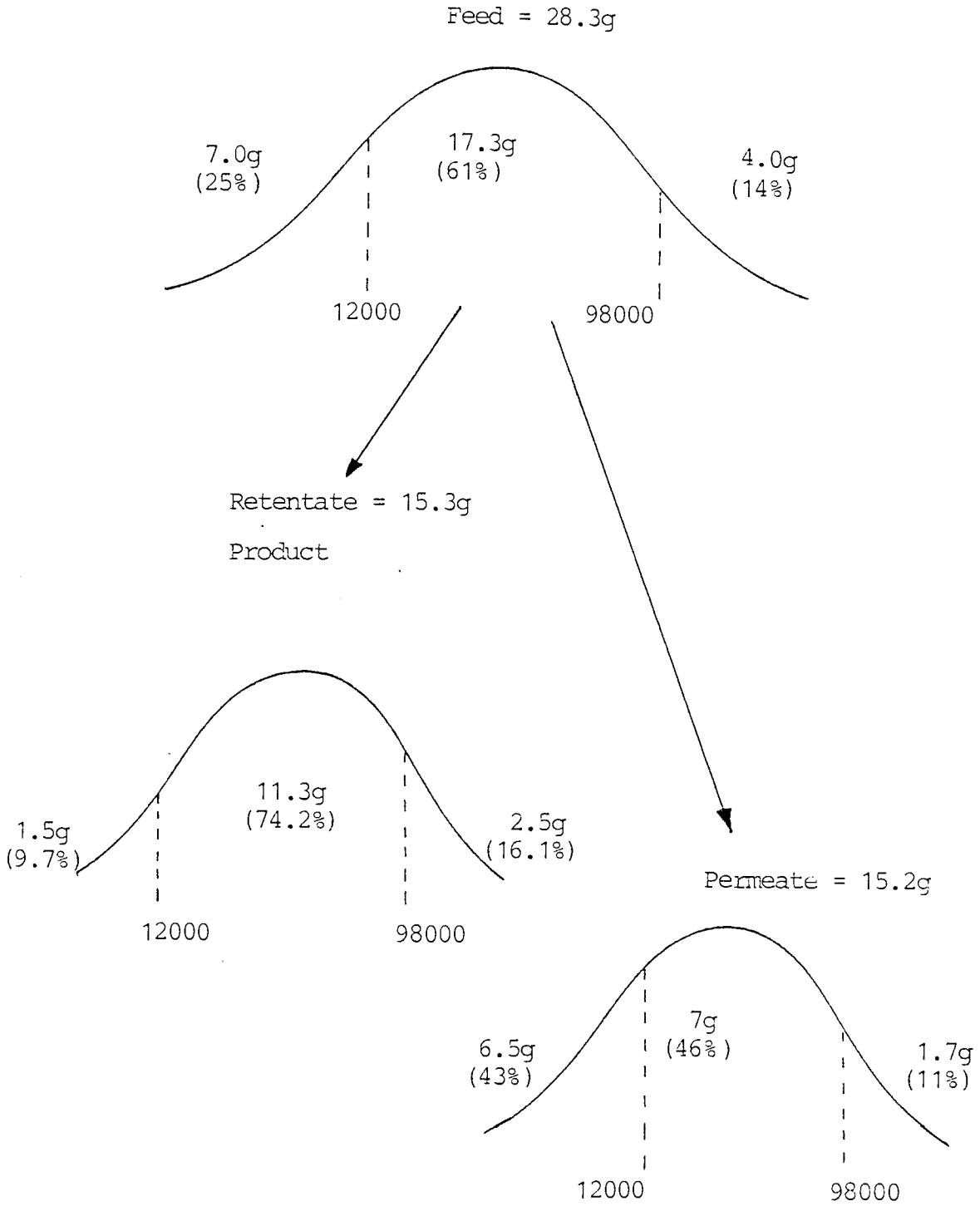

Figure 4.42: Diafiltration Results for Amicon 5 000 Molecular Weight Cut-off Membrane Number Three

	Retentate Product				
Number of Diavolumes Used	Concentration (g/100g solution)	Percentage less than 12 000 mw	Percentage between 12000 & 98000 mw	Percentage above 98000 mw	Efficiency (%) ‡
Feed	1.90	25%	61%	14%	-
2	1.04	18%	68.5%	13.5%	61.5%
4	0.82	12%	71%	17%	50%
5	0.74	9.1%	70.6%	20.3%	45%
6	0.66	6.6%	71.9%	21.5%	41%
7	0.6	5.3%	71.4%	23.3%	37%
8	0.545	4.2%	71.8%	24%	34%
10	0.47	3.7%	67.5%	28.8%	27%

‡ Efficiency = $\frac{\text{Weight of 'saleable' dextran in product}}{\text{Weight of 'saleable' dextran in feed}}$

Figure 4.43: Overall Mass Balance on Amicon 5000 Molecular Weight Cut-off Membrane (Number Three)

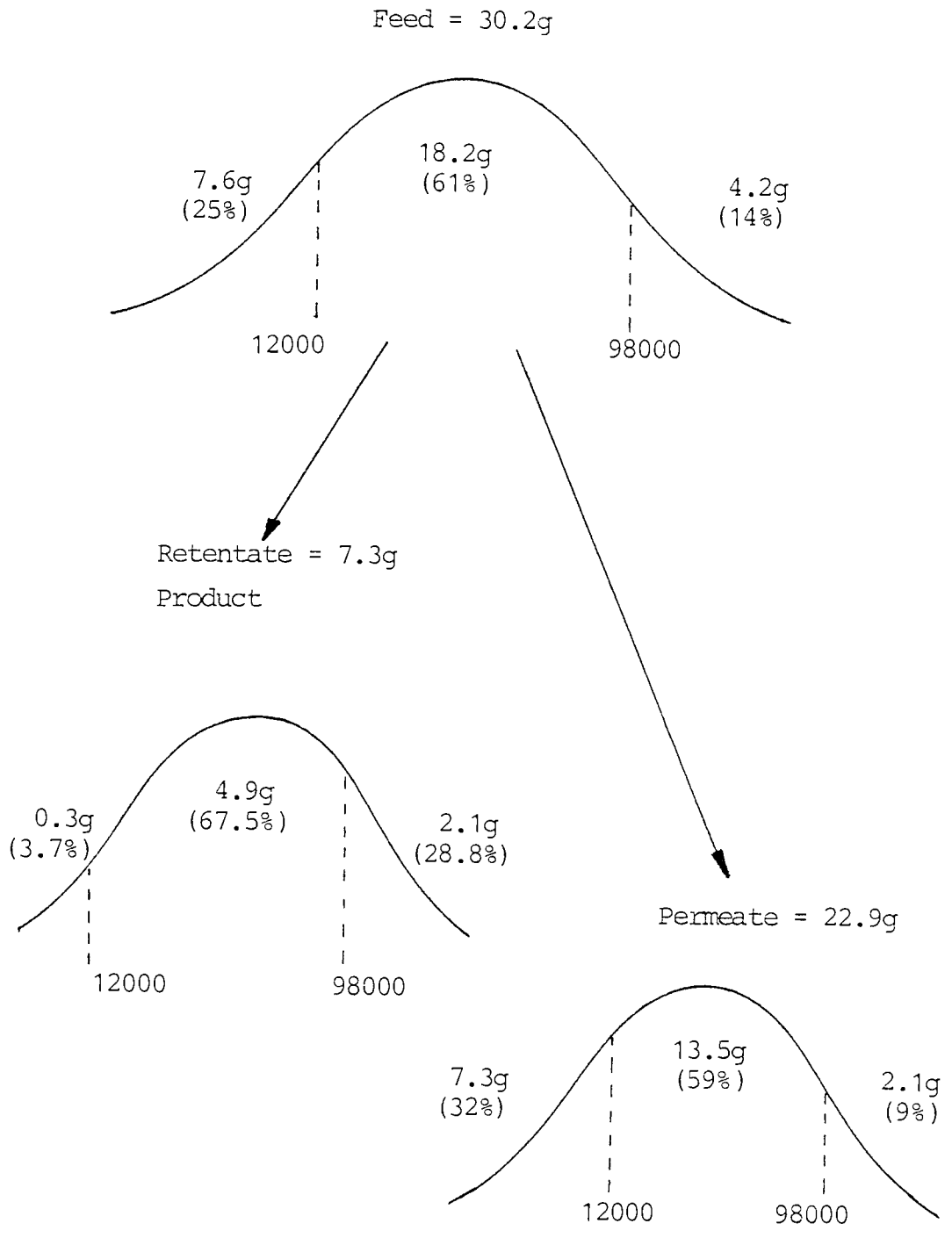

Figure 4.44: Diafiltration Results for Amicon 5 000 Molecular Weight Cut-off Membrane Number Four

		Retentate Product			
Number of Diavolumes Used	Concentration (g/100g solution)	Percentage less than 12 000 mw	Percentage between 12000 & 98000 mw	Percentage above 98000 mw	Efficiency (%) ‡
Feed	1.90	25%	61%	14%	-
1	1.74	22%	65%	13%	97%
2	1.60	17.5%	69.5%	13%	96%
3	1.49	16%	70%	14%	90%
4	1.38	13%	72%	15%	86%
5	1.29	12.3%	71.2%	16.5%	79%
6	1.21	11%	72%	17%	75%
8	1.09	8.4%	73%	18.6%	68%
10	1.0	6.6%	73.4%	20%	63%
12	0.95	6.8%	73.2%	20%	60%

‡ Efficiency = $\frac{\text{Weight of 'saleable' dextran in product}}{\text{Weight of 'saleable' dextran in feed}}$

Figure 4.45: Overall Mass Balance on Amicon 5000 Molecular Weight Cut-off Membrane (Number Four)

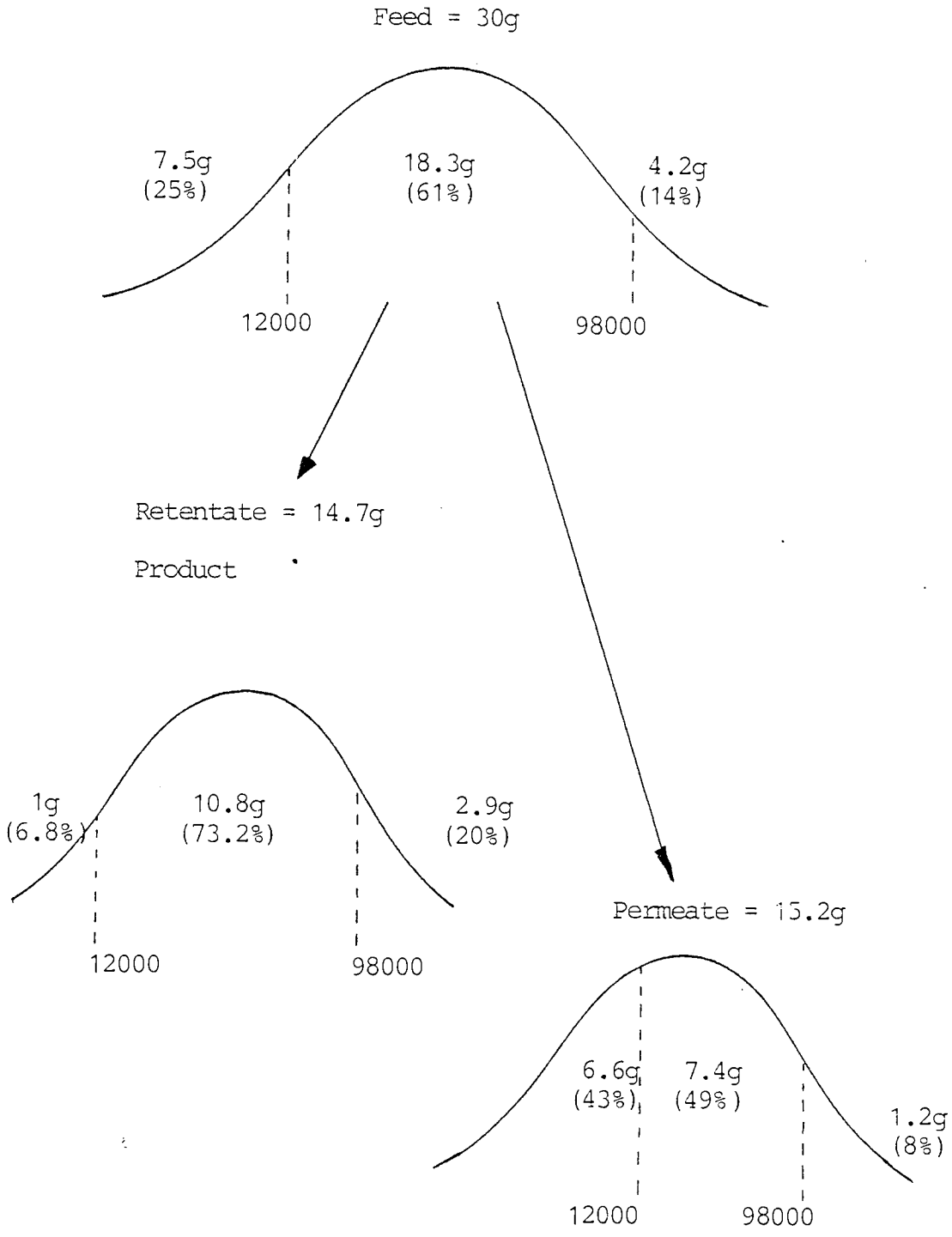

Figure 4.46: Diafiltration Results for Amicon 5 000 Molecular Weight Cut-off Membrane Number Five

		Retentate Product			
Number of Diavolumes Used	Concentration (g/100g solution)	Percentage less than 12 000 mw	Percentage between 12000 & 98000 mw	Percentage above 98000 mw	Efficiency (%) ‡
Feed	1.83	25%	61%	14%	-
1	1.62	20.3%	65.4%	14.3%	95
2	1.48	19.7%	66.3%	14%	88
3	1.37	17%	69%	14%	85
4	1.27	15%	68%	17%	77
5	1.18	13%	70%	17%	74
6	1.09	12%	71%	17%	70
8	0.95	7.7%	72.3%	20%	62
10	0.85	5.3%	72.7%	22%	55
12	0.79	4.4%	73.6%	22%	52

‡ Efficiency = $\frac{\text{Weight of 'saleable' dextran in product}}{\text{Weight of 'saleable' dextran in feed}}$

Figure 4.47: Overall Mass Balance on Amicon 5000 Molecular Weight Cut-off Membrane (Number Five)

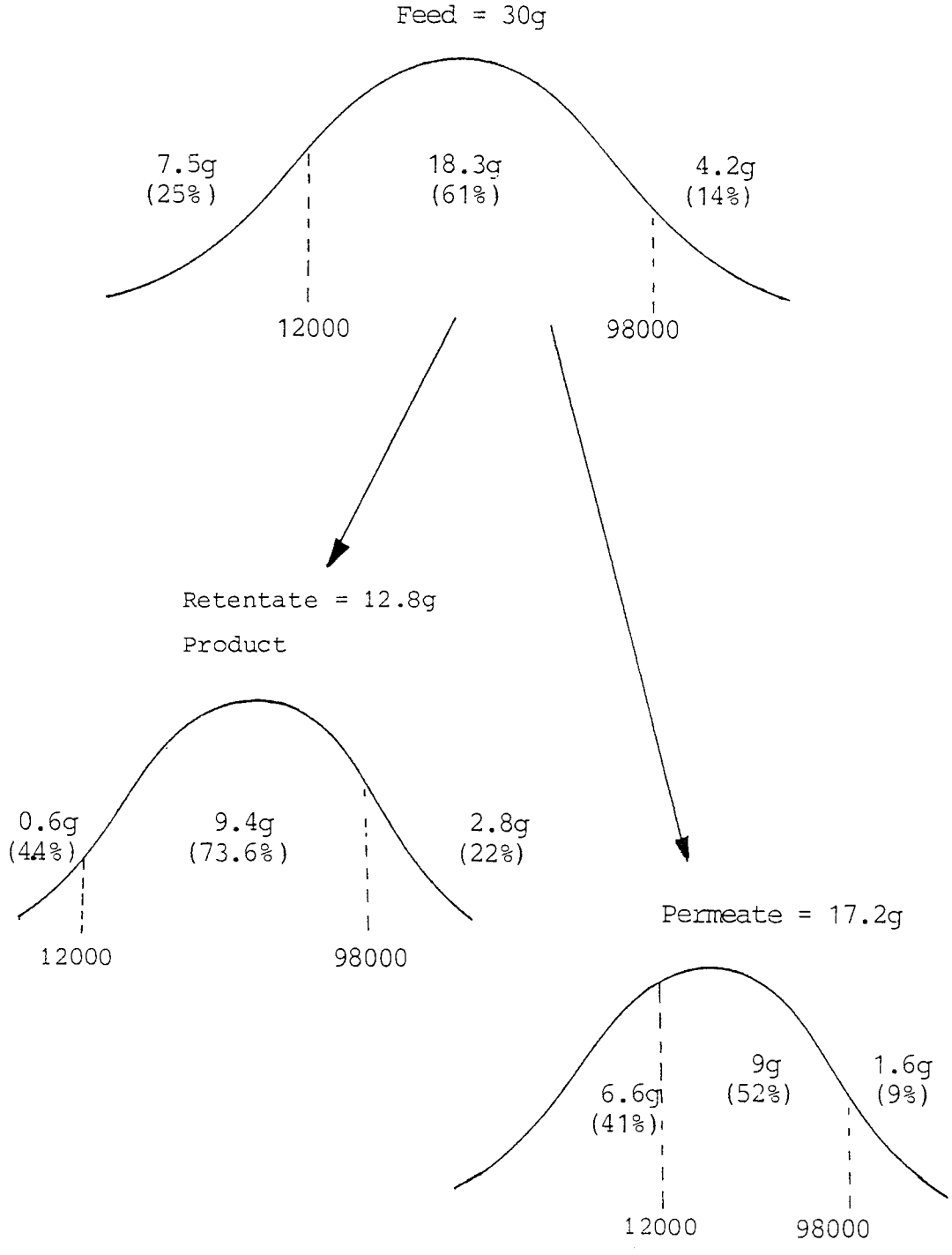

Figure 4.48: Comparison of Old (12) and New Amicon 5000 Molecular Weight Cut-off Membranes

	Flux (cm^3/min 0.06m^2)	Efficiency†
Old membrane	30	71%
New membrane Number 1	11	72%
New Membrane Number 2	11	60%
New Membrane Number 3	18	41%
New Membrane Number 4	12	65%
New Membrane Number 5	12	63%

† Effeciency was measured when product was within specification below 12 000 MW

$$\text{Efficiency} = \frac{\text{Weight of 'saleable' Dextran in Product}}{\text{Weight of 'saleable' Dextran in Feed}}$$

Figure 4.49: Comparison of the Rejection Characteristics of the New Amicon 5000 MW Cut-off Membranes, for Similar Dextran Fractionations

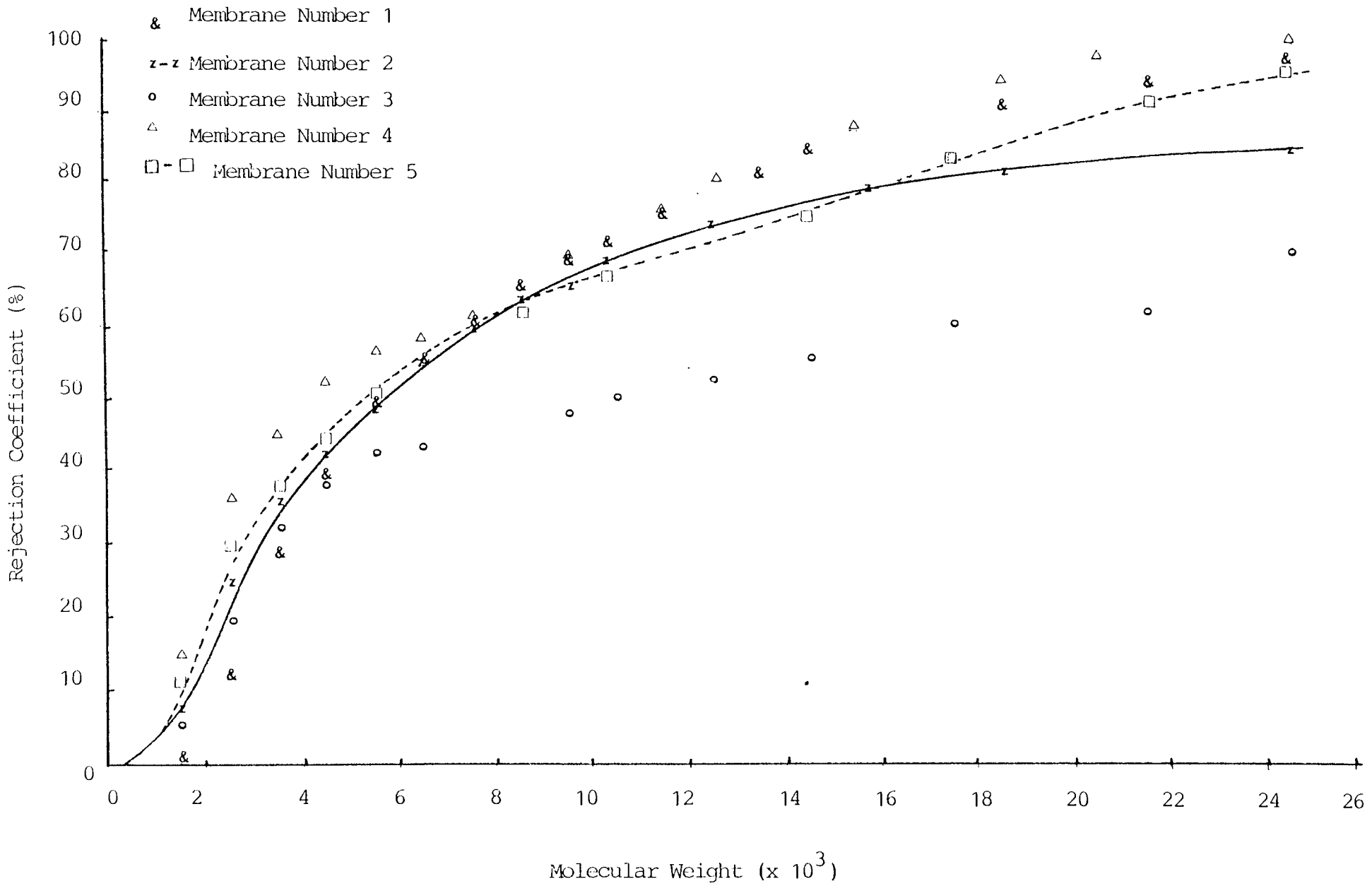

not better than the new membranes. This, therefore, appears to disagree with the previous results.

This occurrence is explained by the change of feed material. When membrane one (the original membrane) was used with the new feed, an efficiency of 87% was obtained to remove 61% of the material below 12 000 daltons. This compared to the 93% efficiency with the HZ16K feed. Therefore, this shows that the lower the percentage of material below 12 000, the lower the efficiency will be to remove the same proportion of this low molecular weight material. This result agrees with the findings of both Cooper (77) and Bottino (79) (see Section 2.4.1). These workers found that increasing the amount of low MW material in a sample, increased a membrane's ability to reject high MW material in the same sample.

The data given in Figure 4.48 shows that the membrane used by Vlachogiannis had a much higher permeate flux than did the new membranes. This higher flux would tend to indicate larger pore sizes and should result in a lower efficiency. This theory was in fact proved correct for membrane number 3. Therefore, taking all these points into account, the 'new' membranes were more efficient than the 'old' membranes used by Vlachogiannis.

As with the other makes of membranes tested the permeate flux remained constant throughout all the experiments conducted. In all cases there was again found to be a gel layer present.

Since these Amicon membranes had a quoted molecular weight cut-off of 5000, their rejection coefficients should have been 100% at and above this weight. However, as can be seen from Figure 4.49 the actual values were 50% at 5000 molecular weight, rising to 100% at and above 25 000 molecular weight. Therefore, in these cases the cut-off of the membranes should be quoted as 25 000. This discrepancy is due to two reasons: one reason is that dextran is a flexible polymer, as mentioned in Section 2.4.2.1.

The second is that under the dia-filtration mode of operation, molecules tend to be 'washed' through the membranes. This is shown in Figure 4.50. As the number of 'washes' increases during an experiment the 50% and 100% rejection points increase in molecular weight.

Ideally, the fractionation would be stopped when the 100% rejection point is at a low molecular weight, ie., 12 000 daltons. However, if this was done the material below 12 000 daltons would not be within specification. Therefore, a balance between the final number of 'washes' used and efficiency must be chosen.

4.5 CONCLUSIONS

From the above results the following conclusions were made:

(a) Out of the membranes tested, Amicon 5000 molecular weight cut-off membranes were the most efficient in fractionating low molecular weight dextran.

(b) Either the DDS 25 000 or 50 000 molecular weight cut-off membranes could be used to fractionate high molecular weight dextran.

(c) Since membranes are calibrated with proteins, the manufacturers recommended values of cut-offs should not be considered to apply to dextran under dia-filtration conditions, ie. membranes with 6000 cut-offs allow through dextran of over 100 000 molecular weight.

(d) Despite being tested at source, some membranes were found to be faulty. Therefore, all membranes should be tested before use.

(e) Even though all the membranes tested were designed to prevent concentration polarization, a gel layer was formed in each case.

Figure 4.50: Variation of Rejection Characteristics of Amicon 5000 Molecular Weight Cut-off Membranes, with Increasing Number of Washes

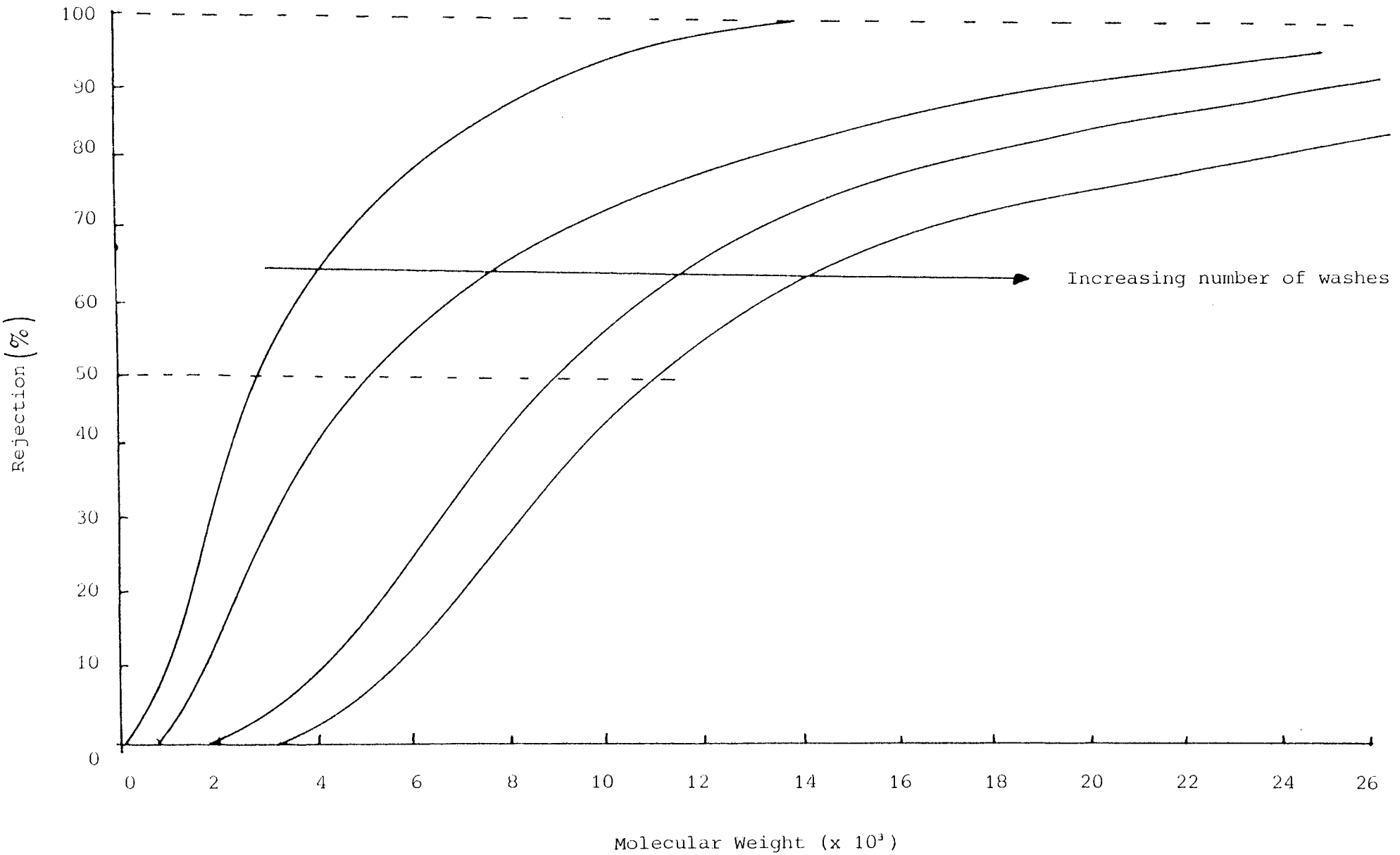

5.0 MEMBRANE CASCADE

5 MEMBRANE CASCADE

5.1 INTRODUCTION

The results obtained with the Amicon 5 000 MW cut-off membranes (Section 4.4) showed that dextran could be fractionated to within the required specification. However, to obtain this specification, 30% to 40% of the 'saleable' dextran (between 12 000 and 98 000 daltons) was lost in the permeate. This membrane efficiency is comparable to the efficiency at present obtained with ethanol fractionation.

If the lower energy costs involved in the membrane fractionation, compared to ethanol, are taken into account, the membrane process might be a more economically efficient method. This will be investigated in Chapter 6. However, it was decided to investigate methods of improving the membrane recovery.

In all the membrane experiments conducted (see Chapter 4) it was noted that initially only small molecules (ie. less than 12 000 daltons) passed through the membrane (Figures 5.1). As the number of diavolumes increased, the size of the molecules passing through the membrane also increased. Therefore, if a membrane is operated in this initial period, only molecules less than 12 000 daltons could be removed. Since no molecules greater than 12 000 daltons are removed this would give an efficiency of 100%. However, if a membrane is operated under these conditions, so little material would be removed that the product would be well outside specification.

Even though this method would be inadequate on its own it was decided to try to incorporate the principle into a system which would give a product within specification.

A possible useable system had been theoretically proposed by Cooper (98) (see Section 2.5.3). A schematic drawing of the proposed system is given in Figure 2.23. Cooper initially suggested this system as a means of reducing the amount of solvent needed in some ultrafiltration applications.

Figure 5.1: Diagram Showing the Variation of the Maximum Molecular Weight of Dextran in the Permeate, with Increasing Number of Diavolumes

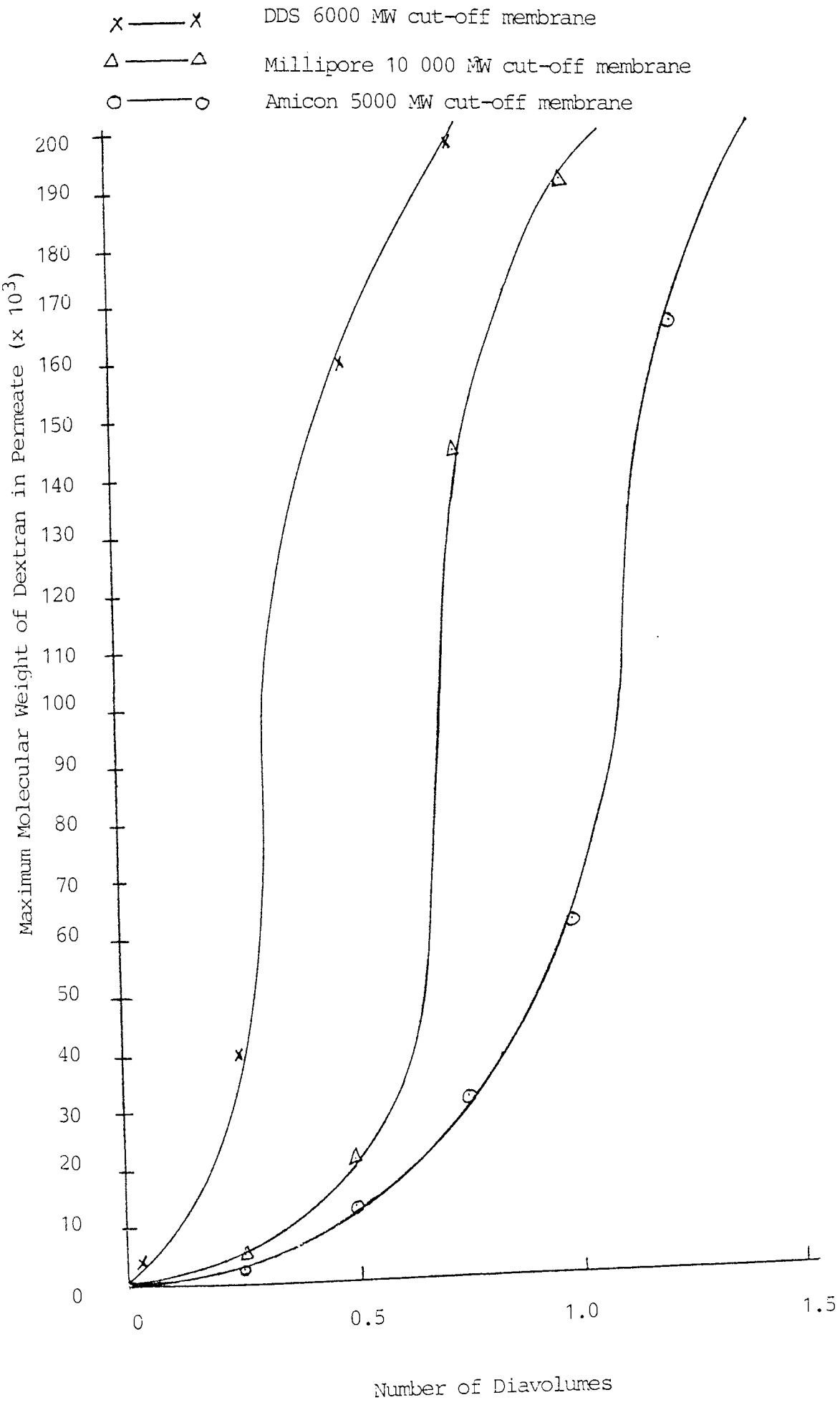

Figure 2.23: Schematic Diagram of Diafiltration Cascade for Decreased Solvent Use (98)

This new system is a multi-staged cascaded batch ultrafiltration process. The feed, containing an impurity solute and a desired solute, initially enters stage K. The feed is then processed under diafiltration conditions. The permeate produced contains some of the impurity and a proportion of the desired solute (depending on each solutes' rejection coefficient). This permeate is waste and the processed retentate then passes to stage (K - 1).

In stage (K - 1) the retentate is again processed under diafiltration conditions. More material of both wanted and unwanted solutes are removed as permeate. However, this permeate from (K - 1) is collected and used as the diafiltration top-up solvent for stage K. If the required solute has a higher rejection coefficient than the impurity, more of the required solute (compared to the impurity) is recovered by this recycle method. Hence, for a given product ratio of solutes the cascade method is more efficient.

The number of cascade units is chosen to give the required product. Since the diafiltration solvent is supplied by the next stage in the cascade, fresh solvent is only supplied in stage 1. This therefore saves (K - 1) volumes of fresh diafiltration solvent.

If this system was to be used with dextran, stage K could be designed to operate in the region where only material less than 12 000 daltons is removed.

Stage (K - 1) would then remove some of the remaining material below 12000 daltons and some of the material above 12000 daltons. The material above 12000 daltons would then be recovered in stage K.

This procedure would then be repeated until the product leaving stage 1 was within specification at the low molecular weight end. Theoretically if this method was adopted, the efficiency should be 100% since only low molecular weight material is removed in stage K.

Since material below 12000 daltons is recycled back to the previous stage, this effectively increases the amount of this material available to be fractionated. As proved in Section 4.4 if there is a large amount of low molecular weight material in a sample, a high proportion can be removed with a low loss of the saleable dextran. Therefore, this factor also would improve the efficiency of a cascade fractionation compared to a batch fractionation.

5.2 COMPUTER SIMULATION OF CASCADE OPERATION

As already stated, if only material below 12000 daltons is removed in stage K an efficiency of 100% can be obtained. However, for all the Amicon membranes tested this phenomena only occurred for the first 0.5 diavolumes, and all the membranes required approximately 12 diavolumes to obtain a product within specification. Since all the stages require the same number of diavolumes this means that a cascade of approximately 24 stages would be required.

This large number of stages was considered prohibitive on a cost basis. It was decided to accept some loss of saleable dextran in stage K and to increase the number of diavolumes per stage to two.

For the purpose of this simulation the membranes were considered to be simple separators acting on three different components. These components were (a) material below 12000 daltons, (b) material between 12000 and 98000 daltons and (c) material greater than 98000 daltons.

For each of these components a rejection coefficient could then be found at intervals of 2 diavolumes. These coefficients were averages of the values obtained for the individual Amicon membranes forming the cascade.

Once these coefficients were found the cascade system then simplified to a recycle mass balance problem. To solve this problem it was decided to use a computer package called 'Process' (written by Simulation Sciences Inc). This package was specifically designed for mass-balance problems and was available on a Harris computer at Aston.

To use this package an operating program (Appendix 3) was written which contained information on all the recycle streams required and the necessary rejection coefficients for each stage.

An example of an output from 'Process' is given in Appendix 4. Using this package, results could quickly be obtained for a varying number of stages in a cascade, and a summary of some results is given in Figure 5.2. These results give the product percentage below 12000 daltons and the efficiency obtained for four to twelve stages in a cascade.

As can be seen from these results there was no difference in the predictions for a change from 6 to 12 stages. When the individual stage compositions, calculated by 'Process' for 12 stages, were compared it was found that for the 6 middle stages no effective change in composition was obtained. Therefore, a maximum of six stages should be used.

Even though six is the recommended number of stages these simulation results show that there is very little difference between four and six stages. Therefore, it was decided that four stages would be the ideal number (on a cost basis) if a cascade rig was to be built.

These results also show that even if four stages are built, the final product will not be within specification. Therefore a secondary set of four cascade units would be needed in series with the first. The feed for this second cascade unit would be the retentate product from the first cascade. The permeate product from the second unit would not be recycled back to the first cascade but would be waste. This would prevent stages becoming ineffective, as happened when the initial cascade unit investigated was increased from six to twelve stages.

"Process" was used to predict the final product from these two cascade units in series. Also the product from three units in series was predicted and the results obtained are summarised in Figure 5.3.

Figure 5.2: Predicted Products from a Four to Twelve Stage Cascade system

Four Stage Cascade

% of product below 12 000 MW = 16%
† Efficiency = 89%

Five Stage Cascade

% of product below 12 000 MW = 16%
† Efficiency = 90%

Six Stage Cascade

% of product below 12 000 MW = 15%
† Efficiency = 90%

Eight Stage Cascade

% of product below 12 000 MW = 15%
† Efficiency = 90%

Ten Stage Cascade

% of product below 12 000 MW = 15%
† Efficiency = 90%

Twelve Stage Cascade

% of product below 12 000 MW = 15%
† Efficiency = 90%

$$\text{† Efficiency} = \frac{\text{Weight of 'saleable' dextran in product}}{\text{Weight of 'saleable' dextran in feed}}$$

Figure 5.3: Predicted Products from One to Three Cascade Units in Series

1st Four Stage Cascade Unit

% of product below 12 000 MW = 16%
† Efficiency = 89%

2nd Four Stage Cascade Unit

% of product below 12 000 MW = 10%
† Efficiency = 76%

3rd Four Stage Cascade Unit

% of product below 12 000 MW = 7%*
† Efficiency = 61%

$$\text{Efficiency} = \frac{\text{Weight of 'saleable' dextran in product}}{\text{Weight of 'saleable' dextran in original feed to cascade unit 1}}$$

* This meets Fisons specification for a Dextran 40

These results show that a product which is within specification at the low molecular weight end should be produced after three cascade units in series. This product is produced for the loss of only 39% of the 'saleable' dextran. This compares with a loss of 44% for the average batch membrane. Therefore, if an actual rig conforms to these predictions an improvement of over 5% should be obtained in using a cascade system compared to the batch system.

5.3 EXPERIMENTAL CASCADE EQUIPMENT

A schematic diagram of the four stage cascade unit which was constructed is given in Figure 5.4 and the actual equipment in Figure 5.5. The unit consisted of four one litre stainless-steel retentate tanks each with a float switch, four two litre stainless-steel diafiltration tanks with one having a float switch, four two litre stainless-steel permeate collection tanks each having a float switch, two dual-head variable speed peristaltic pumps, four needle valves, four pressure switches, four glass filters, four 30 psi pressure guages, a BBC 'B' micro computer, 23 AC solenoid valves and four Amicon 5000 molecular weight cut-off membranes.

The operation of the equipment can be broken down into the following steps:

(i) At the beginning of an experiment all the diafiltration tanks (D) are filled with two litres of de-ionised water. The retentate tanks (F) for stages 2, 3 and 4 are filled with one litre of de-ionised water (until the level switch (LF) registers closed). The retentate tank for stage one is then filled with one litre of feed solution (level switch (LF) closed).

(ii) On stages 2, 3 and 4 the recirculation valves (VF4) were then opened. On stage one the recirculation valve (VF4) and drain valve (VF6) were both opened (Figured 5.6). The peristaltic pump unit for stages 1 and 2 was then started. The speed of the pump was set so that both of the pump's two heads (PH1 and PH2) gave a flowrate of 400cm^3 min^{-1}. One of the heads supplied stage one and the other stage 2. This procedure was then repeated for the second dual-head pump. This second pump supplied stages 3 and 4 (PH3 and PH4) with a flowrate of 400cm^3 min^{-1}. The

Figure 5.4: Schematic Diagram of Four Stage Ultrafiltration Cascade

Key:

D	Diafiltration Tanks (4 of 2 Litres each)
DW	Deionised water supply
F	Feed (Retentate) Tanks (4 of 1 Litres each)
G	Glass filters
LD	Float level switch on Diafiltration Tank of Stage 4
LF	Float level switch on Feed Tanks
LP	Float switch on Permeate Collection Tanks
M	Amicon 5000 MW cut-off membranes
NF	New Feed to Stage 1
NV	Needle values (one per stage)
P	Permeate Collection Tanks (4 of 2 Litres each)
PF	Permeate Flux from Membranes
PH1, 2, 3, 4	Pump Heads 1, 2, 3, 4
PG	Pressure Guage (1 per stage)
PS	Pressure switch (1 per stage)
RP	Final Retentate Product
V	AC Solenoid Valves (23 total)
W	Permeate waste from cascade

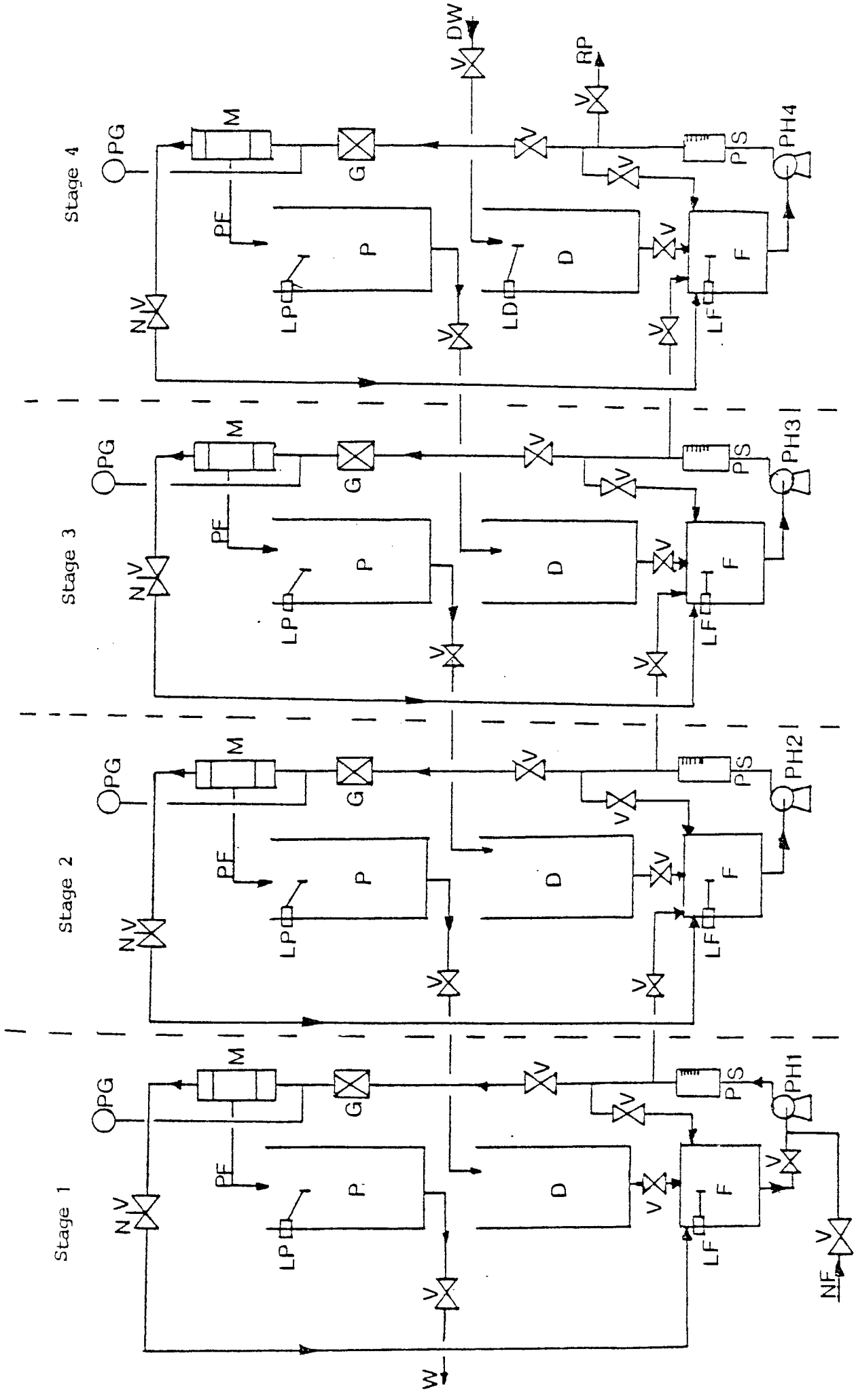
Stage 4
Stage 3
Stage 2
Stage 1
PG
M
G
PF
P
D
F
LP
LD
LF
PS
PH4
PH3
PH2
PH1
DW
RP
W
NF

Figure 5.4

Figure 5.5: Photograph of the Four Stage Membrane Cascade used at Aston

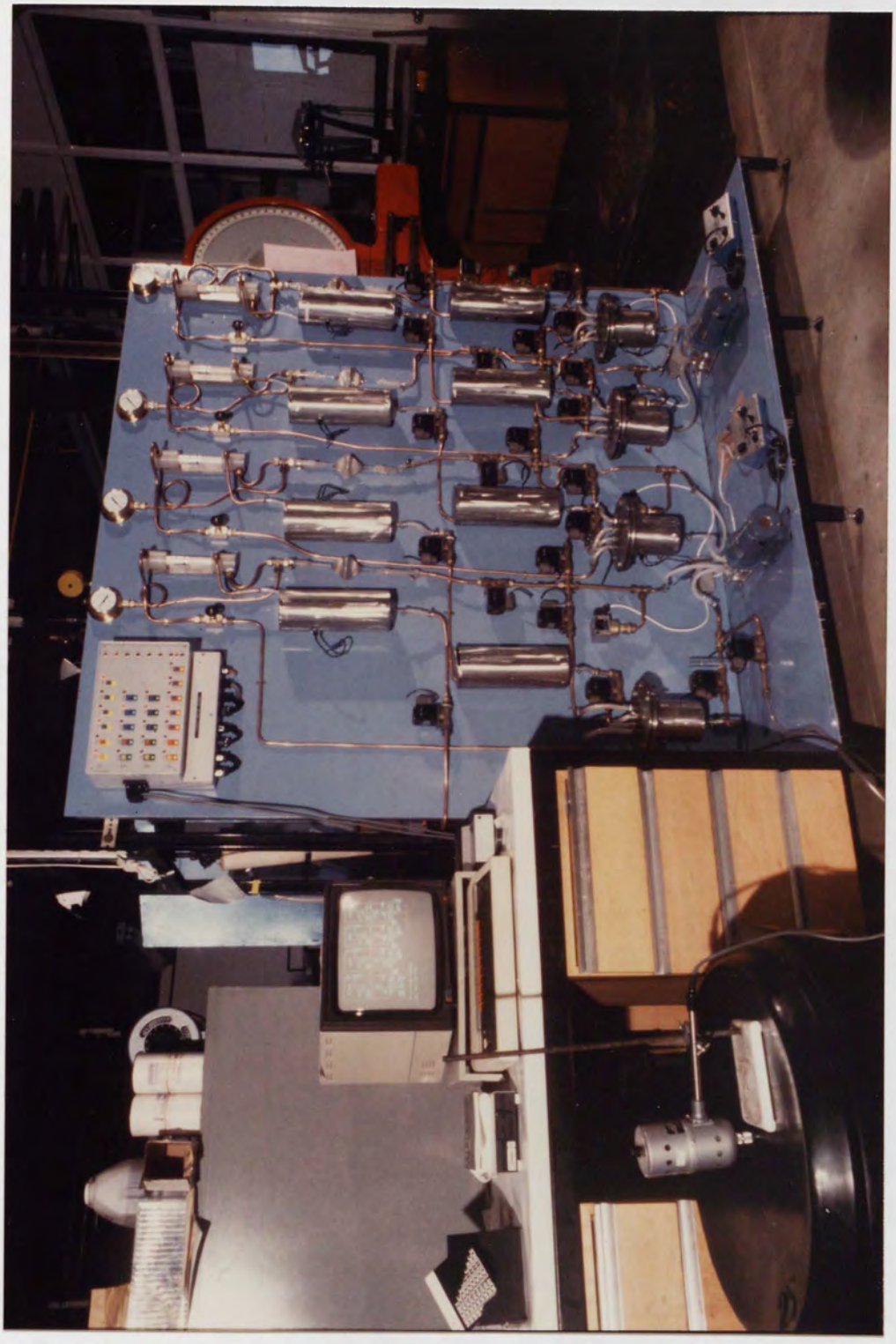

Figure 5.6: Diagram Showing the Valves used for Setting the Recirculation Rate of the Pumps

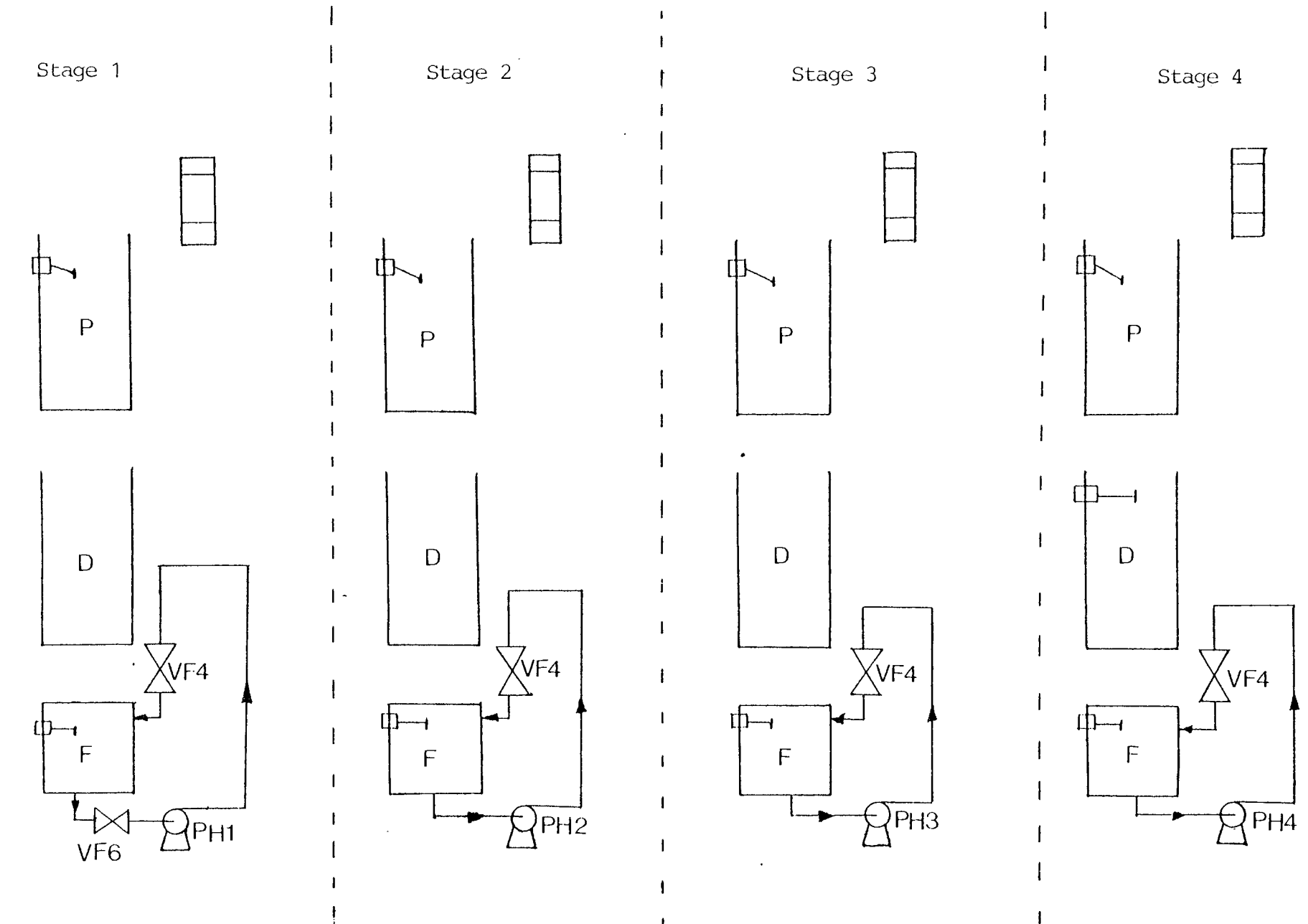

pumps used were Cole-Parmer Masterflex (supplied by Baird & Tatlock, England, UK) and the heads used were capable of flowrates of 16.8 to 1680 cm^3 min^{-1}.

(iii) On stage one the recirculation valve (VF 4) was then closed and the membrane valve (VF 3) opened (Figure 5.7). The retentate solution was then pumped through the Amicon membrane (M). To obtain the correct trans-membrane pressure the metering needle valve (NV) (Hoke Ltd, England, UK) on stage one was adjusted so that the inlet pressure guage (PG) showed 0.8 Kg cm^{-2}. The maximum inlet pressure of the membrane was set at 1.2 Kg cm^{-2} using a pressure switch (PS) (Type DCM-1, Texcel Ltd, St Albans, Herts). When the inlet pressure to the membrane exceeded this value the pressure switch automatically switched off the pump drive unit for stage one. When the pressure decreased below the set value the pump was switched on again.

This procedure was then repeated for stages 2, 3 and 4 (using the same inlet and outlet pressure settings).

(iv) Once the pressures were set, the permeates (PF) produced by the four membranes were then collected in the four permeate (P) tanks (Figure 5.7). The processed retentates were recycled to the retentate (F) tanks. As the level in the P tanks rose the level in the F tanks dropped, which then caused the LF switches to open. When the LF switches registered open the diafiltration (D) tanks' drain valves (VD1) opened. The diafiltration drain valves (VD1) stayed open until enough solution had been added to the F tanks to close the LF switch.

The opening and closing of the VD1 valves continued until the two litres of permeate were collected, ie. when a LP switch registered closed. This use of the VD1 valves kept the volume in the F tanks at an almost constant value.

(v) When a LP valve registered closed on a stage the VF3 valve (for that stage) was automatically shut and the recirculation valve (VF4) opened (Figure 5.8). This procedure prevented any more permeate being collected in that stage. This procedure was repeated independently for each stage. In Figure 5.8 stages one and four have completed their individual cycles. Stages 2 and 3 are incomplete.

Figure 5.7: Diagram Showing the Valves used for Setting Trans-Membrane Pressure, and for Permeate Collection, for Stage One

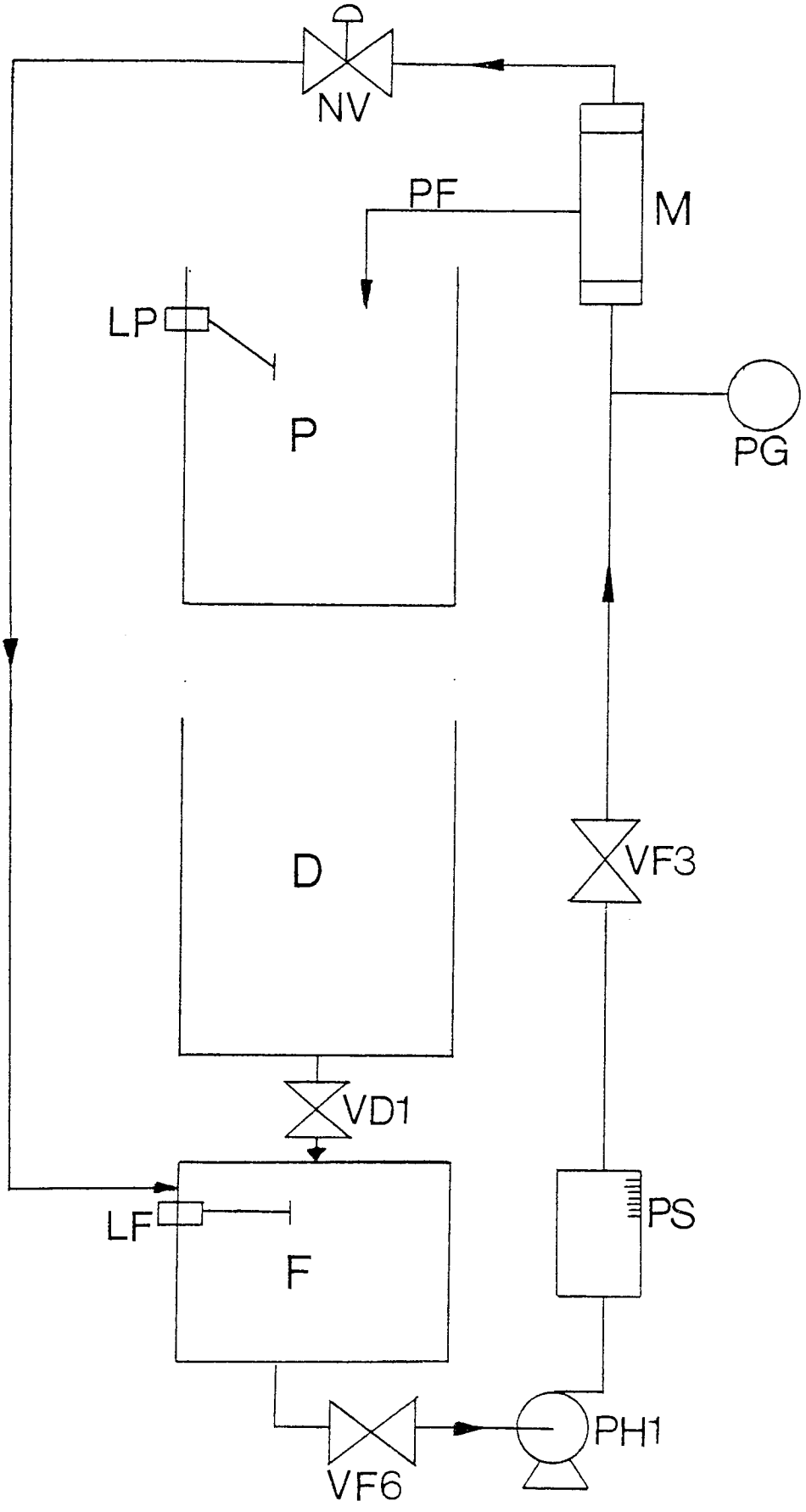

Figure 5.8: Diagram Showing the Valves used for when Stages One and Four have completed a cycle, and Stages Two and Three are still collecting Permeate

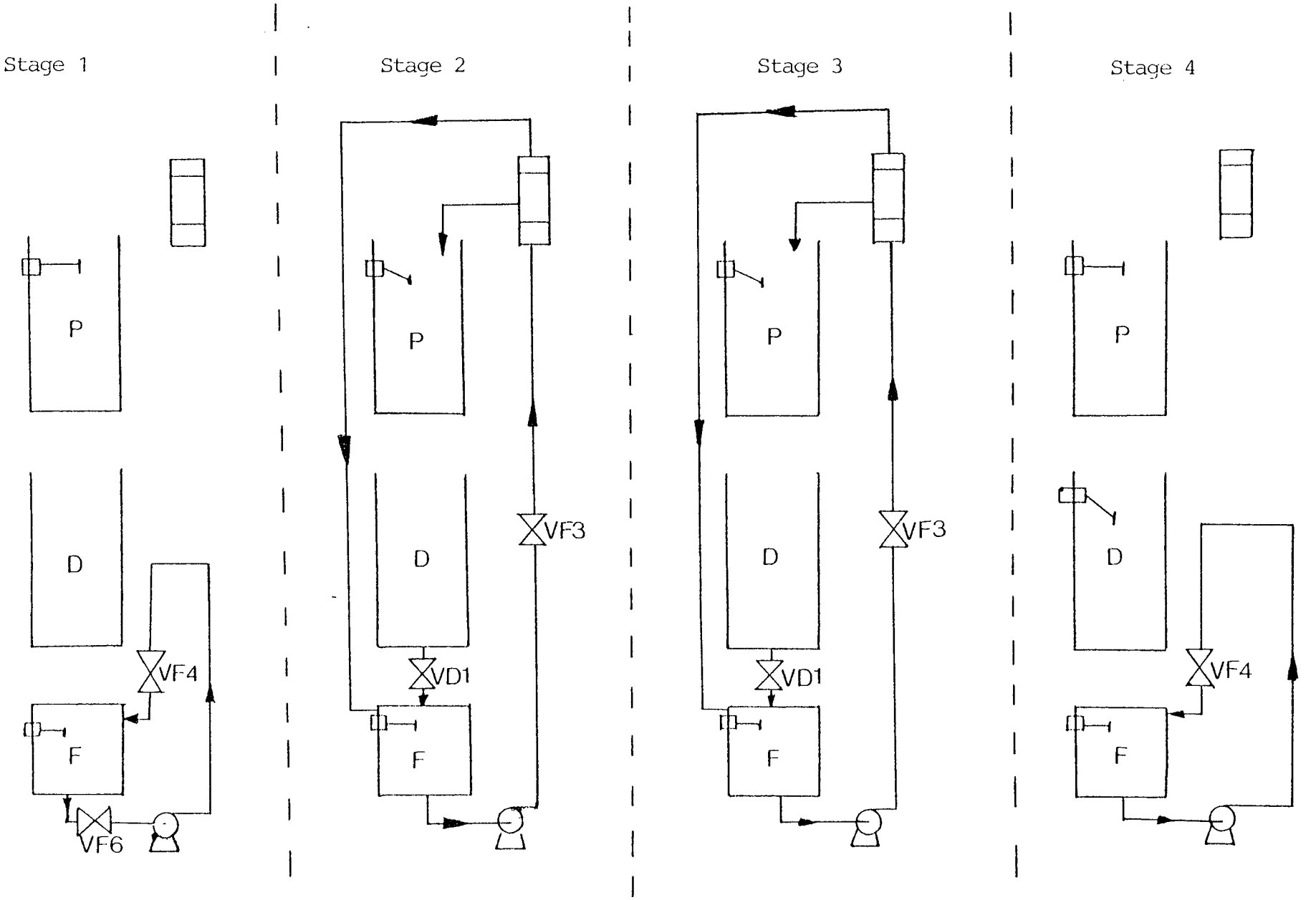

(vi) When all the correct amounts of permeate had been collected (ie. when all the LPs were closed) a cycle was then completed. At this point the recirculation valve (VF4) on stage four was then closed. The product valve (VF6) for stage four was simultaneously opened (Figure 5.9). The exit pipe from VF6 was connected either to a drain or a collection tank. The product from tank four is the final product of the whole cascade unit.

Valve VF6 (on stage four) was left open for a time period which had been pre-set so that tank F was completely drained. Once tank F was drained VF4 was opened and VF6 closed.

(vii) The product from tank F on stage 3 was then transferred to tank F on stage 4 (Figure 5.10). This was accomplished by closing VF4 on stage 3 and opening VF5 on stage 4. The transfer was completed when LF on stage 3 registered open and LF on stage 4 was closed. At this point VF5 on stage 4 was closed and VF4 on stage 3 opened.

This procedure was repeated for the transfer of products from stage 2 to stage 3 and from stage 1 to stage 2.

(viii) Tank F on stage 1 was then filled with fresh feed solution (see Figure 5.11). This was accomplished by closing VF6 and opening VF5 (the inlet to VF5 was connected to a tank containing the feed solution). Fresh feed was pumped into the tank F until the LF switch registered closed. At this point VF5 was closed and VF6 was again opened.

(ix) When the transfer of the retentates was finished the permeate tanks' drain valves (VP2) were opened (Figure 5.12). The permeate from stage 1 was then drained to waste. The permeate from stage 2 filled the diavolume (D) tank for stage 1 (thus recycling the permeate to the previous stage). This was repeated for stages 3 and 4. The VP2 valves were then closed.

Since there was no stage 5, the diavolume tank of stage 4 was filled with de-ionised water from a main storage tank. This was done by opening VP7 until the LD switch registered closed.

Figure 5.9: Diagram Showing the Valves used for Draining the Product from Stage Four

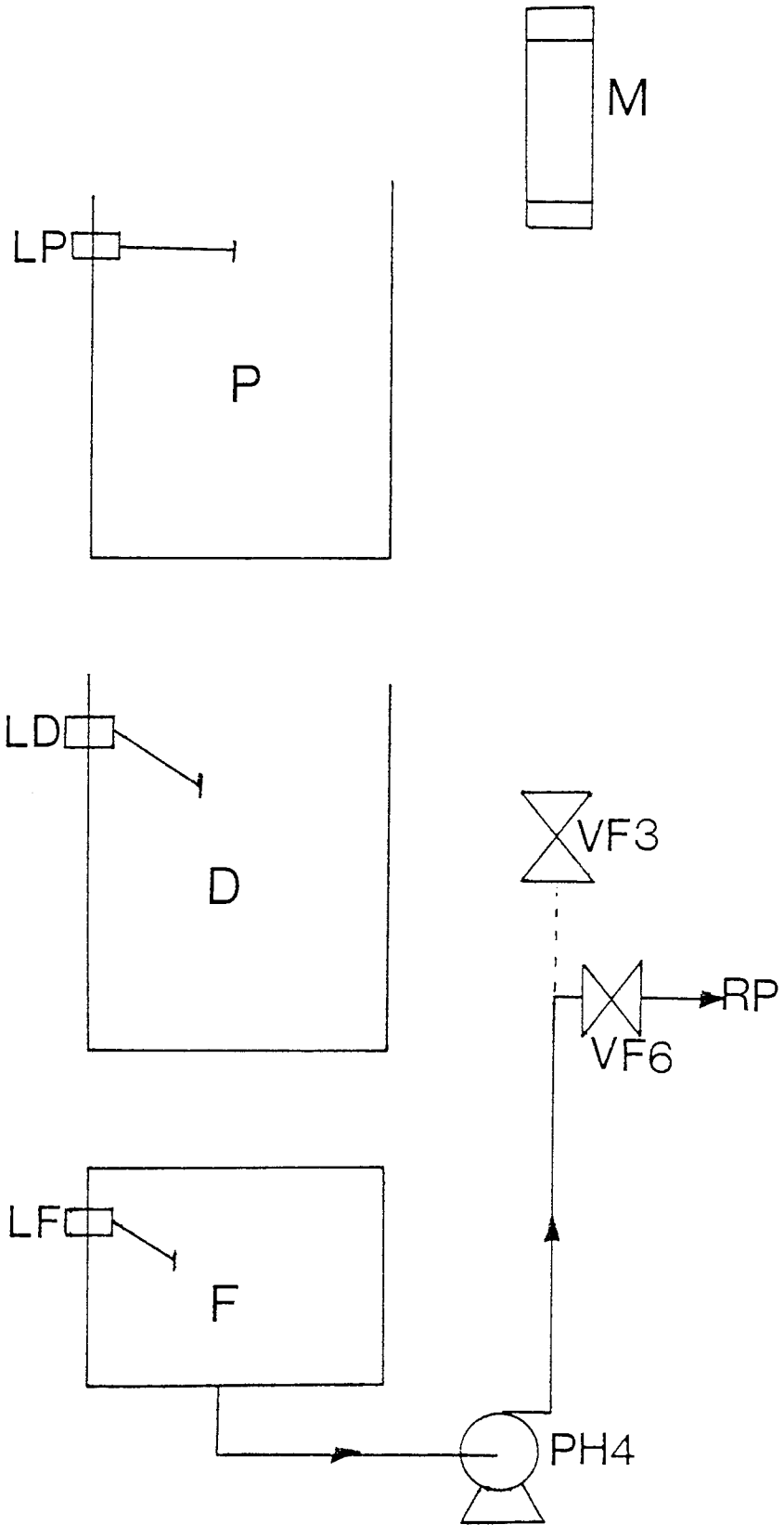

Figure 5.10: Diagram Showing the Transfer of Product from Stage Three to Stage Four

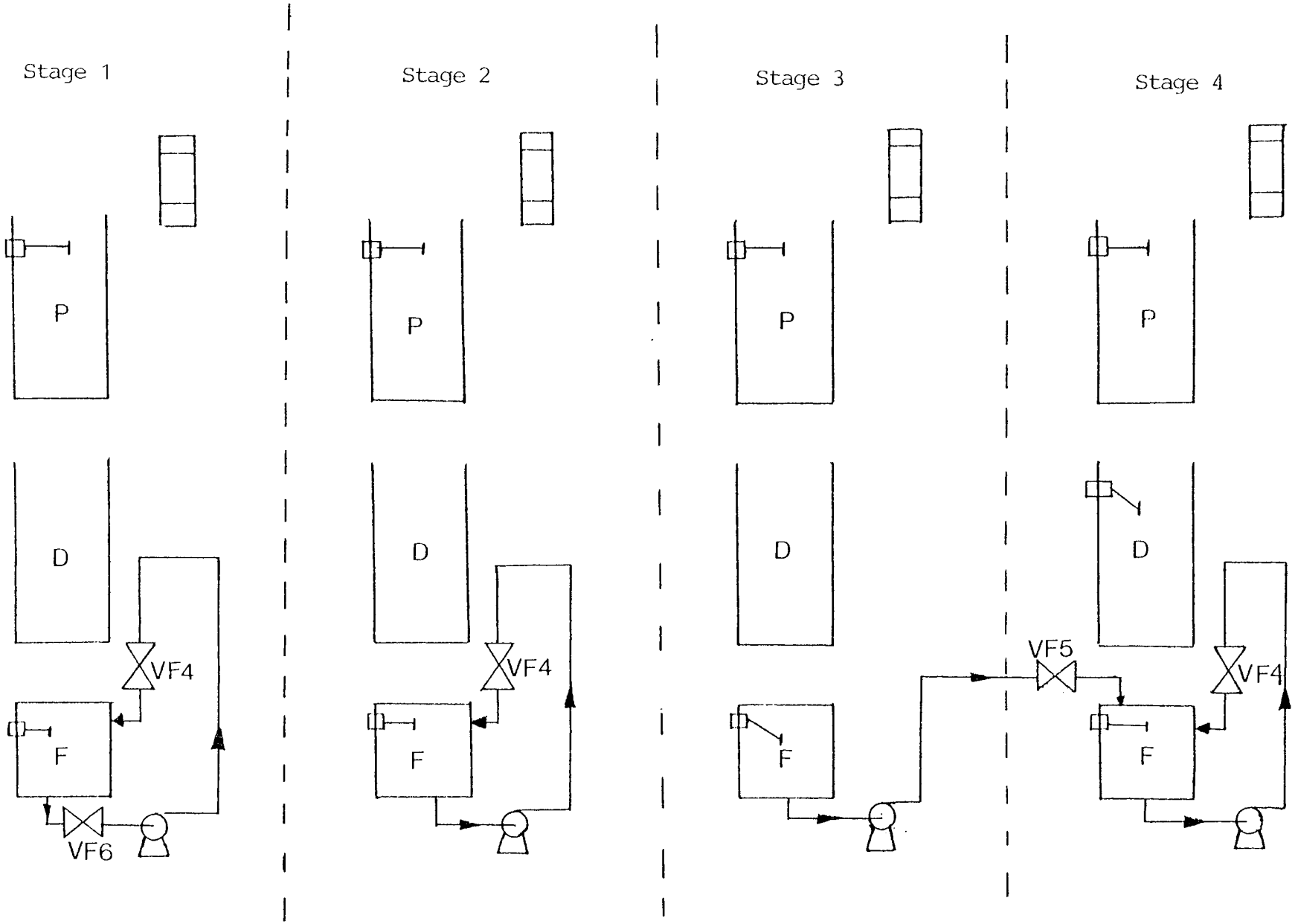

Figure 5.11: Diagram Showing the Replenishment of Stage One with Fresh Feed

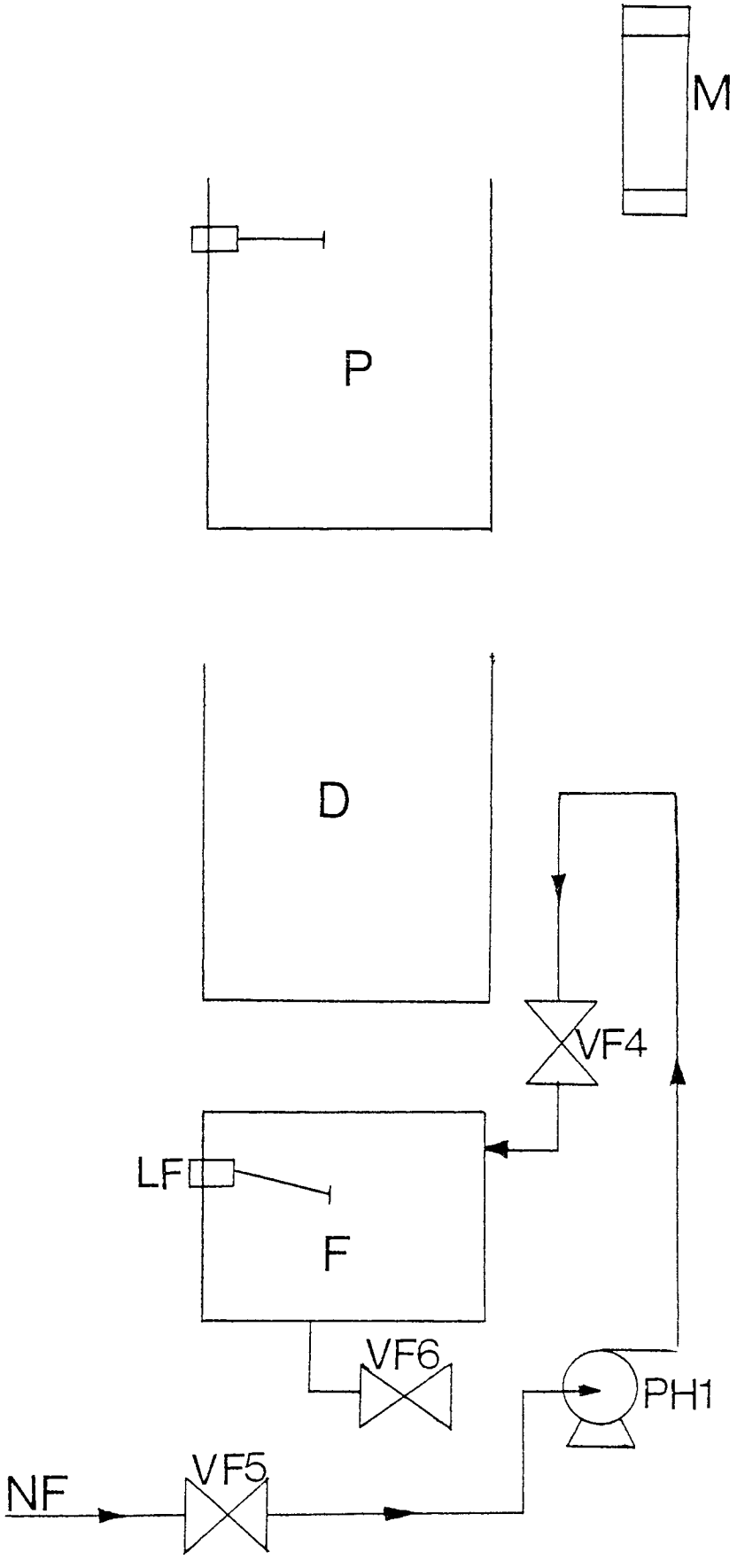

Figure 5.12: Diagram Showing the Recycle of Permeates, and the Addition of Fresh Solvent to Stage Four

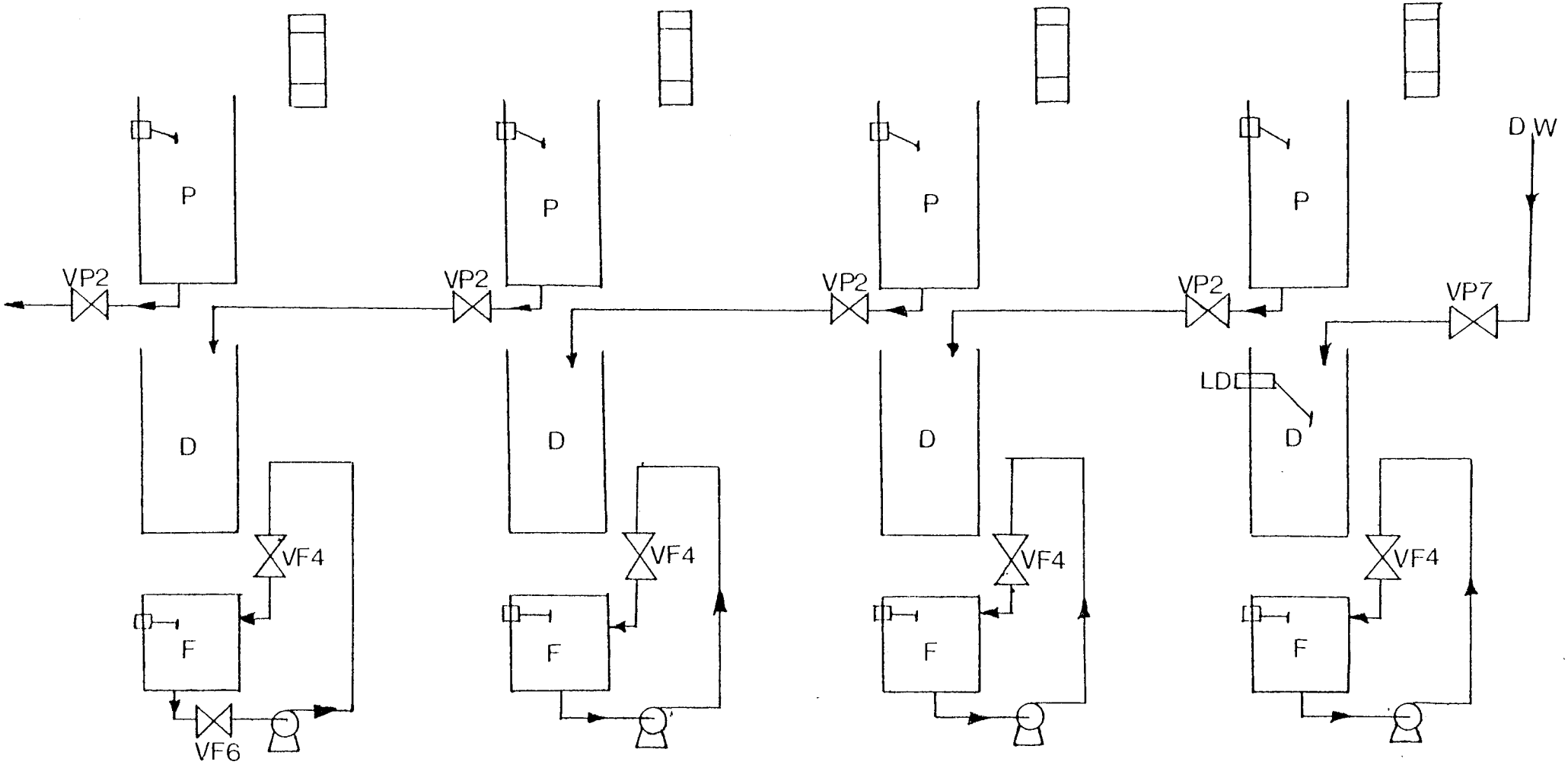

(x) Once all the D tanks were filled the VF4 valves were closed and the VF3 valves opened on all the stages. The next cycle was then started and continued from step (iv) (Figure 5.7).

The opening and closing of the solenoid valves was accomplished by use of a BBC (B) micro computer. The computer also monitored the condition of all the float switches.

The computer controlled the valves via solid state relays (supplied by RS Components Ltd, Birmingham, England). These relays were rated for a continuous 2.5 amps and 250 volts, and the solenoid valves operated at only 240 volts and 100 m Amps. However, even though the relays were rated well above the needs of the solenoid valves great problems were encountered with high voltage and current spikes generated by the AC solenoids. These spikes tended to destroy the relays and therefore anti-surge suppressors were added to the relays. These suppressors were rated for 250 volts and any voltage in excess of this was shorted off by the suppressor. Theoretically this should have prevented any voltage over 250 volts from damaging the relays. Unfortunately, this proved to be incorrect and the relays were still damaged by 'spikes' from the solenoid valves. After extensive work the problem was reduced by lowering the operating voltage of the valves from 250 volts to 160 volts.

To switch a solenoid valve on, the computer would send a small dc voltage to the relay which was connected to the relevant valve. This dc signal would then close a circuit in the relay which would in turn switch on the high AC voltage to the solenoid valve. This AC voltage then opened the valve.

Since the float switches produced only a small dc voltage (when closed) these switches were monitored directly by the computer.

The software needed to monitor the float switches and open the relevant solenoid valves (in the correct sequence) is given in Appendix 5. The program is split

into seven subroutines and each of the subroutines accomplishes one of the steps, from IV to X, mentioned above.

While the computer is controlling the cascade equipment, a schematic of the equipment is continually displayed on the VDU of the computer (see Figure 5.13). This schematic shows which valves are open and whether the level switches are open or closed. In figure 5.13 any valve showing red is open and any level switch showing red is closed and the relevant tank is full of liquid. During an experiment the computer also displays the total number of cycles completed. As well as controlling the opening of the solenoid valves the computer can also test to ensure that some items of equipment are actually working properly. If the computer does detect a problem the software goes into an alarm mode and flashes a warning to the operator. The operator can then correct this problem manually. While the problem is uncorrected the computer will pause in operation, but then continues once the problem is rectified. This feature proved useful in the commissioning of the equipment, when the cascade was left unattended overnight and at weekends.

The computer could only control the equipment once all the tanks were filled with the correct volumes of liquid. Therefore, a manual override was incorporated into the electronics of the system. This override enables the operator to open and close any of the solenoid valves independently of the computer. Therefore, when the rig was initially filled with water, the manual override was used and then the computer took control.

Both the electronics and machine code software used in controlling the rig were developed by D Bleby (Aston University) in conjunction with the author.

To protect the membranes from any debris which might be present in the system a porous glass filter (grade 2) was placed, in-line, before each of the membranes. Also, to prevent bacterial growth in the equipment, sodium azide was added to the feed solution. A concentration of 0.04% w/v was used.

Figure 5.13: Photograph of the Schematic Diagram Displayed by the Computer Controlling the Four Stage Cascade Equipment

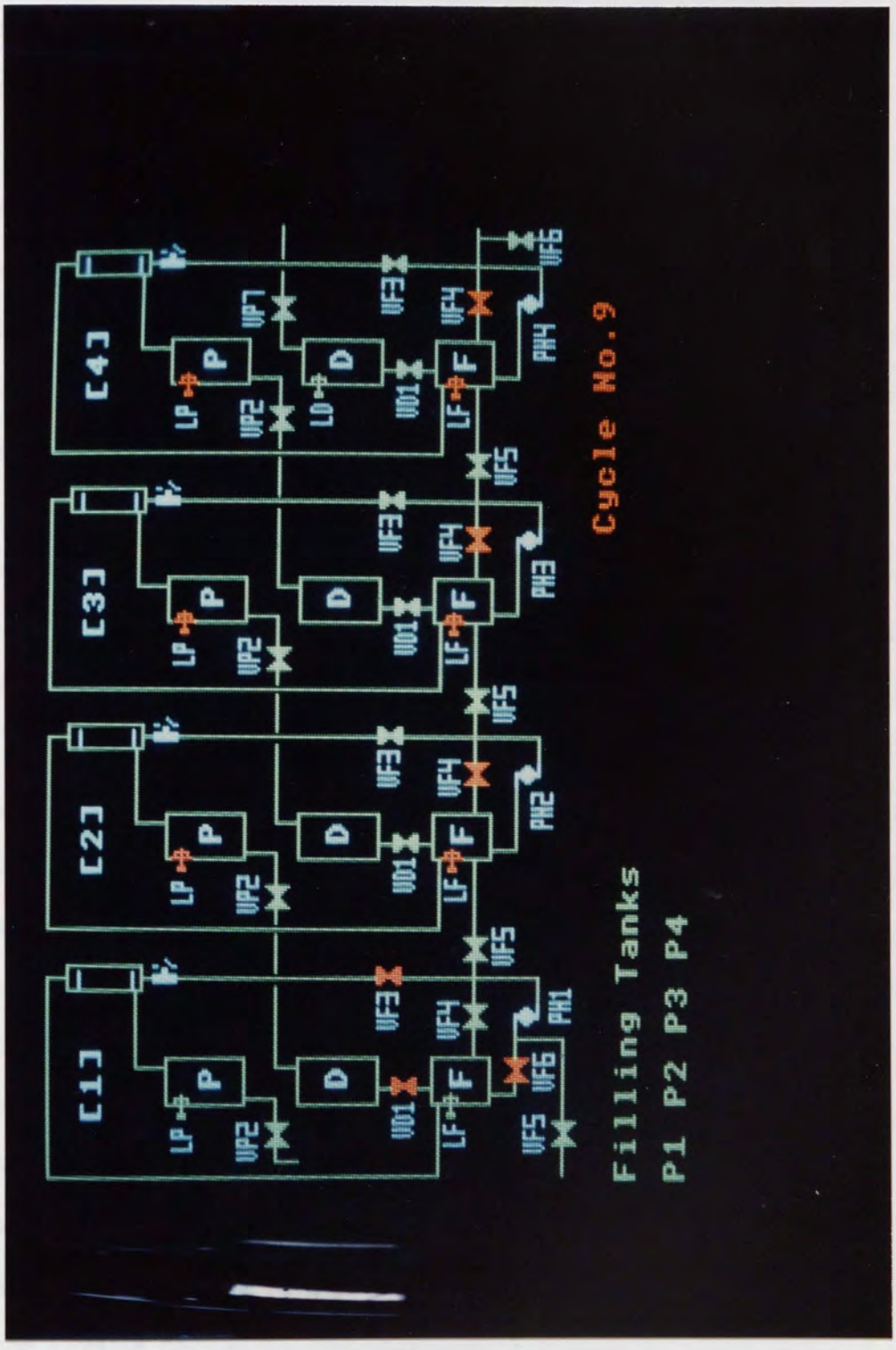

5.4 EXPERIMENTAL RUNS CONDUCTED

As stated in Section 4.4 out of the five Amicon 5000 molecular weight cut-off membranes tested one was considered to be faulty (Number 3). However, in order to assess the effect of a 'faulty' membrane on the performance of the cascade equipment, membrane number 3 was used in the first two experimental runs. The results obtained for these two experiments are summarised in Figures 5.14 to 5.17.

These results were obtained when the cascade equipment had achieved steady-state. This condition was determined by analysing the retentate products of consecutive cycles by GPC and polarimeter. If the analyses agreed to within the limitations of the analytical equipment (2% GPC, 1% polarimeter) steady state was said to be achieved. As can be seen there was a reasonable agreement for both runs over four cycles (Figures 5.15 and 5.16).

The operating conditions of runs 1 and 2 were set at approximately the same values in order to determine the reproducibility of any results obtained. As can be seen from the comparison of the two rejection graphs obtained (Figure 5.17) there was a close agreement.

Figure 5.18 gives a comparison of the average rejection coefficients for the cascade runs 1 and 2, and an average set of rejection coefficients for a comparable batch experiment. These average batch coefficients were found by calculating the individual coefficients of the four membranes used. This is done at an equivalent batch fractionation as that obtained for the cascade equipment. These individual coefficients were then averaged. This comparison shows that for very small dextran molecules (up to 6000 daltons) the cascade had a lower rejection coefficient than the batch method. Therefore, the cascade equipment was better at removing this low molecular weight material. Also the cascade equipment had the highest rejection coefficients for the material above 6000 daltons, indicating that it was recovering more of the 'saleable' dextran than the batch method.

Figure 5.14

EXPERIMENTAL CASCADE RESULTS USING AMICON 5000 MOLECULAR WEIGHT CUT-OFF MEMBRANES

Run Number	Feed Solution				Product Solution				Experiment† Efficiency
	Concentration (g/100g solution)	Percentage less than 12 000 MW	Percentage between 12 000 MW and 98 000 MW	Percentage above 98 000 MW	Concentration (g/100g solution)	Percentage less than 12 000 MW	Percentage between 12 000 and 98 000 MW	Percentage above 98 000 MW	
1	2.06	25	61	14	1.576	18	68	14	85%
2	2.27	25	61	14	1.71	18	69	13	85%
3	2.04	25	61	14	1.676	18	68	14	91.6%
4	2.04	25	61	14	1.63	17	69	14	90%
5	1.765	25	61	14	1.45	18	68	14	91.5%
6*	1.45	18	68	14	1.11	13	73	14	81.6%
7**	1.11	13	73	14	0.83	10	75	15	76.4%

* Feed is product from Run 5

** Feed is product from Run 6

† Efficiency = $\frac{\text{Weight of 'saleable' Dextran in product}}{\text{Weight of 'saleable' Dextran in Feed}}$

Figure 5.15: Comparison of GPC and Polarimeter Results for Four Cycles from Run 1

Sample Concentration (g/100g solution)	% Less than 12 000 MW	% Between 12 000 and 98 000 MW	% Greater than 98 000 MW
Cycle 19 (1.576)	18 19	68 67	14 14
Cycle 21 (1.562)	20 20	66 66	14 14
Cycle 30 (1.576)	19 20	66 66	15 14
Cycle 31 (1.576)	18 18	68 68	14 14

Figure 5.16: Comparison of GPC and Polarimeter Results for Four Cycles From Run 2

Sample Concentration (g/100g solution)	% Less than 12 000 MW	% Between 12 000 and 98 000 MW	% Greater than 98 000 MW
Cycle 20 (1.69)	18 19	68 68	14 13
Cycle 25 (1.71)	18 18	69 69	13 13
Cycle 30 (1.705)	19 18	68 68	13 14
Cycle 31 (1.71)	18 20	69 68	13 12

Figure 5.17: Comparison of Rejection Profiles for Cascade Runs One and Two

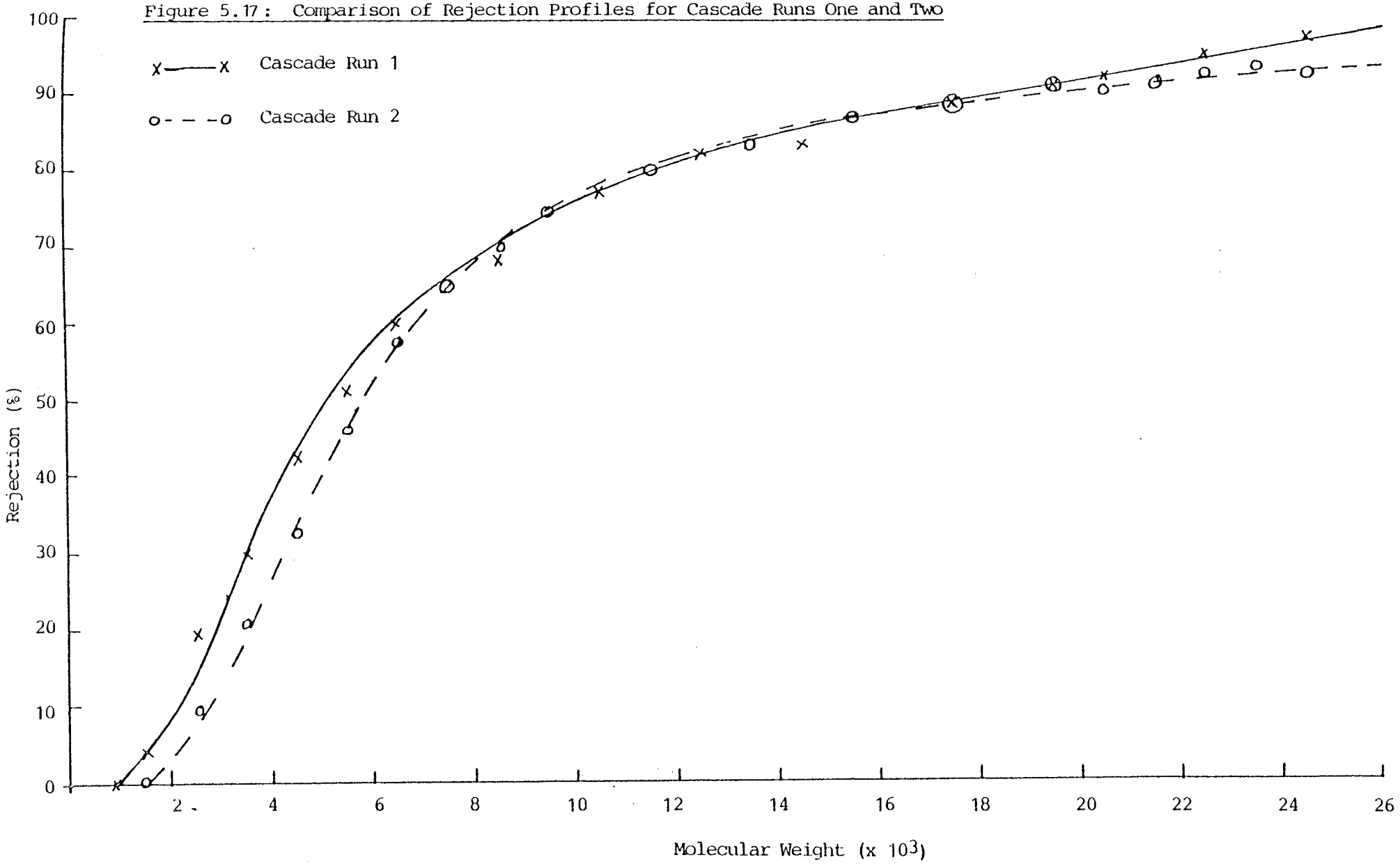

Figure 5.18: Comparison of the Rejection Profiles of the Cascade and Batch Experiments, for Similar Fractionations

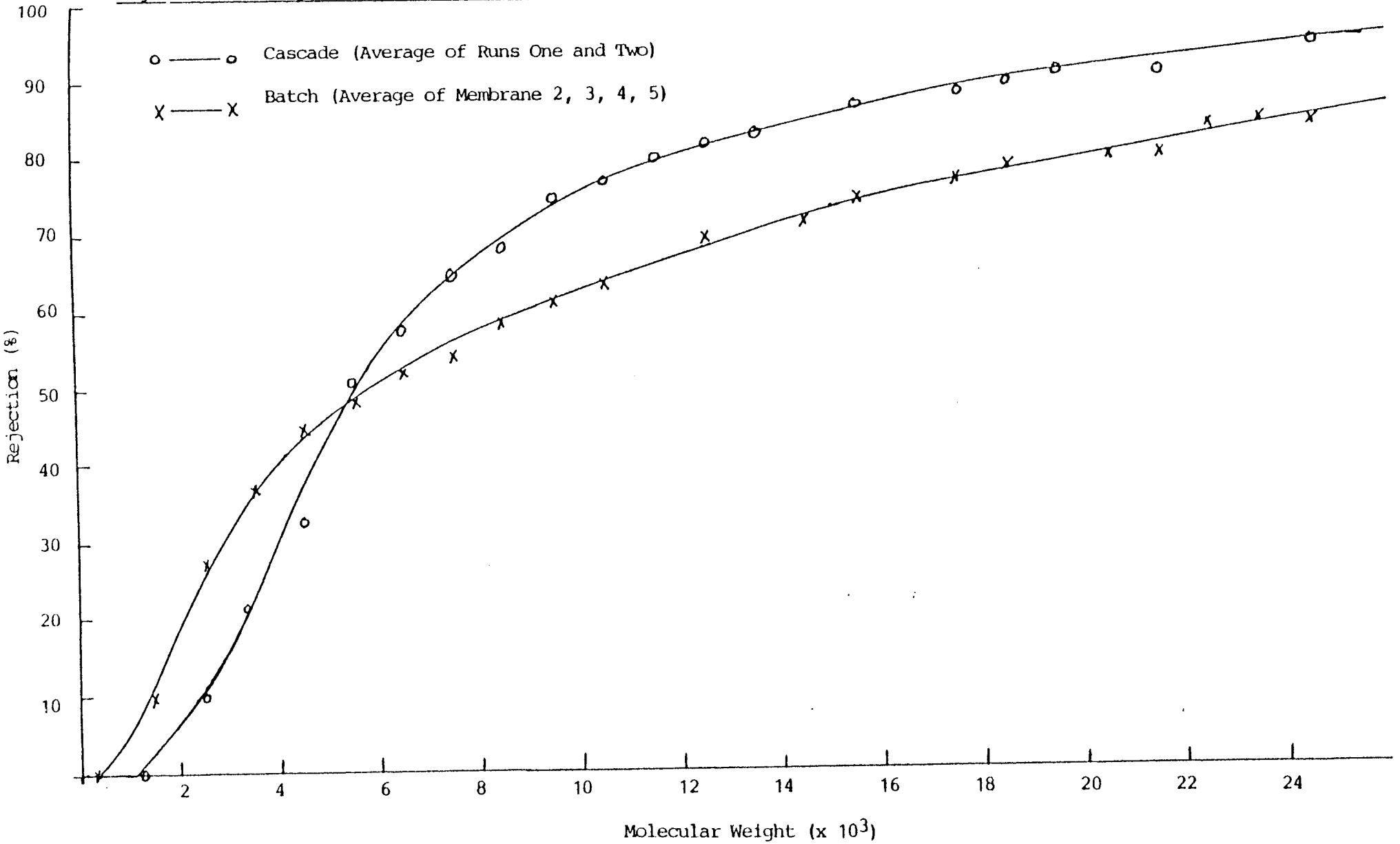

For runs 3 and 4 the 'faulty' membrane (Number 3) was replaced by a 'good' membrane (Number 1). By comparing the results for runs 1 and 2 with runs 3 and 4 the effect of the 'faulty' membrane could be found. The results obtained for runs 3 and 4 are summarised in Figure 5.14 and Figures 5.19 to 5.20.

As with runs one and two there was close agreement between the results obtained for runs three and four indicating reproductibility of experimental results. Also the cascade was again shown to be more efficient than the batch mode in removing the dextran below 6000 daltons and more efficient in recovering dextran above 6000 daltons (Figure 5.20).

When the average of runs one and two are compared with the average of runs three and four (Figure 5.21), the faulty membrane (Number 3) is shown to reduce the cascade's effectiveness at removing the low molecular weight material (below 6000 daltons) and its effectiveness at retaining the material above 6000 daltons. However, on an individual batch basis, membrane 3 had a rejection coefficient of approximately 15% below that of membrane 1 for a molecular weight of 25000 daltons. When the two sets of cascade runs are compared at this molecular weight there is a difference of less than 5%. Therefore, the detrimental effect of the 'bad' membrane was lessened in the cascade equipment by the performance of the 'good' membranes.

Since more than one cascade unit would be required to obtain a dextran product within specification, a two and three cascade unit was simulated. This was accomplished by initially repeating run one. The product from this run was collected over a number of cycles once steady-state had been achieved. This product was then used as feed for run 6. The product from run 6 is equivalent to a product from two cascade units in series. The steady state product from run 6 was again collected over a number of cycles and used as feed for run 7. This is equivalent to three cascade units in series.

The results obtained for runs 5, 6 and 7 are summarised in Figure 5.14 and Figures 5.22 to 5.25.

Figure 5.19 : Comparison of the Rejection Profiles for Cascade Runs Three and Four

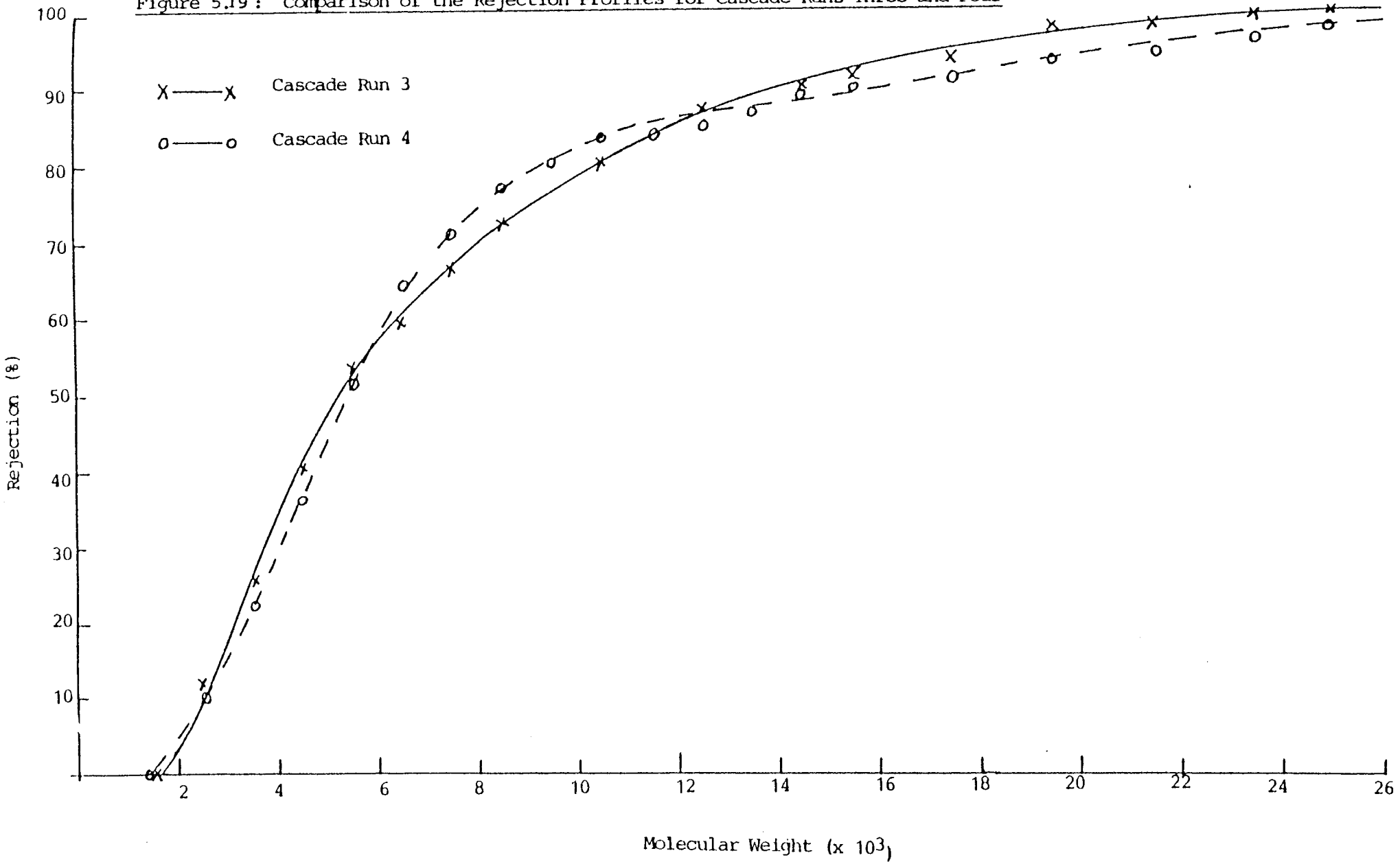

Figure 5.20: Comparison of the Rejection Profiles of Cascade and Batch Experiments, for Similar Fractionations

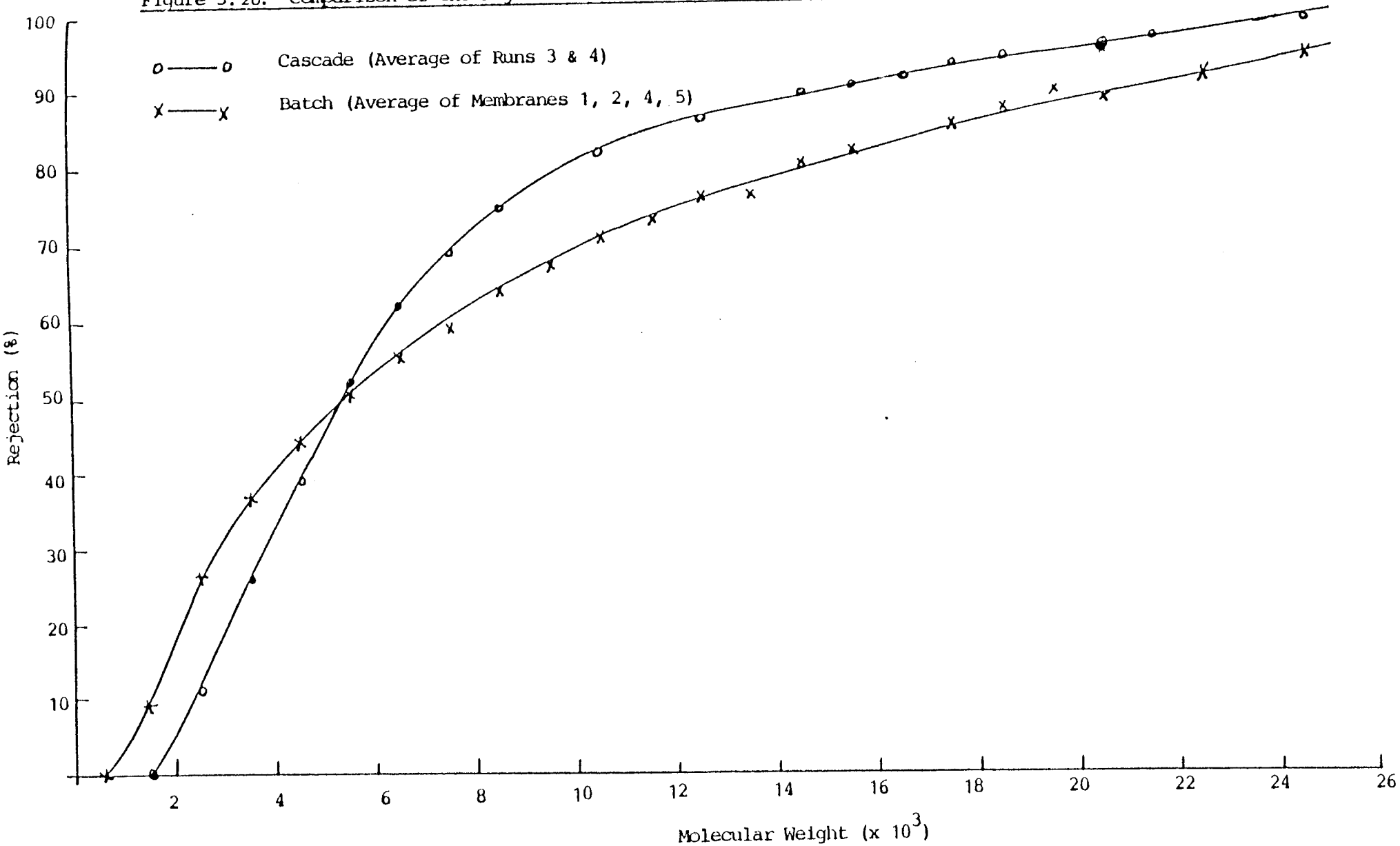

Figure 5.21: Diagram Showing the Effect of a Faulty Membrane on the Rejection Profile of the Cascade System

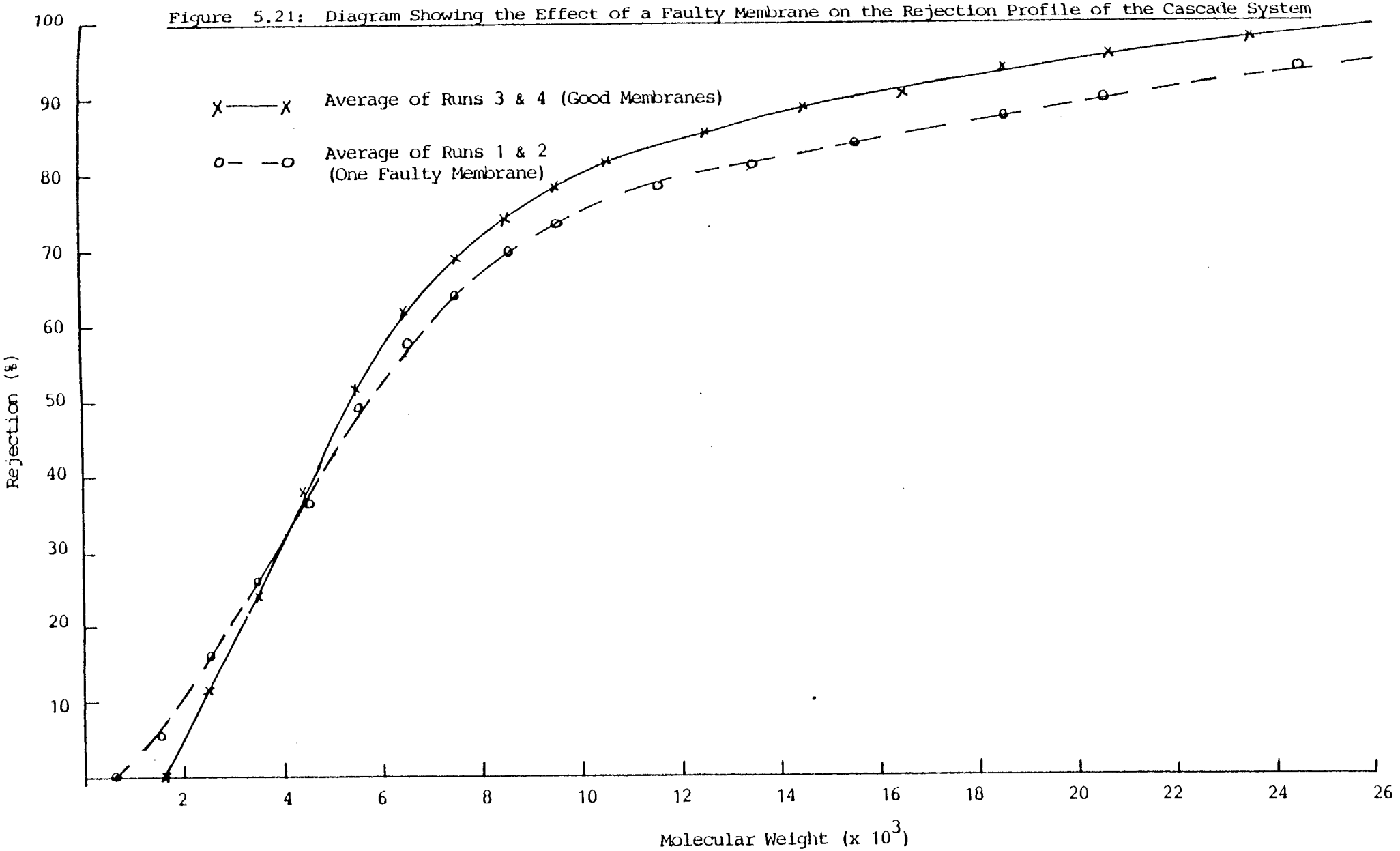

Figure 5.22: Comparison of Rejection Profiles for One, Two, and Three Cascade Units in Series, Based on the Actual Feed to Each Unit

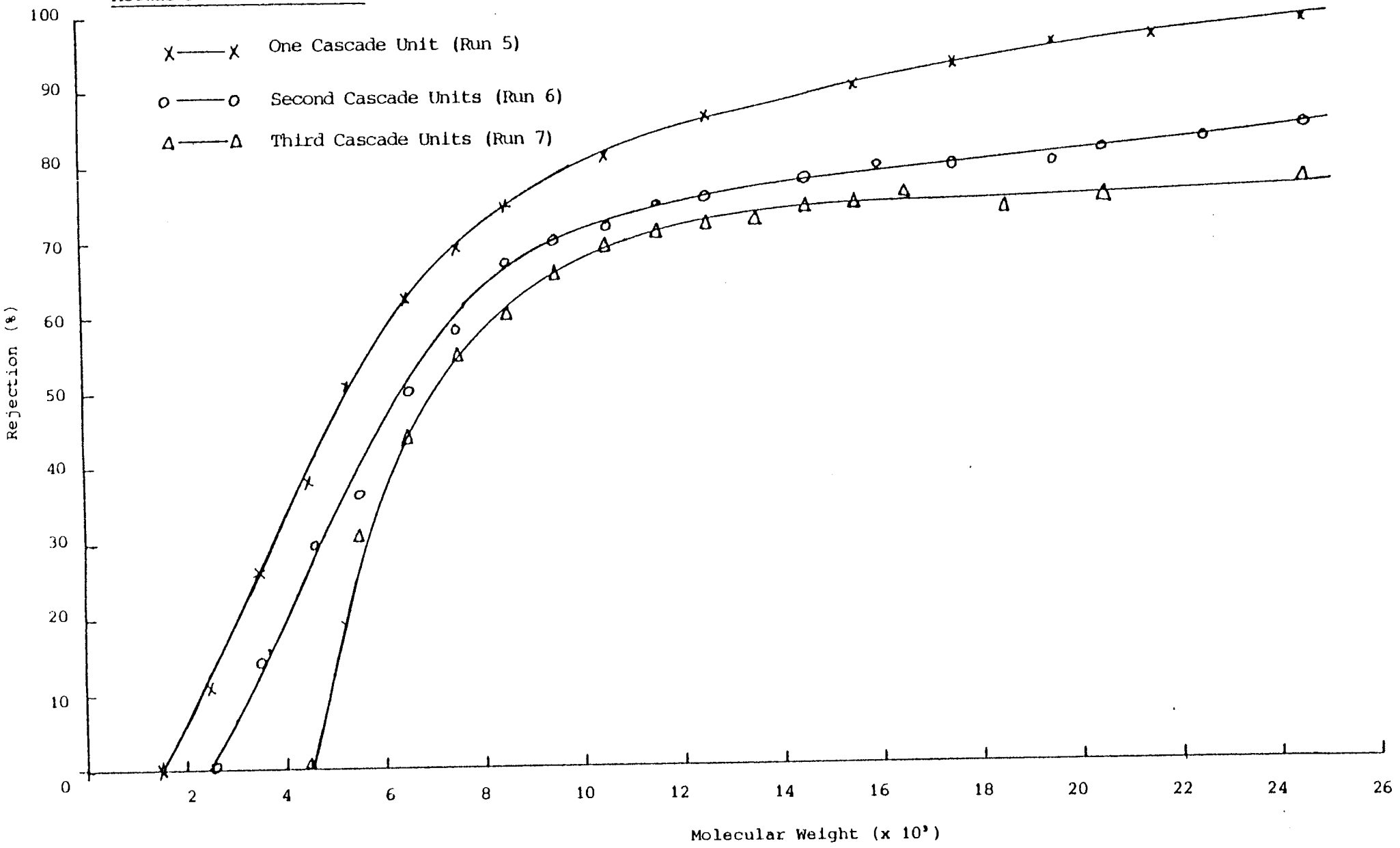

Figure 5.23: Comparison of Rejection Profiles for One, Two and Three Cascade Units in Series, Based on the Feed to Cascade One

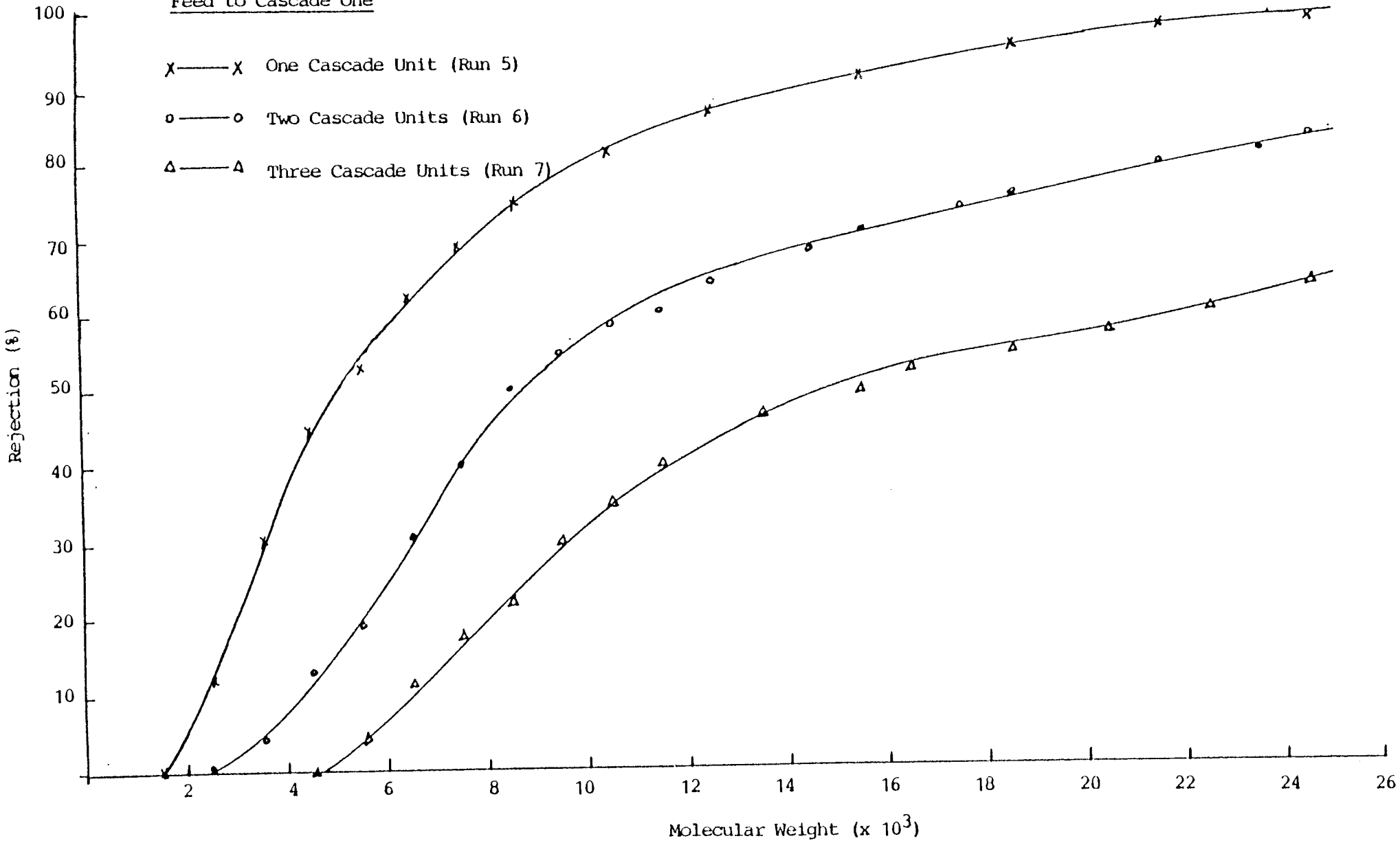

Figure 5.24: Comparison of the Rejection Profiles for Cascade Number Two, and an Equivalent Batch Fractionation

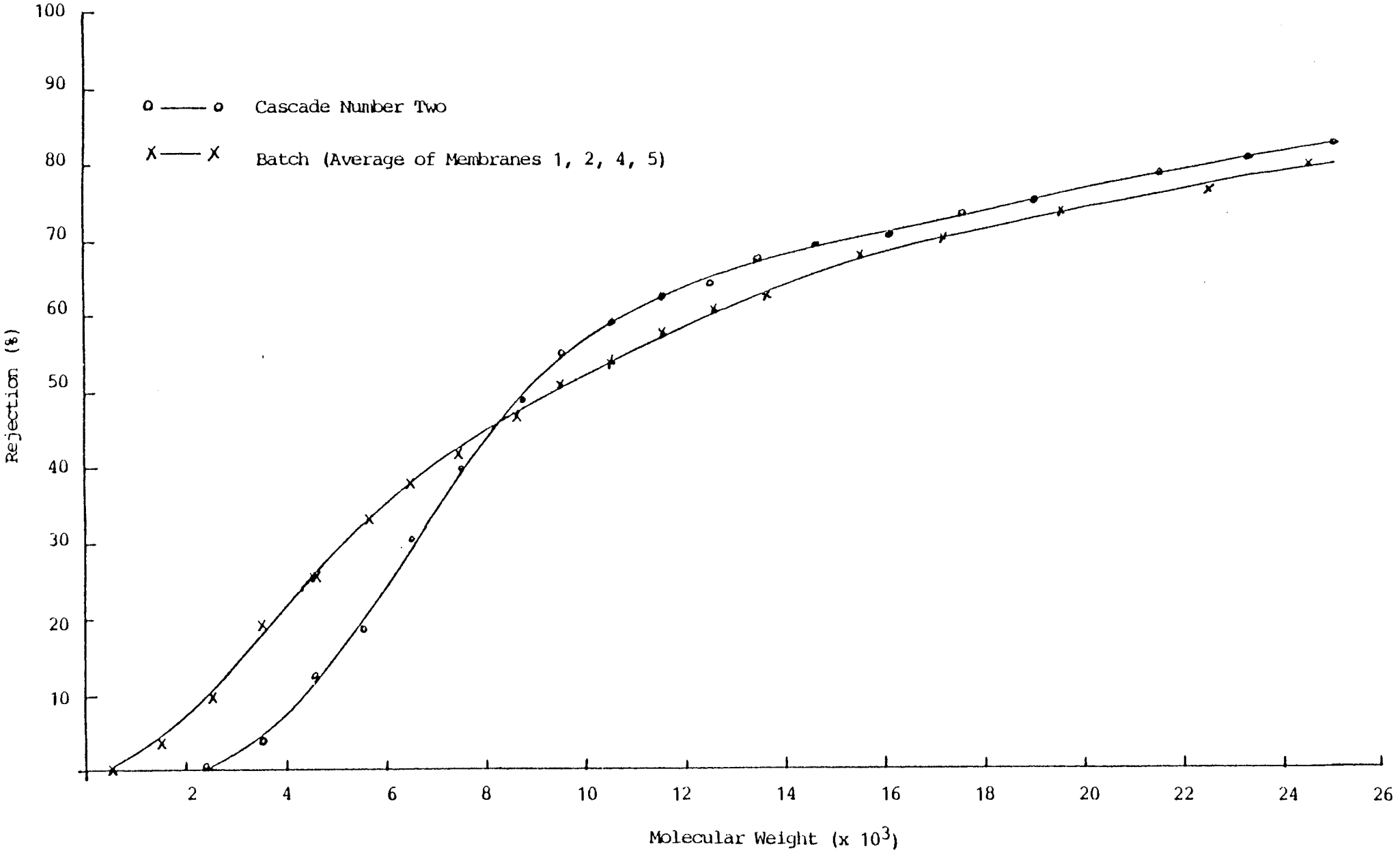

Figure 5.25: Comparison of the Rejection Profiles for Cascade Number Three, and an Equivalent Batch Fractionation

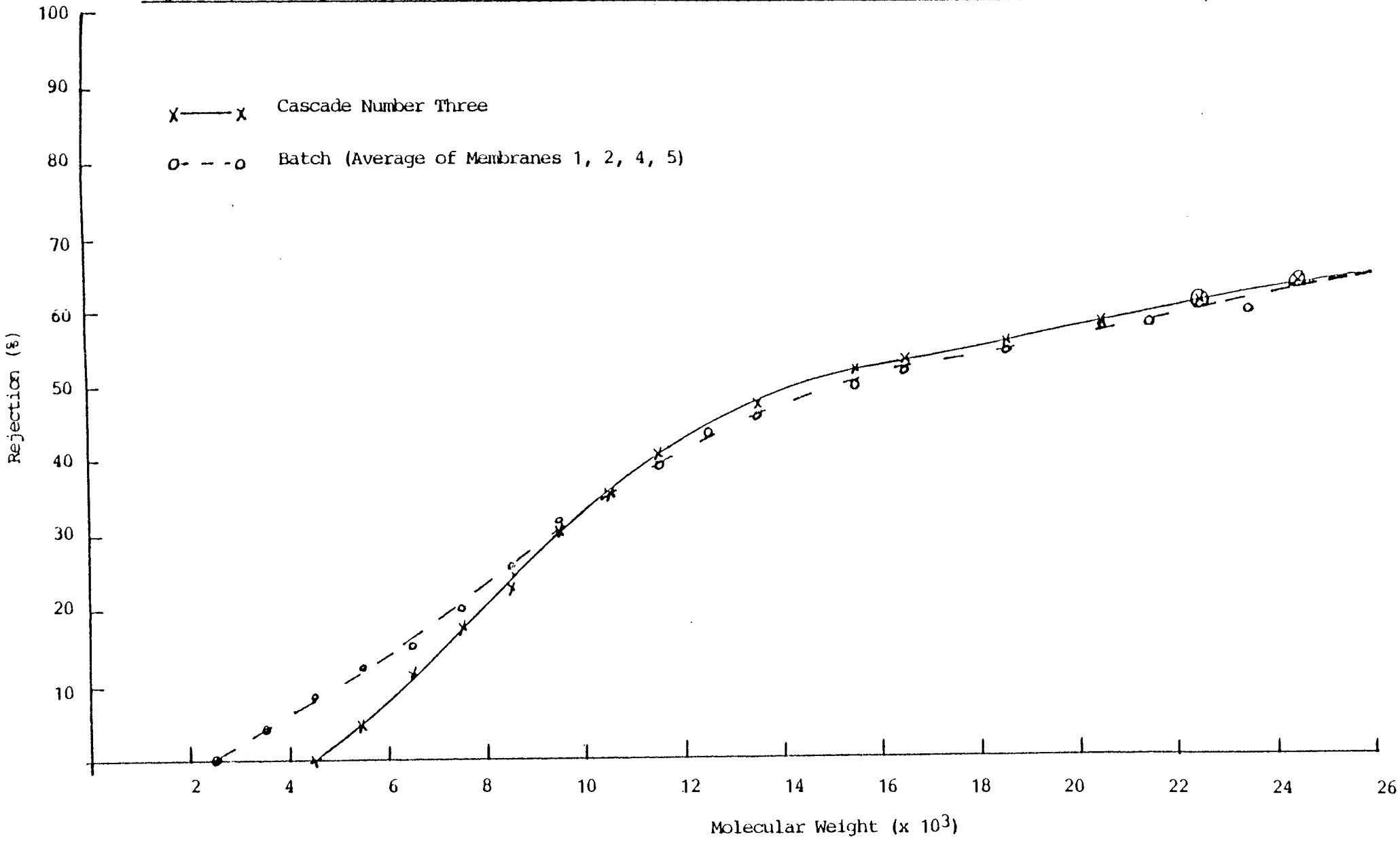

When the rejection coefficients are calculated based on the distribution of the feed used for each pass, Figure 5.22 is obtained. As the number of passes increase the rejection coefficients decrease for all the molecular weights. However, the coefficients for the low molecular weights tend to decrease faster than the higher weights and the rejection curve becomes a more ideal 'sharp' shape. Unfortunately, to obtain this more ideal shape the rejection coefficients for the 25000 dalton molecules drops to only 78%.

When the rejection coefficients are calculated based on the feed used for run five, very flat (non-ideal) curves are obtained (Figure 5.23). However, the batch curves corresponding to an equivalent fractionation had also become less ideal. When the curves are compared (Figures 5.24 and 5.25) it can be seen that the cascade still has lower rejection coefficients for the low molecular weights and slightly higher coefficients for the higher molecular weights.

The cross over point of the cascade and batch curves increases from 6 000 molecular weight (MW) for the first cascade system, to 8 000 MW for the second cascade system, and 10 000 MW for the third cascade system. Since dextran should be fractionated at approximately 10 000 MW the third cascade system comparison is the most ideal. In this case all the 'unwanted' material is being removed more easily by cascade than batch mode, and the 'wanted' material is being retained more easily. However, to reach this point the first two cascade systems have to be operated in the region where 'unwanted' material (ie. material between 6 000 and 10 000, and 8 000 and 10 000 MW) is retained more easily by cascade than batch mode.

This problem could be solved by using 10 000 MW cut-off membranes in the first cascade system instead of 5 000 MW cut-off membranes. This should enable the cascade/batch comparison curves to cross at 10 000 MW instead of 6 000 MW, as with the present 5 000 MW cut-off membranes. This cascade should then remove most of the material below 10 000 MW. The second cascade system could then use

5000 MW cut-off membranes, and the cascade/batch comparison curves should then cross at approximately 10 000 MW. If this could be accomplished the need for the third cascade system could be removed. Also, the new cascade efficiency should be an improvement on the batch mode efficiency. Unfortunately, there was insufficient time in order to prove this assumption.

In the data compared above it was very difficult to calculate batch fractionation results which corresponded exactly with the fractionation obtained by the cascade system. Therefore, to simplify any comparison, Figures 5.26 and 5.27 were plotted. These figures represent the ratio of material below a set (cut) point (ie. 6000 or 12000 daltons) to the material above the set point, and how when the ratio is decreased, the efficiency decreases. Ideally the material below the set point should be removed with no loss of material above the set point, ie. for the 12000 dalton cut point the ratio should be reduced from the starting value of 41% to the required value of 6% with the highest efficiency possible.

For the case of the 6000 dalton set-point (Figure 5.26) the 5 000 MW cut-off membrane cascade was at least 10% more efficient than using membranes in a batch mode, for an equivalent fractionation. However, in the case of the 12000 dalton set-point (Figure 5.27) the batch results were just as efficient as the cascade, if not better. These results are explained by the fact that the cascade rejected more of the material between 6000 and 12000 daltons, than did the batch method. This region contains over 15% of the original feed compared with less than 10% for the zero to 6000 dalton region (which the cascade rejected less). Therefore, the batch membranes could remove a larger proportion of the zero to 12000 dalton region. This could be done with approximately the same efficiency, ie. loss of material above 12000, as the cascade, since both methods had approximately the same rejection coefficients for material between 20000 and 98000 daltons.

Figure 5.27 also shows values of an ethanol fractionation, and results recently obtained by Till (128), at Aston, using the cascade equipment with 10 000 MW cut-off

Figure 5.26: Diagram showing the Relationship Between the Fractionatio of Material below 6000 MW and the Retention of Material above 6000 MW, for Batch Mode Operation and One, Two and Three Cascade Units in Series

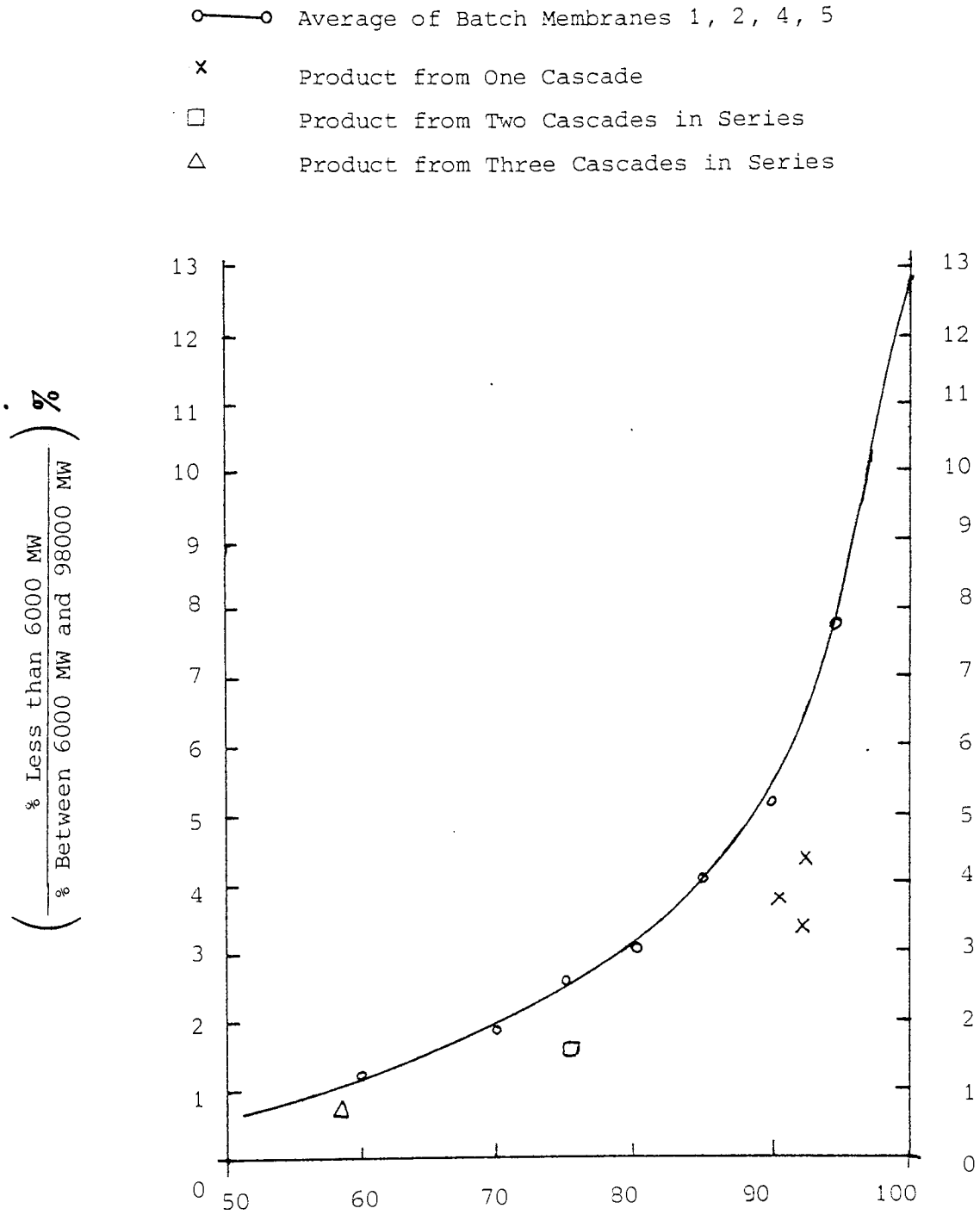

Figure 5.27: Diagram showing the relationship between the fractionati of material below 12 000 MW and the retention of material above 12 000 MW, for batch mode operation and cascade operation

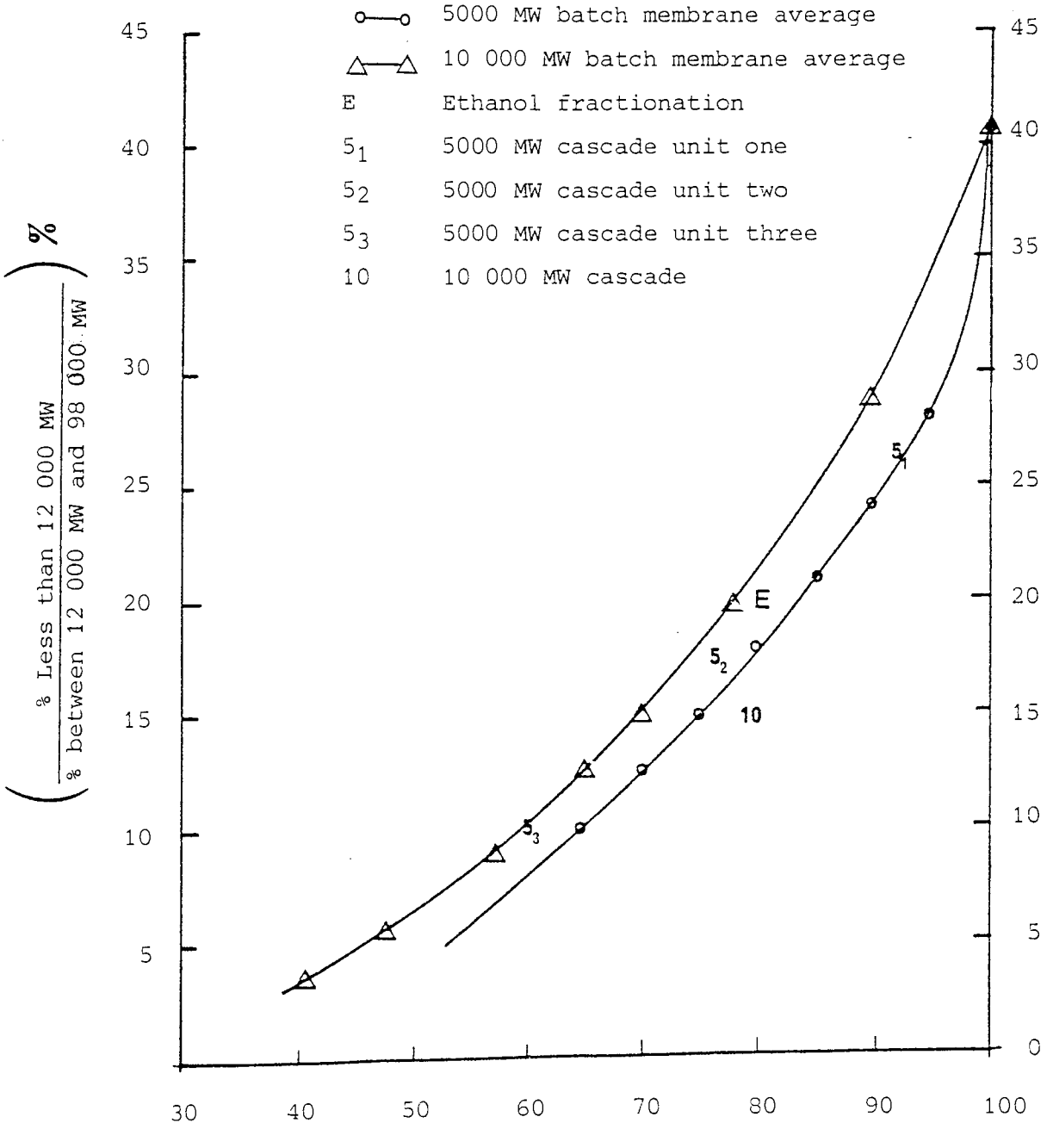

membranes. The ethanol fractionation gave an efficiency comparable to that of membranes operating in the batch mode. The cascade, with 10 000 MW cut-off membranes, gave an efficiency which was approximately 10% better than a batch mode 10 000 membrane, and approximately 5% better than a batch mode 5 000 MW cut-off membrane. This result tends to support the previous hypothesis that a 10 000 MW cut-off membrane cascade could produce a product within the required specification, and with an efficiency greater than the batch mode 5 000 MW cut-off membranes.

In the case of the 6 000 dalton set-point the 5 000 MW cut-off membrane cascade is better since everything above 6 000 is 'wanted' and everything below this limit is 'unwanted'. In both these regions the cascade is better than the batch method.

The predicted cascade results are compared to the actual results in Figure 2.28. It can be seen that the fractionation of the material between 12 000 and 98 000 daltons was predicted reasonably well. However, the prediction of the fractionation of material below 12 000 was in considerable error. This error was because the prediction values were based on batch rejection data, and the cascade rejected the majority of the material below 12 000 MW, more than the individual membranes did in batch mode. Since the rejection coefficients of both cascade and batch mode were so similar for the majority of material above 12 000 MW, the predictions and actual values would be in close agreement.

The difference between the predicted and actual results for the material above 98 000 daltons was mostly due to analytical error. Even though this region accounts for 14% of the original feed this material is spread over a large range of molecular weights. Therefore, slight errors in the analytical GPC can cause large differences in the high molecular weight material measured.

Figure 5.28: Comparison of Predicted and Actual Results for a Cascade Using 5000 Molecular Weight Cut-off Membranes

Molecular Weight Band-Widths (Daltons)	† Percentage of Materials Retained in Band Width					
	Cascade Unit 1		Cascade Unit 2		Cascade Unit 3	
	Predicted	Actual	Predicted	Actual	Predicted	Actual
Zero-12 000	50%	55%-59%	55%	58%	58%	61%
12 000-98 000	89%	90%-92%	85%	82%	80%	77%
98 000+	100%	85%	100%	75%	100%	79%

† Calculations are based on actual feed to cascade unit

5.5 CONCLUSIONS

The results obtained demonstrated that the 5 000 MW cut-off membrane cascade system tested was more efficient than the individual membranes in a batch mode. However, this improved efficiency was only if the dextran was being fractionated at 6000 daltons, which is approximately the quoted molecular weight cut-off of the membranes used. However, if membranes of 10 000 molecular weight cut-off are used in the cascade system these membranes can improve the fractionation efficiency of the cascade at 12000 daltons.

The results obtained from the cascade, using 5000 MW cut-off membranes, were for only one feed concentration (approximately 2%) and for a constant two diavolumes per stage. However, if the feed concentration is increased this will increase the amount of low MW material available for fractionation. Therefore, it might be possible to remove the same amount of low MW material, as at presently obtained, but with a higher efficiency. Also, if the feed concentration is kept constant but the number of diavolumes per stage is changed, a higher efficiency again might be obtainable. Therefore, these operating parameters should be optimised before any definite conclusions can be drawn on the exact improvement of cascade over batch operation.

The values of the predicted results were found to be in disagreement with the actual results. This is due to the way the rejection coefficients of a membrane are strongly dependent upon the molecular weight distribution of the material being fractionated. Therefore, before any reasonable predictions can be found the rejection-distribution relationship must be investigated more extensively, and if possible quantified mathematically.

6.0 DETERMINATION OF THE MOST VIABLE METHOD OF FRACTIONATING DEXTRAN HYDROLYSATE

6 DETERMINATION OF THE MOST VIABLE METHOD OF FRACTIONATING DEXTRAN HYDROLYSATE

6.1 INTRODUCTION

In determining the most viable method of fractionating dextran hydrolysate three main factors must be evaluated. These are, (a) the capital costs involved in the process under consideration, (b) the operating costs of the process, and (c) the recovery of the 'saleable' dextran in the final product. A full design and cost evaluation would take several months to complete for each method of dextran fractionation. Therefore, in the time available only some of the main capital and processing costs have been estimated to give a preliminary insight into the most likely favoured process route. These estimated costs included the main process equipment, but did not include ancillary equipment such as piping and instrumentation. The cost of this ancillary equipment is usually estimated by use of costing coefficients, eg. Lang factors. For the fractionation processes considered in this evaluation these costing coefficients gave approximately the same value for all the alternative processes. Since only a relative cost comparison of processes is required for this evaluation the cost of this ancillary equipment was therefore ignored.

There are currently five main different methods of fractionating dextran hydrolysate. These are, (a) ethanol fractionation, (b) GPC fractionation of high MW dextran followed by UF batch fractionation of low MW dextran, (c) GPC fractionation of high MW dextran followed by UF cascade fractionation of low MW dextran, (d) UF batch fractionation of high and low MW dextran, and (e) UF batch fractionation of high MW dextran followed by UF cascade fractionation of low MW dextran. The relevant costs of these five methods will now be discussed.

6.2 ETHANOL FRACTIONATION

The calculation of the capital and operating costs for ethanol fractionation is given in Appendix 6, and summarised in Figure 6.1.

Figure 6.1: Table of the Main Economic Factors Influencing the Feasibility of Ethanol Fractionation

Capital Costs =	£1 093 600
Operating Costs =	£225 774 pa
Income =	100 tonnes of clinical dextran product at £15/Kg
Income =	£1 500 000 pa
Net income =	£1 500 000 - 225 744
	= £1 274 256 pa
Pay back time =	$\frac{1\ 093\ 600}{1\ 274\ 256}$ x 12 months

Pay back time = 10.3 months

This method of dextran fractionation produces 100 tonnes per annum of final clinical dextran product, from an original starting material of 200 tonnes of dextran hydrolysate. This clinical product is at present sold for £30/Kg. However, this price includes the costs for the actual manufacture of the hydrolysate, the costs of spray drying of the final product, and the profit made on the dextran. Since the costs of dextran manufacture and spray drying have been ignored in these comparison calculations a clinical dextran price of only £15/Kg will be assumed, ie. the cost of the preliminary stages of dextran manufacture and spray drying is equal to £15/Kg.

From Figure 6.1 it can be seen that this ethanol fractionation method has a pay back time of 10.3 months. In reality the actual pay back time would be greater than this figure due to the additional costs of the ancillary equipment required.

6.3 GPC PLUS UF BATCH FRACTIONATION

The calculation of the capital and operating costs for GPC and UF batch fractionation is given in Appendix 6, and summarised in Figure 6.2.

This method of dextran fractionation recovers the same amount of 'saleable' material as ethanol fractionation, ie. 100 tonnes of clinical product from 200 tonnes of hydrolysate. However, due to the lower capital and operating costs for this method the pay back time is only 6.2 months, compared to 10.3 months for ethanol fractionation. Therefore, a GPC plus UF batch fractionation can be considered to be more cost efficient than ethanol fractionation.

6.4 GPC PLUS UF CASCADE FRACTIONATION

The calculation of the capital and operating costs for GPC plus UF cascade fractionation is given in Appendix 6, and summarised in Figure 6.3.

Since this method uses a UF cascade for the fractionation of the low MW dextran, approximately 6 tonnes of extra product can be recovered compared to ethanol

Figure 6.2: Table of the Main Economic Factors Influencing the Feasibility of GPC plus UF Batch Fractionation

Capital Costs

GPC Capital Costs =	137 400
UF Batch Capital Costs =	538 120
Total	£675 520

Operating Costs

GPC Operating Costs =	23 520
UF Batch Operating Costs =	172 100
Total	£195 620pa

Income = 100 tonnes of clinical dextran product at £15/Kg

Income = £1 500 000 pa

Net income = 1 500 000 - 195 620

= £1 304 380pa

Pay back time = $\frac{675\ 520}{1\ 304\ 380}$ x 12 months

Pay back time = 6.2 months

Figure 6.3: Table of the Main Economic Factors Influencing the Feasibility of GPC plus UF Cascade Fractionation

Capital Costs

GPC Capital Costs =	137 400
UF Cascade Capital Costs =	742 780
Total	£880 180

Operating Costs

GPC Operating Costs =	23 520
UF Cascade Operating Costs =	155 900
Total	£179 420pa

Income = 106 tonnes of clinical dextran at £15/Kg

Income = £1 600 000 pa

Net income = 1 600 000 - 179 420

= £1 420 580pa

Pay back time = $\frac{880\ 180}{1\ 420\ 580}$ x 12 months

Pay back time = 7.4 months

fractionation, ie. 106 tonnes of clinical product is produced from 200 tonnes of hydrolysate (see Appendix 6). Since this extra 6 tonnes of product can be considered to be recovered waste material, it will have no dextran production cost (this cost is allowed for in the price of the original 100 tonnes of product), but it will have a product spray drying cost. Therefore, its value to the process can be considered to be approximately £20/Kg (132).

The pay back time for a GPC plus cascade process is longer than for a GPC plus UF batch process. This is because the higher capital costs involved in the cascade fractionation, compared to the UF batch fractionation, far outweigh the savings in operating costs and the recovery of extra 'saleable' dextran. However, GPC plus cascade fractionation is still more viable than ethanol fractionation.

6.5 UF BATCH FRACTIONATION OF HIGH AND LOW MW DEXTRAN

The calculation of the capital and operating costs for UF batch fractionation of high and low MW dextran is given in Appendix 6, and summarised in Figure 6.4.

This method of fractionation has the same recovery of 'saleable' dextran as ethanol fractionation. However, its pay back time and therefore its viability is better than ethanol. When compared to GPC plus UF batch fractionation this method of fractionation is found to be less viable. This is because GPC fractionates the high MW dextran with less capital and operating costs than UF batch fractionation.

UF batch fractionation of the high and low molecular weight dextran is more viable than GPC plus cascade fractionation. This is because of the high capital costs involved in the cascade fractionation.

6.6 UF BATCH PLUS UF CASCADE FRACTIONATION

The calculation of the capital and operating costs for UF batch fractionation of high MW dextran, plus UF cascade fractionation of low MW dextran is given in Appendix 6, and summarised in Figure 6.5.

Figure 6.4: Table of the Main Economic Factors Influencing the Feasibility of UF Batch Fractionation of High and Low Molecular Weight Dextran

Capital Costs

High MW Fractionation =	183 900
Low MW Fractionation =	538 120
Total	£722 020

Operating Costs

High MW Fractionation =	50 300
Low MW Fractionation =	180 200
Total	£230 500 pa

Income = 100 tonnes of clinical dextran product at £15/Kg

Income = £1 500 000 pa

Net income = 1 500 000 - 230 500

= £1 269 500 pa

Pay back time = $\frac{722\,020}{1\,269\,500}$ x 12 months

Pay back time = 6.8 months

Figure 6.5: Table of the Main Economic Factors Influencing the Feasibility of UF Batch Fractionation of High MW Dextran plus UF Cascade Fractionationof Low MW Dextran

Capital Costs

Batch Capital Costs =	183 900
Cascade Capital Costs =	742 780
Total	£926 680

Operating Costs

Batch Operating Costs =	50 300
Cascade Operating Costs =	164 100
Total	£214 400pa

Income = 106 tonnes of clinical dextran product at £15/Kg

Income = £1 600 000pa

Net income = 1 600 000 - 214 400

= £1 385 600pa

Pay back time = $\frac{926\ 680}{1\ 385\ 600}$ x 12 months

Pay back time = 8 months

As with the GPC plus cascade fractionation this method would produce 106 tonnes of clinical product from 200 tonnes of hydrolysate feed. Due to the high operating cost of the batch fractionation, and the high capital cost of the cascade fractionation, this method is only more viable than ethanol fractionation.

6.7 LONG TERM VIABILITY OF THE ALTERNATIVE FRACTIONATION METHODS

In the previous sections the viability of the alternative processes were judged by their individual pay back times. However, this relationship does not take into account the profitability of the processes over their whole operating life. Therefore, cash flow tables for the individual processes were calculated and are given in Figures 6.6 to 6.10.

These tables assumed, (a) a plant life of 10 years, (b) at the end of 10 years 10% of the original capital cost is recovered by scrapping the capital equipment, (c) in year 1 of operation 10% of the annual operating cost is required as working capital, and (d) the working capital is recovered in the final year of operation of the plant.

Figures 6.6 to 6.10 also give the discounted cash flows for 15% and 30% interest rates for each process. These discounted figures indicate whether money invested in a project is worthwhile, or otherwise be better invested in a bank or other securities. Based on these preliminary figures it would appear that even at a 30% interest rate all the alternative projects would be viable, ie. if the capital for each project was invested at an interest rate of 30% for ten years, the return on investment would be less than the return from investing in any one of the alternative fractionation projects. The indications are that one could obtain a much higher return than 30%, but an extensive costing exercise should be performed to verify this hypothesis. These high return on investments are due to the very short pay back times of the processes.

Figure 6.11 shows the alternative methods of fractionation in order of relative economic viability. This figure shows that the GPC plus UF cascade fractionation method is the most long term economically viable process, even though

Figure 6.6: Discounted Cash Flow Table for Ethanol Fractionation

Year	Fixed Investment 10^3 £	Total Operating Costs 10^3 £	Sales Income 10^3 £	Net cash flow (NCF) 10^3 £	Cumulative NCF 10^3 £	Discounted NCF at 15% 10^3 £	Discounted NCF at 30% 10^3 £
0	-1093.6	-	-	-1093.6	-1093.6	-1093.6	-1093.6
1	-	-248.4	+1500	+1251.6	+158	+1088.3	+962.8
2	-	-225.8	+1500	+1274.2	+1432.2	+963.5	+754.0
3	-	-225.8	+1500	+1274.2	+2706.4	+837.8	+580.0
4	-	-225.8	+1500	+1274.2	+3980.6	+728.5	+446.1
5	-	-225.8	+1500	+1274.2	+5254.8	+633.5	+343.2
6	-	-225.8	+1500	+1274.2	+6529.0	+550.9	+263.0
7	-	-225.8	+1500	+1274.2	+7803.2	+479.0	+203.1
8	-	-225.8	+1500	+1274.2	+9077.4	+416.5	+156.2
9	-	-225.8	+1500	+1274.2	+10351.6	+362.2	+120.2
10	+109.4	-203.2	+1500	+1406.2	+11757.8	+347.6	+102.0
Total	-984.2	-2258	+15000	+11757.8	-	+5314.2	+2837

Figure 6.7: Discounted Cash Flow Table for GPC plus UF Batch Fractionation

Year	Fixed Investment 10^3 £	Total Operating Costs 10^3 £	Sales Income 10^3 £	Net cash flow (NCF) 10^3 £	Cumulative NCF 10^3 £	Discounted NCF at 15% 10^3 £	Discounted NCF at 30% 10^3 £
0	-675.5	-	-	-675.5	-675.5	-675.5	-675.5
1	-	-215.2	+1500	+1284.8	+609.3	+1117.2	+988.3
2	-	-195.6	+1500	+1304.4	+1913.7	+986.3	+771.8
3	-	-195.6	+1500	+1304.4	+3218.1	+857.7	+593.7
4	-	-195.6	+1500	+1304.4	+4522.5	+745.8	+456.7
5	-	-195.6	+1500	+1304.4	+5826.9	+648.5	+351.3
6	-	-195.6	+1500	+1304.4	+7131.3	+563.9	+270.2
7	-	-195.6	+1500	+1304.4	+8435.7	+490.4	+207.9
8	-	-195.6	+1500	+1304.4	+9740.1	+426.4	+159.9
9	-	-195.6	+1500	+1304.4	+11044.5	+370.8	+123.0
10	+67.6	-176.0	+1500	+1391.6	+12436.1	+344.0	+100.9
Total	-607.9	-1956	+15000	+12436.1	-	+5875.5	+3348.2

Figure 6.8: Discounted Cash Flow Table for GPC plus Cascade Fractionation

Year	Fixed Investment 10^3 £	Total Operating Costs 10^3 £	Sales Income 10^3 £	Net cash flow (NCF) 10^3 £	Cumulative NCF 10^3 £	Discounted NCF at 15% 10^3 £	Discounted NCF at 30% 10^3 £
0	-880.2	-	-	-880.2	-880.2	-880.2	-880.2
1	-	-197.3	+1600	+1402.7	+522.5	+1219.7	+1079.0
2	-	-179.4	+1600	+1420.6	+1943.1	+1074.2	+840.6
3	-	-179.4	+1600	+1420.6	+3363.7	+934.1	+646.6
4	-	-179.4	+1600	+1420.6	+4784.3	+812.2	+497.4
5	-	-179.4	+1600	+1420.6	+6204.9	+706.3	+382.6
6	-	-179.4	+1600	+1420.6	+7625.5	+614.2	+294.3
7	-	-179.4	+1600	+1420.6	+9046.1	+534.1	+226.4
8	-	-179.4	+1600	+1420.6	+10466.7	+464.4	+174.2
9	-	-179.4	+1600	+1420.6	+11887.3	+403.8	+133.9
10	+88.0	-161.5	+1600	+1526.5	+13413.8	+377.3	+110.7
Total	-792.2	-1794.0	+16000	+13413.8	-	+6260.1	+3505.5

Figure 6.9: Discounted Cash Flow Table for UF Batch Fractionation of High and Low MW Dextran

Year	Fixed Investment 10^3 £	Total Operating Costs 10^3 £	Sales Income 10^3 £	Net cash flow (NCF) 10^3 £	Cumulative NCF 10^3 £	Discounted NCF at 15% 10^3 £	Discounted NCF at 30% 10^3 £
0	-722.0	-	-	-722.0	-722.0	-722.0	-722.0
1	-	-253.6	+1500	+1246.4	+524.4	+1083.8	+958.8
2	-	-230.5	+1500	+1269.5	+1793.9	+960.0	+751.2
3	-	-230.5	+1500	+1269.5	+3063.4	+834.7	+577.8
4	-	-230.5	+1500	+1269.5	+4332.9	+725.8	+444.5
5	-	-230.5	+1500	+1269.5	+5602.4	+631.2	+341.9
6	-	-230.5	+1500	+1269.5	+6871.9	+548.8	+263.0
7	-	-230.5	+1500	+1269.5	+8141.4	+477.3	+202.3
8	-	-230.5	+1500	+1269.5	+9410.9	+415.0	+155.6
9	-	-230.5	+1500	+1269.5	+10680.4	+360.9	+119.7
10	+72.2	-207.5	+1500	+1364.7	+12045.1	+337.3	+99.0
Total	-649.8	-2305.1	+15000	+12045.1	-	+5652.8	+3191.8

Figure 6.10: Discounted Cash Flow Table for UF Batch Fractionation of High MW Dextran plus Cascade Fractionation of Low MW Dextran

Year	Fixed Investment 10^3 £	Total Operating Costs 10^3 £	Sales Income 10^3 £	Net cash flow (NCF) 10^3 £	Cumulative NCF 10^3 £	Discounted NCF at 15% 10^3 £	Discounted NCF at 30% 10^3 £
0	-926.7	-	-	-926.7	-926.7	-926.7	-926.7
1	-	-235.8	+1600	+1364.2	+437.5	+1186.3	+1049.4
2	-	-214.4	+1600	+1385.6	+1823.1	+1047.8	+819.9
3	-	-214.4	+1600	+1385.6	+3208.7	+911.0	+630.7
4	-	-214.4	+1600	+1385.6	+4594.3	+792.2	+485.1
5	-	-214.4	+1600	+1385.6	+5979.9	+688.9	+373.2
6	-	-214.4	+1600	+1385.6	+7365.5	+559.0	+287.1
7	-	-214.4	+1600	+1385.6	+8751.1	+520.9	+220.8
8	-	-214.4	+1600	+1385.6	+10136.7	+452.9	+169.8
9	-	-214.4	+1600	+1385.6	+11522.3	+393.9	+130.7
10	+92.7	-193.0	+1600	+1499.7	+13022.0	+370.7	+108.8
Total	-834	-2144	+16000	+13022.0	-	+6036.9	+3348.8

Figure 6.11: Table Showing the Alternative Methods of Dextran Fractionation in Order of Relative Economic Viability

Fractionation Method	*Short Term Viability	** Long Term Viability
GPC plus Cascade	3rd	1st
UF batch plus Cascade	4th	2nd
GPC plus UF batch	1st	2nd
UF batch plus UF batch	2nd	4th
Ethanol	5th	5th

* based on pay back times

** based on discounted cash flow tables

it was not the best in the short term. This was because it had the highest net income per annum, and its original pay back time was only a few months longer than the other fractionation methods. Therefore, the higher net income has a greater effect over the ten year plant life than does the higher capital cost. For this same reason the UF batch plus cascade process is just as viable in the long term as the GPC plus UF batch process. In both short term and long term viability ethanol fractionation was found to be the less favoured process route.

6.8 FEASIBILITY OF OPERATING THE NEW ALTERNATIVE PROCESSES IN STERILE CONDITIONS

Even though the new alternative fractionation processes may be more economically viable they are of no use if they cannot be operated under pyrogen free conditions. The present ethanol process is pyrogen free due to the presence of the ethanol, and the distillation steps required for the ethanol recovery.

The pyrogen free operation of the new processes would fall into two parts. The first part is the initial sanitisation of the new processes to remove any presence of bacteria. This is accomplished by cleaning the process tanks with steam, and flushing a sanitising agent, such as hypochlorite, through the GPC and UF membranes. This agent would then be washed out of the system with pyrogen free water. Also, the membranes could be further protected by autoclaving.

Once the processes have been sanitised the second part would be to then keep the processes pyrogen free. This is accomplished by using only pyrogen free water in all the process streams. This water is manufactured on the present ethanol process by using membranes. In the present study the new processes would obtain their feeds from the present dextran fermentation plant. This plant is operated in an ethanol environment and would therefore be pyrogen free.

During the operation of all the alternative processes there is some time period when all the process tanks are empty of solution. At this time the tanks can be cleaned with plant steam. All the pumps costed in this economic evaluation are made from stainless steel and are normally employed in the food and beverage industries.

In the evaluation of the membrane costs the number of membranes required was calculated so that one batch was processed every 112 hours. However, in this evaluation the flux of the membranes was deliberately underestimated. In reality each batch could be processed in less than 112 hours, and this would therefore allow time for the membranes to be sanitised between batches. This reduction in process time could also allow more batches to be processed per year, and would therefore increase the throughput of the membrane processes for the same capital costs. This would then enhance the viability of the processes which incorporate membrane fractionation.

6.9 CONCLUSIONS

Out of the new alternative processes evaluated, the GPC plus UF cascade fractionation method was found to be the most viable in the long term. It was also found to be more viable than the ethanol fractionation method in the short term evaluation.

In practice the viability of the GPC plus cascade fractionation could be improved for several reasons:

(a) In these calculations the life of the membranes was taken as three years. This figure was based on experience at Aston, where the membranes used have only been washed with de-ionised water. However, these membranes can also be washed with 0.1N sodium hydroxide. The life of these membranes could then exceed 3 years, and this would therefore reduce the operating cost of the process. This principle also applies to the porous silica packing in the GPC columns where a life of five years was assumed, but this packing has been known to last at least 10 years.

(b) The large capital cost of the cascade fractionation is due to the number of stages required, and the number of diavolumes per stage required. As mentioned in Chapter 5, it is possible that the number of stages required could be reduced by having cascades, containing either 10000 or 5000 MW cut-off membranes, in series. Also, it might be possible that the number of diavolumes could be reduced with only a small change in performance. If both these factors could be accomplished they could greatly reduce the capital cost of the cascade, and therefore improve its viability.

The GPC plus cascade does have one disadvantage in that some dextran is lost in reaching steady-state in both rigs. However, if the non steady-state products from the process are recycled back to the initial stored hydrolysate, then these losses can be avoided.

In the process proposed by Vlachogiannis (Figure 1.2) an ion exchange column was incorporated at the end of the process. This column removed any silica eluted from the GPC columns. By placing the exchange column at the end of the process some silica is lost through the concentration membranes. If the permeate from those membranes was recycled back into the process this silica would build up in the system. Therefore, the best position for the ion-exchange column would be immediately after the GPC rig. This column costs approximately £3000 and does not therefore greatly effect the relative cost of the new process. This also applies to the cost of the packing lost from the GPC. The actual amount of packing lost is negligible but any traces must be removed before the final dextran product can be classed as clinical.

Since the final dextran product is a clinical product it must be pyrogen free. It would appear that it is possible to operate the new GPC plus UF cascade under pyrogen free conditions. However, this can only be confirmed by the actual operation of a GPC and cascade under the proposed conditions.

7.0 CONCLUSIONS AND RECOMMENDATIONS

7.0 CONCLUSIONS AND RECOMMENDATIONS

During this research project the suitability of UF membranes for the fractionation of dextran hydrolysate has been considered. Three different makes of membrane were tested in a batch diafiltration mode of operation. These membranes were of the Millipore cassette configuration, DDS flat-sheet configuration, and the Amicon hollow fibre configuration. From these experiments it was concluded that:

(a) Amicon hollow fibre membranes, of 5000 MW cut-off were the most efficient membranes for the fractionation of low molecular weight dextran. These membranes gave a fractionation efficiency of between 60% and 70%, which is comparable to that obtained with ethanol fractionation.

(b) The manufacturers' quoted values for a membrane's molecular weight cut-off did not apply when dextran was being processed. This was because the manufacturers calibrate their membranes using globular proteins of specific molecular weight. These proteins are usually considered to act as solid spheres. Dextran, however, can be considered to be a flexible polymer coil, and in the high shear forces present in the UF membranes these coils become deformed and stretched straight. Therefore, when large dextran molecules, ie. 70 000+ molecular weight, become distorted they can pass through the pores of a 5000 molecular weight cut-off membrane. Hence, a dextran molecule behaves as a protein of one-tenth its molecular weight. The best expression for a membrane's performance with dextran is its rejection - molecular weight relationship for a set fractionation of a given feed material.

(c) Even though membranes, of the same quoted molecular weight cut-off, can be tested and passed by the manufactures, their actual performance in rejecting dextran of specific molecular weights can vary by up to 15%. It is recommended that all membranes should be tested before use by determining their rejection-molecular weight relationship. This will then show up any membranes that are below specification.

(d) The molecular weight distribution of the dextran sample to be fractionated can effect the rejection-molecular weight relationship of the membrane being used. Using a given membrane, a sample containing a large percentage of low molecular weight (MW)

material can have a high proportion of this low MW material removed with a high efficiency. If the same proportion of low material is then removed from a sample with a lower percentage of low molecular weight material, a lower efficiency is obtained.

Since the best fractionation efficiency obtained with a batch mode membrane was only comparable to that of ethanol fractionation, different methods of improving this efficiency were considered. Based on the experience gained from batch mode experiments and theoretical equipment proposed in the literature, a four stage membrane cascade was constructed. This cascade recycles permeates in a counter-current direction to the retentates. Using this equipment, with Amicon 5000 molecular weight cut-off membranes, it was demonstrated that a membrane cascade configuration can obtain a fractionation efficiency of at least 10% greater than that obtained with the same membranes in a batch mode. However, this improved efficiency was obtained at a fractionation of 6000 molecular weight. Below this molecular weight the cascade rejected material less than the membranes did in a batch mode, and above 6000 molecular weight the cascade rejected material more effectively than in the batch mode. At a 12 000 molecular weight fractionation point the cascade efficiency was found to be worse than the batch mode membranes. This discrepency could be rectified by the operation of the cascade using 10 000 molecular weight cut-off membranes.

The performance of the cascade unit was modelled using a computer package called 'Process'. This package predicted the rejection of the material above 12 000 molecular weight reasonably well. However, the prediction of the material below 12000 molecular weight was inadequate. This was because the model used the rejection characteristics of the batch mode membranes in the prediction of the cascade results. When low molecular weight material was recycled in the permeates of the cascade this effected the distribution of the retentates, and caused the rejection characteristics of the membranes in the cascade to vary from their batch characteristics. This problem can be rectified if the dependence of the membranes' rejection characteristics can be related to the molecular weight distribution of the sample being fractionated. This relationship

could then be used in the prediction of any cascade experiment, and the modelling of the cascade should then simplify to a mass balance problem.

The experiments conducted using the cascade were for only one constant set of operating conditions. To determine the best method of operating the cascade these operating conditions, eg. feed concentration, number of diavolumes per stage and positioning of membranes, must be optimised.

Estimates of the capital and operating costs of the present ethanol fractionation method have been made available (132). Estimates were then found for alternative methods of fractionation based on GPC, UF batch membranes, and UF cascade. On a long term economic basis it was found that a GPC plus UF cascade fractionation process would be more viable than ethanol fractionation. By using this new process an increase in income of approximately £146 000 per annum could be obtained, with a saving of approximately £200 000 on capital costs.

The future work on this project should include:

(a) The improvement of the cascade fractionation at 12 000 molecular weight by use of 10 000 molecular weight cut-off membranes.

(b) The improvement of the cascade fractionation efficiency by means of optimising the operating parameters.

(c) The improvement of the modelling of the cascade performance by obtaining data on the rejection characteristics of membranes with feed of differing molecular weight distributions.

APPENDIX 1: LISTING OF THE COMPUTER PROGRAM USED FOR DATA ACQUISITION ON THE GPC ANALYTICAL SYSTEM

```
1Ø        DIM A(4ØØ),Z(5)
6ØØØ      I=1:T1=TI:Y=1
6Ø1Ø      GO SUB 7ØØØ
6Ø2Ø      E=TI-T1
6Ø3Ø      IF E<12Ø THEN 6Ø2Ø
6Ø4Ø      IF Y=5 THEN 6Ø9Ø
6Ø5Ø      Y=Y+1:T1=TI
6Ø6Ø      GO TO 6Ø1Ø
6Ø9Ø      T1=TI
61ØØ      A(I)=Z(1)+Z(2)+Z(3)+Z(4)+Z(5))/5
61Ø5      PRINT"READING";I/6;"=";A(I),A(I)/4
651Ø      IF I<36Ø THEN 675Ø
655Ø      FOR Q=156 TO I
656Ø      OPEN 1,4,I
657Ø      OPEN 2,4,2
658Ø      F$="9999.99    S9999.99    S9999.99"
659Ø      PRINT#2,FI
66ØØ      PRINT#1,Q/6,A(Q),A(Q)/4
661Ø      CLOSE1:CLOSE2
662Ø      NEXT Q
665Ø      END
675Ø      Y=1.Ø:I=I+1
676Ø      GO TO 6Ø1Ø
7ØØO      OPEN 1,9,I
7Ø1Ø      GET#1,J$,K$
7Ø2Ø      IF K$="" THEN K=-224: GO TO 7Ø4Ø
7Ø3Ø      K=ASC(K$)-224
7Ø4Ø      IF K<Ø THEN D=(K+32)*-1
7Ø5Ø      IF K>=Ø THEN D=K
7Ø6Ø      D=D*256
7Ø7Ø      IF J$="" THEN J=Ø:GO TO 7Ø9Ø
7Ø8Ø      J=ASC(J$)
7Ø9Ø      IF K<Ø THEN J=J*-1
71ØØ      Z(Y)=J+D
71Ø5      PRINT Z(Y),Z(Y)/4
7110      CLOSE1
712Ø      RETURN
```

APPENDIX 2: EXAMPLE OF A DEXTRAN MOLECULAR WEIGHT DISTRIBUTION, AND A LISTING OF THE COMPUTER PROGRAM USED TO CALCULATE THE DISTRIBUTION

Batch Number: SYR - 111

Date of Analysis: 12/5/86

Flowrate = .903900986
VO = 16.16
VE1 = 23.33
VI = 30.83
VT = 33.66

Weight Average Mol Weight = 12097.0917
Number Average Mol Weight = 9957.294
MW/MN Ratio = 1.21489751

Point	KD Value	Mol Weight	Height	Wght Frac	Cumm %
16	.838	2905.	.00	.00000	.00
15	.809	4000.	54.00	1.74418	1.74
14	.781	5413.	204.00	6.58914	8.33
13	.752	7230.	534.00	17.24806	25.58
12	.724	9569.	837.00	27.03488	52.61
11	.695	12540.	762.00	24.61240	77.22
10	.666	16349.	438.00	14.14728	91.37
9	.638	21211.	167.00	5.39405	96.77
8	.609	27418.	52.00	1.67958	98.44
7	.581	35349.	20.00	.64599	99.09
6	.552	45494.	10.00	.32299	99.41
5	.524	58497.	7.00	.22609	99.64
4	.495	75204.	5.00	.16149	99.80
3	.466	96737.	4.00	.12919	99.93
2	.438	124592.	2.00	.06459	100.00
1	.409	160781.	.00	.00000	100.00

Aston GPC Calibration Constants

B1 = -12.511
B2 = 7.007
B3 = 4.307
B4 = 16.237
B5 = 510.032

```
1         DIM H(17Ø), VIN(17Ø), AMIN( 17Ø), S(17Ø), S5(17Ø)
2         PRINT"TYPE"IN THE BATCH NUMBER"
3         INPUT KRS
4         PRINT"TYPE IN DATE"
5         INPUT KS
7         PRINT"TYPE IN NMAX, VØ, VE1, VI, VT"
8         INPUT NMAX, DØ, D1, D2, D3
9         PRINT"TYPE IN THE HEIGHTS"
1Ø        FOR I=1 TO NMAX: INPUT H(I): NEXT I
2Ø        GO SUB 1ØØØ: GO SUB 5ØØØ
25        OPEN1,4
26        OPEN2,4,1
27        OPEN3,4,2
28        FS="999 99999.999 9999999999. 9999.99 999999.999 9999.99"
29        PRINT #3,FS
3Ø        PRINT #1,CHRI(1)"BATCH NUMBER";KRS
31        PRINT#1: PRINT #1
33        PRINT#1,CHRI(1)"DATE OF ANALYSIS";KS
34        PRINT#1:PRINT#1
35        PRINT#1,"FLOWRATE="; RATE
36        PRINT#1,"      VØ=";DØ
37        PRINT#1,"     VEI=";D1
38        PRINT#1,"      VI=";D2
39        PRINT#1,"      VT=";D3
4Ø        PRINT#1
42        PRINT#1,"WEIGHT AVERAGE MOLECULAR WEIGHT=";AAAW
43        PRINT#1,"NUMBER AVERAGE MOLECULAR WEIGHT=";AVMN
44        PRINT#1,"                                  Mw/Mn RATIO=";SPR
45        PRINT#1:PRINT#1:PRINT#1
5Ø        HDS="POINT"+"       "+"KD VALUE"+"              "
51        GHS="MOL.WEIGHT"+"     "
52        FHS="HEIGHT"+"         "+"WGHT FRAC"+"   CUMM%"
53        EHS=HDS+GHS+FHS
54        PRINT#1,EHS
6Ø        FOR I=NMAX TO 1 STEP -1
62        PRINT#2,I,VIN(I),AMIN(I),H(I),S(I),S5(I)
8Ø        NEXT I
81        PRINT#1:PRINT#1:PRINT#1
82        PRINT#1,"ASTONVGPC CALIBRATION CONSTANTS"
83        PRINT#1,"    B1=";B1
84        PRINT#1,"    B2=";B2
85        PRINT#1,"    B3=";B3
86        PRINT#1,"    B4=";B4
87        PRINT#1,"    B5=";B5
9Ø        CLOSE1:CLOSE2:CLOSE3
1ØØ       END
1ØØØ      RATE=57.ØØØ/D3
1Ø1Ø      VIE=D1*RATE
1Ø2Ø      VFE=D2*RATE
1Ø3Ø      VI=(VIE-28.586)/28.415
1Ø4Ø      VF=(VFE-28.596)/28.415
1Ø5Ø      VH=(VF-VI)/(NMAN-1)
11ØØ      RETURN
```

```
5ØØØ    REM CALCULATE M.W.D.
5Ø1Ø    B1=-16.6334:B2=21.7Ø2:B3=16.Ø67:B5=87.798
5Ø2Ø    S1=Ø.Ø:S2=Ø.Ø:S3=Ø.Ø
5Ø3Ø    FOR I=1 TO NMAX
5Ø4Ø    VIN(I)=VI+VH*(I-1)
5Ø5Ø    IF VIN(I)>1.Ø THEN 5Ø8Ø
5Ø6Ø    IF VIN(I)<Ø.Ø THEN 5Ø9Ø
5Ø65    AKIN(I)=B4+B1*VIN(I)+B2*(VIN(I)**2+B3*(VIN(I)**3)
5Ø7Ø    AAMIN(I)=B5+EXP(AKIN(I))
5Ø72    GO TO 51ØØ
5Ø8Ø    AMIN(I)=B5+EXP(B4+B1+B2+B3)
5Ø85    GO TO 51ØØ
5Ø9Ø    AMIN(I)=B5+EXP(B4)
51ØØ    S1=S1+H(I):S2=S2+(AMIN(I)*H(I))
511Ø    S3=S3+(H(I)/AMIN(I)):NEXT I
512Ø    AAAW=S2/S1
5125    AVMN=S1/S3
513Ø    SPR=AAAW/AVMN
518Ø    PRINT"WEIGHT AVERGE MOLECULAR WEIGHT=";AAAW
519Ø    PRINT"NUMBER AVERAGE MOLECULAR WEIGHT=";AVMN
5195    PRINT"                                Mw/Mn RATIO =";SPR
52ØØ    S4=Ø.Ø
521Ø    FOR I=1 TO NMAX:S4=S4+H(I):NEXT I
522Ø    FOR I=1 TO NMAX:S(I)=H(I)*1ØØ/S4:NEXT I
5225    S5 (NMAX+1)=Ø.Ø
523Ø    FOR I=NMAX TO 1 STEP -1
5235    S5(I)+S5(I+1)+S(I)
524Ø    NEXT I
55ØØ    RETURN
```

APPENDIX 3: A LISTING OF THE OPERATING PROGRAM USED WITH THE 'PROCESS' FLOW PACKAGE

```
TITLE PROJECT=UFCAS,PROBLEM=ONE,USER=K.R.POLAND,DATE=15.3.84
DESCRIPTION MASS BALANCE ON ONE STAGE CASCADE
DIMENSION METRIC,PRESS=BAR,TEMP=C
PRINT FRACTION,EXTENSIVE
CALCULATION NOHBALANCE
COMPONENT DATA
LIBID 1,WATER
NONLIB 2,DEXT12/3,DEXT40/4,DEXT98
MW 2,12000/3,40000/4,98000
SPGR 2,1.0/3,1.0/4,1.0
ACENTRIC 2,1/3,1/4,1
TC 2,1000/3,1000/4,1000
PC 2,1000/3,1000/4,1000
CHAO 2,,2000,/3,,2000,/4,,2000
STREAM DATA
PROPERTY STRM=F0,PRESS=1,TEMP=25,RATE=1020.6,COMP=1,1000/2,5.56/3,12.57/4,2.47
PROPERTY STRM=Y0,PRESS=1,TEMP=25,RATE=1000,COMP=1,1000/2,0/3,0/4,0
UNIT OPERATIONS
SEPARATOR UID=S1,NAME=STAGEONE
FEED F0,Y2
OVHD STRM=Y1,PHASE=L,PRESSURE=1,TEMPERATURE=25
BTMS STRM=F1,PHASE=L,PRESSURE=1,TEMPERATURE=25
FOVHD 1,,0.5/2,,0.4010/3,,0.0504/4,,0.0
SEPARATOR UID=S2,NAME=STAGE TWO
FEED F1,Y3
OVHD STRM=Y2,PHASE=L,PRESSURE=1,TEMPERATURE=25
BTMS STRM=F2,PHASE=L,PRESSURE=1,TEMPERATURE=25
FOVHD 1,,0.5/2,,0.3313/3,,0.0428/4,,0.0014
SEPARATOR UID=S3,NAME=STAGE THREE
FEED=F2,Y4
OVHD STRM=Y3,PHASE=L,PRESSURE=1,TEMPERATURE=25
BTMS STRM=F3,PHASE=L,PRESSURE=1,TEMPERATURE=25
FOVHD 1,,0.5/2,,0.3274/3,,0.0424/4,,0.0014
SEPARATOR UID=S4,NAME=STAGE FOUR
FEED=F3
OVHD STRM=Y4,PHASE=L,PRESSURE=1,TEMPERATURE=25
BTMS STRM=F4,PHASE=L,PRESSURE=1,TEMPERATURE=25
FOVHD 1,,0.5/2,,0.32/3,,0.043/4,,0.0014
SEPARATOR UID=S5,NAME=STAGE FIVE
FEED=F4,Y6
OVHD STRM=Y5,PHASE=L,PRESSURE=1,TEMPERATURE=25
BTMS STRM=F5,PHASE=L,PRESSURE=1,TEMPERATURE=25
FOVHD 1,,0.5/2,,0.32/3,,0.045/4,,0.0014
SEPARATOR UID=S6,NAME=STAGE SIX
FEED=F5,Y7
OVHD STRM=Y6,PHASE=L,PRESSURE=1,TEMPERATURE=25
BTMS STRM=F6,PHASE=L,PRESSURE=1,TEMPERATURE=25
FOVHD 1,,0.5/2,,0.32/3,,0.045/4,,0.0014
SEPARATOR UID=S7,NAME=STAGE SEVEN
FEED=F6,Y8
OVHD STRM=Y7,PHASE=L,PRESSURE=1,TEMPERATURE=25
BTMS STRM=F7,PHASE=L,PRESSURE=1,TEMPERATURE=25
FOVHD 1,,0.5/2,,0.32/3,,0.045/4,,0.0014
```

```
SEPARATOR UID=S8,NAME=STAGE EIGHT
FEED=F7
OVHD STRM=Y8,PHASE=L,PRESSURE=1,TEMPERATURE=25
BTMS STRM=F8,PHASE=L,PRESSURE=1,TEMPERATURE=25
FOVHD 1,,0.5/2,,0.32/3,,0.045/4,,0.0014
SEPARATOR UID=S9,NAME=STAGE NINE
FEED=F8,Y10
OVHD STRM=Y9,PHASE=L,PRESSURE=1,TEMPERATURE=25
BTMS STRM=F9,PHASE=L,PRESSURE=1,TEMPERATURE=25
FOVHD 1,,0.5/2,,0.32/3,,0.045/4,,0.0014
SEPARATOR UID=S10,NAME=STAGE TEN
FEED F9,Y11
OVHD STRM=Y10,PHASE=L,PRESSURE=1,TEMPERATURE=25
BTMS STRM=F10,PHASE=L,PRESSURE=1,TEMPERATURE=25
FOVHD 1,,0.5/2,,0.32/3,,0.045/4,,0.0014
SEPARATOR UID=S11,NAME=STAGE ELEVEN
FEED F10,Y12
OVHD STRM=Y11,PHASE=L,PRESSURE=1,TEMPERATURE=25
BTMS STRM=F11,PHASE=L,PRESSURE=1,TEMPERATURE=25
FOVHD 1,,0.5/2,,0.32/3,,0.045/4,,0.0014
SEPARATOR UID=S12,NAME=STAGE TWELVE
FEED F11,YO
OVHD STRM=Y12,PHASE=L,PRESSURE=1,TEMPERATURE=25
BTMS STRM=F12,PHASE=L,PRESSURE=1,TEMPERATURE=25
FOVHD 1,,0.5/2,,0.32/3,,0.045/4,,0.0014
RECYCLE
ACCELERATION TYPE=WEGS,STRM=Y3,Y4,Y6,Y7,Y8,Y10,Y11,Y12
LOOP NO=1,START=S1,END=S2,TRIAL=10,TOLER=0.01
LOOP NO=2,START=S1,END=S3,TRIAL=10,TOLER=0.01
LOOP NO=3,START=S1,END=S4,TRIAL=10,TOLER=0.01
LOOP NO=4,START=S1,END=S5,TRIAL=10,TOLER=0.01
LOOP NO=5,START=S1,END=S6,TRIAL=10,TOLER=0.01
LOOP NO=6,START=S1,END=S7,TRIAL=10,TOLER=0.01
LOOP NO=7,START=S1,END=S8,TRIAL=10,TOLER=0.01
LOOP NO=8,START=S1,END=S9,TRIAL=10,TOLER=0.01
LOOP NO=9,START=S1,END=S10,TRIAL=10,TOLER=0.01
LOOP NO=10,START=S1,END=S11,TRIAL=10,TOLER=0.01
LOOP NO=11,START=S1,END=S12,TRIAL=10,TOLER=0.01
```

APPENDIX 4: AN EXAMPLE OF THE OUTPUT FROM THE 'PROCESS' FLOW PACKAGE

VIIIA UNIT STREAM CORRELATION MATRIX

UNIT NO	1	2	3	4	5	6	7	8	9	10	11	12
ID	S1	S2	S3	S4	S5	S6	S7	S8	S9	S10	S11	S12
STREAM ID												
F0	F	–	–	–	–	–	–	–	–	–	–	–
F1	P	F	–	–	–	–	–	–	–	–	–	–
F2	–	P	F	–	–	–	–	–	–	–	–	–
F3	–	–	P	F	–	–	–	–	–	–	–	–
F4	–	–	–	P	F	–	–	–	–	–	–	–
F5	–	–	–	–	P	F	–	–	–	–	–	–
F6	–	–	–	–	–	P	F	–	–	–	–	–
F7	–	–	–	–	–	–	P	F	–	–	–	–
F8	–	–	–	–	–	–	–	P	F	–	–	–
F9	–	–	–	–	–	–	–	–	P	F	–	–
Y0	–	–	–	–	–	–	–	–	–	–	–	F
Y1	P	–	–	–	–	–	–	–	–	–	–	–
Y2	F	P	–	–	–	–	–	–	–	–	–	–
Y3	–	F	P	–	–	–	–	–	–	–	–	–
Y4	–	–	F	P	–	–	–	–	–	–	–	–
Y5	–	–	–	–	P	–	–	–	–	–	–	–
Y6	–	–	–	–	F	P	–	–	–	–	–	–
Y7	–	–	–	–	–	F	P	–	–	–	–	–
Y8	–	–	–	–	–	–	F	P	–	–	–	–
Y9	–	–	–	–	–	–	–	–	P	–	–	–
F10	–	–	–	–	–	–	–	–	–	P	F	–
F11	–	–	–	–	–	–	–	–	–	–	P	F

F12	-	-	-	-	-	-	-	-	-	-	-	P
Y10	-	-	-	-	-	-	-	-	F	P	-	-
Y11	-	-	-	-	-	-	-	-	-	F	P	-
Y12	-	-	-	-	-	-	-	-	-	-	F	P

VIIIB CALCULATIONAL SEQUENCE IS DEFINED BY INPUT

VIIIC RECYCLE LOOPS ARE DEFINED BY INPUT

VIIID RECYCLE STREAMS

STREAM	FROM UNIT	TO UNIT	LOOP
Y2	2,S2	1,S1	1
Y3	3,S3	2,S2	2
Y4	4,S4	3,S3	3
Y6	6,S6	5,S5	5
Y7	7,S7	6,S6	6
Y8	8,S8	7,S7	7
Y10	10,S10	9,S9	9
Y11	11,S11	10,S10	10
Y12	12,S12	11,S11	11

STREAM COMPONENT FLOW RATES - KG MOLS/HR

STREAM ID NAME	F0	F1	F2	F3	F4	F5	F6
PHASE	LIQUID	LIQUID	LIQUID	LIQUID	LIQUID	LIQUID	LIQUID
1 WATER	1000.0000	800.0000	600.0000	400.0000	200.0000	160.0000	120.0000
2 DEXT12	5.5600	4.5952	4.2617	3.6526	2.4838	2.4178	2.2775
3 DEXT40	12.5700	12.4655	12.4594	12.4435	11.9084	11.9083	11.9072
4 DEXT98	2.4700	2.4735	2.4735	2.4735	2.4700	2.4700	2.4700
TOTALS	1020.6000	819.5341	619.1945	418.5695	216.8622	176.7961	136.6546
TEMPERATURE, DEG C	25.0000	25.0000	25.0000	25.0000	25.0000	25.0000	25.0000
PRESSURE, BAR	1.0000	1.0000	1.0000	1.0000	1.0000	1.0000	1.0000
H, MM KCAL/HR	0.0000	0.0000	0.0000	0.0000	0.0000	0.0000	0.0000
MOLE FRACT LIQUID	1.0000	1.0000	1.0000	1.0000	1.0000	1.0000	1.0000
MOLE FRACT WATER	0.9798	0.0000	0.0000	0.0000	0.0000	0.0000	0.0000
RECYCLE CONVERGENCE	0.0000	0.0000	0.0000	0.0000	0.0000	0.0000	0.0000

STREAM ID NAME	F7	F8	F9	Y0	Y1	Y2	Y3
PHASE	LIQUID	LIQUID	LIQUID	LIQUID	LIQUID	LIQUID	LIQUID
1 WATER	80.0000	40.0000	229.6327	1000.0000	800.0000	600.0000	400.0000
2 DEXT12	1.9794	1.3460	1.3100	0.0000	3.0762	2.1114	1.7780
3 DEXT40	11.8820	11.3473	11.3472	0.0000	0.6616	0.5571	0.5510
4 DEXT98	2.4700	2.4665	2.4665	0.0000	0.0000	0.0035	0.0035
TOTALS	96.3314	55.1598	244.7564	1000.0000	803.7379	602.6721	402.3324
TEMPERATURE, DEG C	25.0000	25.0000	25.0000	25.0000	25.0000	25.0000	25.0000

PRESSURE, BAR	1.0000	1.0000	1.0000	1.0000	1.0000	1.0000	1.0000
H, MM KCAL/HR	0.0000	0.0000	0.0000	0.0000	0.0000	0.0000	0.0000
MOLE FRACT LIQUID	1.0000	1.0000	1.0000	1.0000	1.0000	1.0000	1.0000
MOLE FRACT WATER	0.0000	0.0000	0.0000	0.0000	0.0000	0.0000	0.0000
RECYCLE CONVERGENCE	0.0000	0.0000	0.0000	0.0000	0.0000	0.0000	0.0000

STREAM ID NAME	Y4	Y5	Y6	Y7	Y8	Y9	F10
PHASE	LIQUID	LIQUID	LIQUID	LIQUID	LIQUID	LIQUID	LIQUID
1 WATER	200.0000	160.0000	120.0000	80.0000	40.0000	229.6327	422.8163
2 DEXT12	1.1688	1.1378	1.0718	0.9315	0.6334	0.6165	1.2340
3 DEXT40	0.5351	0.5611	0.5611	0.5599	0.5347	0.5347	11.3461
4 DEXT98	0.0035	0.0035	0.0035	0.0035	0.0035	0.0035	2.4665
TOTALS	201.7074	161.7024	121.6363	81.4948	41.1716	230.7873	437.8629
TEMPERATURE, DEG C	25.0000	25.0000	25.0000	25.0000	25.0000	25.0000	25.0000
PRESSURE, BAR	1.0000	1.0000	1.0000	1.0000	1.0000	1.0000	1.0000
H, MM KCAL/HR	0.0000	0.0000	0.0000	0.0000	0.0000	0.0000	0.0000
MOLE FRACT LIQUID	1.0000	1.0000	1.0000	1.0000	1.0000	1.0000	1.0000
MOLE FRACT WATER	0.0000	0.0000	0.0000	0.0000	0.0000	0.0000	0.0000
RECYCLE CONVERGENCE	0.0000	0.0000	0.0000	0.0000	0.0000	0.0000	0.0000

STREAM COMPONENT FLOW RATES - KG MOLS/HR

STREAM ID NAME	F11	F12	Y10	Y11	Y12
PHASE	LIQUID	LIQUID	LIQUID	LIQUID	LIQUID
1 WATER	615.4080	807.7040	422.8163	615.4080	807.7040
2 DEXT12	1.0726	0.7293	0.5807	0.5047	0.3432
3 DEXT40	11.3221	10.8126	0.5346	0.5335	0.5095
4 DEXT98	2.4665	2.4631	0.0035	0.0035	0.0035
TOTALS	630.2692	821.7090	423.9351	616.4497	808.5602
TEMPERATURE, DEG C	25.0000	25.0000	25.0000	25.0000	25.0000
PRESSURE, BAR	1.0000	1.0000	1.0000	1.0000	1.0000
H, MM KCAL/HR	0.0000	0.0000	0.0000	0.0000	0.0000
MOLE FRACT LIQUID	1.0000	1.0000	1.0000	1.0000	1.0000
MOLE FRACT WATER	0.0000	0.0000	0.0000	0.0000	0.0000
RECYCLE CONVERGENCE	0.0000	0.0000	0.0084	-0.0010	-0.0004

APPENDIX 5: A LISTING OF THE COMPUTER PROGRAM USED TO CONTROL THE FOUR STAGE MEMBRANE CASCADE

```
   10  REM HOPE
   20  :
   25  ON ERROR GOTO 1800
   30  *TV255,1
   40  *KEY10 *FX13,4|M?&FCC1=00|M?&FCC2=00|M?&FCC3=00|M?&
FCC4=00|MMODE3|MOLD|M VDU19,1,2,0,0,0|N|M
   50  :
   60  MODE1:VDU23;8202;0;0;0;
   70  PROCsetup:PROCinit
   80  REPEAT:PROCcycle:PROCone:PROCtwo:PROCthree:PROCfour
   90    PROCfive:PROCsix:PROCseven:cycle%=cycle%+1
  100    UNTIL FALSE:END
  110  :
  120  DEF PROCinit
  130  PROCvalve("VF16","ON"):PROCvalve("VF14","ON")
  140  PROCvalve("VF24","ON"):PROCvalve("VF34","ON")
  150  PROCvalve("VF44","ON"):CALLdisplay
  160  *FX21,0
  170  INPUT'"CYCLE Number "cycle%
  180  ENDPROC
  190  :
  200  DEF PROCcycle
  210  VDU28,25,22,39,22:CLS:COLOUR 1:PRINT"  Cycle No.";c
ycle%;
  220  VDU28,0,31,24,22:COLOUR 3:ENDPROC
  230  :
  240  DEF PROCone
  250  PROCvalve("VF14","OFF"):PROCvalve("VF13","ON")
  260  PROCvalve("VF24","OFF");:PROCvalve("VF23","ON")
  270  PROCvalve("VF34","OFF"):PROCvalve("VF33","ON")
  280  PROCvalve("VF44","OFF"):PROCvalve("VF43","ON")
  290  CLS:PRINT'"Filling Tanks"''"P1 P2 P3 P4"
  300  B1%=0:B2%=0:B3%=0:B4%=0:TIME=0
  310  REPEAT:CALL display
  320    IF FNLP(1) THEN PROCvalve("VF13","OFF"):PROCvalve
("VF14","ON"):B1%=1
  330    IF FNLF(1) THEN PROCvalve("VD11","OFF") ELSE PROC
valve("VD11","ON")
  340    IF FNLP(2) THEN PROCvalve("VF23","OFF"):PROCvalve
("VF24","ON"):B2%=1
  350    IF FNLF(2) THEN PROCvalve("VD21","OFF") ELSE PROC
valve("VD21","ON")
  360    IF FNLP(3) THEN PROCvalve("VF33","OFF"):PROCvalve
("VF34","ON"):B3%=1
  370    IF FNLF(3) THEN PROCvalve("VD31","OFF") ELSE PROC
valve("VD31","ON")
  380    IF FNLP(4) THEN PROCdelay(1,57000)
  390    IF FNdelay(1) THEN PROCvalve("VF43","OFF"):PROCva
lve("VF44","ON"):B4%=1
  400    IF FNLF(4) THEN PROCvalve("VD41","OFF") ELSE PROC
valve("VD41","ON")
  410    UNTIL B1%=1 AND B2%=1 AND B3%=1 AND B4%=1
  420  CALL display:PROCresetdelays:ENDPROC
  430  :
  440  DEF PROCtwo
  450  PROCvalve("VD11","ON"):PROCvalve("VD21","ON")
  460  PROCvalve("VD31","ON"):PROCvalve("VD41","ON")
```

```
  47Ø  CLS:PRINT'"Draining Tanks"''"D1 D2 D3 D4"''"into Ta
nks"''"F1 F2 F3 F4"
  48Ø  B1%=Ø:B2%=Ø:B3%=Ø:B4%=Ø:time%=TIME
  49Ø  REPEAT:CALLdisplay
  5ØØ    IF TIME>time%+3ØØØ THEN PROCfault(1)
  51Ø    IF FNLF(1) THEN PROCvalve("VD11","OFF"):B1%=1
  52Ø    IF FNLF(2) THEN PROCvalve("VD21","OFF"):B2%=1
  53Ø    IF FNLF(3) THEN PROCvalve("VD31","OFF"):B3%=1
  54Ø    IF FNLF(4) THEN PROCvalve("VD41","OFF"):B4%=1
  55Ø    UNTIL B1%=1 AND B2%=1 AND B3%=1 AND B4%=1
  56Ø  ENDPROC
  57Ø  :
  58Ø  DEF PROCthree
  59Ø  PROCvalve("VF44","OFF"):PROCvalve("VF46","ON")
  6ØØ  CLS:PRINT'"Draining Tank 4"
  61Ø  REPEAT:PROCdelay(1,28ØØØ):CALLdisplay:UNTIL FNdelay
(1)
  62Ø  PROCresetdelays:IF FNLF(4) THEN 6ØØ
  63Ø  PROCvalve("VF46","OFF"):PROCvalve("VF44","ON")
  64Ø  CALLdisplay:ENDPROC
  65Ø  :
  66Ø  DEF PROCfour
  67Ø  RESTORE 75Ø
  68Ø  FOR O%=3 TO 1 STEP-1:READ V1$,V2$
  69Ø    PROCvalve(V1$,"OFF"):PROCvalve(V2$,"ON")
  7ØØ    time=TIME:CLS:PRINT'"Transfering F";O%;" to F";O%
+1
  71Ø    REPEAT:CALLdisplay:IF TIME>time+65ØØØØ THEN PROCf
ault(2)
  72Ø      UNTIL FNLF(O%+1) AND NOT FNLF(O%)
  73Ø    PROCvalve(V2$,"OFF"):PROCvalve(V1$,"ON")
  74Ø    CALLdisplay:NEXT:ENDPROC
  75Ø  DATA VF34,VF45,VF24,VF35,VF14,VF25
  76Ø  :
  77Ø  DEF PROCfive
  78Ø  PROCvalve("VF16","OFF"):PROCvalve("VF15","ON")
  79Ø  CLS:PRINT'"Filling tank F1"
  8ØØ  REPEAT:CALLdisplay:UNTIL FNLF(1)
  81Ø  PROCvalve("VF15","OFF"):PROCvalve("VF16","ON")
  82Ø  CALL display:ENDPROC
  83Ø  :
  84Ø  DEF PROCsix
  85Ø  PROCvalve("VP12","ON"):PROCvalve("VP22","ON")
  86Ø  PROCvalve("VP32","ON"):PROCvalve("VP42","ON")
  87Ø  CLS:PRINT'"Draining P tanks"
  88Ø  REPEAT:PROCdelay(1,12ØØØ):CALL display:UNTIL FNdela
y(1)
  89Ø  IF FNLP(1) OR FNLP(2) OR FNLP(3) OR FNLP(4) THEN PR
OCfault(3)
  9ØØ  PROCvalve("VP12","OFF"):PROCvalve("VP22","OFF")
  91Ø  PROCvalve("VP32","OFF"):PROCvalve("VP42","OFF")
  92Ø  CALL display:PROCresetdelays:ENDPROC
  93Ø  :
  94Ø  DEF PROCseven
  95Ø  B%=Ø:TIME=Ø:CLS:PRINT'"Filling tank D4"
  96Ø  REPEAT:CALL display
  97Ø    IF NOT FNLD(4) THEN PROCvalve("VP47","ON") ELSE P
ROCdelay(2,1ØØØ)
```

```
  98Ø  UNTIL FNdelay(2):PROCvalve("VP47","OFF"):CALL displ
ay:CLS
  99Ø  PROCresetdelays:ENDPROC
 1ØØØ  :
 1Ø1Ø  DEF PROCsetup
 1Ø2Ø  VDU19,3,2,Ø,Ø,Ø,19,2,6,Ø,Ø,Ø:VDU28,Ø,31,24,22
 1Ø3Ø  *LOAD"O.CHAR"
 1Ø4Ø  *LOAD"O.CODE"
 1Ø5Ø  *LOAD"O.TABLE"
 1Ø6Ø  *LOAD"SCREEN"
 1Ø7Ø  ?&22Ø=&BØ:?&221=&Ø9:?&A48=&ØØ:?&A49=&ØØ
 1Ø8Ø  display=&9ØØ:CALLdisplay
 1Ø9Ø  REM to start INT.(*FX14,4).to stop INT.(*FX13,4)
 11ØØ  *FX14,4
 111Ø  DIM DEL(4):ENDPROC
 112Ø  :
 113Ø  DEF FNLF(num%)
 114Ø  IF (?&A48 AND 2^(num%-1))=2^(num%-1) THEN num%=TRUE
 ELSE num%=FALSE
 115Ø  =num%
 116Ø  DEF FNLP(num%)
 117Ø  IF (?&A49 AND 2^(num%-1))=2^(num%-1) THEN num%=TRUE
 ELSE num%=FALSE
 118Ø  =num%
 119Ø  DEF FNLD(num%)
 12ØØ  IF (?&A48 AND &1Ø)=&1Ø THEN num%=TRUE ELSE num%=FAL
SE
 121Ø  =num%
 122Ø  :
 123Ø  DEF PROCvalve(V$,P$)
 124Ø  S%=VAL(MID$(V$,3,1)):V%=VAL(RIGHT$(V$,1))
 125Ø  IF V%=Ø OR S%=Ø OR S%>4 THEN 132Ø
 126Ø  IF S%=4 AND V%>7 THEN 132Ø
 127Ø  IF S%=1 AND V%>6 THEN 132Ø
 128Ø  IF (S%=2 OR S%=3) AND V%>5 THEN 132Ø
 129Ø  V%=2^(V%-1):S%=&A4E-S%
 13ØØ  IF P$="ON" THEN ?S%=?S% OR V% : ENDPROC
 131Ø  IF P$="OFF" THEN ?S%=?S% AND (V% EOR &FF) : ENDPROC
 132Ø  PRINT"Not Possible !":FOR D%=Ø TO 1ØØØ:NEXT D%:ENDP
ROC
 133Ø  :
 134Ø  DEF PROCdelay(denum%,delay%)
 135Ø  IF DEL(denum%)=Ø THEN DEL(denum%)=(TIME+delay%)
 136Ø  PROCprintdelay:ENDPROC
 137Ø  :
 138Ø  DEF PROCprintdelay
 139Ø  VDU28,25,31,39,23:CLS
 14ØØ  FOR denum%=1 TO 4:IF DEL(denum%)=Ø THEN 145Ø
 141Ø    IF (DEL(denum%)-TIME)<Ø THEN 145Ø
 142Ø    min%=((DEL(denum%)-TIME)DIV6ØØØ)MOD6Ø
 143Ø    sec%=((DEL(denum%)-TIME)DIV1ØØ)MOD6Ø
 144Ø    PRINT'" Delay ";denum%;" = ";min%;".";sec%
 145Ø    NEXT denum%:VDU28,Ø,31,24,22
 146Ø  ENDPROC
 147Ø  :
 148Ø  DEF PROCresetdelays
 149Ø  FOR denum%=1 TO 4:DEL(denum%)=Ø.NEXT denum%
```

```
 15ØØ  VDU28,25,31,39,23:CLS:VDU28,Ø,31,24,22
 151Ø  ENDPROC
 152Ø  :
 153Ø  DEF FNdelay(denum%)
 154Ø  IF DEL(denum%)>TIME THEN over%=FALSE ELSE over%=TRU
E
 155Ø  IF DEL(denum%)=Ø THEN over%=FALSE
 156Ø  =over%
 157Ø  :
 158Ø  DEF PROCfault(F%)
 159Ø  VDU19,128,143,Ø,Ø,Ø:n%=Ø
 16ØØ  REPEAT:key=INKEY(1):n%=n%+1
 161Ø    REM SOUND&1Ø+RND(3),-15,n%MOD5Ø,5
 162Ø    UNTIL key=32:VDU19,128,128,Ø,Ø,Ø
 163Ø  CLS:COLOUR 1
 164Ø  ON F% GOTO 166Ø,169Ø,17ØØ
 165Ø  :
 166Ø  FOR N%=1 TO 4
 167Ø    IF NOT FNLF(N%) THEN PRINT"Tank F";N%;" Failed to
 Fill"
 168Ø    NEXT:PROCwait:ENDPROC
 169Ø  PRINT'"Transfer from F";O%;" to F";O%+1;" not compl
ete":PROCwait:ENDPROC
 17ØØ  FOR N%=1 TO 4
 171Ø    IF FNLF(N%) THEN PRINT"Tank P";N%;" Failed to Dra
in"
 172Ø    NEXT:PROCwait:ENDPROC
 173Ø  :
 174Ø  DEF PROCwait
 175Ø  COLOUR2:REPEAT:key=INKEY(5):CALLdisplay
 176Ø    PRINT'"Press spacebar to Cont."
 177Ø    UNTIL key=32:COLOUR3:CLS:ENDPROC
 178Ø  :
 18ØØ  IF ERR=17 THEN STOP
 181Ø  *FX13,4
 182Ø  ?&FCC1=ØØ:?&FCC2=ØØ:?&FCC3=ØØ:?&FCC4=ØØ
 183Ø  REPORT:PRINT" at line ";ERL
 184Ø  END
```

APPENDIX 6: EVALUATION OF THE MOST COST EFFICIENT METHOD OF FRACTIONATING DEXTRAN HYDROLYSATE

APPENDIX 6: Evaluation of the Most Cost Efficient Method of Fractionating Dextran Hydrolysate

6.1 Introduction

In this determination of the most cost efficient method of fractionating dextran hydrolysate three main factors have been investigated. These are (a) operating costs, (b) capital costs and (c) the recovery of the 'saleable' dextran in the product, compared to the original amount in the feed.

In these calculations the costs for ethanol fractionation have been derived from actual plant data wherever possible. The costs for GPC and UF fractionations have been derived from experimental experience gained at Aston.

6.2 Process Time Required per Batch

The present Fisons process is designed to obtain at least 100 tonnes per year of clinical dextran. Data obtained from Fisons indicated that a typical hydrolysate batch contained 2 800 Kg of dextran. From this feed 1 400 Kg of final product could be obtained. Therefore, at least 72 batches were required per annum.

To obtain a process time per batch, for latter calculations, a year was assumed to consist of 48 processing weeks. Therefore, 1.5 batches were required per week, or 1 batch every 112 hours.

This batch time of 112 hours was used in the calculations for the new alternative processes. This batch time was kept constant since any new process would obtain the dextran hydrolysate from the existing fermentation plant.

6.3 Ethanol Fractionation

6.3.1 Operating Costs

Data obtained from Fisons showed that to fractionate 2 800 Kg of dextran hydrolysate, down to 1 400 Kg of clinical dextran, required the use and recovery of 41 350 Kg of water and 39 700 Kg of ethanol.

This ethanol and water is removed by steam heated distillation columns. The cost of this steam is one of the main operating costs of the existing plant and its value will now be calculated.

From Plant Data

Inlet feed temperature to distillation columns = 12°C

Average operating temperature of columns = 82°C

Reflux ratio of columns = 0.85

Cost of steam/tonne = £12.00

Energy required per batch to raise mixture to boiling point

Ethanol (Q_1) = mass x specific heat capacity x temperature rise

$$Q_1 = 39\,700 \text{ Kg} \times 2.6 \frac{\text{KJ}}{\text{Kg K}} \times 70 \text{ K}$$

$Q_1 = 7\,225 \times 10^3$ KJ

Water (Q_2) = 41 350 Kg x 4.19 KJ/Kg K x 70 K

$Q_2 = 12\,128 \times 10^3$ KJ

Total (Q_3) = $19\,353 \times 10^3$ KJ

Energy required per batch to vapourise mixture

Ethanol (Q_4) = mass x latent heat of vapourisation

$$Q_4 = 39\,700 \text{ Kg} \times 1090 \frac{\text{KJ}}{\text{Kg}}$$

$Q_4 = 43\,273 \times 10^3$ KJ

Water (Q_5) = 41 350 x 2 260

Q_5 = 93 451 x 10^3 KJ

Total (Q_6) = 136 724 x 10^3 KJ

Taking into account column reflux:

Total energy required for vapourisation = 1.85 x (Q_6)

Q_7 = 252 939 x 10^3 KJ

Hence,

Total distillation energy required (Q_8) = Q_7 + Q_3

Q_8 = 272 292 x 10^3 KJ

If the steam providing this energy is at a temperature of 138°C (from steam tables), then the energy provided can be assumed to be solely from the steam condensing. Therefore, assuming 100% efficiency in heat transfer:

Energy provided by steam = mass of steam (M) x heat of vapourisation of water (λ)

Therefore M λ = Q_8

Therefore M = 120 483 Kg

Therefore M = 120.5 tonnes

Hence,

Cost of steam = 120.5 x £12

Cost of steam = £1446 per batch

Cost of steam = £104 112 per annum

Even though this cost for steam ignores all heat losses and makes the major assumption of a 100% efficiency in heat transfer, it is known that this figure does bear some comparison to the actual plant costs for steam. Therefore, this figure will be used for future comparisons.

As well as the cost of steam, the other major plant processing costs are: (a) cost of ethanol losses, (b) cost of fresh pyrogen free de-ionised water, (c) cost of the power required for the necessary pumps, (d) cost of effluent disposal, and (e) utilities, eg. canteens, administration, and labour.

From plant data the ethanol losses are approximately 2% of the total ethanol requirement, and this is equal to £33 210 per annum.

The ethanol fractionation requires approximately 41.7 tonnes of fresh pyrogen free water per batch. This water costs approximately £1.50 per tonne, and therefore the cost of this fresh water is approximately £4 500 per annum. This figure does not make any allowance for any non pyrogen free (mains) water required on the plant, eg. for the condensers on the distillation columns. This mains water is on a closed circuit and the losses can be considered negligible.

The present process requires six 20 Kw pumps for pumping the non pyrogen-free water (mains water) at a maximum rate of approximately 300 000 L hr^{-1}. Plant data shows that four of these six pumps operate for 160 hours per week and two for 100 hours per week. This gives a total of 806 400 Kw per annum. This power costs £0.055 per Kw hr, and therefore the cost of the power for these pumps is £44 352 per annum.

The ethanol process also requires at least four 18.5 Kw pumps and four 4 Kw pumps for the process streams (see later). The cost of the power required for these process stream pumps is equal to £39 600 per annum. Hence, the total cost of the pumping power can be considered to be equal to £83 952 per annum.

The mains water system passes through two cooling towers, both of which contain large fans. No data could be obtained for the power of these fans, and therefore their power was ignored.

The present process recycles many of its 'waste' products and therefore the cost of effluent disposal can be considered negligible.

Since the new alternative fractionation processes under consideration will require approximately the same amount of labour, and since the requirement for utilities will be the same for all processes, these costs will also be considered negligible.

Hence, the total operating cost for ethanol fractionation can be considered to be equal to £225 774 per annum.

6.3.2 Capital Costs

To calculate an accurate cost for every single piece of capital equipment, eg. piping, instrumentation, steam lines etc, would take several months. However, the cost of the major pieces of capital equipment can be estimated. These major pieces consist of distillation columns, settling tanks (for precipitating the chosen MWs), storage tanks and pumps. The cost of these pieces will now be considered.

The distillation columns used in the industrial ethanol fractionation process are 1.4 metres in diameter, 8.5 metres high and have 15 plates. Using a computer package written, at Aston, by Momo (130) the cost of such a column was calculated to be £293200. This price includes the costs of the necessary reboiler and the reflux condenser. The present ethanol fractionation takes place over four stages, with each stage producing a different quantity and mixture of ethanol/water solution. Therefore, in order to be able to distill off the necessary alcohol from each stage, the present process uses three of the above distillation columns. Hence, the total cost of the distillation columns would be £879 600.

Since a four stage fractionation is used, four settling tanks are required. These tanks consist of one tank of 40m^3 capacity, two tanks of 50 m^3 capacity, and one tank of 55m^3 capacity. Since increasing the volume of a tank does not greatly affect its cost, all these tanks can be considered to be of equal volume and all cost approximately £15 000 each. This cost includes an allowance for an agitator in each tank for mixing the ethanol and water solutions. Therefore, the total cost of the settling tanks is £60 000.

Once a particular fractionation stage has been completed, the required product is sent to a storage tank before the next fractionation, and the 'waste' product is sent to a storage tank before its alcohol content is removed by distillation. Therefore, a total of eight storage tanks is required. Four of these tanks require a volume of 10m^3 and cost

£4500 each, three require a volume of $50m^3$ and cost £10 000 each, and one tank of $30m^3$ is required which costs £7 000. Also, one tank is required for the storage of the initial ethanol. This tank must have a volume of $60m^3$ and costs approximately £11 000. Therefore, the total cost of these storage tanks is £66 000.

Since all pumping must be undertaken in a potentially explosive atmosphere, all the pumps used must be flame proof. This greatly increases the cost of the pumps needed. For the first stage fractionation one pump of 4 Kw is required for transfer of solution between the 'waste' product storage tank and the distillation columns, and one 18.5 Kw pump is required for transfer of solution from the settling tanks to the storage tanks. The second pump is of a higher power requirement since the precipitated dextran leaving the settling tank is very viscous. These pumps cost approximately £4 000 and £6 000 respectively. Similar pumps are required on the second, third and fourth precipitation stages. Hence, the total cost of the process stream pumps is £40 000.

As stated in Appendix 6.3.1, six 20 Kw pumps are required for pumping the mains water streams. These pumps cost a total of £48 000. As previously stated this mains water passes through two cooling towers. No accurate costs could be obtained for these cooling towers, and therefore their cost will be ignored even though it is expected their cost could be considerable.

Hence, the total capital cost of the ethanol fractionation process can be considered to be approximately £1 093 600.

6.4 GPC and UF Fractionation

As stated at the beginning of this PhD thesis, Vlachogiannis (14) showed that a process incorporating both GPC and UF could fractionate dextran as efficiently as ethanol fractionation. However, no actual operating costs were calculated for comparison. Therefore, based on the work of Vlachogiannis these costs will now be determined.

6.4.1 GPC Fractionation

6.4.1.1 Operating Costs

(a) GPC Equipment Operating Costs

The main costs of GPC fractionation are, (a) the cost of the GPC packing, (b) the energy required to run the GPC equipment at 60°C (as recommended by Vlachogiannis), and (c) the energy required for pumping the feed, eluent and purge solutions.

To produce 100 tonnes per annum of clinical dextran a GPC rig containing 2.54m^3 of packing is required. This packing costs approximately £8 700/m^3 and therefore the initial packing cost is £22 000. However, the useful life of this packing is at least 5 years and so the annual cost is only £4 400.

The energy required to run the equipment at 60°C is equal to the energy required to heat the feed solutions to 60°C, and the energy required to maintain the equipment at 60°C. These costs have been calculated by Ganetsos (129) and are:

Cost of heating feeds = £5 550 pa

Cost of heating equipment = £7 500 pa

To obtain the necessary flowrates in the feed, eluent and purge lines, three pumps each of 2.2 Kw are required (see later). Therefore the cost of the pumping power is £2 900 per annum.

The 'waste' stream from the GPC consists almost totally of high molecular weight dextran. The majority of this material can be recycled back to the acid hydrolysis section of the dextran production process. Therefore, the effluent from GPC fractionation can be considered negligible. As with ethanol fractionation the cost of utilities and labour will be ignored.

Hence, the operating cost of the GPC equipment can be considered to be equal to £20 350 per annum. The cost of the pyrogen-free water required by the GPC will be discussed later.

(b) GPC Product Concentration Operating Costs

If a dextran feed of 2 800 Kg of hydrolysate is fractionated by GPC, a product containing 2 345 Kg of dextran is produced at a concentration of 1.4% w/w. The ideal feed concentration for UF fractionation, of the low molecular weight material, is 2.0% w/w. Therefore, the GPC products must be concentrated.

This concentration can be accomplished either by evaporation or by using UF membranes. The respective costs of these two methods will now be investigated.

(i) Evaporation:

Amount of water in 1.4% solution = 167 400 Kg

Amount of water in 2.0% solution = 117 100 Kg

Therefore:

Amount of water to be removed = 50 300 Kg/batch

Assuming the feed solution enters the evaporator at 100^{o}C, energy is supplied by steam condensing and 100% heat transfer efficiency, then:

Amount of steam required = 50 300 Kg/batch

= 50.3 tonne/batch

Hence,

cost of steam = 50.3 x 12

= £604/batch

= <u>£43 488 pa</u>

(ii) UF Concentration:

Vlachogiannis showed that an Amicon 2000 molecular weight cut-off membrane can be used to concentrate dextran solutions. This concentration can be accomplished with a negligible loss of dextran; any dextran which is lost is below 12000 MW. The number, and cost of the membranes required will now be calculated:

Amount of water to be removed = 50 300 Kg/batch

Since 1 batch takes 112 hours, therefore:

Amount of water to be removed = 449 Kg/hr = 449 L/hr

Flux of a $0.06m^2$ membrane of 2 000 MW cut-off = 8.4 cm^3/min

Therefore:

$$\text{Flux of Amicon } 5m^2 \text{ membrane} = \frac{8.4}{10^3} \times 60 \times \frac{5}{0.06}$$

Therefore:

$$\text{flux} = 42 \text{ L/hr}$$

Hence,

$$\text{Number of membranes required} = \frac{449}{42} = 10.7$$

$$= 11$$

Cost of one membrane = £600

Therefore,

Total cost of membranes = £6 600.

Since the concentration of the solutions being processed never exceed 2% w/w, from experimental experience these membranes should have a life of at least 3 years. Therefore:

Annual cost of membranes = £2 200

To produce the necessary retentate recirculation rates and pressures required by these membranes a 2.2 Kw pump is required, with an annual electricity cost of £968.

Therefore, the total cost of this membrane concentration step is £3168 per annum. Hence, concentration by membranes is £40 320 per annum cheaper than concentration by evaporation.

Hence, the total operating cost for GPC fractionation is approximately £23520.

6.4.1.2 Capital Costs

In order to process the necessary amount of dextran hydrolysate, the GPC equipment required would consist of 13 columns each of 1.9 metres in height and 0.42 metres in diameter. From experience at Aston, these columns should approximately cost a total of £102 000.

As well as the chromatographic columns the GPC will also require ancilliary equipment such as pumps, heaters, and feed and product tanks. As stated previously one 2.2 Kw feed pump, one 2.2 Kw purge pump and one 2.2 Kw eluent pump are required. Even though these pumps are all of the same power, by varying their impeller sizes, eg. from 6 inches to 6½ inches, the required flowrates and pressures can be obtained. These pumps each cost £1 300.

In order to operate the GPC equipment at the required 60°C, four heaters are required. These consist of one feed heater, one eluent heater, one purge heater, and one 'space' heater. The 'space' heater is used to maintain the actual metal and packing of the GPC columns at the required temperature. This 'space' heater costs approximately £2000, and the three process stream heaters cost £1400 each.

Since the GPC equipment operates ideally under steady-state conditions, a constant feed composition is required. However, the present production method for dextran hydrolysate gives a product of slightly varying composition. Therefore, the GPC would require a feed tank of at least 70 000 litres. This feed tank could then store at least four batches of hydrolysate, and would therefore tend to 'smooth' out any irregularities in the GPC feed. This tank would cost approximately £10 000.

As well as the feed tank, two tanks each of 10 000 litres would be required for storing quantities of pyrogen free water for use as eluent and purge. These two tanks would cost approximately £3 500 each.

As stated previously, the product from the GPC must be concentrated before the next fractionation step, and this concentration step has to be accomplished under a batch mode if membranes are used. Therefore, two GPC product tanks, each of 10 000 litres, are required. These tanks would each require 6.5 hours to be concentrated and transferred to the next stage, with the GPC filling one tank every 6.7 hours. These product tanks would cost £3 500 each.

The concentration of the GPC products would require a 2.2 Kw pump. This is so that the necessary retentate recirculation rate, and pressure required for the concentrating membranes can be obtained. This pump would cost £1300.

The GPC equipment would also require valves to control the flows into and out of the columns, and some means of controlling the valves themselves. However, the present ethanol fractionation method uses extensive control for both process and non-process streams. Since no accurate comparative cost could be determined for the ethanol process control system, the cost of the GPC control system will be considered to be negligible. Hence, the capital cost of GPC fractionation can be considered to be £137400.

6.4.2 UF Fractionation of Low MW Dextran

The UF fractionation of the low molecular weight dextran can be accomplished in two ways. The first method is batch diafiltration using Amicon 5000 molecular weight cut-off membranes. The second is by using the cascade mentioned in Chapter 5, with Amicon 10 000 molecular weight cut-off membranes. The relevant costs of these two methods will now be discussed.

6.4.2.1 Batch Fractionation

(a) Operating costs

From experiments conducted with Amicon membranes in Chapter 4:

Number of diavolumes required (using 5000 MW cut-off membranes) = 12

Therefore,

Volume of water to be processed = 12 x 117 100 L

$= 1405 \times 10^3$ L/batch

Since one batch must be processed in 112 hours:

Total flux required = 12 546 L/hr

Flux of Amicon 5000 MW cut-off membrane (5 m^2) = 75 L/hr

Therefore:

Number of membranes required = $\frac{12\,546}{75}$

$= 167.3$

$= 168$

Initial cost of membranes = 168 x £600

= £101 000

As with the 2000 cut-off membranes a life of at least 3 years can be assumed. Therefore:

Annual cost of membranes = £34 000

This fractionation will produce 1 403 Kg of final clinical dextran dissolved in 117 100 Kg of water (~ 1.2% w/w concentration). However, before this product can be spray dried it must have a concentration of between 25-30% w/w. Therefore another concentration step is required:

Required concentration of final product = 25-30 ~ 27% w/w

Amount of water in final product = $\frac{1403}{0.27}$ = 5200 Kg

Therefore:

Amount of water to be removed = 117 100 - 5200

= 111 900 Kg/batch

= 1 000 kg/hr

= 1 000 L/hr

Work done by Vlachogiannis with the Amicon 2000 MW cut-off membrane indicates that the membrane flux would drop from 42 L/hr to 10 L/hr with the high final concentration involved. Therefore:

Average membrane flux = 25 L/hr

Hence,

Number of membranes required = $\frac{1000}{25}$

= 40

Initial cost of membranes = 40 x £600

= £24 000

Since high concentrations are used, a life of only one year should be assumed.

Annual cost of membranes = £24 000

One of the major operating costs for this UF batch fractionation would be the cost of the pyrogen free water required (1405 x 10^3 L per batch). Therefore, to try to

reduce this requirement the waste product from the fractionation can be concentrated from its original concentration of 0.07% to a final concentration of 10%. This would require the removal of 1395 580 L of water per batch, or 12460 L/hr. As with the previous concentration step Amicon 2000 MW cut-off membranes can be used. A flux of 42 L/hr can be assumed since the maximum concentration is 10%. Therefore:

Number of $5m^2$ membranes of 2000 MW cut-off required = $\frac{12460}{42}$ = 297

Hence,

Initial cost of membranes = £178 200

With a maximum concentration of 10%, a life of 3 years can be assumed, therefore:

Cost of membranes = £59 400 per annum

Hence,

Total cost of membranes for batch fractionation = 34 000 + 24 000 + 59 400

= £117 400 per annum

Even though the majority of water used by both the GPC and UF fractionations is recovered during the overall process, approximately 64 tonnes/batch is still required (see Figure A6-1). This water costs £6 900 per annum.

Since the effluent from the batch UF fractionation is concentrated to 10% w/w, this product can be recycled and used for the manufacture of other dextran products eg. iron dextran. Therefore, the effluent can be considered to be zero.

This batch UF fractionation and concentration would require at least 8 x 1.1 Kw pumps, 8 x 4 Kw pumps,14 x 2.2 Kw pumps and at least two 18.5 Kw pumps. The 18.5 Kw pumps would be required for use with the high (27% w/w) concentrations involved in the final concentration step. These pumps would require electricity worth £47 800 per annum.

Hence,

Cost of UF batch fractionation = Total cost of membranes + cost of pumping power + cost of pyrogen free water.

Cost of UF batch fractionation = 117 400 + 47 800 + 6 900 = £172 100 pa.

Figure A6-1: Pyrogen Free Water Balance for a GPC and Batch UF Fractionation

Requirements

GPC Eluent =	65.6 x 10^3 L/batch
GPC purge =	151 x 10^3 L/batch
UF batch diafiltration =	1405 x 10^3 L/batch
Total	1621.6 x 10^3 L/batch

Recovery

Concentration step between GPC + UF =	50 300 L/batch
Concentration step between UF + spray drying =	111 900 L/batch
Concentration of waste product from UF fractionation =	1395 580 L/batch
Total	1557.78 x 10^3 L/batch

Therefore net amount of water required = 63.82 x 10^3 L/batch

(b) Capital Costs

In order to fractionate the required amount of dextran in the required time, 168 membranes are necessary (see previous section). If all these membranes were used on one single batch unit one very large pump would be required to obtain the necessary retentate recirculation rate and transmembrane pressures. Also, controlling the flow distribution, from one pump, into so many membranes could be very difficult. Therefore, in order to simplify these problems the batch fractionation can be considered to take place in eight identical units simultaneously, where each one of these eight units would contain 21 membranes.

Since the dextran solution is processed in eight simultaneous batches, eight retentate feed tanks of $20m^3$, eight diafiltration solvent storage tanks of $180m^3$ and eight permeate collection tanks of $180m^3$ would be required. These tanks would cost a total of £43 200, £128 000 and £128 000 respectively. One initial bulk feed tank of 120 m^3 would also be required, and would cost £13 000.

To obtain the necessary retentate flowrates a 4 Kw pump would be required per batch unit. This pump would cost £1300 and since eight pumps are required the total cost of these pumps is £10 400.

Since this fractionation is accomplished under diafiltration conditions, eight 1.1 Kw pumps would be required to transfer the diafiltration solvent from its storage tanks to the retentate tanks. These pumps would cost a total of £7 520.

Even though the dextran is processed in eight separate batches, only two product tanks, each of $60m^3$, are required. Each one of these product tanks would supply the feed to 20 membranes which would then concentrate the batch fractionated product to the required 27% w/w final concentration. These product tanks would cost £9000 each. In order to obtain the necessary retentate flowrates at these high final concentrations a 18.5 Kw pump would be required per product tank. This pump would cost £1900.

As mentioned in the previous section, the 'waste' product from the batch fractionation is concentrated in order to recover pyrogen free water. As with the dextran fractionation this concentration is best achieved by several simultaneous batch operations. For this case fourteen separate batch units would be required, and therefore fourteen 'waste' product tanks, each of $100m^3$, would be necessary. These tanks would cost £12 000 each.

To obtain the require retentate flowrates for this concentration step fourteen 2.2 Kw pumps are required, and would cost a total of £18 200.

As with the GPC fractionation calculations the cost of instrumentation, valves and a control system has been considered negligible. This is because no accurate costs could be determined for the ethanol process for comparison. Hence, the total capital cost of UF batch fractionation of low MW dextran can be considered to be £538 120.

6.4.2.2 Cascade Fractionation

(a) Operating Costs

Work recently done by Till (128), using the cascade equipment of Chapter 5 and Amicon 10 000 MW cut-off membranes, indicates that an improvement in recovery of 5% in 'saleable' dextran can be achieved over the batch fractionation. This fractionation would be accomplished by using a four stage cascade, with three of such units in series. At each stage 2 diavolumes would be processed. Since each stage would be processing at the same time, the time to process only two diavolumes need be considered. Therefore:

Volume to be processed = 2 x 117 100

= 234 200 L/batch

= 2091 L/hr

Flux of Amicon 0.06 m^2 membrane of 10 000 MW cut-off = 22 cm^3/min

Hence,

$$\text{Flux of Amicon } 5m^2 \text{ membrane} = 22 \times 60 \times \frac{5}{10^3} \times \frac{}{0.06}$$

= 110 L/hr

Therefore number of membranes required per stage = 19 (20)

Therefore total number of membranes required = 19 x 4 x 3

= 228

Therefore initial cost = 228 x £600

= £136 800

Assuming a life equal to 3 years:

Cost of membranes = £45 600 pa

As with the batch fractionation the product from this stage has to be concentrated before spray drying:

Weight of dextran in product from cascade = 1472 Kg

Weight of water in product from cascade = 117 110 Kg

Weight of water in concentrated product = $\frac{1472}{0.27}$ = 5452 Kg

Hence,

Water to be removed = 111 648 L/batch

= 1000 L/hr

Average membrane flux = 25 L/hr

Hence,

Number of membranes required = 40

Initial cost = £24 000

Assume a life equal to one year.

Cost of membranes = £24 000 pa

As with the UF batch fractionation, the 'waste' product from the cascade must be concentrated in order to recover some of the pyrogen free water. If this 'waste' product is concentrated from its initial concentration of 0.1% w/w to a final concentration of 10% w/w, 693 870 L of pure water per batch can be recovered. This concentration would require 148 membranes at a cost of £29 600 pa.

Hence:

Total cost of membranes for cascade fractionation = 45 600 + 24 000 + 29 600

= £99 200 pa

From Figure A6-2 it can be seen that a GPC plus cascade fractionation process would require 63.4 tonnes/batch of fresh pyrogen free water. This water would cost £6800 pa.

Since the effluent from the cascade is concentrated to 10% w/w, this product can be recycled and used for the manufacture of other dextran products. Therefore, the effluent can be considered to be zero.

The cascade fractionation would require 12 x 4 Kw pumps for retentate recycling, and 12 x 1.1 Kw pumps for permeate transfer. These pumps would require electricity worth £26 900 pa. The two concentration steps would require seven pumps of 2.2 Kw, and two pumps of 18.5 Kw for the very concentrated solutions. These nine pumps would require £23 000 worth of electricity per annum.

Hence,

Operating cost of UF cascade fractionation = total cost of membranes + cost of pyrogen free water + cost of pumping power.

= 99 200 + 6800 + 26 900 + 23 000 = £155 900 pa

(b) Capital Costs

As stated in the previous section this cascade fractionation is accomplished by using a four stage cascade configuration, with three of such units in series. Therefore, twelve retentate tanks, twelve permeate collection tanks, and twelve diafiltration solvent storage tanks are required. The retentate tanks are of $120m^3$ volume, and the permeate and diafiltration tanks are of $240m^3$ volume. These tanks each cost £13 000 and £18 000 respectively.

On each of the twelve stages a retentate recirculation pump of 4 Kw, and a permeate transfer pump of 1.1 Kw are required. Therefore, the cost of these pumps for the twleve stages is £15 600 and £11 280 respectively.

Figure A6-2: Pyrogen-free Water Balance for a GPC and UF Cascade Fractionation

Requirements

GPC eluent =	65.6×10^3 L/batch
GPC purge =	151×10^3 L/batch
UF cascade =	702.6×10^3 L/batch
Total	919.2×10^3 L/batch

Recovery

Concentration step between GPC and UF =	50.3×10^3 L/batch
Concentration step between UF and spray drying =	111.648×10^3 L/batch
Concentration of waste product from cascade =	693.87×10^3 L/batch
Total	855.818×10^3 L/batch

Therefore net amount of water required = 63.4×10^3 L/batch

As well as the tanks required on the actual cascade stages, one initial feed tank of 120m^3, and two final product tanks of 60m^3 each, are required. These tanks each cost £13 000 and £9000 respectively. To concentrate the solutions in the final product tanks two 18.5 Kw pumps are required, and cost a total of £3 800.

As with the batch fractionation the 'waste' product streams from the cascade are processed in seven simultaneous batches. Therefore, seven 'waste' product collection tanks, each of 100m^3, and seven 2.2 Kw recirculation pumps are required. The tanks cost £12 000 each and the pumps are £1 300 each.

As with the GPC and UF batch fractionation calculations, the cost of instrumentation, valves and a control system has been considered negligible. Therefore, the capital cost of a UF cascade low MW dextran fractionation can be considered to be £742 780.

6.5 UF Fractionation of High and Low MW Dextran

6.5.1 UF Fractionation of High MW Dextran

6.5.1.1 Operating Costs

As well as using GPC to fractionate the high MW dextran, it has been shown (Chapter 4) that UF can also achieve the required fractionation with the same efficiency as GPC. Therefore, the best metohd to use would be the one which has the least operating and capital costs.

The data reported earlier shows that DDS membranes with either 25 000 or 50000 MW cut-offs obtain the required product within six diavolumes. However, instead of investigating the costs of these membranes it was decided to use an Amicon 30000 MW cut-off membrane. This was because, (a) the Amicon configuration has been shown consistantly to be the best for fractionating dextran, (b) the capital costs of membrane housings would be less for Amicon membranes compared to DDS, and (c) since Amicon membranes operate at lower pressures the pumping costs would be less. It was thought appropriate to operate the Amicon membranes for six diavolumes however. The operating costs of these Amicon membranes will now be found.

Initial feed concentration = 2% w/w

Therefore,

Water in feed = 140 x 10^3 L

Hence,

Volume of water to be processed = 6 x 140 x 10^3

= 840 x 10^3 L/batch

= 7500 L/hr

Flux of 0.06 m^2 Amicon 30 000 membrane (131) = 30 cm^3/min

Therefore flux of Amicon 5m^2 membrane = 150 L/hr

Therefore number of membranes required = 50

Hence,

Initial cost of membranes = £30 000

Assuming a life of 3 years:

Cost of membranes = £10 000 pa

For this fractionation the product is in the permeate and has a concentration of approximately 0.3% w/w. This must, therefore, be concentrated to 2% w/w before use in the next UF fractionation stage.

Amount of water in 2% solution = 117 110 L

Therefore:

Amount of water to be removed = 840 000 - 117 100

= 722 900 L/batch

= 6 454 L/hr

Flux of Amicon 2000 MW cut-off membrane (5 m^2) = 42 L/hr

Therefore:

Number of membranes required = 154

Initial cost = £92 400

Assuming a life equal to three years:

Cost of Membranes = £31 000 pa

Hence,

Cost of membranes for UF fractionation of high MW dextran = 10 000 + 31 000

= £41 000 pa

In order to obtain the required retentate flowrates through the membranes, the fractionation of the high MW dextran would be accomplished in two equal simultaneously operated batches. This would therefore require two 4 Kw pumps, which would use electricity worth £3,500 pa.

The concentration of the permeate product would be accomplished in six simultaneous batches. This would therefore require six 2.2 Kw pumps, which would use electricity worth £5 800 pa.

The 'waste' product from this fractionation would be the retentate, and would contain mostly very high MW dextran. This 'waste' can be recycled back to the acid hydrolysis section of the dextran process. Therefore, the effluent from this process can be considered to be zero.

The fresh pyrogen free water requirement of this high MW fractionation will be discussed later. Therefore, the operating cost can be assumed to be £50 300 per annum.

6.5.1.2 Capital Costs

This method of high MW dextran fractionation would require two retentate tanks of $80m^3$, two permeate collection tanks of $420m^3$, and one initial feed tank of $150m^3$. These tanks would each cost £11 000, £25 000 and £14 500 respectively. The two 4 Kw pumps required would each cost £1300.

The concentration of the permeate product would require six $150m^3$ retentate tanks at a total cost of £87 000. The six 2.2 Kw pumps required would cost a total of £7800. Hence, the capital cost for this UF batch fractionation of the high MW dextran is £183 900.

6.5.2 UF Fractionation of Low MW Dextran

6.5.2.1 Batch Fractionation

Since UF batch fractionation of high MW dextran has the same efficiency as GPC, the operating conditions and therefore the majority of the operating costs will be the same as with GPC and UF fractionation. Therefore, from Appendix 6.4.2.1:

Total cost of membranes for fractionation = £117 400 pa

Total cost of pumping power = £47 800 pa

Effluent disposal costs = Zero

The one operating cost which is different from Appendix 6.4.2.1 is the cost of the fresh pyrogen free water. Figure A6-3 gives a water balance for the batch fractionation of both high and low MW dextran. As can be seen from this Figure water is required to dilute the feed solution before the initial high MW fractionation. This is because the original hydrolysate feed concentration was too high and had to be reduced to 2%. The net amount of pyrogen free water required is approximately 138 tonnes/batch, and the cost of this water is £15 000 per annum. Therefore, the operating cost for the batch UF fractionation of the low MW dextran can be considered to be £180 200 per annum.

Since the operating conditions for this UF batch low MW dextran fractionation are exactly the same as in Appendix 6.4.2.1, the capital cost will also be the same, and therefore is equal to £538 120.

6.5.2.2 Cascade Fractionation

Since the operating conditions for this fractionation are the same as in Appendix 6.4.2.2, the majority of the operating costs will be the same. Therefore:

Total cost of membranes for fractionation = £99 200 pa

Total cost of pumping power = £49 900 pa

Effluent disposal costs = Zero

Figure A6-4 gives a water balance for the batch fractionation of the high MW dextran and the cascade fractionation of the low MW dextran. The net amount of

Figure A6-3: Pyrogen Free Water Balance for a UF Batch Fractionation of High and Low MW Dextran

Requirements

Dilution of feed =	123.6×10^3 L/batch
UF High MW Fractionation =	840×10^3 L/batch
UF Low MW Fractionation =	1405×10^3 L/batch
Total	2368.6×10^3 L/batch

Recovery

Concentration Step Between High and Low MW Fractionations =	722.9×10^3 L/batch
Concentration Step Between Low MW Fractionation + Spray Drying =	111.900×10^3 L/batch
Concentration of Waste Product from Low MW Fractionation =	1395.58×10^3 L/batch
Total	2230.38×10^3 L/batch

Therefore net amount of water required = 138.22×10^3 L/batch

Figure A6-4: Pyrogen Free Water Balance for a UF Batch Fractionation of High MW Dextran and a UF Cascade Fractionation of Low MW Dextran

Requirements

Dilution of feed =	123.6×10^3 L/batch
UF High MW Fractionation =	840×10^3 L/batch
Cascade Fractionation =	702.6×10^3 L/batch
Total	1666.2×10^3 L/batch

Recovery

Concentration Step Between High and Low Fractionation =	722.9×10^3 L/batch
Concentration Step Between Cascade + Spray Drying =	111.5×10^3 L/batch
Concentration of Waste Product from Cascade =	693.87×10^3 L/batch
Total	1528.42×10^3 L/batch

Therefore net amount of water required = 137.78×10^3 L/batch

pyrogen free water required is approximately 138 tonnes/batch, and the cost of this water is £15 000 per annum. Therefore, the operating cost for this cascade fractionation of the low MW dextran is £164 100 per annum.

From Appendix 6.4.2.2, the capital cost for the cascade fractionation is £742 780.

NOMENCLATURE

A_s	Asymmetry factor of a GPC column
B	Back diffusion of a solute
b_{1-5}	GPC calibration constants
C_b	Concentration of solute in the bulk solution
C_g	Concentration of the gel layer
C_i	Concentration of component i
C_o	Initial concentration of solute
C_p	Concentration of solute in permeate
C_r	Concentration of solute in retentate
C_t	Concentration of solute at time t
C_w	Concentration of solute at membrane wall
D	Diffusivity of the solute (Chapter 2)
D	Polydispersity of a dextran sample (Chapter 3)
d_p	Diameter of a membrane pore
F(V)	Surface area per unit volume
h_i	GPC chromatogram height of component i
J_1	Membrane solvent flux
J_2	Membrane solute flux
J_v	Total volume of membrane flux
K	Overall mass transfer coefficient
K_c	Carman factor
K_d	GPC column distribution coefficient
K_m	Mass transfer coefficient of solute
K_1, K_2	Solute drag coefficients
k_B	Boltzmann Constant
L	Length of pore
L_p	Membrane permeability constant
M_N	Number average molecular weight

M_W	Weight average molecular weight
M_V	Viscosity average molecular weight
N	Number of monomer units in a polymer chain (Chapter 2)
N	Theoretical number of plates (Chapter 3)
N_A	Avogadro's number
P	Permeability of solute
P_p	Permeate pressure
R	Rejection coefficient
R_F	Flory radius of gyration
R_o	Observed rejection
R_{perm}	Rejection based on permeate
R_{ret}	Rejection based on retentate
r	Radius of membrane pore
r_e	Einstein radius of solute
r_R	Reptation time
r_Z	Zimm relaxation frequency of a polymer chain
r_2	Solute radius
r_3	Membrane capillary radius
S_c	Critical shear rate
T	Kelvin temperature
V_o	Initial retentate volume (Chapter 2)
V_p	Volume of permeate (Chapter 2)
V_t	Retentate volume at time t (Chapter 2)
V_o	Void volume (Chapter 3)
V_R	Elution volume (Chapter 3)
V_t	Total liquid volume (Chapter 3)
W	Hindrance to convection
$W_{0.5}$	Peak width at one-half peak height
X	Thickness of membrane
X_e	Effective free area of a membrane
Y_B	Boundary layer thickness

GREEK LETTERS

Γ	Virial coefficient
ε	Fraction of membrane skin containing pores
η	Intrinsic viscosity
η_0	Viscosity of solvent
η_2	Viscosity of solute
λ	Ratio of solute radius to pore radius
μ	Fluid viscosity
π	Osmotic pressure
σ_g	Reflection coefficient of gel layer
σ_m	Reflection coefficient of membrane
Φ	Sieving coefficient

REFERENCES

1 THOREN L Dextran as a Plasma Substitute. Blood Substitutes and Plasma Expanders. Progress in Clinical and Biological Research. 19, Alan R Liss Inc (1978) 265-282

2 MARTIN LE Dextran: A Plasma Volume Expander. Chemistry and Industry, 8, (1955) 184-191

3 ATIK M Dextran 40 and Dextran 70. Arch Surg, 94 (1967) 664-671

4 NILSSON K, SODERLUND G Clinical Dextrans. Specification and Quality of Preparations on the Market. Acta Pharm Suec. 15, (1978) 439-454

5 FOSTER FH Dextran-Manufacture and Use. Part 1. Process Biochem, Feb 1968, 15-19

6 FOSTER FH Dextran-Manufacture and Use. Part 2. Process Biochem, March 1968, 55-62

7 BARKER PE, ELLISON FJ, HATT BW A New Process for the Continuous Fractionation of Dextran. Ind Eng Chem Process Des Dev, 17 (3), (1978) 302-309

8 BARKER PE, HATT BW, WILLIAMS AN Fractionation of a Polymer Using a Preparative Scale Continuous Chromatograph. Chromatographia, 11 (9), (1978) 487-493

9 ENGLAND K A Comparison of Batch and Continuous Chromatography Equipment for the Separation of Organic Mixtures, PhD Thesis, University of Aston in Birmingham, 1979

10 ELLISON FJ Polymer Fractionation by Continuous Chromatography, PhD Thesis, University of Aston in Birmingham, 1976

11 WILLIAMS AN Fractionation and Separation by Continuous Liquid-Liquid Chromatography, PhD Thesis, University of Aston in Birmingham, 1977

12 VLACHOGIANNIS GJ Dextran Polymer Fractionation by Production Scale Chromatography and Ultrafiltration. PhD Thesis, University of Aston in Birmingham, 1982

13 ALSOP RM, BARKER PE, VLACHOGIANNIS GJ Efficient Production of Clinical Dextran from Dextran Hydrolysate. Chem Eng, 399, 1984, 24-27,

14 BARKER PE, ALSOP RM, VLACHOGIANNIS GJ Fractionation, Purification and Concentration of Dextran Solutions by UF. J Membr Sci. 20 (1984) 79-91

15 BARKER PE, ENGLAND K, VLACHOGIANNIS GJ Mathamatical Model for the Fractionation of Dextran on a Semi-Continuous Counter-current Simulated Moving Bed Chromatograph. Chem Eng Res Des, 61 (4), (1983) 241-247

16 BARKER PE, VLACHOGIANNIS GJ, ALSOP RM Dextran Fractionation on a Semi-Continuous Counter-current Simulated Moving Bed Chromatograph. Chromatographia, 17 (3), (1983) 149-152

17 MEARES P Membrane Separation Processes. Elsevier Scientific Publishing Company, Amsterdam, (1976)

18 KEDEM O, KATCHALSKY A A Physical Interpretation of the Phenomenological Coefficients of Membrane Permeability, J Gen Physiol, 45, (1961) 143

19 KATOH M, SUZUKI S Am Chem Soc Symp Ser (1981), 153 (1981), 247

20 LACEY RE Industrial Processing with Membranes. Robert E Krieger Publishing Company, New York, (1979)

21 RAUTENBACH R, ALBRECHT R Separation by Membranes, Ger Chem Eng, 5, 329

22 KIMURA S, SOURIRAJAN K Analysis of Data in Reverse Osmosis with Porous Cellulose Acetate Membranes Used. AIChE J, 13 (3), (1967) 497-503

23 SHERWOOD TK, BRIAN PLT, FISHER RE, DRESNER L Salt Concentration at Phase Boundaries in Desalination by Reverse Osmosis. Ind Eng Chem Fundamentals, 4 (2), (1965) 113

24 MICHAELS AS New Separation Technique for CPI. Chem Eng Prog, 64, 12, 31

25 BLATT WF, DAVID A, MICHAELS AS, NELSON L Solute Polarisation and Cake Formation in Membrane Ultrafiltration Causes, Consequences and Control Techniques. Membrane Science and Technology, Ed Flinn JE, Plenum Press, p 47

26 STRATHMANN H Membrane Separation Processes. J Membrane Science 9, (1981), 121-189

27 PORTER MC Concentration Polarization with Membrane Ultrafiltration. Ind Eng Chem Prod Res Develop. 11, No 3 (1972), pp 234-248

28 GRAETZ L Ann Phys Chem, 18, (1883)

29 LEVEQUE MA Ann Mines, 13 (April 1928)

30 GOLDSMITH RL Macromolecular Ultration with Microporous Membranes. Ind Eng Chem Fundam. 10 (1), (1971) 113-120

31 TANFORD C Physical Chemistry of Macromolecules. Wiley, N York (1961)

32 TRETTIN DR, DOSHI MR Pressure-independent Ultrafiltration - is it Gel Limited or Osmotic Pressure Limited in Synthetic Membranes, Vol II, Hyper and Ultrafiltration Uses. Ed. AF Turbak. American Chemical Society, Washington, (1981), 373

33 FLORY PJ Principles of Polymer Chemistry. Cornell University Press (1953)

34 WALES M Pressure Drop Across Polarization Layers in Ultrafiltration. ACS Symposium Series, 1, (1981) 159-170

35 CLIFTON MJ, ABIDINE N Growth of the Polarization Layer in UF with Hollow-Fibre Membranes. Submitted for publication in J of Memb Sci.

36 WIJAMS JG, NAKAO S, VAN DEN BERG JWA Hydrodynamic Resistance of Concentration Polarisation Boundary Layers in Ultrafiltration. J Memb Sci, 22, (1985) 117-135

37 COLTON CK, FRIEDMAN S, WILSON DE, LEES M Ultrafiltration of Lipoproteins Through a Synthetic Membrane. J Clin Inv, 51 (1972) 2472-2481

38 NGUYEN QT, NEEL J Characterization of Ultrafiltration Membranes. Part III. Role of Solvent Media and Conformational Changes in Ultrafiltration of Synthetic Polymers. J Membrane Science, 14 (2) (1983) 97-109

39 CAPANNELLI G, VIGO F, MANARI S Ultrafiltration Membranes - Characterization Methods. J Membrane Science, 15 (3), (1983) 289-313

40 NAKAO S, KIMURA S Effect of Gel Layer on Rejection and Fractionation of Different Molecular Weight Solutes by Ultrafiltration. ACS Symposium Series 2, (154), (1981), 119-132

41 NAKAO S, YUMOTO S, KIMURA S Analysis of Rejection Characteristics of Macromolecular Gel Layer for Low Molecular Weight Solutes in UF. J Chem Eng Jpn, 15, 6, (1982) 463-8

42 JAGUR-GRODZINSKI J, KEDEM O Transport Coefficients and Salt Rejection in Unchanged Hyperfiltration Membranes Desalination, 1, (1966) 327

43 LOPEZ-LEIVA M Prediction of Permeate Fluxes in UF/RO Systems. Polymer Science and Technology, 13, (1980) 269-281

44 DOSHI MR, TRETTIN DR UF of Colloidal Suspensions and Macromolecular Solutions in an Unstirred Batch Cell. Ind Eng Chem Fundam, 20 (3), (1981) 221-9

45 TANNY GB Dynamic Membranes in UF and Reverse Osmosis. Separation and Purification Methods, 7 (2), (1978) 183-220

46 LE MS, HOWELL JA Alternative Model for UF. Chem Eng Res Des, 62 (Nov 84) pp 373-380

47 BLATT WF Hollow Fibres: A Transition Point in Membrane Technology. American Laboratory, Oct 1972, 78-85

48 PORTER MC, NELSON L Ultrafiltration in the Chemical, Food Processing, Pharmaceutical and Medical Industries. Recent Developments in Separation Science, Vol II, CRC Press

49 CHUDACEK MW, FANE AG The Dynamics of Polarisation in Unstirred and Stirred Ultrafiltration. J Membrane Science, 21 (2), (1984) 145-160

50 CHAN K, MATSUURA T, SOURIRAJAN S Interfacial Forces, Average Pore Size, and Pore Size Distribution of UF Membranes. Ind Eng Chem Prod Res Dev, 21, (1982) 605-612

51 KLEIN E, HOLLAND FF, DONNAUD A Diffusive and Hydraulic Permeabilities of Commercially Available Hemodialysis Films and Hollow Fibres. J Membrane Science, 2, (1977), 349

52 BECHHOLD HZ Phys Chem, 64, (1908) 328

53 FERRY JD Ultrafilter Membranes and Ultrafiltration. Chem Rev, 18 (1936) 373

54 DU BOIS R The Role of Membrane Parameters and of Filtration Pressure in the Determination of the Shape of the Polyvinyl Pyrrolidone Sieving Curve, Contr Nephol, 1, (1975), 9

55 SCHWARZ HH, BOSSIN E Skin Layer Characterization of Anistropic Membranes for UF. J Membrane Science, 12, (1), (1982), 101-106

56 BODZEK M Physico-Chemical Characterization of Ultrafiltration Membranes. Polish Journal of Chemistry, 56, (1983) 919-930

57 FANE AG, FELL CJD, WATERS AG The Relationship Between Membrane Surface Pore Characteristics and Flux for UF Membranes. J Membrane Science, 9 (1981) (3) pp 245-262

58 GREEN DM, ANTWILER GD, MONCRIEF JW, DECHERD JF Trans Am Soc Artif Int Organs, 22, (1976) 627

59 MICHAELS AS Analysis and Prediction of Sieving Curves for Ultrafiltration Membranes: A Universal Correlation? Sep Sci Technol 15 (6), (1980) 1305-1322

60 TINGHUL L, CHAN K, MATSUURA T Determination of Interaction Forces and Average Pore Size and Pore Size Distribution and their Effects of Fouling of UF Membranes. Ind Eng Chem Prod Res Dev, 23, (1984) 116-124

61 KLEIN E, FELDHOFF P, TURNHAM T Molecular Weight Spectra of Ultrafilter Rejection II Measurements on Highly Rejecting Filters. Jnl of Membrane Science 15 (3) (1983), 245-257

62 ZEMAN L, WALES M Polymer Solute Rejection by Ultrafiltration Membranes. ACS Symposium Series, 2, (154) (1981) 411-434

63 HOWELL JA, VELICANGIL O Protein Ultrafiltration: Theory of Membrane Fouling and its Treatment with Immobilized Proteins. Ultrafiltration Membranes and Applications. AR Cooper (Ed), Plenum Press, N York, (1980), pp 217-229

64 INGHAM KC, BUSBY TF, SAHLESTROM Y, CASTINO F Separation of Macromolecules by Ultrafiltration, Influence of Protein Adsorption, Protein-Protein Interactions and Concentration Polarisation. Ultrafiltration Membranes and Applications. AR Cooper (Ed), Plenum Press, N York, (1980), pp 141-158

65 ROWLAND FW, EIRICH FR Flow Rates of Polymer Solutions Through Porous Disks as a Function of Solute. J Polym Sci, A-1, 4 (1966), 2401

66 ZEMAN, LJ Adsorption Effects in Rejection of Macromolecules by UF Membranes. Journal of Membrane Science, 15 (3) (1983) 213-230

67 KLEIN E, FELDHOFF P, TURNHAM T Molecular Weight Spectra of Ultrafilter Rejection. I. A Simple HPLC Method using Homologous Maltodextrin Polymers. J Mem Science, 15, (1), pp 15-26, (1983)

68 NGUYEN QT, APTEL P, NEEL J Characterisation of Ultrafiltration Membranes. Part I, Water and Organic Solvent Permeabilities. J Mem Science, 5 (1979) 235-251

69 KAMIDE K, MANABLE S Mechanism of Permselectivity of Porous Polymeric Membranes in Ultrafiltration Process. Polymer Journal, 13 (5), (1981) 459-479

70 FELDHOFF P, TURNHAM T, KLEIN E Effect of Plasma Proteins on the Sieving Spectra of Hemofilters. Artificial Organs, 8 (2), (1984) 186-192

71 KIMURA S, JITSUHARA I Transport Through Charged UF Membranes. Desalination, 46 (1983), 407-416

72 KALINA IK, SUDAREUA NN Functional Characteristics of Semipermeable Membranes and Their Calibration Against Various Substances. Jnl of Applied Chemistry of the USSR, 54 (5), (1981), pp 909-11

73 MADSEN RF, KOFOD NIELSEN W Thin-Channel Ultrafiltration, Theoretical and Experimental Approaches. Polymer Science and Technology, 13, (1980) 423-438

74 BAKER RW Methods of Fractionating Polymers by UF. Journ of Applied Polymer Science, Vol 13, (1969) 369-376

75 BAKER RW, STRATHMANN H Ultrafiltration of Macromolecular Solutions with High Flux Membranes. Journal of Applied Polymer Science, Vol 14, pp 1197-1214 (1970)

76 EDBERG SC, BRONSON, PM The Fractionation of Hydrolysed Dextran by UF Through a Series of Anisotropic Cellulose Acetate Membranes. Preparative Biochemistry 1 (3), (1971) 249-257

77 COOPER AR, VAN DER VEER DS Ultrafiltration Membrane Characterisation. 2nd World Filtration Congress, 1979, pp 455-461

78 NGUYEN QT, APTEL P, NEEL J Characterisation of Ultrafiltration Membranes. Part II. Mass Transport Measurements for Low and High MW Synthetic Polymers in Water Solutions. J Membrane Science, 7, (1980) 141-155

79 BOTTINO A, CAPANNELLI G, IMPERATO A, MUNARI S Ultrafiltration of Hydrosoluble Polymers. Effect of Operating Conditions on the Perforamnce of the Membrane. J Mem Sci, 21, (1984), 247-267

80 ARTURSON G, GRANATH K Dextrans as Test Molecules in Studies of the Functional Ultrastructure of Biological Membranes. Clin Chim Acta, 37 (1972) 309-322

81 DE GENNES PG Coil-Stretch Transition of Dilute Flexible Polymers Under Ultra High Velocity Gradients. Journal of Chemical Physics, 60, No 12, (1974), pp 5030-5042

82 DE GENNES PG Dynamics of Entangled Polymer Solution, I. The Rouse Model, Macromolecules. 9, (1976) 587

83 DAOUDI S, BROCHARD F Flow of Flexible Polymer Solutions in Pores Macromolecules. 11 (1978) 751-758

84 EDWARDS SF The Statistical Mechanics of Polymerized Material. Proc Phys Soc, 92, (1967), 9-16

85 QUANG TRONG NGUYEN Characterisation of UF Membranes. Part IV. Influence of the Deformation of Macromolecular Solutes on the Transport Through Ultrafiltration Membranes. J Mem Science, 14, (1983) 111-128

86 BRENNER H, GAYDOS JL The Constrained Brownian Movement of Spherical Particles in Cylindrical Pores of Comparable Radius. J Colloid Interface Sci, 58, 312 (1977)

87 ZEMAN L, WALES M Steric Rejection of Polymeric Solutes by Membranes with Uniform Pore Size Distribution. Sep Sci Technol (1981), 16, 3, 275-90

88 PAINE PL, SCHERR P Drag Coefficients for the Movement of Rigid Spheres Through Liquid Filled Cylindrical Pores. Biophys J, 15, 1087, (1975)

89 LONG TD, JACOBS DL Configurational Effects on Membrane Rejection. J Mem Scien, 9, (1981) 13-27

90 DEEN WM, BOHRER MP, EPSTEIN NB Effects of Molecular Size and Configuration on Diffusion in Microporous Membranes. AIChE J, 27 (6), pp 952-959, Nov 1981

91 MUNCH WD, ZESTER LP, ANDERSON JL Rejection of Polyelectrolytes from Microporous Membranes. J Membrane Sci, 5 (1979) 77

92 TUTANJIAN RS, RETI AR Molecular Fractionation by Staged Ultrafiltration. AIChE Symp Ser, (1978), 178 210-16

93 KINOSHITA M, NARUSE Y Improvement of the Mathematical Simulation Model for a Multicomponent Separating Cascade. Nucl Science and Eng, (1982), 82 (4), 469-75

94 GRUZDEV EB, LAGUNTSOV NI A Method of Calculating Membrane Element Cascades for Separating Multi Component Mixtures. Atomnaya Energiya, 57 (2), pp 117-120, August 1984

95 ASH R, FOLEY T Transcient-State Transport in Some Finite Systems. Part 1. A Simple (Two-Stage) Cascade. J Memb Sci, 13 (1983) 205-232

96 FRANKLIN NL Counterflow Cascades: Part 1. Chem Eng Res Des, 64, Jan 1986

97 PORTER MC, MICHAELS AS Membrane Ultrafiltration. Chem Technol, 1, (1971) pp 56-63

98 COOPER AR, PETTINGILL DB Improved UF Processes by Partial Recycle of Ultrafiltrate. Journal of Membrane Science, 15 (1983) 3-13

99 NODA I, GRYTE C Multi-Stage Membrane Separation Processes for the Continuous Fractionation of Solutes Having Similar Permeabilities. AIChE, 1981 27, 6, 904-12

100 BHAMBRA KS The Fractionation of Dextran using Ethanol. PhD Thesis, University of Aston in Birmingham, 1985

101 ALSOP RM, BYRNE GA, DONE JN, EAR IE, GIBBS R Quality Assurance in Clinical Dextran Manufacture by Molecular Weight Characterisation. Proc Biochem (1977, Dec), 15-22

102 TSK-GEL, Technical Data Bulletin, Toya Soda Manufacturing Co Ltd, Tokyo, Japan, Toyo-Soda Publication (1980)

103 BARKER PE, HATT BW, VLACHOGIANNIS GJ Suitability of TSK-Gel Toyo Pearl Packing for Gel Permeation Chromatographic Analysis of Dextran. J of Chromatography, 208, (1981) 74-77

104 ALSOP RM, VLACHOGIANNIS GJ Determination of the Molecular Weight of Clinical Dextran by Gel Permeation Chromatography on TSK-PW Type Columns. Jou of Chromatography, 246, (1982), 227-240

105 YAU WW, KIRKLAND JJ, BLY DD Modern Size Exclusion Liquid Chromatography. John Wiley and Sons (1979)

106 HATT BW Polymer Molecular Weight Distribution by Gel Permeation Chromatography, Developments in Chromatography-1; Knapman, CEH, Applied Science Publ, Essex (1979), 157-199

107 GRABISTIC Z, REMPP R, BENOIT H A Universal Calibration for Gel Permeation Chromatography, Jou Polym Sci, Part B, 5, (1967) 753-759

108 FRANK FC, WARD IM, WILLIAMS T Calibration Procedure for Gel Permeation Chromatography. Jou Polm Sci, A-2, 6 (1968), 1357-1369

109 BALKE ST, HAMIELEC AE Gel Permeation Chromatography Calibration Curve From Polydisperse Standards. Ind Eng Prod Res Dev, 8, (1969) 54-57

110 CERVENKA A, BATES TW Characterisation of Polydisperse Branched Polymers by Means of Gel Permeation Chromatography. Jou of Chromatography, 53, (1970), 85-93

111 LANSING W, KRAEMER E A New Method of GPC Calibration Using Dextran Fractions of Low Polydispersity. Jou Am Chem Soc, 57, (1935), 1369-1385

112 McCRACKIN FL Calibration of GPC Columns Using Polydisperse Polymer Standards. Jou Appl Polm Sci, 21, (1977), 191-198

113 CHAPLIN RP, CHING W Accurate Calibration of GPC by Use of Broad Molecular Weight Distribution Standards. J Macromol Sci Chem, A14, (1980), 257-263

114 MALOWER EG, MONTANA AJ Algorithm for the Determination of Linear GPC Calibration Curve of a Polydisperse Standard. Jou Polym Sci, Polym Phys Ed, 118, (1980), 2303-2305

115 NILSSON G, NILSSON K Molecular Weight Distribution Determination of Clinical Dextran by GPC. Jou of Chromatography, 101, (1974), 137-153

116 HARTLEY HO The Modified Gauss-Newton Method for Fitting of Non-Linear Regression Functions by Least Squares. Technometrices, 3, (1961), 269-280

117 BOOTH GC, GOLD V Molecular Weight Studies of Dextran. Jou Chem Soc (1956), 3380-3385

118 PHARMACIA FINE CHEMICALS Molecular Weight and Molecular Size Determination. Separation News (March 1972)

119 HASEL JA Computer Manipulation and Substraction of GPC Chromatograms. Jou Polym Sci, Polm Lett Ed, 17, (1979), 111-113

120 OUANO AC Qualitative Data Interpretation Techniques in GPC. Jou Macromol Sci Rev Macromol Chem, 9 (1), (1973), 123-148

121 JORDAN RC, CHRIST PJ A Data System for Polymer Characterisation, Application to GPC. Am Lab, 11 (1979), 71-72, 74, 76, 78-81

122 INSTRUCTIONS MANUAL Differential Refractometer R401, Waters Associates Ltd, Hartford, Cheshire.

123 INSTRUCTIONS MANUAL Servoscribe RE 541 20, Smiths Industries Ltd, Cricklewood, London, UK.

124 AMICON LTD Products for Separations Technology, Stonehouse, Glos, GL10 2BJ

125 MILLIPORE (UK) LTD Molecular Separation and Cell Harvesting with the Pellicon Cassette System, Technical Publication PBO84, Harrow, Middlesex, HA1 2YH

126 DDS DDS Ro-System UF Module, DK-4900 Nakskov, Denmark

127 PIERPOINT D Fractionation of Dextran 40 Hydrolysate at the High Molecular Weight End by UF on the DDS System. Fisons Internal Development Report.

128 TILL A Chemical Engineering Department, Aston University, Birmingham. Personal communication.

129 GANETSOS G Production of 100 tonnes per annum of Clinical Dextran using a Non-alcoholic Route. Final Year Design Project, Aston University, Birmingham, April 1983.

130 MOMO S, Chemical Engineering Department, Aston University, Birmingham. Personal communication.

131 ZAFAR IA Chemical Engineering Department, Aston University, Birmingham. Personal communication.

132 Personal Communication